

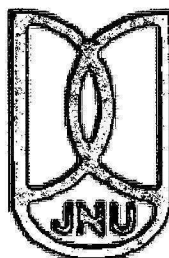
**Transcriptional Activation Of p53 Gene And
Stabilization Of p53 By Its Amino-Terminus Domain**

**Thesis Submitted To The Jawaharlal Nehru University
In Partial Fulfillment For The Award Of The Degree Of**

**DOCTOR OF PHILOSOPHY
IN
BIOTECHNOLOGY**

By

ANUJ KUMAR SHARMA



**SCHOOL OF BIOTECHNOLOGY
JAWAHARLAL NEHRU UNIVERSITY
NEW DELHI-110067**

INDIA

2009





Jawaharlal Nehru University
New Delhi
India

Certificate

This is to certify that the work entitled 'Transcriptional Activation Of p53 And Stabilization Of p53 By Its Amino-Terminus Domain' submitted to the School of Biotechnology, Jawaharlal Nehru University, New Delhi in partial fulfillment of the requirements for the award of the degree of Doctor of Philosophy, embodies faithful record of original research work carried out by Anuj Kumar Sharma. This work is original and has not been submitted so far in part or full for any other degree or diploma of any other university.

Anuj Kumar Sharma
(Ph.D. Candidate)

School of Biotechnology
Jawaharlal Nehru University
New Delhi (INDIA)-110067

Prof. Uttam Pati
(Supervisor)

School of Biotechnology
Jawaharlal Nehru University
New Delhi (INDIA)-110067

Prof. Rajiv Bhat
(Dean)

School of Biotechnology
Jawaharlal Nehru University
New Delhi (INDIA)-110067

LIST OF PUBLICATIONS

SCIENTIFIC PUBLICATIONS

- ◆ **Sharma AK**, Akhaury P and Pati U. Tumor suppressor p53 auto-regulates p53 gene expression via differential DBS selection under physiological and stress conditions. Manuscript under preparation.
- ◆ **Sharma AK**, Khan AA, Gogna R, Singh AK, and Pati U. p53 amino-terminus region (1-125) stabilizes and restores heat denatured p53 wild phenotype. Submitted after revision to **PLoS ONE**.
- ◆ **Sharma K**, **Sharma AK**, Vincent TK Chow and Lal SK. The SARS-CoV 9b Accessory Protein uses passive transport for import, active NES dependent nucleocytoplasmic export and triggers caspase 3 mediated apoptosis when retained in the nucleus of mammalian cells. Submitted to **Biochemistry**.
- ◆ **Dubey SK**, **Sharma AK**, Misra K, Pati U and Pandey R. Design and synthesis of a modified RNA-curcumin demethylenated piperoyl conjugate as a telomerase targeted antisense prodrug; its activity against human cancer cell lines HeLa & KB. Submitted to **Indian Journal of Pharmacology**.
- ◆ **Dubey SK**, **Sharma AK**, Narain U, Misra K, Pati U. Design, synthesis and characterization of some bioactive conjugates of curcumin with glycine, glutamic acid, valine and demethylenated piperic acid and study of their antimicrobial and antiproliferative properties. **European Journal of Medicinal Chemistry**. 43 (2008) 1837-1846.
- ◆ **Kapoor N**, **Sharma AK**, Dwivedi V, Kumar A, Pati U, Misra K. Telomerase targeted anticancer bioactive prodrug by antisense-based approach. **Cancer Letters**. 248 (2007) 245–250.

ABSTRACTS

- ◆ **Dubey SK**, **Sharma AK**, Misra K, Pandey A, Pati U, Pandey RK. A combined antisense and prodrug approach to target human telomerase. International Symposium on Chromosomes to genomes, 2007.
- ◆ **Kapoor N**, **Sharma AK**, Kumar A, Pati U, Misra K. Telomerase targeted anticancer bioactive prodrug by antisense-based approach. 8th National Symposium on Biochemical Engineering and Biotechnology, 2006.

*Dedicated to
Beloved Parents*

ACKNOWLEDGEMENTS

It is by Gods grace and his willingness that I hereby place on record my deep sense of gratitude and respect to all those who helped and encouraged me to complete this work. In the past six years, I have learnt that research is a journey. In many ways similar to the journey of life in which hope, adventure, joy, pride and disappointments all meet you in equal measure. A journey in which learning comes with experience and experience comes with struggle.

Foremost, I am grateful to Prof. Uttam Pati, my guide and mentor through this journey for his constant support, encouragement, supervision and freedom to realize my scientific pursuit and having reposed unstinting faith in my abilities. I owe him lot of gratitude for having shown me the path of research. I believe it will be a driving force to accept the challenges cheerfully in all my future endeavors. This piece of work would have been a distant dream without him. Thank you very much, Sir.

I am indebted to the Dean Prof. Rajiv Bhat for providing the research facilities in the school. I would further like to convey my heartfelt gratitude to Prof. Rakesh Bhatnagar, Prof. S. K. Kar, Prof. Aparna Dixit, Prof. K. J. Mukherjee, Dr. Devpriya Chaudhary, Dr. S.S. Maitra, Dr. Ranjana Arya, Dr. Swati Tiwari and Dr. Maitreyi S. Rajala for their support and encouragement.

I also acknowledge the financial aid provided by UGC for junior and senior research fellowship during the course of work.

I am grateful to my seniors, Prerna, Sarita, Hossein, Veenu, Amzad for familiarizing me with the intricacies of molecular biology and cell culture.

I am thankful to them for giving me valuable help and support.

I would further acknowledge my labmates Anoop, Trinath, Janpriya (JP), Madhu, Kamia, Gargi, Flora, Kiran, Amir, Anupam, Rajan for being by my side during smooth and rough phases. Big thanks to all of them for their precious help and much needed advice. Jaspreet, Jai, Pradeep, Rajesh, Neha, Rosaline, Bharti, Naveen have always provided me cheerful company in the lab. Saurav Pathak, though with me for a short time period; will always be part of my fond moments.

My friends Jitendra, Chaitali, Samarпита have always cheered me up. Their company and support was highly valuable during my work.

Special thanks to Shushma ma'am who in spite of the physical distances has always been close to me and kept me energized and always going.

The special care and concern extended to me by Puneet Sir, Yogi Sir, Yash Sir, Khushoo Sir, Neeraj Sir, Saurav Sir, Sujeet Sir is heartily acknowledged. They were not just my seniors but my friends, playmates and source of sustenance. They always inspired me and paved the path for me to aim high.

The friendly environment and help provided by Subhash, Megha, Sheeba, Mohan, Shuchi, Jyotsna, Manpreet, Shivangi, Amit, Tanu, Parul, Kanchan, Manish, Divya, Alli, Gautam, Rajkumar, Sahu, Preeti, Amit, Puneet Prabha, Shivani, Shailesh, Vibhuti, Sunita, Sanjay Sir, Swapnil, Rajni, Manish, Neida made my working tasks easier.

My hostel friends, especially Imam, Vishal, Rakesh Sir, Abhay Sir, Bipul, Sangeet, Monu, Yogesh, Anil, Nipun, Rajkumar, Ravinder, Asim, Aditya, Padmesh, Alok provided me with a home away from home atmosphere and made living during this distant journey much easier. Dhabagiri, midnight B'day celebration, hostel nites and other times spent with them will always be part of my cherished memories.

Big thanks to G9, for their company in JNU during my initial phase.

My outside-campus friends especially Jitender, Sandeep, Anuraag, Pankaj, Manish, Amit, Shagufta, Pooja ma'am, Sunman, Richesh ji are acknowledged for their constant and timely help, support and inspiration.

Anil ji, Rajesh, Sanjay deserve special thanks for keeping the lab clean and organized, and helping with daily lab chores. Help extended by Naipal ji, Sindhu ma'am, Yadav ji, and Sajjan Bhaiya on numerous occasions is duly acknowledged. I acknowledge the cooperation of the office staff Tyagi Sir, Manuj Sir, Tewari ji, Neena Ma'am, Vedpal ji, Sachdeva ma'am, Dilbagh ji, Ajay and lab attendants. Umesh ji, Ghanshyam ji, Amresh ji, and Taposh have been helpful, time and again. I also sincerely thank Rajesh Bhaiya for refreshing doodh-patti and samosas.

To everybody that has been a part of my life but I failed to mention, thank you very much.

I am short of words in expressing my acknowledgement and gratitude to Manpreet for her endless patience, care and encouragement throughout this entire journey. She is gem of a person and a true friend. Without her, I would have struggled to find the inspiration and motivation needed to complete this work. "You are the best girl I have ever met"!

The unconditional love and support provided by Jija Ji, Didi, Bhaiya and Bhabhi deserve special mention. I am indebted to them for all their sacrifices and for creating an environment in which following this path seemed so natural. My beloved nieces and nephew - Aditi, Khushboo, Anuja, Stuti and Ashu deserve special mention here whose love and care has always made my life beautiful, great and a lot easier than it would have been.

Above all, I am forever indebted to the- two most important persons in my life, my parents. Their love and support in all that I have done until now are the keys of all my achievements. This thesis is dedicated to them.

Anuj

LIST OF ABBREVIATIONS

%	Percentage
β ME	Beta mercaptoethanol
μg	Microgram
μl	Microliter
μM	Micromolar
μCi	Microcurie
~	Approximately
A ₂₆₀	Absorbance at 260 nm
A ₂₈₀	Absorbance at 280 nm
A ₆₀₀	Absorbance at 600 nm.
Ab	Antibody
Amp	Ampicillin
AP	Alkaline phosphatase
APS	Ammonium persulphate
ATCC	American type culture collection
ATP	Adenosine Triphosphate
BCIP	5-bromo-4-chloro-3-indolyl phosphate
bp	Base pair
BSA	Bovine Serum Albumin
Ci	Curie
cpm	Counts per minute
C-terminal	Carboxy terminal
ddH ₂ O	Double distilled water
ddNTP	Di-deoxyribose nucleotide triphosphate
DMEM	Dulbecco's modified Eagle medium
DMF	Dimethylformamide.
DNA/RNA	Deoxyribose/Ribose nucleic acid
dNTP	Deoxyribose nucleotide triphosphate
ds	Double stranded
DTT	Dithiothreitol

EDTA	Ethylene diamine tetracetic acid
ELISA	Enzyme Linked Immuno Sorbent Assay
EtBr	Ethidium Bromide
FCS/FBS	Fetal calf/bovine serum
fmole	Femtomole
g	Gravitational force
Gms (gm)	Grams
HEPES	N-2-hydroxyethylpiperzine-N-2 ethane sulphonic acid
hr/hrs	Hour/hours
IPTG	Isopropyl- β -D-thio-galactopyranoside
kb	Kilo base
kDa	Kilo Dalton
LB	Luria Bertani medium
M	Molarity
mCi	Milli Curie
mg	Milligram
MG-132	Z-Leu-Leu-Leu-CHO
min/mins	Minute/Minutes
ml	Millilitres
mM	Milli Molar
mRNA	Messenger RNA
MT(Mt)	Mutant
MTT	3-(4,5-dimethylthiazol-2-yl)-5-diphenyltetrazolium bromide
N-terminal	Amino-Terminal
N	Normality
NBT	Nitro blue tetrazolium chloride
NCCS	National Centre for Cell Science
ng	Nanogram
Ni ²⁺ -NTA	Nickel-nitrilotriacetic acid
O/N	Overnight
°C	Degree celsius
OD	Optical Density

PAGE	Poly Acrylamide Gel Electrophoresis
PBS	Phosphate Buffer Saline
PCR	Polymerase chain reaction
PMSF	Phenyl Methyl sulfonyl fluoride
PNK	Polynucleotide kinase
RNase	Ribonuclease
rpm	Revolution per minute
RT	Room Temperature
SDS	Sodium Dodecyl Sulphate
SDS-PAGE	Sodium Dodecyl Sulphate- Poly Acrylamide Gel Electrophoresis
sec	Seconds
T4	T4 bacteriophage
TAE	Tris acetate EDTA
TBE	Tris-borate EDTA
TBS	Tris buffered Saline with Tween 20
TE	Tris-EDTA
TEMED	N, N, N', N', tetramethyl ethylene diamine
Tris.	Tris (hydroxymethyl) amino acid
U	Unit(s)
UV	Ultra Violet
WT	Wild-type
xg	Times gravity (centrifugal force)

TABLE OF CONTENTS

1. INTRODUCTION	1-21
○ p53 TUMOR SUPPRESSOR PROTEIN	1
○ p53 FUNCTION	1
• Cell Cycle Arrest	2
• DNA Repair	2
• Apoptosis	3
• Angiogenesis, Antioxidant Activity and Metabolism	5
○ REGULATION OF p53 TRANSCRIPTION FUNCTION	6
○ p53 STRUCTURE	8
• p53 Gene Structure and Organization	8
• p53 Promoter, Expression and Auto-regulation	9
• p53 Protein Structure	11
▪ p53-N-terminus (Amino-terminus Domain)	12
▪ p53 Central Core (DNA-Binding Domain)	12
▪ p53 C-terminus (Carboxy-terminus Domain)	14
○ p53 CONFORMATION	15
• Importance in Stabilization, DNA binding and Sub-cellular localization	15
○ p53-NTD (AMINO-TERMINUS DOMAIN)	17
• Role in p53 Activation and Stabilization: Post-translational Modifications at N-terminus	17
• Role in Stabilization and Regulation of p53 Activity	19
○ Aims and Objectives	20
2. MATERIAL AND METHODS	22-43
○ MATERIALS	22
• Chemicals	22
• Enzymes, Reagents and Antibodies	23
• Bacterial strains and Bacterial expression vectors	23
• Cell culture reagents, cell lines and mammalian expression vectors	23
• ELISA plates	24
○ METHODS	26
• Maintenance of mammalian cell lines and cell culture	26
• Preservation of cell lines/ Freeze down preparation	26
• Revival of cell lines	26
• Transient transfection and heat shock treatment	27
• Stable Transfection/Generation of cell lines expressing HA-NTD125	28
• Preparation of nuclear proteins extract and whole cell lysate	28
• Immunofluorescence staining	29
• Western blotting	30
• Immunoprecipitation and co-immunoprecipitation assay	30
• Two Site-ELISA (<i>in vivo</i> ELISA) from Cell lysate	31
• Luciferase assay	31

• Chromatin Immunoprecipitation (ChIP) Assay	32
• Silver staining: DNA and proteins	33
▪ <i>Silver staining of native polyacrylamide gels for DNA visualization</i>	33
▪ <i>Silver staining of native polyacrylamide gels for protein visualization</i>	34
• Recombinant protein expression	34
• Purification of protein by Ni ²⁺ - NTA affinity chromatography	34
• Thermal denaturation analysis	35
• <i>In vitro</i> co-immunoprecipitation and protection assay	35
• Polyacrylamide gel electrophoresis: Native and SDS-PAGE	35
▪ <i>Native polyacrylamide gel</i>	35
▪ <i>SDS-polyacrylamide gel</i>	36
• Coomassie Blue staining	36
• Kination and purification of oligonucleotides	36
• Electrophoretic Mobility Shift Assay (EMSA)	37
• Bacterial Cultures	38
• Preparation of Competent Cells	38
• Determination of competency	38
• Transformation	38
• Plasmid DNA Isolation	39
▪ <i>Mini-Prep</i>	39
▪ <i>Midi-Prep</i>	39
• Agarose gel electrophoresis and DNA quantitation	40
• DNA elution from agarose gels	40
• DNA elution from polyacrylamide gels	41
• PCR amplification	41
• Restriction enzyme digestion of DNA	42
• Ligation	43
3. RESULTS	44-85
○ NTD125 is natively unfolded and highly thermostable	44
○ NTD125 interacts with WT p53 <i>in vitro</i>	47
○ NTD125 protects and restores wild type conformation of p53 <i>in vitro</i>	49
○ NTD125 protects and restores p53 DNA binding activity <i>in vitro</i>	52
○ Cloning of NTD125, NTD93, NTD61 and NTD55 cDNA in pNHA1 vector	60
○ NTD125 interacts with p53 in cell	62
○ NTD125 also protects wild type conformation of endogenous p53 in cell	63
○ NTD125 stabilizes p53 [*] protein levels and quenches MDM2	67
○ NTD125 localizes in the nucleus	69
○ NTD125 activates p53 gene transcription	71
○ NTD125 induces apoptosis in KB cells	78
○ NTD125 affects the gene expression profile of stably expressing NTD125 KB cells (KB-125)	80
4. DISCUSSION	86-95
5. BIBLIOGRAPHY	96-111
6. APPENDIX	
7. PUBLICATIONS	

Introduction

p53 TUMOR SUPPRESSOR PROTEIN

p53 is a phospho-nuclear protein that functions as a transcriptional factor and found inactive in more than half of human cancers. Importance of p53 in the cellular system can be estimated by the fact that since 1990, on an average every month a new protein is reported to interact with p53 and every week a new transcriptional target is added to the list. It is regarded as “Cellular Gatekeeper” and “Guardian of the Genome” due to its extensive role in cell cycle control and DNA damage repair (Lane, 1992; Levine, 1997). p53 is an extraordinary protein whose activities lie at the heart of a remarkable number of basic cellular processes. Activated p53 results in DNA repair, cell cycle arrest and apoptosis by targeting the genes involved in the process (Levine, 2006). p53 transactivates genes by actively binding to its response elements (RE) in the promoter of related genes, simultaneously p53 also auto-regulates its own expression (Wang and El-Deiry, 2006). In 1979, p53 was first identified as a simian virus 40 (SV40) large T antigen interacting protein. This 53-kDa protein was immunoprecipitated from SV40-transformed mouse cell lysate and from uninfected mouse embryonal carcinoma cells using anti-large T serum isolated from rabbits, hamsters, mice and monkeys (Chang *et al.*, 1979; Kress *et al.*, 1979; Lane and Crawford, 1979; Linzer and Levine, 1979). It was initially considered as an oncogene. By early 1990's, studies established p53 as a tumour suppressor gene rather than an oncogene (Finlay *et al.*, 1989).

p53 FUNCTION

p53 is maintained at low levels in normal growing cells but in response to cellular stress it gets stabilized, activated and regulates signal transduction pathways of variety of genes and proteins to deal with the stress aptly. Largely, activated WT p53 suppresses the tumorigenesis by transcriptionally regulating the target genes. p53 pathways are activated by many different types of cellular stress including (but not limited to) DNA damage, oncogene activation, hypoxia, heat shock and glucose starvation (Pluquet and Hainaut, 2001; Levine *et al.*, 2006). Activated p53 binds in a sequence-specific manner to regions of DNA containing p53 consensus binding sites in different target genes to overcome the stress (Kern *et al.*, 1991; El-Deiry *et al.*, 1992). The products of target genes cover a wide range of functions,

and result in several distinct cellular outcomes; mainly cell cycle arrest, apoptosis and DNA repair (Levine *et al.*, 2006).

Cell Cycle Arrest

p53 functions to check the cell cycle if the DNA is damaged and requires repair. Key players in p53-mediated cell cycle arrest include p21, 14-3-3 σ , pRb, BTG-2 and MCG10. p21 also known as cyclin-dependent kinase (Cdk)-interacting protein (Cip1) or wild-type p53-activated fragment 1 (WAF1) was identified as a WT p53 inducible gene (Harper *et al.*, 1993; El-Deiry *et al.*, 1993). p21 interacts with Cdk2/CDK4 and hinders their kinase activity; it also inhibits the phosphorylation of retinoblastoma protein (Rb) through cyclin-Cdk complexes involved in the G1-S transition of the cell cycle (Harper *et al.*, 1993). p21 was found to inhibit cell growth of cancer cells and facilitated p53-mediated G1-arrest (El-Deiry *et al.*, 1993). Using serial analysis of gene expression (SAGE) to compare genes upregulated in colorectal cancer cells in response to ionizing radiation (IR), 14-3-3 σ was identified as p53 induced gene (Hermeking *et al.*, 1997). Over-expression of 14-3-3 σ causes a G2/M arrest in multiple cell lines (Hermeking *et al.*, 1997) and mediates G2/M arrest by sequestering cell division cycle 2 (Cdc2)-cyclin B1 complexes in response to DNA damage (Chan *et al.*, 1999). The Growth Arrest and DNA Damage gene (GADD45) plays a role in checking genomic stability by arresting cells at G2/M checkpoint in p53 dependent manner (Wang *et al.*, 1999). WT p53-Induced Phosphatase Gene (WIP1) arrests cells in G1 on exposure to ionizing radiation in p53 regulated manner (Fiscella *et al.*, 1997). p53 also regulates Cyclin D1; several findings are consistent with a model in which cyclin D1 serves as a key sensor and integrator of extracellular signals of cells in early to mid-G1 phase in p53 dependent manner. The abundance of cyclin D1 is induced by growth factors including epithelial growth factor and IGF-I (Fu *et al.*, 2004). Some other p53 regulated genes such as BTG2 (inhibits cyclin E1) (Rouault *et al.*, 1996) and MCG10 (Zhu and Chen, 2000) also contribute to the p53 dependent G1 block.

DNA Repair

DNA repair is the primary aim of p53 during damage induced cell cycle arrest.

Prime p53 target genes involved in DNA repair are p48 (DDB2/XPE) (Hwang *et al.*, 1999), XPC (Adimoolam and Ford, 2002) and p53-inducible ribonucleotide reductase small subunit 2 (p53R2) homologue (Tanaka *et al.*, 2000). p48 plays a role in nucleotide excision repair (NER) and aids in the removal of lesions in DNA caused by UV. p48 gets upregulated in response to UV in cells containing WT p53 but not in cells deficient of p53. Further, a p53 consensus binding site was identified in the 5' untranslated region (UTR) of the p48 gene (Tan and Chu, 2002). p53 protein induces DNA polymerase-eta (η) (Liu and Chen, 2006) which assists DNA repair at the replication fork. WT p53 can also inhibit processes that involve homologous recombination, not only through activity modulation owing to the direct binding to factors such as RPA, RAD51, WRN and BLM, but also through the transcription of RAD51 (Arias-Lopez *et al.*, 2006), WRN (Yamabe *et al.*, 1998) and Rec Q4 (Sengupta *et al.*, 2005) genes. The cells lacking functional p53 exhibited defective repair of UV damage and were more sensitive to UV irradiation than those having WT p53 (Smith *et al.*, 1995; Ford and Hanawalt, 1995; Havre *et al.*, 1995; Cistulli and Kaufman, 1998; El-Mahdy *et al.*, 2000; McKay *et al.*, 2000). Several groups concluded that p53 played a role in DNA repair of UV damage by the nucleotide excision repair (NER) pathway (Levine, 1997). Certain factors of the DNA mismatch repair, such as MSH2, PCNA (Scherer *et al.*, 2000), MLH1 (Xu and Morris, 1999) and PMS2 (Shimodaira *et al.*, 2003; Chen and Sadowski, 2005) are also encoded by p53-inducible genes. Furthermore, p53 induces the p53R2 gene, which is important for maintenance of nucleotide pools during the DNA repair (Kimura *et al.*, 2003). Upregulation of p53R2 enables a dNTP supply to be available for DNA repair in response to damage.

Apoptosis

Apoptosis is genetically programmed cell death that plays role in tissue development, homeostasis and diseases (Danial and Korsmeyer, 2004; Braithwaite *et al.*, 2005). p53 stimulates a wide network of apoptotic signals that act through two key pathways: i) extrinsic pathway and ii) intrinsic pathway. p53 target genes have been identified in both extrinsic and intrinsic pathways. The extrinsic death receptor pathway involves binding of death ligands to death receptors triggering

the activation of caspase cascade resulting in cell death. p53 can activate the apoptosis through induction of genes encoding trans-membrane proteins. Fas/APO-1 (also known as CD95) is a member of the tumor necrosis factor receptor (TNFR) super-family (Nagata and Golstein, 1995). Upon binding of ligand (TNF) to the receptor (TNFR1), it activates and recruits adaptor molecules like TNFR1-associated (TRADD) death domain and FAS-associated death domain (FADD), which further employ and activate procaspase-8. Procaspase-8 subsequently triggers the executioner caspases that modulate apoptosis (Ashkenazi and Dixit, 1998). Further studies in cancer cell lines treated with chemotherapeutic agents, showed an increase in apoptosis through higher cell-surface expression of the Fas/APO-1. Activation of receptor was found to be WT p53 dependent (Muller *et al.*, 1998). KILLER/DR5 (also called APO-2), a member of the TNF-related apoptosis inducing ligand (TRAIL) family of death receptors, was also hypothesized to be a potential p53 target gene. It expresses in response to DNA damaging agents in the presence of WT p53 and promotes cell death through caspase 8 (Ashkenazi and Dixit, 1998). Along with the expression of p53 by adenovirus in p53 null cancer cell lines, it resulted in up-regulation of KILLER/DR5 (Wu *et al.*, 1997), through p53 consensus binding site in the first intron of the KILLER/DR5 gene (Takimoto and El-Deiry, 2000). Another very important apoptotic gene - p53 apoptosis effector related to PMP-22 (PERP) is a putative tetraspan transmembrane protein that represents a new member of the PMP-22/gas family of proteins engaged in cell growth regulation. Induction of PERP in response to DNA damage and presence of p53 response element in PERP promoter supports its role in apoptosis in p53 dependent manner. Further high levels of PERP mRNA in apoptotic cells in comparison to arresting cells confirm its direct involvement in the process; however, mechanism of action remains to be explored (Attardi *et al.*, 2000).

The intrinsic (mitochondrial) pathway is dominated by the Bcl-2 family of proteins, which governs the release of cytochrome c (Cyt c) from the mitochondria (Cory and Adams, 2002; Kuwana *et al.*, 2002). The pathway shifts the balance in the Bcl-2 family from anti-apoptotic (pro-survival) towards the pro-apoptotic members. Bax (Miyashita and Reed, 1995), Noxa (Oda *et al.*, 2000), Puma (Yu *et al.*, 2001; Nakano and Vousden, 2001), BID (Sax *et al.*, 2002),

APAF-1 (Moroni *et al.*, 2001), p53AIP-1 (Oda *et al.*, 2000) are few examples among the numerous pro-apoptotic genes targeted by p53 (presence of p53 binding consensus site in promoter), which are involved in intrinsic pathways. Bax, NOXA, Puma are members of the Bcl-2 family. Bax forms homodimers and heterodimers with Bcl-2 and Bcl-XL anti-apoptotic proteins, and releases Cyt c from the mitochondria (Skulachev, 1998), which results in caspase-9 activation (Adams and Cory, 1998). PUMA and Noxa are BH3-only members of the Bcl-2 family those are able to bind and inhibit anti-apoptotic Bcl-2 members in the mitochondria. This inhibition results in the release of Cyt c leading to apoptosis (Oda *et al.*, 2000; Yu *et al.*, 2001; Nakano and Vousden, 2001). The PUMA gene is directly induced by p53 in response to DNA damage. A vital balance between PUMA and p21 determines the onset of arrest or death, in response to exogenous p53 expression and hypoxia in human colorectal cancer cells. PUMA expression promotes mitochondrial translocation and multimerization of Bax culminating in induction of apoptosis (Yu *et al.*, 2003). Another p53-targeted gene Noxa contains a single p53 response element and is induced in response to X-ray irradiation (Oda *et al.*, 2000). Since, Noxa also encodes BH-3 domain, it is also considered to function in a manner similar to PUMA and Bax, although its mechanism is not yet determined. p53 also induces APAF-1, which is required for stress-induced p53-dependent apoptosis of fibroblasts and for induction of apoptosis by Myc in which caspase-9 is an essential downstream component (Soengas *et al.*, 1999). Interestingly, p53 also boosts the activation of caspase cascade in both transcription-dependent and independent manner.

Angiogenesis, Antioxidant Activity and Metabolism

Besides, cell cycle arrest, DNA repair and apoptosis, p53 is also involved in cellular processes like angiogenesis, metabolism and antioxidant function, which are equally important during cancer progression. p53-regulated genes include angiogenesis inhibitor thrombospondin (TSP-1) (Dameron *et al.*, 1994), GD-AIF (Van Meir *et al.*, 1994), BAI1 (Nishimori *et al.*, 1997), inhibitors of tumor invasion and metastasis KAI1 (Mashimo *et al.*, 1998), collagenase MMP2 (Bian and Sun, 1997), MASPIN (Zou *et al.*, 2000), an inhibitor of the plasminogen activator protein PAI-1 (Kunz *et al.*, 1995) and several secreting protein factors, which hinder proliferation of exposed cells (Komarova *et al.*, 1998). In addition,

p53-induced not only genes, which elevate intracellular levels of ROS but also a group of genes that encode a set of antioxidant proteins; e.g. glutathione peroxidases Gpx1 (Hussain *et al.*, 2004), Gpx2 (Yan and Chen, 2006), superoxide dismutase Sod2 (Hussain *et al.*, 2004), aldehyde dehydrogenase Aldh4A1 (Yoon *et al.*, 2004), and two members of the sestrin family PA26 (Sesn1) (Velasco-Miguel *et al.*, 1999) and Hi95 (Sesn2) (Budanov *et al.*, 2004). Therefore, the antioxidant function of p53 is one of the most important components of its suppressor activity that prevents tumor formation. p53 also induces transcription of the synthesis of Cyt c oxidase homologue 2 (SCO2) gene, which encodes a protein factor required for the assembly of mitochondrial respiratory complex Cyclooxygenase II (COXII) (Matoba *et al.*, 2006). Another p53-regulated gene TIGAR is important for the regulation of the glycolytic pathway. The gene encodes a protein that is homologous to phosphofructokinase, the glycolytic enzyme converting glucose-6-phosphate to fructose-2, 6-biphosphate (Bensaad *et al.*, 2006). Relative deficit of NAD(P)H and the increased ROS, along with the enhanced glycolysis and reduced respiration represent common consequences of the p53 deficiency (Bensaad and Vousden, 2007).

p53 plays a central role and controls a number of downstream targets in a synchronized manner against stress. For example, when a cell undergoes DNA damage stress, p53 arrests the cell in undergoing phase and activates the genes involved in repair, but if the damage is non-repairable it can lead to apoptosis thus getting rid of the diseased cell. Hence, p53 maintain the cellular integrity. Any error in p53 and downstream process can lead to defective growth resulting in diseased condition.

REGULATION OF p53 TRANSCRIPTION FUNCTION

WT p53 is a sequence-specific DNA-binding protein that can activate transcription of genes containing p53 response elements both *in vitro* and *in vivo* (El-Deiry, 1998). The consensus sequence of a p53 Response Element (RE) consists of two copies of a degenerate 10-bp motif of palindromic DNA sequence, 5'-RRRCW(A/T)W(T/A)GYYY-3' with a spacer of up to 13 bps (El-Deiry *et al.*, 1992; Funk *et al.*, 1992). p53 binds to its consensus site as a tetramer and the

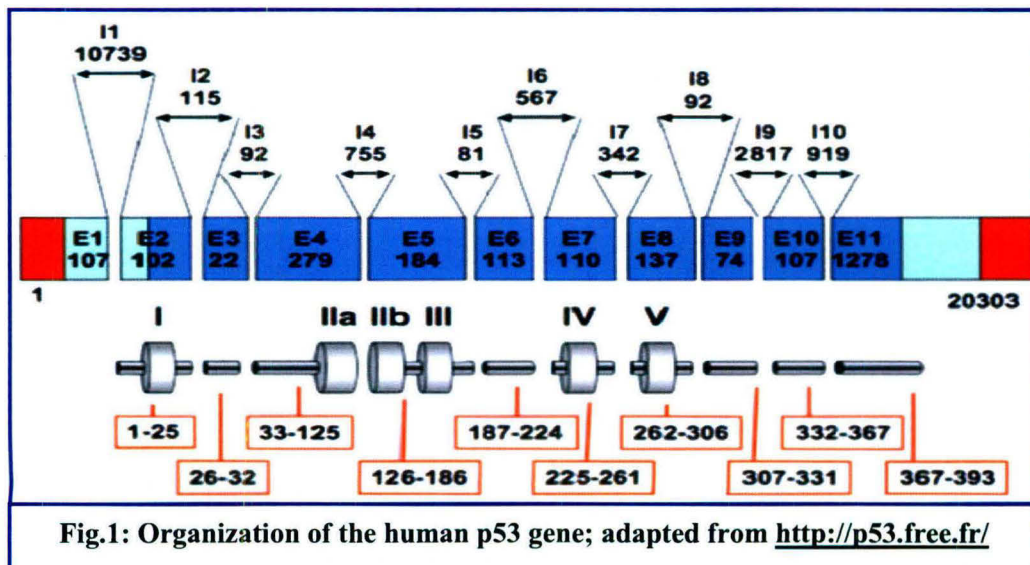
binding of p53 to its DNA-binding site (DBS) *in vivo* may significantly vary from *in vitro* binding that depends on factors like length of consensus sequence, length and sequence of spacer region and co-factors. GADD45 (Kastan *et al.*, 1992), p21 (El-Deiry *et al.*, 1993), MDM2 (Momand *et al.*, 1992; Wu *et al.*, 1993), Cyclin D (Okamoto and Beach, 1994), Bax (Miyashita and Reed, 1995), IGF-BP3 (Buckbinder *et al.*, 1995), PIG-3 (Polyak *et al.*, 1997) and 14-3-3 σ (Hermeking *et al.*, 1997) genes are amongst the earlier identified genes, which contain p53 response elements in their respective promoters and are activated by induction of p53. Later, a computer based programme screened ~2600 human genes and ~1700 mouse orthologs, having putative p53 response elements through the human and mouse genome, respectively (Hoh *et al.*, 2002). Further, out of over half a million paired-end ditag (PET) sequence, Wei *et al.* characterized 65,572 unique p53 ChIP DNA fragments and established overlapping PET clusters; thus identified at least 542 binding loci with redefined consensus p53 binding motif through human genome and discovered 98 previously unidentified p53 target genes (Wei *et al.*, 2006). Recently, Roblick *et al.* identified 55 new p53 responsive genes and highlighted the role of transcription-independent effect for the p53-induced biological response (Rahman-Roblick *et al.*, 2007). Even though the number of p53-targeted genes is increasing day by day, it remains unclear what mechanism(s) direct the *in vivo* selectivity to different sites. In a recent review on mechanisms of regulatory diversity within the p53 transcriptional network, Espinosa proposed two alternative models to explain how this regulatory diversity is achieved: i) **The Selective Binding Model**: to bind or not to bind? and ii) **The Selective Context Model**: life (and death) after DNA binding (Espinosa, 2008). The study of kinetics of p53 binding to target gene promoter shows differential selection to relevant sites. Increased expression of genes was observed in the case of higher affinity RE while in case of low affinity RE; although binding is there still the expression is delayed (Szak *et al.*, 2001). Specific p53 mutations might lead to define changes in the transactivation pattern that are compatible or advantageous during tumorigenesis and could be selected in particular cellular and genetic environments (Inga *et al.*, 2002). A systematic study of known and potential p53 DBSs shows that p53 efficiently utilizes the DBS of MDM2, and of genes connected to cell cycle arrest, DNA repair and the death receptor pathway

of apoptosis; however p53 was unable to utilize two-third of the isolated DBS of the apoptosis-related genes (Qian *et al.*, 2002). Thus, a major regulation of p53 activity occurs at the level of p53 DBS themselves. A sequence analysis of p53 response-elements suggests multiple binding modes of the p53 tetramer to DNA targets (Ma *et al.*, 2007). While, the symmetries in the p53 response-element encode binding modes for the p53 tetramer to recognize DNA, here inverse repeat p53 REs favor the H14 mode. Direct repeat p53 REs may have high possibilities of other modes (Ma and Levine, 2007). The difference in affinity typically observed is so great that it can be easily detected with Chromatin-immunoprecipitation (ChIP) assay. This is more reliable and sensitive than the band shift assay, which can not scrutinize a key property of nuclear environment that overcomes the inhibitory effects of the p53 basic domain *in vivo*. ChIP based screening was successfully employed to identify p53 transcription factor binding sites that links to transcriptionally regulated target genes in the genome (Hearnes *et al.*, 2005).

p53 STRUCTURE

p53 Gene Structure and Organization

The human p53 gene is located on the short arm of seventeenth chromosome 17p13.1 (Benchimol *et al.*, 1985; McBride *et al.*, 1986; Isobe *et al.*, 1986; van Tuinen *et al.*, 1987). Until now, the p53 gene structure is very simple. Around 20,000 bps long p53 gene contains 11 exons and generates a final mRNA of ~2500 bps (Bourdon *et al.*, 2005) that translates into 393 aa long polypeptide (Fig.1).



p53 Promoter, Expression and Auto-regulation

p53 controls a number of proteins at genetic level but the factors, which affect its own transcription, remain a mystery. p53 protein appears to be expressed constitutively at relatively low levels but there are a number of experimental systems in which cellular p53 protein levels change in response to external stimuli. In such systems, p53 protein levels closely parallel the levels of p53 mRNA (Benchimol *et al.*, 1984); raising the possibility, that p53 might be transcriptionally regulated. Reisman *et al.* (1988) characterized the regulatory regions of the human p53 gene using chloramphenicol acetyltransferase (CAT) assay. They identified 2 promoters: the first (hp53P1) is located 100 to 250 bps upstream of the first exon and is responsible for transcription of the major p53 mRNA species. The second (hp53P2) is stronger promoter than the first and is located within the 10,738-bp of first intron, approximately 1,000 bp downstream of exon 1 (Reisman *et al.*, 1988). A 85 base-pair fragment residing within first exon was shown to be required for full promoter activity (Tuck and Crawford, 1989). Like other housekeeping genes, p53 also has a TATA-less promoter (Ozbun and Butel, 1995). Most of the conspicuous effects of p53 are associated with transcription level higher than the basal level. Therefore, we can expect various levels of transcription of p53 corresponding to the different effects (leaving aside the various post-translational modifications which might occur). The findings of the various studies on p53's cellular transcriptional controls are as follows-

- 1) NF- κ B activates p53 binding to its site located +49 to +68 in p53 promoter. NF- κ B induction of p53 may be a mechanism by which cell growth can be stopped so as to repair the damage induced by stress (Wu and Lozano, 1994).
- 2) YY1 and NF1 both activate the human p53 promoter by alternatively binding to a composite element and YY1 and E1A cooperate to amplify p53 promoter activity (Furlong *et al.*, 1996).
- 3) ETS transcription factors (binding site -491 bp to -503 bp) also upregulate p53 (Venanzoni *et al.*, 1996).
- 4) The PAX protein (binding site -7 bp to -12 bp) downregulates p53 (Stuart *et al.*, 1995).

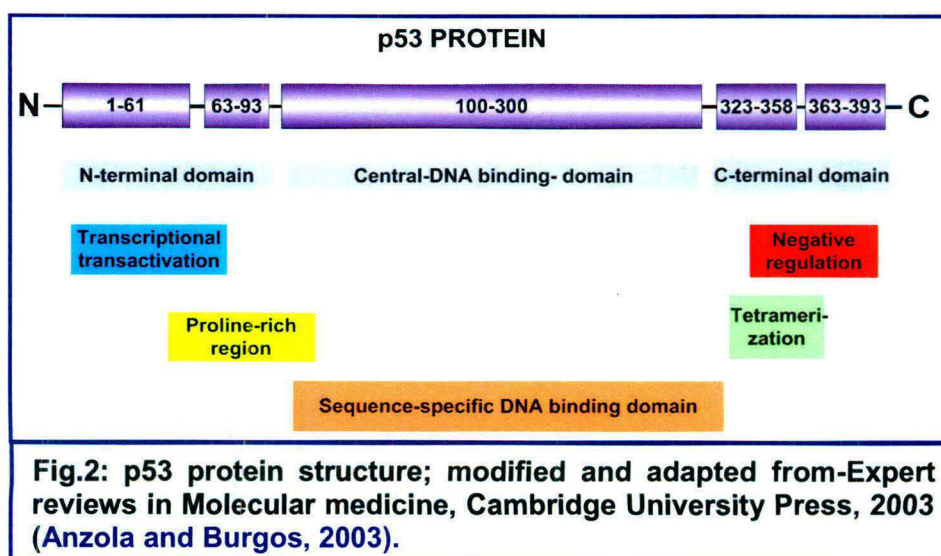
- 5) HOXA5 upregulates p53 promoter through HOX binding sites (Raman *et al.*, 2000).
- 6) BCL6 represses p53 transcription by binding two specific DNA sites within p53 promoter (Phan and Dalla-Favera, 2004).
- 7) C/EBP β -2, which plays a central role in the regulation of p53 transcription during the transition into S phase, binds within a positive *cis*-acting element (-972 to -953). (Boggs and Reisman, 2006; 2007).
- 8) p53 can transactivate endogenous p53 expression by binding to p53 promoter (Wang and El-Deiry *et al.*, 2006).

In spite of these diverse reports, no central regulatory mechanism of p53 gene expression has been proposed so far. In this context, it would be interesting to study p53 regulation in the light of its molecular interactions. The binding of p53 to the cell cycle-arrest gene promoters was found to be 50 times stronger than the pro-apoptotic gene promoters (Weinberg *et al.*, 2005). Thus, a major regulation of p53 activity occurs at the level of p53 DBS itself by posing additional requirement for the successful utilization of apoptosis-related DBS (Qian *et al.*, 2002). How p53 chooses against the response, to be activated is critical in understanding its role as a tumor suppressor. It has become apparent that a number of variables such as co-factor recruitment, post-translational modification, sub-cellular localization of p53, p53-mediated gene activation, differential-binding affinity of p53 for DNA; all play a role in dictating p53 response giving rise to the “p53 smart” model of activation (Vousden, 2000). In fact, multiple interactions with co-activators and co-repressors as well as with the components of the general transcriptional machinery allow p53 to either promote or inhibit transcription of different target genes (Laptenko and Prives, 2006). It has been shown that p53 cancer mutants exhibited differential DNA binding properties and transcriptional activities when tested with several p53 DBS (Campomenosi *et al.*, 2001; Akhaury, 2003). It is also reported that WT p53 may adopt more than one conformation to utilize certain DBS (Halazonetis, 1993), although, DNA conformation is of equal importance for sequence specific binding (Kim *et al.*, 1997). Szak *et al.*, 2001, have demonstrated by gel shift assays that the PIG3 DBS is a low-affinity p53 DBS, as compared to the p21, 5' site and MDM2 DBS.

Although the mechanism(s) behind this role of p53 largely remains unclear, the ability of p53 to distinguish between cell-cycle arrest and apoptosis targets might be due to intrinsic differences in the regulatory regions of these genes; either within the response element itself or in surrounding sequences. p53 promoter itself has three p53 DNA binding sites but their significance in auto-regulation is not well studied. DBS II (Deffie *et al.*, 1993) which constitutes the Class-1 type, where as DBS I (Hudson *et al.*, 1995) and DBS III (Tiwari, 2003, Tripathi *et al.*, 2007) which constitute the Class-2 type showed binding with p53; both *in vitro* and *in vivo*. While role of DBS II in upregulation of p53 expression has been established (Hudson *et al.*, 1995), role of DBS I and DBS III remains unexplored.

p53 Protein Structure

p53 is a 393 amino acids long protein that has a theoretical molecular mass of 43,500 daltons whereas it migrates at 53,000 daltons on SDS-PAGE. It is because p53 is ~40 % intrinsically disordered and shows retarded migration on SDS-PAGE. Out of 393 residues of p53, only residues 100-300 and residues 324-355 are folded (Shakked, 2007). Biophysical studies confer that at the physiological temperature, WT p53 is more than 50 % unfolded due to the presence of large unstructured regions in its N and C-terminus (Bell *et al.*, 2002). Structurally, p53 is composed of several structural and functional domains (Fig. 2). N-terminus (residues 1-100), core domain (residues 101-300) and C-terminus (residues 301-393) are the three main structural domains which may be further divided into various functional domains.



p53-N-terminus (Amino-terminus Domain)

The N-terminal domain (residues 1-100) of p53 is natively unfolded (Bell *et al.*, 2002; Dawson *et al.*, 2003), although a residual secondary structure is observed in regions of functionally important hydrophobic residues (Lee *et al.*, 2000). The first 73 amino acid residues of N-terminus of p53 contain the acidic- transcription activation domain (TAD) (Fields and Jang, 1990). Length of TAD region is described dissimilar by different workers. The TAD is further subdivided into two subdomains- TAD1 (residues 1-40) and TAD2 (residues 40-61) (Chang *et al.*, 1995). Within NTD, and region adjoining to the TAD is referred to the proline-rich domain, which consist of amino acid residues 64-92 and contains five repeats of the sequence PXXP, where P: proline, and X: any amino acid (Walker and Levine, 1996). The proline-rich region of p53 was found to be important for the ability of p53 to induce apoptosis (Sakamuro *et al.*, 1997).

NMR studies on p53 TAD (1-70) also showed that it is largely disordered under physiological conditions. Three small regions within the TAD have been shown to have minimally-structured motifs, a helix and two nascent turns (Lee *et al.*, 2000). A helix formed by residues 18-26 can be most clearly identified and preexists even in the absence of any target protein. This helix coincides with the amphipathic helix that was reported to be induced upon MDM2 binding (Kussie *et al.*, 1996; Botuyan *et al.*, 1997). Recently, two additional mini-motifs (turn I, residues 40-45 and turn II, 49-54) were reported and shown to bind to MDM2 (Chi *et al.*, 2005). In particular, the turn II motif has a higher MDM2-binding affinity than the turn I and targets the same site in MDM2 as the helix. These motifs correspond directly with the RPA-binding helices H1 and H2 of p53 and suggest that this region of p53 may be multifunctional in its ability to interact with multiple protein partners (Bochkareva *et al.*, 2005).

p53 Central Core (DNA-Binding Domain)

Another essential functional domain of p53 is the DNA-Binding Domain (DBD), located in the central region of the p53 protein (amino acids 100-300). p53 Core consists of an immunoglobulin-like β -sandwich that provides the basic scaffold for the DNA-binding surface. This surface can be subdivided into two structural

motifs that bind to the minor groove and major groove of target DNA, respectively (Cho *et al.*, 1994; Joerger and Fersht, 2008). Human p53-DBD is highly unstable and melts at temperature slightly above the body temperature, i.e., 44 °C - 45 °C, which dictates the stability rather the instability of the full length protein (Bullock *et al.*, 2000; Butler and Loh, 2003). By creating mutations in core domain, thermostable p53 variants having a half-life of 100 minutes at 37 °C have been generated (Matsumura and Ellington, 1999). DNA binding domain also contains conserved regions and major mutation hot spot sites (Pavletich *et al.*, 1993). In 1991, p53 was found to have the capability to bind to DNA in a sequence-specific manner (Kern *et al.*, 1991). Soon thereafter, the same group defined the sequence of the p53 consensus-binding site (El-Deiry *et al.*, 1992). p53 was then shown to directly activate transcription through this consensus binding site (Farmer *et al.*, 1992). Later studies proved that p53 requires this sequence-specific transcriptional activity to function as a tumor suppressor (Pietenpol *et al.*, 1994). Important structural information was first obtained by crystallizing p53 with the consensus DNA (Cho *et al.*, 1994). Cho *et al.*, for the first time revealed that the core domain consists of a β -sandwich that serves as a scaffold for two large loops (bind to Zn ion) and a loop-sheet-helix motif (bind to major groove of DNA). As with the N-terminus, proteins that interact with the DBD of p53 can affect the function of p53. The SV40 large T antigen binds to the DBD of p53 to inhibit its function (Tan *et al.*, 1986). The HPV E6 protein also binds to the core domain of p53 to promote its degradation (Li and Coffino, 1996). Two additional cofactors, p53 binding protein 1 (53BP1) and p53 binding protein 2 (53BP2) also interact with the p53 DBD (Iwabuchi *et al.*, 1994; Gorina and Pavletich, 1996). 53BP1 and 2 have the ability to act as transcriptional cofactors and enhance p53 transactivation function (Iwabuchi *et al.*, 1998). Also, heat shock cognate protein 70 (Hsc70) binds to the DBD of p53 mutant proteins containing mutations in residues such as R175 and V143 that alter the structure of the protein (Fourie *et al.*, 1997; Hinds *et al.*, 1990). Such properties of the p53-DBD illustrate its essential role in p53-mediated transcriptional regulation.

p53 C-terminus (Carboxy-terminus Domain)

The C-terminus of p53, amino acid residues 300-393 are also important for several aspects of p53 function and regulation. C-terminal region is subdivided into tetramerization/oligomerization domain (residues 325-356) and extreme C-terminal-regulatory domain (CTD, residues 363-393). Amino acids 300-318 constitute a flexible linker region that connects the central core and the C-terminus of p53 (Cho *et al.*, 1994). When binding to DNA, p53 oligomerizes to form tetramers by means of the oligomerization domain (Wang *et al.*, 1994). As stated, tetramerization is necessary for p53 to proficiently transactivate target genes and suppress growth of cancer cell lines (Pietenpol *et al.*, 1994). Tetramerization domain is also a well structured domain of p53 and forms reversible tetramers of full-length p53 (Sakaguchi *et al.*, 1997; Veprintsev *et al.*, 2006). The tetrameric structure of the domain, as revealed by X-ray crystallography (Jeffrey *et al.*, 1995; Mittl *et al.*, 1998) and in solution by NMR (Clore *et al.*, 1995) is best described as a dimer of primary dimers. The C-terminus of p53 also contains three nuclear localization signals (NLS) spanning residues 316-325, 369-375 and 379-384. Out of which, NLS (316-325) contains the greatest nuclear localization ability and is conserved in several species with best match to the consensus sequence of a typical NLS (Dang and Lee, 1989; Shaulsky *et al.*, 1990). A nuclear export signal (NES) was also identified in the C-terminus of p53, located specifically within the oligomerization domain. It was also proposed that when p53 tetramerizes and binds to DNA, this NES is masked, preventing p53 export from the nucleus (Stommel *et al.*, 1999).

Lastly, extreme carboxy-terminus of p53 (residues 363-393) which comprises a basic domain has the ability to negatively control p53 sequence-specific DNA binding (Hupp *et al.*, 1992; Gu and Roeder, 1997). Single stranded DNA or non-specific DNA binding site also coincides within this region (Selivanova *et al.*, 1996; Kim and Deppert, 2006). Deletion of the C-terminal domain or quenching by the p53 monoclonal antibody PAb421 at the p53 C-terminus counteracts the negative regulation and activates sequence-specific binding by relieving the allosteric inhibition of DNA binding after inducing a conformational change in the protein (Hupp and Lane, 1994). Post-translational modifications in the C-terminus domain also activate sequence-specific DNA binding (Hupp *et al.*, 1992; Hupp *et*

al., 1993; Hupp and Lane, 1994; Appella and Anderson, 2001). In a nutshell, the extreme C-terminus of p53 also plays a regulatory role in several important aspects of p53 function.

p53 CONFORMATION

Importance in Stabilization, DNA binding and Sub-cellular localization

Apart from role of post-translational modifications in stabilization of p53, there is another important factor for the stability of the tumor suppressor function of p53 and that is its conformation. WT p53 is believed to exist in two biological conformations, i) *Active or wild-type* and ii) *Latent or mutant conformation* (Fig. 3). These are recognized with the help of monoclonal antibodies exclusive for

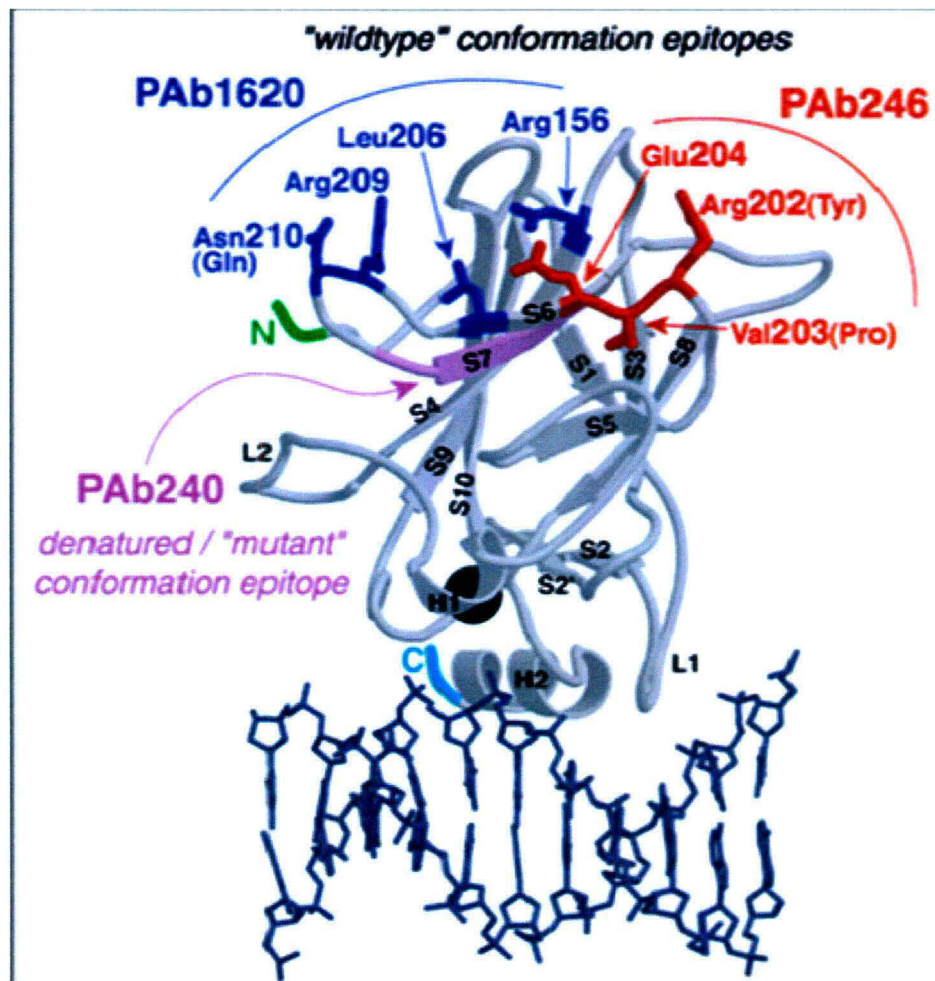


Fig.3: Reprinted by permission from Macmillan Publishers Ltd: [ONCOGENE] (Wang *et al.*, 2001. The 'wildtype' conformation of p53: epitope mapping using hybrid proteins. Vol. 20, 2318-2324), copyright (2001).

target conformation i.e. PAb1620 (human) or PAb246 (mouse), which recognizes wild-type conformation whereas PAb240 binds to mutant conformation (Gannon *et al.*, 1990; Wang *et al.*, 2001). The results of experimental data till date suggest that WT p53 is structurally unstable protein and exists in a state of equilibrium between wild and mutant conformations (Tripathi *et al.*, 2007) and the equilibrium must shift from mutant to wild phenotype during stress to activate p53; either by post-translational modification or through conformational stabilization. Murine fibroblast having genotypically WT p53 showed change from wild type to mutant conformation on serum starvation (Milner and Watson, 1990). Redox regulation of p53 protein conformation has also been noted (Hainaut and Milner, 1993). Hainaut *et al.* later on showed that even in the presence of Cu (II), WT p53 could alter from wild type to mutant conformation (Hainaut *et al.*, 1995).

WT p53 is demonstrated as a cytoplasmic protein in normal cells but it is located in the nucleus in transformed, stressed and actively growing cells (Rotter, 1983; Inoue *et al.*, 2005). Sub-cellular localization is very important for the proper functioning as well as stability of p53 therefore its nucleo-cytoplasmic transport is tightly regulated (Shaulsky *et al.*, 1990; Vousden, 2000) by numerous factors including oligomerization (Stommel *et al.*, 1999), MDM2-interaction (Roth *et al.*, 1998; Tao and Levine, 1999), phosphorylation (Takahashi *et al.*, 1993; Wang and Prives, 1995) and heat shock proteins/chaperones (Zylicz *et al.*, 2001). WT p53 was shown to be in mutant conformation in cytoplasm, genotoxic stress caused p53 to fold into wild conformation, and to concentrate in nucleus suggesting that nuclear translocation of p53 can result in the change in its conformation from mutant to wild type (Gaitonde *et al.*, 2000). Recent studies also showed the localization of (PAb1620+/PAb240-) positive p53 wild phenotype in nucleus and found wild conformation more stable in comparison to cytoplasmic p53 mutant phenotype (PAb1620-/PAb240+) (Nie *et al.*, 2007). Thus, the combined activation of the sequence-specific DNA binding function of p53 by either post-translational modification or conformational modulation decides the sub-cellular localization of p53.

p53-NTD (AMINO-TERMINUS DOMAIN)

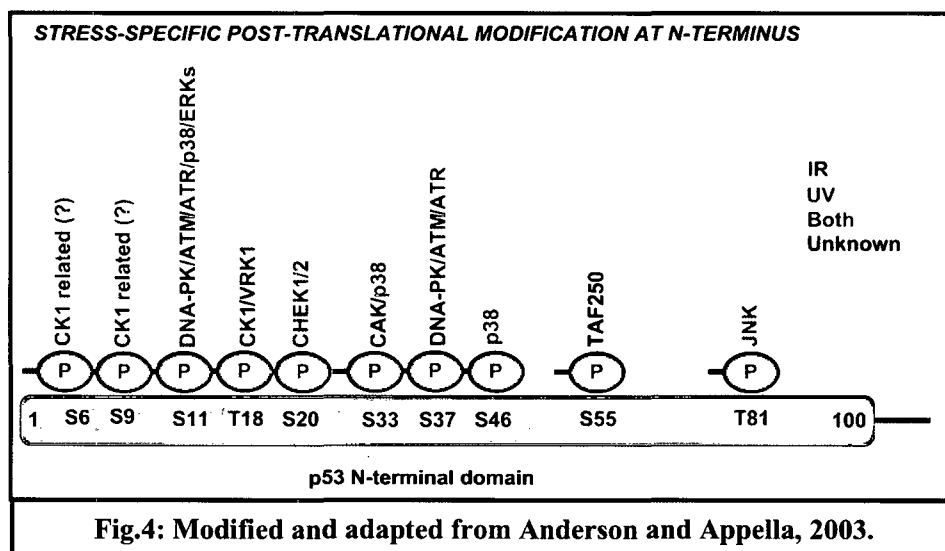
Role in p53 Activation and Stabilization: Post-translational Modifications at N-terminus

Under normal conditions of cellular functioning, p53 protein levels are very low due to its short half-life (Maltzman and Czyzyk, 1984) and rapid turnover mediated through its interaction with MDM2 creating a feed back loop. However, when cells encounter genotoxic stress, the p53 protein is activated because of many different types of post-translational modifications (Appella and Anderson, 2001). Most of them occur at N-terminus.

Phosphorylation is one of the most important modifications of p53 and increases its sequence-specific binding ability (Hupp and Lane, 1994). At amino-terminus of p53, serines (S) 6, 9, 15, 20, 33, 37 and 46 and threonines (T) 18 and 81 are targets of phosphorylation in response to genotoxic stress. Phosphorylation of S15 of p53 contributes to the disruption of the p53/MDM2 complex resulting in the stabilization of p53 protein (Shieh *et al.*, 1997). Zhang and Xiong (2001) reported the presence of another NES in p53 consisting of amino acid residues 11-27 in the N-terminus. Upon phosphorylation of S15 within this region, p53 is no longer exported from the nucleus (Zhang and Xiong, 2001) so activated p53 is maintained within the nucleus. Phosphorylation of p53 at S15 increases the ability of p53 to bind to p300/CBP that acetylates p53 at the C-terminus (Lambert *et al.*, 1998). A few Serine/ Threonine kinases, which phosphorylate at N-terminus are ataxia telangiectasia mutated (ATM), ATM- and Rad3-related (ATR), checkpoint kinases 1 and 2 (Chk1, Chk2), c-jun N-terminal kinase (JNK), casein kinase 1 and 2 (CK1, CK2), protein kinase C (PKC), p38 stress activated kinase and DNA-dependent protein kinase (DNAPK) (Bode and Dong, 2004). Largely, phosphorylation at N-terminus of p53 results in enhanced transcriptional activation ability and stability.

NTD is also the region where many important proteins bind to p53. NTD is important for the ability of p53 to activate transcription; components of the transcription initiation factor IID (TFIID) associate with the N-terminus of p53. Specifically, TATA box binding protein (TBP) (Seto *et al.*, 1992) and TBP-

associated factors (TAFs) - TAFII32 and TAFII70 interact with the N-terminus of p53 (Lu and Levine, 1995; Thut *et al.*, 1995). In addition, cAMP response element-binding protein (CREB)-binding protein (CBP)/p300 complex is known to interact with p53 at its N-terminus. CBP/p300 serves as a transcriptional coactivator and potentiates p53-mediated transcription (Gu *et al.*, 1997; Lill *et al.*, 1997; Avantaggiati *et al.*, 1997). CBP/p300 has histone acetyltransferase (HAT) activity and is able to acetylate histones in regions of transcriptionally active chromatin (Bannister and Kouzarides, 1996; Ogryzko *et al.*, 1996). CBP/p300 and PCAF also acetylate p53, which enhances its sequence specific DNA binding ability in response to DNA damage (Gu and Roeder, 1997, Liu *et al.*, 1999). The adenovirus E1b protein also binds to p53 within N-terminus region and inhibits transcriptional activation function (Kao *et al.*, 1990). One of the most important p53 interacting proteins, which bind to p53 at the N-terminus, is MDM2 (Oliner *et al.*, 1993). MDM2 negatively regulates p53 by associating with the NTD and inhibiting p53 transactivation (Oliner *et al.*, 1993). It also targets p53 for ubiquitination and rapid degradation by the 26S proteasome (Haupt *et al.*, 1997; Kubbutat *et al.*, 1998). Key p53-N-terminal modifications are summarized in Fig. 4.



Role in Stabilization and Regulation of p53 Activity

It has been established that the post-translational modifications at N-terminus play very important role in p53 stability and transactivational activity. Various studies have been carried out in this context to elucidate the role of NTD in regulation of p53 stability, DNA binding activity, and conformation. The first and foremost role of p53-NTD is transactivation (Lin *et al.*, 1994) because the N-terminal truncated isoform of p53 is not only unable to transactivate downstream genes but it also inhibits function of WT p53 through dominant negative effect (Bourdan *et al.*, 2005). However, much remains to be explored. N-terminus was shown to negatively regulate p53 DNA binding activity by dissociating p53-DNA complex *in vitro* (Cain *et al.*, 2000); this activity was higher in bacterially expressed protein in comparison to that of insect cell (post translationally modified). Thus, postulating auto-inhibitory function for NTD that is mechanically different from C-terminus inhibitory function (Cain *et al.*, 2000). Integrity of the NTD is required for proper functioning of WT p53 to cause apoptosis and for mutant p53 to block the drug-induced apoptosis, *in vivo* (Matas *et al.*, 2001). A group studying the allosteric regulation of thermostability and DNA binding activity by specific interacting proteins postulated the role of NTD in conformational regulation of p53 but not in DNA binding activity (Hansen *et al.*, 1996). Further exploration of NTD and utilization of DNA shuffling trick led to identification of 20 amino acid residues in the core (residues 101-120) responsible for the thermostable phenotype (Xirodimas and Lane, 1999). Such mutants were also able to restore PAb1620⁺ conformation of WT p53 at higher temperature. Studying the regulation of wild type murine p53 by ATP and ADP, a putative ATP binding site in NTD (residues 1-67) and a putative ADP binding site in core (residues 98-303) was predicted (Warnock and Raines, 2004). Therefore, it is very important to understand the regulation of p53 conformation, as ultimately p53 transcriptional function is crucial for assessing how the system utilizes the p53 downstream pathways to withstand stress. Recent studies focusing on structural aspect of NTD established its important role in p53 stabilization. Structural determination of NTD by using residual dipolar couplings (RDCs) from NMR spectroscopy and small-angle X-ray scattering (SAXS) revealed that NTD is stiffer in the proline-rich region (64-92), which has a tendency to adopt a polyproline II (PPII) structure and projects TAD away from the core (Wells *et al.*, 2008). RDC data showed that

the isolated NTD of p53 (1-93) is an intrinsically disordered protein (ITP) with two regions of nascent secondary structure (Wells *et al.*, 2008). Further, study showed amyloid formation of TAD (1-63) at acidic pH and amyloid aggregation of whole protein under suitable destabilizing conditions (Rigacci *et al.*, 2008). Cytotoxic nature of these amyloids provides new and important function to NTD.

Structure studies on NTD showed that it is an unstructured or natively unfolded domain of p53. Chaperones also possess almost 40 % of unstructured region and these regions are important for chaperoning activity (Tompa and Csermely, 2004). Small protein chaperones like α -synuclien and α -catenine are few examples which are fully unstructured or less structured proteins and can function as a chaperone (Horwitz, 1992; Park *et al.*, 2002). These small chaperones molecules are very important for cellular processes and any defect in their activity leads to diseases like Parkinson's disease and Alzheimer.

With this background information, we aimed to explore the role of p53-NTD in p53 stabilization and gene activation. Further, we investigated thermostability and the intermolecular interaction between NTD125 and WT p53 both *in vitro* and *in vivo*. Role of NTD125 on p53 thermostability and DNA-binding activity was also probed. Consequences of NTD125 expression in KB cells in relation with p53 were studied and considering the effect of NTD125 on p53 thermostability and gene activation, we postulated that NTD125 possess chaperone like activity. In view of this, following were the main aims and objectives of the study undertaken:

Aims and Objectives-

- ❖ To study the *in vitro* thermostability of NTD125 and its interaction with WT p53.
- ❖ To study the effect of NTD125 on WT p53 conformation at physiologically higher temperatures and on p53 DNA binding activity, *in vitro*.
- ❖ To assess the sub-cellular localization of exogenously transfected HA-tagged-NTD125 in KB cells.

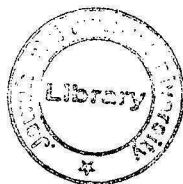
- ❖ To investigate the interaction of NTD125 and p53 in cellular system and consequences of interaction of p53 conformational modulation and cellular localization.
- ❖ To investigate the role of NTD125 in p53 mediated transcriptional regulation of p53 gene.
- ❖ To investigate the outcome of NTD125 regulated (stabilized), highly expressed WT p53 in the system.
- ❖ To examine the gene expression profile of stably expressing NTD125 in KB cells.

TH-16347

572.86

Sh233

T_r.



*Materials
&
Methods*

MATERIALS

Chemicals:

Ammonium Persulphate, Ampicillin, Aprotinin, 5-Bromo 4-Chloro 3-Indolyl Phosphate (BCIP), Boric Acid, Bovine Serum Albumin, Bromophenol Blue, Calcium Chloride, Cellulose Phosphate, Chloroform, Citric Acid, Coomassie Brilliant Blue, Dithiothreitol, Ethidium Bromide, Ethylene Diamine Tetracetic Acid (EDTA), Ficoll, Formaldehyde, Glacial Acetic acid, Glutathione Sepharose, Glycine, Glycerol, Guanidium Hydrochloride, HEPES, Imidazole Hydrochloride, Isoamyl Alcohol, Isopropyl Alcohol, Kanamycin, Leupeptin, Magnesium chloride, Methanol, Nitro Blue Tetrazolium Chloride (NBT), N, N, N', N'-Tetramethyl-Ethylenediamine (TEMED), Ni²⁺-NTA, Nonidet P-40 (NP-40), Phenol, Phenyl Methyl Sulphonyl Fluoride (PMSF), Polyvinyl Pyrrolidone, poly (dI-dC), p-Nitrophenyl Phosphate (PNPP), Potassium Dihydrogen Phosphate, Potassium Acetate, Potassium Chloride, Protein A Sepharose, Reduced Glutathione, Salmon Sperm DNA, Sigmacote, Sodium Acetate, Sodium Azide, Sodium Chloride, Sodium Deoxycholate, Sodium Dihydrogen Phosphate, Sodium Hydrogen Diphosphate, Sodium dodecyl (lauryl) sulphate, Sodium hydroxide, Sodium pyruvate, Tris-Base (Trizma Base), Triton X-100, Tween-20, Trypsin Inhibitor, Xylene Cyanol, Yeast Extract, β -mercaptomethanol and other chemicals were purchased from Sigma Chemical Company, USA, GE Healthcare, UK and Calbiochem, USA. Absolute alcohol was purchased from E. Merck, Germany. Acrylamide, Agarose, Bis-Acrylamide, Luria Bertani (LB) medium, Luria Bertani Agar, Sephadex G-50 were obtained from GE Healthcare, UK. Concentrated Hydrochloric acid, Concentrated Sulphuric acid, Concentrated Nitric acid, Glucose, Nickel Chloride, Nickel Sulphate, Potassium dichromate, Silver nitrate, Sodium bicarbonate, Sodium carbonate and Sodium thiosulphate were purchased from Qualigens Chemicals, India. Bradford reagent for protein quantitation was obtained from Bio-Rad, USA. Nitrocellulose membrane was purchased from Bio-Rad and Millipore, USA. Dialysis tubing was procured from Sigma-Aldrich, USA. Radioactive chemicals γ -³²P-ATP was purchased from Board of Radiation and Isotope Technology (BRIT), Jonaki, Hyderabad, India. X ray films, Fixer and Developer used for autoradiography were from Kodak, USA.

Enzymes, Reagents and Antibodies:

RNase A, T4 DNA ligase and T4 polynucleotide kinase were purchased from New England Biolabs (USA), Restriction Endonucleases *Bam*HI, *Eco*RI, *Kpn*I, *Bgl*II, *Xba*I and GFX mini-preparation kit for plasmid DNA isolation were purchased from GE Healthcare, UK. *Nhe*I and *Taq* DNA polymerase were purchased from Bangalore Genei India. *Pfu* DNA polymerase was purchased from Fermentas, USA. All the oligonucleotides used were obtained from Microsynth, Switzerland, Sigma Genosys, USA and Ocimum Biosolutions, Hyderabad. Enterokinase enzyme, midi and maxi prep plasmid DNA isolation kits, and agarose gel elution kit were purchased from Novagen, USA and Qiagen, Germany. Anti-p53 antibodies (PAb1801, PAb421, PAb1620 and PAb240) were purchased from Calbiochem, USA. Anti-GST anti-His, PAbFL-393, PAb C-19, anti-MDM2, anti-CHIP primary antibodies, anti-Mouse, anti-Rabbit and anti-Goat secondary antibodies (AP-conjugated), were purchased from Santa-Cruz, Biotechnology USA. FITC-conjugated anti-Mouse secondary antibodies was purchased from Sigma-Aldrich, USA.

Bacterial strains and Bacterial expression vectors:

Escherichia coli DH5 α strain was used for transforming the ligated product in the cloning experiments and for plasmid DNA preparation, whereas *E. coli* BL-21 (DE-3) strain was used for the over-expression of the recombinant protein. pET21c, pET28a and pET32a vectors (Novagen, USA) were used for preparing proteins with 6X-His tag, and pGEX-4T-1 (GE Healthcare, UK) vector system was used for preparing proteins with GST-tag.

Cell culture reagents, cell lines and mammalian expression vectors:

Dulbecco's Modified Eagle Media (DMEM), Penstrep (Mixture of two antibiotics: Penicillin and Streptomycin), Phosphate buffered saline (PBS) and Trypsin-EDTA were obtained from Sigma-Aldrich, USA. Fetal bovine serum was purchased from Gibco-BRL, USA. DMSO for preservation of cell lines was purchased from Sigma-Aldrich, USA. Transfection reagents Gene juice and Effectine were bought from Novagen, USA and Qiagen, Germany respectively. Luciferase assay kit (comprising cell lysis buffer and luciferase substrate) was

purchased from Promega Corporation, USA. Cell culture plastic wares were obtained from BD Falcon, USA. KB, Saos-2 and CHO-K1 cells were obtained from National Centre for Cell Science, Pune, India. Expression vectors used for the studies were pBABE-puro (Akhaury, 2003) and pNHA1 (Tewari, 2003). The pGL2-promoter vector for luciferase assay was purchased from Promega Corporation, USA. pSV- β -gal vector (Promega) was used for expression of β -galactosidase for normalization of luciferase activity.

ELISA plates:

For performing two sites ELISA from cell lysate (*in vivo* ELISA), 96 well flat bottomed Maxisorp ELISA plates were purchased from Nunc, Denmark.

Table 1. Oligonucleotides used in the study:

Sr. No	Oligo. Name/ Id No.	Oligonucleotide Sequence (Microsynth/Sigma-Aldrich/Ocimum Biosolutions)	No. of bases/ T _m (°C)	Purpose of Use
1.	DBS I sense/ 151394	5'-GGGGTACCCCATGGGATTGGGGTTTTCCCCTCCCAT AGATCTTC-3'	44/ 77.8	EMSA
2.	DBS I anti-sense/ 151395	3'-CCCCATGGGGTACCCTAACCCCAAAGGGGAGGGT ATCTAGAAG-5'	44/ 77.8	EMSA
3.	DBS II sense/ 151392	5'-GGGGTACCCCTTACTTGCCCTTACTTGTGTCAGAAGAT CTC-3'	40/ 73.5	EMSA
4.	DBS II anti-sense/ 151393	3'-CCCCATGGGGAATGAACGGGAATGAACAGTCTTCT AGAAG-5'	40/ 73.5	EMSA
5.	DBS III sense/ 151387	5'-GGGGTACCCACAATGCAGGATTCTCCAAAATGA AGATCTTC-3'	43/ 74.19	EMSA
6.	DBS III anti-sense/ 151391	3'-CCCCATGGGGTGTTACGTCTAAGGAGGTTTTACTT CTAGAAG-5'	43/ 74.19	EMSA
7.	p21-5'-DBS sense/ 151398	5'-GAAAGATCTCGAGCAACATGTTGGGACATGTTCTT CGAGAATTGGTACCCC-3'	51/ 76.6	EMSA
8.	p21-5'-DBS anti-sense/ 151388	3'-CTTTCTAGAGCTCGTTGTACAACCCTGTACAAGGAG CTCCTAACCATGGGG-5'	51/ 76.6	EMSA
9.	NTD125 sense/ 31928-001	5'-CTAGCTAGCTCTAGAATGGAGGAGCCCCAGTCAGA TCC-3'	38/ 78.2	PCR-based Cloning
10.	NTD125 anti-sense / 31928-002	5'-CCGGAATTCTTACGTGCAAGTCACAGACTTGGC-3'	33/ 79	PCR-based Cloning

11.	NTD93 anti-sense / 31928-003	5'-CCGGAATTCTTACAGGGGCCAGGAGGGGGCTGG-3'	33/ 85.8	PCR-based Cloning
12.	NTD61 anti-sense/ 31928-004	5'-CCGGAATTCTTAATCTGGACCTGGGTCTTCAGTGAA CC-3'	38/ 80.2	PCR-based Cloning
13.	NTD55 anti-sense/ 31928-005	5'-CCGGAATTCTTATTGGGACGGCAAGGGGGACAG-3'	33/ 82.8	PCR-based Cloning
14.	DBS I sense/ 156165	5'-GGGGTACCTGGGATTGGGGTTTTC-3'	24/ 65.38	PCR-based Cloning
15.	DBS I anti-sense/ 159992	5'-GGAAGATCTGAAGCTCAAACCTTTT-3'	24/ 57.5	PCR-based Cloning, ChIP assay
16.	DBS II sense/ 156164	5'-GGGGTACCCGGATTACTTGCCCTT-3'	24/ 66.2	PCR-based Cloning, ChIP assay
17.	DBS II anti-sense/ 425151	5'-GGAAGATCTTCTGGCACAAAGCT-3'	24/ 59.6	PCR-based Cloning, ChIP assay
18.	DBS III sense/ 156163	5'-GGGGTACCGCAGGATTCCTCCAAA-3'	24/ 66	PCR-based Cloning, ChIP assay
19.	DBS III anti-sense/ 425152	5'-GGAAGATCTGGGTGGAAAATTCTG-3'	24/ 57.9	PCR-Cloning, ChIP assay
20.	p21-5'-DBS sense/ 2701-006	5'-GGGGTACCCTTGGGCAGCAGTGAT-3'	24/ 75.1	ChIP assay
21.	p21-5'-DBS anti-sense/ 2700-049	5'-GGAAGATCTAGCCCACGGACAAAAT-3'	25/ 69.5	ChIP assay
22.	pGL-2 Seq primer 5'/ 25771	5'-GTCCAAACTCATCAATG-3'	17/ 42	PCR for confirmation of clone
23.	pGL-2 Seq primer 3'/ 46050	5'-GGCGGACTATGGTTGCTGAC-3'	21/ 58	PCR for confirmation of clone

METHODS

Maintenance of mammalian cell lines and cell culture

KB, Saos-2 and H-1299 cell lines were used for *in vivo* experiments. All the cells were procured from NCCS, Pune. Cells were grown in Dulbecco's Modified Eagle's medium (DMEM) supplemented with 10 % FCS and incubated at 37 °C in a CO₂ incubator maintaining 5 % CO₂. Cells were subcultured (split) every 3rd - 5th day when confluency reached to ~90-100 % by trypsinization. For the same, firstly, the consumed media was removed and cells were washed with 1 X PBS. Cells were then treated with 1 X TE solution, followed by its removal and incubation of plates for 2 mins at 37 °C. After the incubation period, TE was neutralized by adding 1 ml of complete DMEM media to the plate, detached cells were collected and counted. Finally, equal number of cells was plated in fresh plates for further growth.

Preservation of cell lines/ Freeze down preparation

For preservation of cell lines, freeze downs were prepared and stored at -80 °C for short-term storage and at -196 °C (liquid nitrogen) for long-term storage. Healthy growing cells were harvested at ~70-80 % confluent stage for preservation. After trypsinization, cells were collected in a 15 ml centrifuge tube by centrifuging at 1000 rpm for 3 mins followed by thorough washing with 1X PBS. PBS was then removed and cells were resuspended in the preservation solution containing 90 % FCS and 10 % DMSO and added to cryovials. The vials were immediately transferred to -80 °C deep freezer/liquid nitrogen can. For best revival efficiency ~ 1×10⁶ cells were added per vial. A week post storage, 1 freeze down per cell type was revived and checked for the cell viability.

Revival of cell lines

For revival of cells from freeze downs, cells (cryovials) were taken out from -80 °C deep freezer/liquid nitrogen and thawed at 37 °C. Cells were subsequently transferred to 15 ml centrifuge tube having 2 ml of complete DMEM media and centrifuged at 1000 rpm for 3 mins in a centrifuge with a swinging bucket rotor. The supernatant was then discarded and cells were washed with 1 X PBS. Again, cells were homogenously resuspended in 5 ml of complete media and were plated

in 60 mm petriplates. Centrifuging the cells helps to remove DMSO used during cryopreservation. DMSO has toxic effect on cell growth.

Transient transfection and heat shock treatment

Transient transfections were done using lipofectamine reagents according to manufacturer's protocol. A day before transfection, cells were trypsinized, counted and then plated equally into culture plates. The number of cells were calculated in a manner such that they become 70 % confluent after an incubation of 16 hrs. For Gene juice (Novagen), for 1 μg of DNA, 3 μl of reagent was added in 100 μl of serum free media (SFM) and incubated for 5 mins. DNA was then added to it and further incubated for 5-15 mins. SFM was then added to the mixture to make up the volume to 1 ml. Meanwhile, cells were washed twice with PBS. When incubation period was over, transfection mixture was added to the petriplates drop by drop; plates were rocked gently and kept in CO_2 incubator at 37 $^\circ\text{C}$ for 6 hrs. After 6 hrs incubation, incomplete media was aspirated off and fresh complete DMEM media with 10 % FCS was added to the plates. Cells were further allowed to grow for 24-26 hrs and processed according to experiments.

In case of Effectene (Qiagen), entire procedure was same except that in place of incomplete medium, complete medium was used and for first 6 hrs, cells were kept in lesser volume of medium and then supplemented with full volume of medium.

For luciferase assay, in co-transfection experiments, 2 μg of either pNHA1-p53 or pNHA1-NTD125 construct was transfected together with 1 μg of reporter construct (pGL2-Pr-constructs) into 35 mm culture dish. Respective empty vectors were used to maintain the equal amount of DNA in all the transfection reactions. 0.5 μg of pSV- β -gal reporter plasmid was co-transfected with all samples.

For two-site ELISA and immunoprecipitation assay, 5 μg of pNHA1-NTD125, pNHA1-NTD93, pNHA1-NTD61 or pNHA1-NTD55 plasmid DNA was transfected per 60 mm dish. For co-immunoprecipitation assay, 5 μg pNHA1-NTD125/60 mm plate was used for transfection. For apoptosis assay, different

concentration of pNHA1-NTD125 (0-5 µg) DNA was transfected per plate. For immunofluorescence assay, 2 µg of pNHA1-NTD125 was transfected per 35 mm dish.

- For heat shock experiments, cells were grown at 42 °C for 70 mins in CO₂ incubator and used after incubation was over.

Stable Transfection/Generation of cell lines expressing HA-NTD125

For generating HA-tagged NTD125 expressing cells, 2 µg pNHA1-NTD125 plasmid was transfected into 40 % confluent 60 mm plate. Cells were then allowed to grow and were once split in normal growing media (without selection antibiotics). 12 hrs post seeding, media was replaced with selection media containing Neomycin (2 mg/ml). Antibiotic concentration for selection was determined by death assay at different concentrations. Cells were further grown and split in selection media. Untransfected cells started dying after three days post addition of selection media, further media was changed on every 3rd day. The remaining surviving population of cells kept on growing on selection media and started forming colonies. After allowing them to grow for few days, when colonies became big and thick, they were pooled for subculturing. Selection was further continued for 6 weeks. Stably transfected cells were then checked for expression of NTD125 and p53.

Preparation of nuclear proteins extract and whole cell lysate

The method used is a modification of that described by Dignam (Dignam, 1990). Cells (1.5×10^7) were harvested and centrifuged at 250g for 10 min. The pellet was washed with PBS and centrifuged at 250g for 10 min. After decanting the supernatant, the pellet was resuspended in 5 volumes of Buffer A (10 mM HEPES, pH 7.9, 1.5 mM MgCl₂, 10 mM KCl, 0.5 mM DTT, 0.5 mM PMSF). It was incubated on ice for 10 min and then centrifuged at 250g for 10 mins. The pellet was again resuspended in 3 volumes of Buffer A containing NP-40 at a final concentration of 0.05 %. The resuspension was homogenized with 20 strokes of a tight fitting Dounce homogenizer to release the nuclei, followed by centrifugation at 250g for 10 mins to pellet the nuclei. The nuclei pellet was resuspended in 1 ml

Buffer C (5 mM HEPES, pH 7.9, 26 % glycerol (v/v), 1.5 mM MgCl₂, 0.2 mM EDTA, 0.5 mM PMSF) having NaCl with the final concentration of 300 mM. The solution was mixed well by inversion and incubated on ice for 30 min. It was centrifuged at 24,000g for 20 mins. All the centrifugation steps were carried out at 4 °C. Finally, supernatant was aliquoted in fresh tubes, and freezed at -80 °C. The protein concentration of nuclear extract preparation was estimated using Bradford protein detection kit (Bio-Rad) (Bradford, 1976).

Immunofluorescence staining

For immunofluorescence analysis, cells were grown on coverslip in 35 mm culture dish. Twenty-four hrs post-transfection cells were gently washed twice with cold PBS and fixed in 4 % paraformaldehyde at RT for 15 mins. Subsequently, cells were washed with cold wash buffer (0.01 % BSA and 0.1 % sodium azide in 1 X PBS) followed by permeabilization with chilled permeabilization buffer (0.1 % Triton X-100 and 0.5 % Saponin in 1X PBS and stored at 4 °C). Blocking was done with blocking buffer (1% BSA in 1X PBS) followed by washing with cold wash buffer. For staining, primary antibodies against p53 i.e. PAb C-19 (raised in rabbit) and anti-HA i.e. 12CA5 (raised in mouse) were diluted (1:100) in antibodies dilution buffer (0.01 % Saponin, 1 % BSA and 0.1% Sodium Azide (Nan3) in 1 X PBS and stored at 4 °C). 100 µl of diluted antibodies was spread on a piece of parafilm and coverslip was then kept inverted on it and incubated at 37 °C for 90 mins. After incubation, cells were washed twice with washing buffer. FITC-conjugated anti-mouse secondary antibodies (diluted 1:100) were used to detect p53 and HA-tagged NTD125 separately. Secondary antibodies incubation was carried out in the same manner as primary antibodies, but for 2 hrs and in dark. After washing twice with ice-cold washing buffer and once with PBS, cells were then mounted on DABCO containing mounting media. Slides were sealed with Fevibond and observed through confocal microscope LSM-510 (Carl Zeiss, Germany) or fluorescence microscope (Nikon) attached to a digital camera. Images were then processed using LSM-510 image view (Carl Zeiss) and Image J (Pubmed).

Western blotting

After protein samples were resolved on SDS-PAGE, gel was equilibrated with transfer buffer for 10 mins, followed by transfer of proteins on to the nitrocellulose membrane by semi dry gel transfer apparatus (Bio-Rad) or the wet blot system (Bio-Rad). Post-transfer, membrane was transferred to blocking buffer (PBS, 1.0 % BSA, and 0.05 % Tween-20), after 1 hr incubation at RT, washing was done thrice (each wash for 5-10 mins) with washing buffer (PBS, 0.1 % BSA and 0.05 % Tween-20). Subsequently the membrane was incubated with primary antibodies diluted in wash buffer (1:2000) for 1 hr followed by washing thrice (10 mins each wash) with washing buffer, followed by incubation of the membrane with secondary antibodies conjugated to alkaline phosphatase for another hr. After subsequent washing, blot was developed in developing buffer (100 mM Tris-Cl, pH 9.5, 50 mM MgCl₂, and 100 mM NaCl) containing NBT and BCIP.

Immunoprecipitation and co-immunoprecipitation assay

For co-immunoprecipitation assay, cells were transfected, at 70 % confluency, with plasmid DNA as per the manufacturer's instructions. Cells were grown further for 24-26 hrs, harvested and lysed in NP-40 lysis buffer (20 mM Tris-Cl, pH 7.4, 100 mM NaCl, 10 % Glycerol, 1 % NP-40 and 1 mM EDTA, 1 X Protease inhibitor cocktail). Whole cell lysate was pre-cleared and 1 µg of anti-p53, anti-HA, anti-MDM2 antibodies were used for immunoprecipitation. After 2 hrs of incubation, 40 µl of 10 % protein A-agarose in NP-40 buffer was added to the lysate and further incubated at 4 °C for 2 hrs. Washing was done twice with NP-40 buffer and once with radio-immunoprecipitation assay (RIPA) buffer (50 mM Tris-Cl, pH 7.4, 150 mM NaCl, 1 % Triton X-100, 0.1% SDS, 1 % sodium deoxycholate, 1 X Protease inhibitor cocktail). Immunocomplex was released by addition of SDS loading dye followed by boiling for 5 mins, centrifugation and analysis on 10 % SDS-PAGE. Proteins were transferred onto nitrocellulose membrane and immunoblotted with target antibodies. To assess the effect of NTD125 on the conformation of p53 under heat shock conditions, KB cells were transfected with pNHA1-NTD125, followed by immunoprecipitation using anti-p53 antibodies (PAb1620 and PAb240) as described above. Blot was developed using C-ter specific anti-p53 antibodies (PAb C-19).

Two Site ELISA (*in vivo* ELISA) from cell lysate

Sandwich ELISA from cell lysate was done with some modifications of that described earlier (Liu *et al.*, 2001). Briefly, wells were coated with 100 μ l of 5 μ g/ml anti-p53 antibodies (PAb1620, PAb240 and PAb C-19) overnight at 4 °C. After washing thrice with TBS buffer (0.05 % Tween-20 in PBS), blocking was done using 5 % skimmed milk in TBS for 2 hrs at 4 °C. The wells were then washed thrice with TBS and 200 μ g cell lysate in NP-40 lysis buffer (normal/heat shocked) 1:1 v/v diluted in 5 % milk in TBS was added to each well and incubated at 4 °C for 2 hrs. Further, 100 μ l of anti-p53 polyclonal antibodies FL-393 (1:1000 diluted) was added to each well and incubated at 4 °C for 2 hrs. Subsequently, 100 μ l of AP-conjugated anti-rabbit secondary antibodies (1:1000) was added to each well and kept at RT for 2 hrs. After two quick washes with TBST, ELISA was developed using 100 μ l of 1mg/ml PNPP solution in AP- buffer (pH 9.5) for 30 mins; after terminating the reaction by adding 0.1 mM EDTA, absorbance was recorded at 405 nm on Micro plate reader (Bio-Rad). Readings were recorded from three independent experiments and data were expressed as mean \pm S.D. for each sample.

Luciferase assay

Luciferase assay was performed using Luciferase reporter gene assay kit (Promega) according to manufacturer's instructions. A day before transfection, 2×10^5 cells were seeded in 35 mm culture plates and 24 hrs post-transfection, the assay was performed. The media was aspirated from the plate and cells were washed thrice with cold PBS. Then 200 μ l of 1 X lysis buffer (diluted in PBS from 5 X stock) was added to the plate. The plates were incubated at 4 °C temperature for 15-20 mins. The entire lysed cell's supernatant was transferred into eppendorf tubes. The tubes containing the lysate were vortexed once followed by centrifugation at 10,000 rpm for 5 mins and the clear supernatant was transferred into fresh tubes. For detection, to 100 μ l of Luciferin solution (luciferase substrate), 20 μ l of the supernatant was added and mixed well. Luminisence was immediately measured on a luminometer. Luciferase activity (units obtained) was normalized by the β -galactosidase activity and the data from triplicate determinations were expressed as mean \pm S.D.

Chromatin Immunoprecipitation (ChIP) Assay

ChIP assay was standardized and performed as described ahead. Cells from 100 mm culture plate ($\sim 5 \times 10^7$ cells) were cross-linked with 1 % formaldehyde at 37 °C for 10 mins in complete media and cross-linking was stopped by adding 125 mM glycine and further incubating the plate at 37 °C for 5 mins. Cells were then rinsed twice with ice-cold PBS, scraped and pelleted by centrifugation at 3,000 rpm at 4 °C. The cell pellet was then resuspended in 0.6 ml of lysis buffer (1 % SDS, 10 mM EDTA, 50 mM Tris-Cl, pH 8.1, 1 X Protease inhibitor cocktail) and kept on ice for 20 mins. Afterwards, lysate was sonicated 10 times, 5 sec each at the interval of 2 mins at submaximal input (at the power of 3.0, in Mesonix sonicator), followed by centrifugation at 10,000 rpm for 10 mins. Supernatant was then collected in a new tube and estimated for total protein using Bradford assay (Bio-Rad kit). Total of 3 mg protein was diluted to 5 ml in dilution buffer (1 % Triton X-100, 2 mM EDTA, 150 mM NaCl and 20 mM Tris-Cl, pH 8.1, 1 X Protease inhibitor cocktail) followed by immunoclearing by 20 μ l preimmune serum and protein A-agarose (50 μ l of 10 % protein A-agarose slurry in dilution buffer) for 2 hrs at 4 °C. Immunoprecipitation was performed overnight with 1 μ g of suitable antibodies. After immunoprecipitation, 50 μ l of protein A-agarose (10 % slurry) pre-saturated with salmon sperm DNA was added to the solution and then incubation was continued for another hr. Agarose beads bound immune-DNA complex was pelleted by centrifuging the tubes at 2000 rpm for 5 mins. Further agarose beads were washed and pelleted sequentially in TSE I (0.1 % SDS, 1 % Triton X -100, 2 mM EDTA, 20 mM Tris-Cl, pH 8.1 and 150 mM NaCl, 1 X Protease inhibitor cocktail), TSE II (0.1 % SDS, 1 % Triton X -100, 2 mM EDTA, 20 mM Tris-Cl, pH 8.1 and 150 mM NaCl, 1 X Protease inhibitor cocktail) and buffer III (0.25 M LiCl, 1 % NP-40, 1 % sodium deoxycholate, 1 mM EDTA, and 10 mM Tris-Cl, pH 8.1 and 1 X Protease inhibitor cocktail) with 10 mins incubation on rotatory shaker for each wash. Beads were then washed once with TE buffer (20 mM Tris-Cl, pH 8.1 and 1 mM EDTA) and DNA-protein-antibody complex was extracted in 150 μ l of elution buffer (1 % SDS and 0.1M NaHCO₃) three times by incubating at RT for 15 mins, every time. DNA-protein cross-linking was reversed by incubating the eluted samples at 65 °C for 4 hrs followed by proteinase K digestion at 37 °C for an hr. The DNA was then

extracted with phenol-chloroform, and precipitated overnight with ethanol at -80 °C. After 70 % ethanol washing, DNA was air dried and finally dissolved in 20 µl of ddH₂O/MQ. 1 µl of eluted samples was taken for PCR amplification using suitable primers. For negative control, the complete procedure was repeated in the absence or with non-specific antibodies. For input control, sample after sonication was subjected to proteinase K digestion and total DNA was extracted by phenol-chloroform method. DNA was finally diluted in 50 µl of water and 1 µl of sample was taken for PCR reaction. Same amount of all PCR products were loaded on 10 % native PAGE followed by silver staining to visualize the amplified product.

Silver staining: DNA and proteins

Silver staining of gels for visualization of samples in polyacrylamide gel is a very sensitive technique. It is able to detect as little as 2-3 ng of DNA and 0.1-1 ng of polypeptides. All the buffers required for silver staining need to be prepared freshly at the time of the staining. Steps after the oxidizer treatment have to be strictly undertaken in dark.

Silver staining of native polyacrylamide gels for DNA visualization

The gel was incubated in Fixative A (50 % methanol and 10 % acetic acid) for 30 mins with mild shaking. The solution was decanted. Fixative B (10 % ethanol and 5 % acetic acid) was added and kept for 20 mins with gentle shaking. The solution was changed and again Fixative B was added for another 10 mins. After decanting Fixative B, oxidizer solution (3.4 mM K₂Cr₂O₇ and 3.2 mM Nitric acid) was added and incubated for 8 mins with constant shaking. The gel was washed twice with MQ water, each wash for 5 mins. Silver nitrate (12 mM AgNO₃) solution was added onto gel and incubated under shaking conditions for 30 mins in dark. The gel was washed with water for 30 mins. The gel was then treated with developer (0.28 nM Na₂CO₃ and 0.05 % formaldehyde) for 6-8 mins or until the bands develop. The reaction was stopped by washing the gel thoroughly with excess of water. The gel was then stored in 10 % acetic acid solution or air-dried.

Silver staining of native polyacrylamide gels for protein visualization

The gel was incubated in Fixative A for 30 mins with mild shaking. The gel was then rinsed with MQ water thrice, each wash of 15 min. After the last wash, oxidizer solution was added and incubated for 1 min. The gel was washed twice with MQ water, each wash for 1 min. Silver nitrate solution was added on to gel and incubated under shaking conditions for 20 mins in dark. The gel was washed thrice with water, each wash for 1 min. The gel was then treated with developer for 6-8 mins or until the bands appeared. Stopping solution (10 % acetic acid or 10 % citric acid) was added to stop the reaction.

Recombinant protein expression

Plasmids harboring the genes of interest (10 ng) were transformed in *E. coli* BL21 (DE3) competent cells. Single colony was picked from the plate, inoculated into fresh LB medium and incubated overnight at 37 °C. From this overnight grown culture, 1 % inoculum was inoculated in LB medium and incubated at 37 °C for 3-4 hrs till OD reached 0.8 to 1. Cultures harboring p53 and NTD125 genes were induced with 0.25 and 0.5 mM IPTG for overexpression of p53 and NTD125 respectively and were allowed to grow at 25 °C for 4 hrs. Expression of recombinant protein was analyzed was checked by lysis of 1 ml cell pellet in lysis buffer and resolving the clarified lysates on 12 % SDS- PAGE.

Purification of protein by Ni²⁺- NTA affinity chromatography

Purification was done as described earlier (Ali, 2008). Briefly, for purification of the His-tagged protein Ni²⁺- NTA column was used. Induced cells were harvested after completion of induction period, resuspended in native lysis buffer (50 mM NaH₂PO₄, 300 mM NaCl, 10 mM imidazole, pH 8.0) and further incubated on ice for 20 mins. Cells were then sonicated for their lysis and after centrifugation; supernatant was loaded onto the metal affinity column for binding of His-tagged proteins. The protein bound column was washed with 50 mM imidazole in lysis buffer. Further, protein was eluted with varying imidazole concentrations (200-500 mM) in lysis buffer. Fractions containing purified proteins were pooled, dialyzed against pre-Chilled 1 X PBS containing 1 X protease inhibitor for 4 hrs. Dialyzed proteins were used for experiments or stored at -80 °C in 5 % glycerol.

Thermal denaturation analysis

The thermal denaturation curves were analysed by recording the change in absorbance of proteins at 280 nm wavelength in UV-visible spectrophotometer (CARY, 100 Bio, Varian) attached to temperature controller. Before experiment, 100 µg of p53 or NTD125 were diluted in 1 ml cold PBS and scanned between 25 °C to 75 °C temperature range. The variation in temperature was done at the rate of 1 °C/min. PBS alone was included as a control.

***In vitro* co-immunoprecipitation and protection assay**

For co-immunoprecipitation assay, 2 µg of recombinant p53 was incubated with or without recombinant NTD125 in 1:1 molar ratio. Protein mixture was further diluted to 100 µl in PBS (with protease inhibitor cocktail) and incubated at different temperatures (RT, 37 °C, 40 °C, 42 °C and 45 °C) for 1 hr. Again the sample was diluted to 500 µl with PBS and 1 µg of PAb C-19/ PAb1620/ PAb240 was added to the mixture and incubated on a rotatory shaker for 1 hr at 4 °C. After that 50 µl of 10 % protein-A agarose (pre-saturated with BSA) was added to the sample and incubated for 2 hrs at 4 °C with continuous stirring. After pelleting, beads were washed thrice with NP-40 washing buffer (0.5 % NP-40 in 1 X PBS and 1 X protease inhibitor cocktail) and finally immune-complex was released in 50 µl of NP-40 washing buffer by adding SDS loading dye and boiling for 3 mins. For *in vitro* protection assay, the above procedure was repeated with 2 µg of p53 protein with or without NTD125 (1:5) molar ratio. CHIP protein (1:2) molar ratio was used as positive control for p53 chaperoning at higher temperatures. For immunoblotting, 20 µl of eluted sample was resolved on 12 % SDS-PAGE and semi-dry blotted onto nitrocellulose membrane. Western blot was developed using PAb1801/ PAbDO1 monoclonal antibodies.

Polyacrylamide gel electrophoresis: Native and SDS-PAGE

Native polyacrylamide gel

Native-PAGE was preferred only for small DNA fragments. A stock solution of 30 % acrylamide was made in a ratio of 29:1 (Acrylamide: *N,N'*-methylbisacrylamide, w/w) in water and then was added according to the percentage of the gel required for the DNA sample. The gel was prepared in 0.5 X

TBE buffer. For 10 ml gel volume, 100 μ l of 10 % APS and 10 μ l of TEMED were added. The total volume was made to 10 ml by adding water. The gel was run in 0.5 % TBE buffer at 120 Volts.

SDS-polyacrylamide gel

It was used for proteins, for the purpose of showing over expression, purification, protein-protein interactions and western blot studies. Different percentage of resolving gel (10, 12 and 15 %) was used according to the size of proteins; stacking gel was used at 4 %. Samples were prepared in 5 X SDS-loading dye. Running buffer used was 1 X Tris-glycine. The stock solutions of buffers used for the preparation gel were 1.5 M Tris-Cl, pH-8.8 for resolving, and 1 M Tris-Cl pH-6.8 for stacking gel.

Coomassie Blue staining

After running the gel, it was transferred to the Coomassie brilliant blue stain solution and incubated for 30 mins with constant shaking at room temperature. Gel was then destained by placing it in the destain solution and incubating it at room temperature with constant shaking. Used destain was replaced with fresh destain solution until the background was cleared and the bands become evident.

Kination and purification of oligonucleotides

Oligonucleotides were 5'-end labeled using T4 Polynucleotide kinase (T4 PNK) and γ -³²P-ATP to make radiolabeled DNA probes. γ -³²P-ATP catalyzes the transfer of gamma phosphate of ribonucleoside 5'- triphosphate to the 5'- hydroxyl group of DNA. The composition of the reaction mixture prepared for kination is as follows:

Oligonucleotide	50 ng
10 X buffer	3 μ l
T4 PNK enzyme	10 U
γ -P ³² -ATP	1 μ l
MQ-H ₂ O	Made up the volume to 30 μ l

The reaction mixture was incubated at 37 °C for 30 mins. Purification of radiolabeled oligonucleotide from unincorporated γ -P³²-ATP was done by Sephadex G-50 resin packed in 1 ml syringe. Slurry of Sephadex G-50 (50 %) was made in sterile water. Column was prepared by plugging glass wool at the bottom of syringe and then packing the column with hydrated Sephadex G-50. The column was centrifuged at 2500 rpm for 3 mins. After packing the column, the sample was loaded on to it. Eluted DNA was collected in a microcentrifuge tube kept beneath a 15 ml tube upon spinning the column at 3000 rpm for 5 mins. Counts were taken for 1 μ l sample in the β -counter and accordingly used in an EMSA reaction.

Electrophoretic Mobility Shift Assay (EMSA)

The DNA binding activity of p53 was monitored by EMSA. The oligonucleotides containing different p53 binding sites as described (Table. 1) were synthesized from Microsynth/Sigma-aldrich. Sense and anti-sense oligonucleotides were separately end labeled by T4 polynucleotide kinase using γ -P³²-ATP, annealed and then purified by G-50 column, as described above. EMSA buffer (5 X), 100 ng of poly dI-dC, 100 ng of recombinant p53 protein (\pm NTD125), 3 ng of radiolabeled DNA were added to the reaction mixture and water was added to make up the volume to loading volume (25 μ l). Reaction mixture was then incubated for 30 mins at RT. The reaction mixture after incubation was loaded onto 4 % native-PAG containing 0.5 X TBE buffer and electrophoresed for suitable time. Gel was then dried and exposed on to the X-ray film for autoradiography. Cassette was then incubated at -80 °C until the film was developed for visualizing the bands.

To observe the effect of NTD125 on DNA binding activity of p53, recombinant NTD125 (in various amounts) was mixed with p53 prior to incubation at 37 °C for an hr. Further, to rule out the presence of any chaperone like protein in purified p53 and NTD125, culture was induced in the presence of 5 μ M of geldanamycin. Subsequently, 5 μ M of geldanamycin was maintained in the reaction mixture throughout. In addition, to observe any effect of NTD125 on DNA binding activity of p53 in the presence of ATP, 5 mM ATP was added in the reaction mixture prior to setting up the EMSA reaction.

Bacterial Cultures

All bacterial cultures were grown in LB medium at 37 °C with shaking in the presence of appropriate antibiotics. The medium was sterilized by autoclaving at a pressure of 15 lbs/square inch for 15 mins. For preserving the bacterial cultures, cells were allowed to grow in LB medium with appropriate antibiotics. When the cells reached log phase, 300 µl of culture was added into the micro-centrifuge tube containing 300 µl of 100 % glycerol. The cells were vortexed thoroughly until the solution became homogenous and further stored at -80 °C.

Preparation of competent cells

Competent cells of *E. coli* strains DH5 α , BL-21(DE3) were prepared with a slight modification in the standard protocol (Sambrook *et al.*, 1989). A single colony was picked from a freshly grown plate and then inoculated in 10 ml of LB broth and the culture was incubated for O/N at 37 °C. After 16 hrs, 1 ml of this culture was transferred to 100 ml LB broth (1 % final concentration). The cells were grown at 37 °C till absorbance at 600 (A_{600}) reached 0.4-0.6. The culture was then removed and chilled by putting on ice with slight rotation for 20 mins. Culture was then aseptically transferred to sterile oakridge tubes. Cells were pelleted down at 4000 rpm for 5 mins at 4 °C. Supernatant was discarded and the cell pellet was resuspended in 25 ml of chilled 100 mM $CaCl_2$ and incubated on ice for 30 mins. The cells were again centrifuged at 4000 rpm for 5 mins at 4 °C and then resuspended in 5 ml of 100 mM $CaCl_2$ supplemented with 15 % glycerol. The cells were left on ice for 4-6 hrs, the resuspended cells were then aliquoted in 200 µl batches and were stored at -80 °C.

Determination of competency

One aliquot of 200 µl competent cells was thawed on ice followed by addition of 10 ng of standard plasmid DNA. The efficiency of the competent cells per µg of supercoiled plasmid DNA is represented as the number of colonies obtained per-µg of supercoiled plasmid DNA.

Transformation

Frozen competent cells were thawed on ice and the plasmid DNA or ligation mixture was added to the cell suspension, mixed properly and incubated on ice for

30 mins. Cells were then given a heat shock at 42 °C for 90 seconds in a water bath. Further, cells were incubated on ice for 2–3 mins prior to addition of 800 µl of LB broth, mixed and incubated at 37 °C for 1 hr in shaker. Cells were then pelleted down at 10,000 rpm for 30 sec; supernatant was discarded and cell pellet was resuspended in 25-50 µl media left in the tube and spread on the LB agar plate containing appropriate antibiotics.

Plasmid DNA Isolation

Mini-Prep

Miniprep plasmid isolation procedure used was a slight modification of the original protocol (Sambrook *et al.*, 1989). 3 ml of overnight grown (15-16 hrs) bacterial culture was transferred to a microfuge tube and centrifuged at 10,000 rpm at RT for 1 min. Supernatant was discarded. 100 µl of Solution I was added to the tube and mixed by vortexing. 200 µl of freshly prepared Solution II was added to it and gently mixed by turning the microfuge tube upside down, couple of times, followed by incubation on ice for 5 mins. After that, 150 µl of Solution III was added to it, mixed vigorously and left on ice for 5 mins. The tubes were spun at 4 °C for 10 mins at 14000 rpm. The clear supernatant was transferred to other tube (if the supernatant was not clear, it was recentrifuged). 2.5 volume of chilled 100 % ethanol was added to the supernatant and the tubes were kept at –80 °C for 30 mins. After incubation, tubes were centrifuged for 20 mins at RT. The supernatant was decanted and then after 70 % ethanol was pellet was air-dried. 30 µl of TE/MQ along with 1 µl of RNAase A was added and incubated at 37 °C, for 30 mins. Plasmid DNA was run on 1 % agarose gel at constant voltage of 75 volts and the DNA bands were visualized under UV transilluminator following EtBr staining.

Midi-Prep

Large-scale plasmid preparation for ultra pure DNA was done using Midi-Prep DNA isolation kits provided by Novagen/ Qiagen according to the manufacturer's protocol. The final DNA was dissolved in autoclaved MQ and 260/280 ratio was checked for assessing the quality of DNA.

Agarose gel electrophoresis and DNA quantitation

The agarose gel used varied from 0.8 to 1.2 % according to the size of DNA to be resolved. The agarose was resuspended in 0.5 X TAE and dissolved by boiling; ethidium bromide was then added to a final concentration of 0.5 µg/ml. The agarose solution was poured in the gel casting mould, further combs were inserted and the solution was left to solidify. Combs were then removed and gel was kept in the electrophoresis tank containing 0.5 X TAE. The DNA sample was mixed with tracking dye and loaded into the wells of the gel and electrophoresis was carried out at a constant voltage of 5 to 15 volt/cm and then bands were visualized using short wavelength UV transilluminator. For the quantitation of plasmid DNA by spectrometry, DNA was diluted in water and absorbance at 260nm (A_{260}) and at 280 nm (A_{280}) was measured in quartz cuvette. $A_{260}=1$ is equivalent to 50 µg/ml of plasmid DNA. The ratio of A_{260} / A_{280} was taken to check the purity of the DNA preparation. The ratio of the protein free pure DNA ranges from 1.8-2.

DNA elution from agarose gels

GeneClean kit (SpinPrep™ Gel DNA Kit, Novagen) was used to purify PCR amplified products and restriction enzyme digested DNA fragments to obtain DNA free of all salts, proteins and other interfering agents. The purified DNA was then used for ligation and other purposes. For GeneClean, desired DNA band was excised from the gel and put in a microcentrifuge tube. The weight of agarose piece was measured. Three volumes of Spin Prep Gel Melting Solution (A) was added and the gel slice in the tube was heated at 50 °C for 10 mins or till the agarose slice dissolves. Spin Prep Filter was placed on a receiver tube, the solution was loaded onto it; centrifuged to full speed for 30 sec, and flow-through was discarded. Again, 400 µl of fresh Spin Prep Gel Melting Solution (A) was added to the filter and the spinning step was repeated. Further, 650 µl of spin Prep Wash Buffer (B) was added to filter and spun. Flow-through was discarded and column was spun for 2 mins for removing any traces of wash buffer. Finally, filter was transferred to Elute receiver tube and 50 µl of pre-warmed (50 °C) Spin Prep Elute Buffer (C) was added to the filter. Filter was incubated at 50 °C for three min and then immediately centrifuged to collect the eluted DNA. This process of

elution was repeated once more. The eluted DNA product was analyzed on 1.2 % agarose gel.

DNA elution from polyacrylamide gels

After electrophoresis, the gel was either stained with ethidium bromide for cold DNA samples or exposed for radioactive DNA samples. The autoradiogram was developed and the DNA band was aligned. The desired DNA band was excised from the gel. The gel piece was crushed to give fine slurry. Approximate volume of the crushed slice was calculated and three volumes DNA elution buffer was added to the crushed gel in the tube. The tube was kept on a rotary shaker for 8-10 hrs. Samples were centrifuged after the incubation period and the upper layer of supernatant was collected in a fresh tube. This elution process was repeated twice or thrice depending on the DNA size and the gel percentage. Larger sized DNA fragments require more elution time and are recovered with a lesser efficiency as compared to the small sized DNA fragments. Finally, the DNA was ethanol precipitated, washed with 70 % ethanol, and air-dried. The dried pellet was dissolved in required volume of buffer for further experiments.

PCR amplification

For amplification of cDNA NTD125 and deleted constructs, PCR amplification was done using the p53 cDNA cloned in pNHA1 as template with *Pfu* DNA Polymerase. For amplification of DBS II and DBS III, PCR amplification was done using hp53-Luc (Moshe Oren, Weizman, Israel) as template. The PCR reaction was set in a 0.2 ml PCR tubes on Gene Amp PCR system 2400 (Perkin Elmer). The reaction mixture is as follows

DNA template	10-20 ng (1 μ l in ChIP assay)
Sense Primer	50 ng
Anti- sense Primer	50 ng
10 X Vent Buffer	5 μ l
<i>Taq/Pfu</i> DNA polymerase	2 U
MQ water	added to make up the volume 50 μ l

Table.2. Details of the PCR machine programming are depicted in the following table:

Primers	Purpose	Denatura ⁿ Temp. (°C)/ Time (sec.)	Annealing Temp. (°C)/ Time (sec.)	Extn. Temp. (°C)/ Time (sec.)	No. of Cycle s	Final Extn. Temp. (°C)/ Time (min.)
319228-001/31928-02	Cloning of NTD125	95/30	73/30	72/45	30	72/5
319228-001/31928-03	Cloning of NTD93	95/30	73/30	72/45	30	72/5
319228-001/31928-04	Cloning of NTD61	95/30	73/30	72/45	30	72/5
319228-001/31928-05	Cloning of NTD55	95/30	73/30	72/45	30	72/5
156163/159992	Cloning of DBS I, II, III	95/30	55/30	72/45	25	72/5
156162/159992	Cloning of DBS I, II	95/30	55/30	72/45	25	72/5
156161/159992	Cloning of DBS I/ ChIP assay	95/30	55/30	72/45	25/30	72/5
156162/425151	Cloning of DBS II/ ChIP assay	95/30	55/30	72/45	25/30	72/5
156163/425152	Cloning of DBS III/ ChIP assay	95/30	55/30	72/45	25/30	72/5
2701-006/2400-49	ChIP assay p21-5' DBS	95/30	55/30	72/45	30	72/5

Restriction enzyme digestion of DNA

The DNA samples were digested with restriction endonucleases in an appropriate 1 X reaction buffer (supplied with the enzyme). DNA sample (1-2 µg) was digested in a reaction volume of 25-50 µl and incubated at temperatures specific for individual enzymes in a water bath for 4-5 hrs. The digested DNA was ethanol precipitated and air-dried. The DNA was dissolved in autoclaved MQ, and if second digestion was required, it was further digested with the desired restriction enzyme.

Ligation

Vector and insert DNA were digested with complementary restriction sites. The plasmid vector and insert were added in a molar ratio of 1:5 or 1:10 in a total reaction volume of 10 μ l. The reaction mixture was incubated for 16 hrs at 16 °C. The cohesive end ligation needs the final concentration of 1 mM ATP. The ligation reaction is set as follows:

Incubation temperature	16 °C
T4 DNA igase	1-2 U
ATP concentration	1 mM

After the completion of the incubation period, samples were transformed or stored at -20 °C until further used.

Results

Loss of active or wild conformation leads to non-functional p53 under heat stress and in many cancers because conformation specific activation of p53 from latent to active form (mutant to wild phenotype) is essential for WT p53 to be translocated from cytoplasm to nucleus and function as a transcriptional factor (Gaitonde *et al.*, 2000). As reported, under heat stress both native p53 and bacterially expressed recombinant p53 attain mutant phenotype, which is functionally inactive and unable to perform tumor suppressor function. At the same time, there are molecular chaperones that assist restoration of wild phenotype of WT p53 e.g. Hsp90, Hsp70, CHIP, MDM2 under elevated temperature. These chaperone molecules interact either with mutant phenotype and convert it to wild form or interact with wild phenotype and hold it in wild form under unfavorable conditions. Molecular chaperones play significant role in modulating p53 activity under unfavorable conditions. Most of the biological chaperones have dual activity e.g. chaperoning/ATPase or chaperoning/ubiquitination and so far, no switch between the two is recognized. Due to this, research is focused on identification of small molecules/peptides, which can chaperone p53 to its active conformation and lack other functions and side effects. Many such molecules have been identified which can restore wild conformation of WT p53 or MT p53 and can initiate apoptosis (Beretta *et al.*, 2008). Here we explored the role of p53-NTD in stabilization of p53 protein as well as transcriptional activation of p53 gene.

1. NTD125 is natively unfolded and highly thermostable-

As NTD125 is a novel protein as an independent molecule, we firstly subjected NTD125 to various available bioinformatic tools for *in silico* characterization. Using ProtParam (ExPASy tools; Gasteiger *et al.*, 2005), we determined theoretical pI and molecular mass which were 4.12 and 13.4 kDa, respectively. Stability analysis predicted NTD125 as an unstable protein (details shown in Table. 3). We also analyzed NTD125 for intrinsic disorder using IUPred (Dosztanyi *et al.*, 2005) and found that it falls under the category of disordered proteins showing the presence of only few small organized regions by different methods; long disorder, short disorder and structured region (Fig. 5). According to prediction, region above 95 residues showed presence of some structured region. Residues 20-40

ProtParam

NTD125:

```

      10           20           30           40           50           60
MEEPQSDPSV  EPPLSQETFS  DLWKLLPENN  VLSPLPSQAM  DDLMLSPDDI  EQWFTEDPGP
      70           80           90          100          110          120
DEAPRMPEAA  PRVAPAPAAP  TPAAPAPAPS  WPLSSSVPSQ  KTYQGSYGFR  LGFLHSGTAK
      125
SVTCT

```

Number of amino acids: 125

Molecular weight: 13402.9

Theoretical pI: 4.12

Total number of negatively charged residues (Asp + Glu): 17

Total number of positively charged residues (Arg + Lys): 6

Atomic composition:

Carbon	C	596	Formula: C ₅₉₆ H ₉₀₄ N ₁₅₀ O ₁₉₂ S ₅
Hydrogen	H	904	
Nitrogen	N	150	Total number of atoms: 1847
Oxygen	O	192	
Sulfur	S	5	

Extinction coefficients:

In units of M⁻¹ cm⁻¹, at 280 nm measured in water.

Ext. coefficient -19480

Abs 0.1% (=1 g/l)-1.453, assuming ALL Cys residues appear as half cystines

Ext. coefficient -19480

Abs 0.1% (=1 g/l)-1.453, assuming NO Cys residues appear as half cystines

Estimated half-life:

The N-terminal of the sequence considered is M (Met).

The estimated half-life is: **30 hrs** (mammalian reticulocytes, *in vitro*)

>20 hrs (yeast, *in vivo*).

>10 hrs (Escherichia coli, *in vivo*).

Instability index:

The instability index (II) is computed to be 84.09

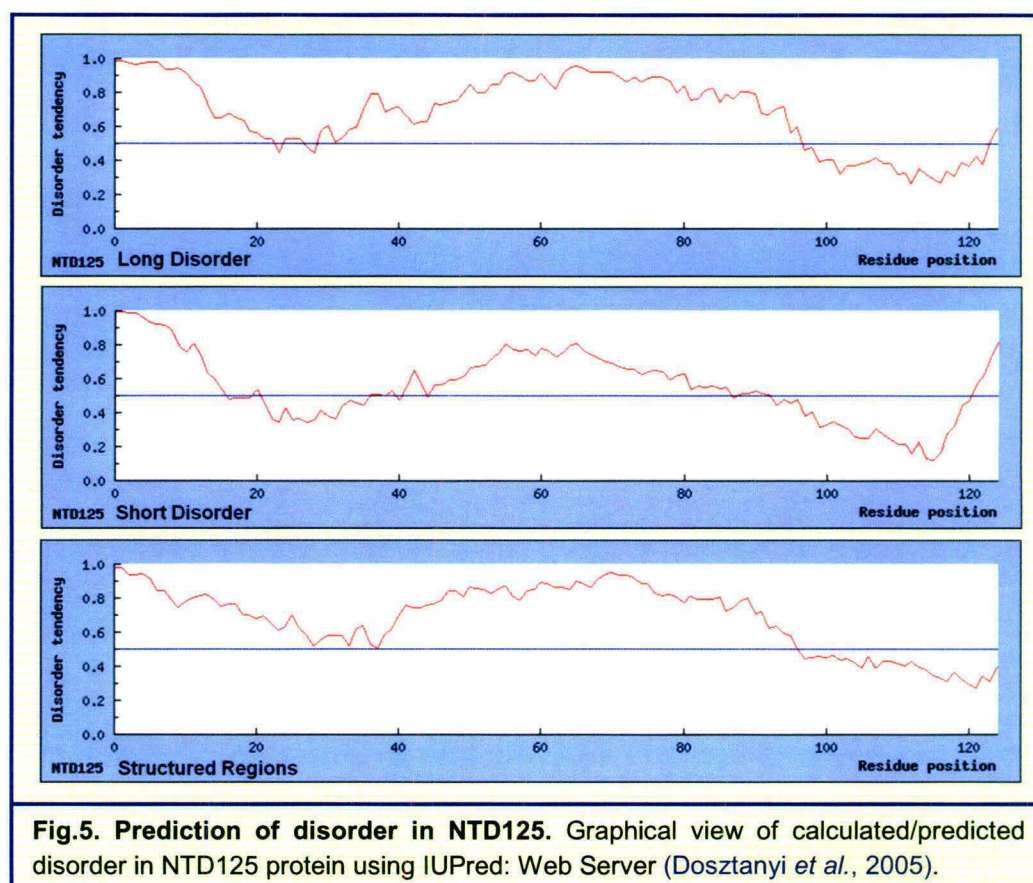
This classifies the protein as unstable.

Aliphatic index: 59.44

Grand average of hydropathicity (GRAVY): -0.506

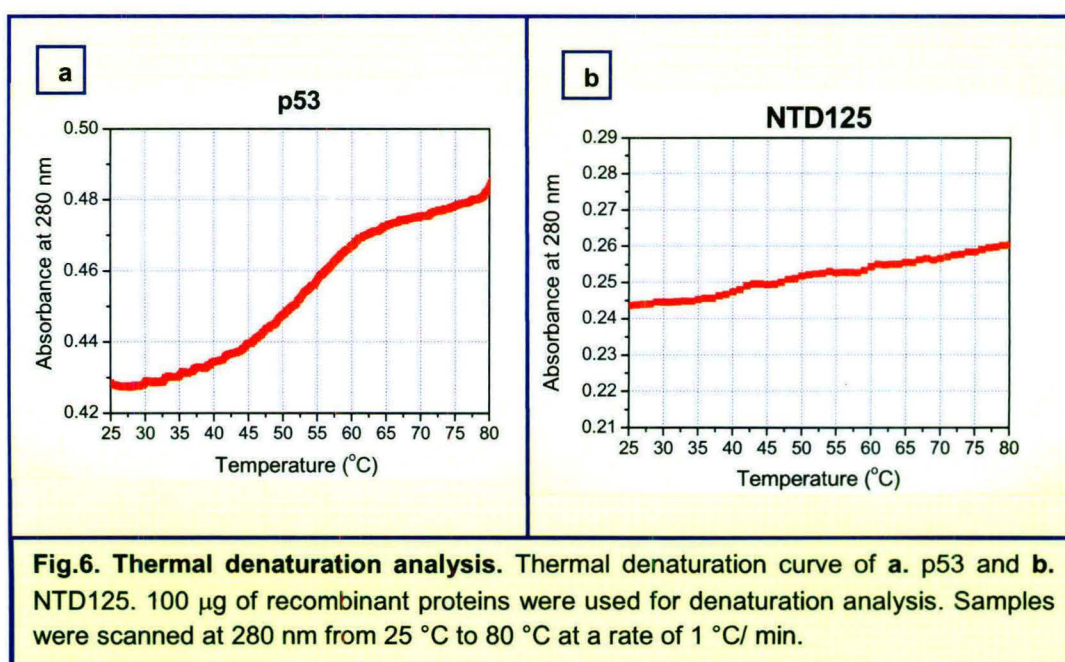
Table.3. Prediction of physical properties. *In silico* prediction of various physical characteristics of NTD125 by ProtParam (Expasy).

also exhibit slight presence of structure. Such bioinformatics based analysis predicts behavior of NTD125; but only on theoretical basis.



Therefore, in view of information attained by bioinformatics tools, we started our experiments with bacterially expressed and highly purified NTD125 and p53 to assess *in vitro* thermostability and intermolecular interaction between the two. The proteins were expressed and purified using pET32a-p53 and pET21c-NTD125 plasmid vectors (Ali, 2008) transformed in *E. coli* BL-21 (DE3) cells, grown in 1.5 X LB medium at 37 °C. Over expressed proteins were purified through Ni²⁺-NTA affinity chromatography. The purified proteins were dialyzed against cold PBS containing PMSF and protease inhibitor cocktail. The proteins had ≥ 95 % purity. Protein concentration was estimated using Bradford reagent (Bio-Rad). Freshly prepared proteins were used for experiments. To analyze thermal stability of NTD125 and p53, we subjected both the proteins to thermal denaturation studies using UV-visible spectroscopy. For thermal denaturation experiment, we

took 100 μg of each protein in cold PBS, the sample was then brought to 25 $^{\circ}\text{C}$ and scanned at 280 nm from 25 $^{\circ}\text{C}$ to 80 $^{\circ}\text{C}$ at a rate of 1 $^{\circ}\text{C}/\text{min}$ in Cary-100, UV-visible spectrophotometer (Varian). Spectra revealed that while p53 starts melting at ~ 35 $^{\circ}\text{C}$ and melts rapidly (Fig. 6a), NTD125 did not show clear denaturation transitions, and showed very less changes in absorbance, which could be due to its unfolded structure (Fig. 6b). These observations established NTD125 as a thermostable protein. Being structurally disordered, we were expecting NTD125 to show thermal stability at higher temperatures. Similarly, Far-UV CD spectra analysis also proved the thermal stability of NTD125 (Sharma *et al.*, 2009). As the denaturation/melting curve results due to opening up of higher-level structures of molecule, p53's thermal denaturation curve also helps us to understand the temperature dependent aggregation of purified p53 because open molecules are more prone to aggregation. So, p53 shows faster aggregation in fluorescence spectroscopy analysis at higher temperature (Sharma *et al.*, 2009).

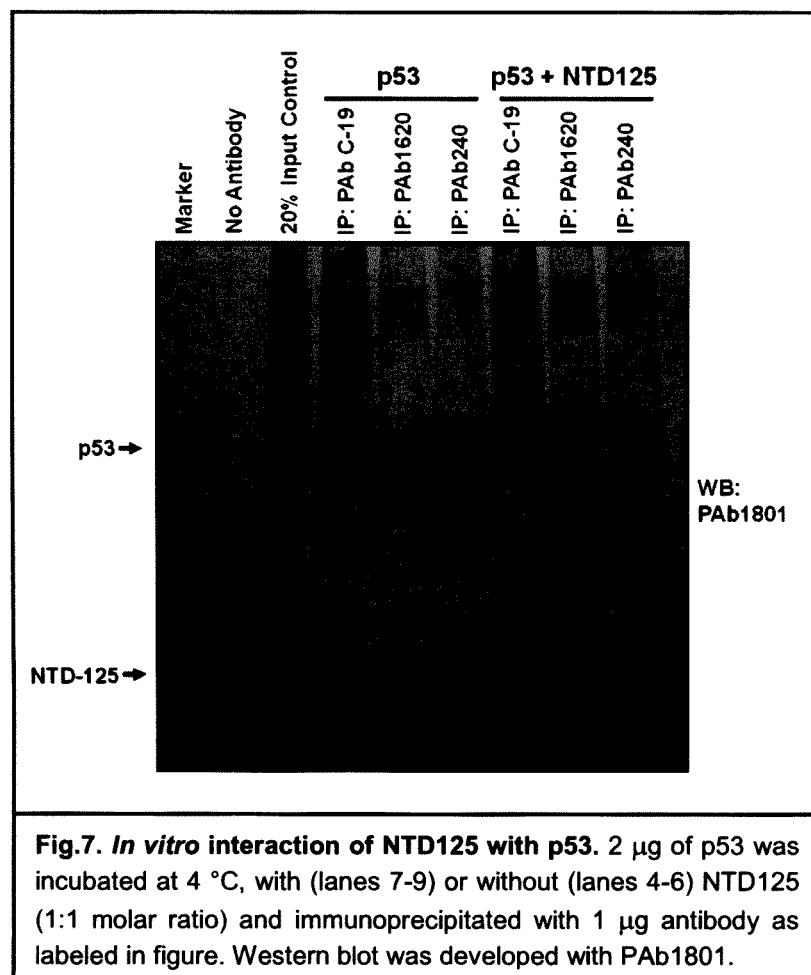


2. NTD125 interacts with WT p53 *in vitro*-

While studying the solution structure of tetrameric p53 through cryo-electron microscopy, Okorokov *et al.* observed the interaction of N-terminal-TAD region with C-terminal-basic region during dimer and tetramer formation (Okorokov *et al.*, 2006). They also confirmed direct N-C terminal interaction by GST-pull down

assay with purified, isolated domains (Okorokov *et al.*, 2006). This data suggests the possibility of interaction of NTD125 with the p53 through its C-terminus.

For confirming the intermolecular interaction between p53 and NTD125 *in vitro*, we incubated NTD125 with p53 in equimolar ratio at 4 °C and then immunoprecipitated p53 with anti-p53 specific antibodies i.e. PAb C-19, PAb1620 and PAb240. PAb C-19 which interacts within the C-terminus of p53, can only pull p53 from the solution and not NTD125 unless in complex, whereas PAb1620 and PAb240 are two conformation specific antibodies and exclusive for wild type and mutant type conformation of p53, respectively. Immunoprecipitation showed that p53 interacted with NTD125. NTD125 is immunoprecipitated with all three antibodies used; with almost equal intensity (Fig. 7). The result suggested that NTD125 could interact with both wild and mutant conformation of p53.



Immunoprecipitation results established the intermolecular interaction between thermosensitive p53 and thermostable NTD125. Confirmation of interaction between the two proteins led us to further investigate whether NTD125 could stabilize WT p53 at higher temperature. We were also interested to explore the effect of this interaction on p53 DNA binding activity.

3. NTD125 protects and restores wild type conformation of p53 *in vitro*-

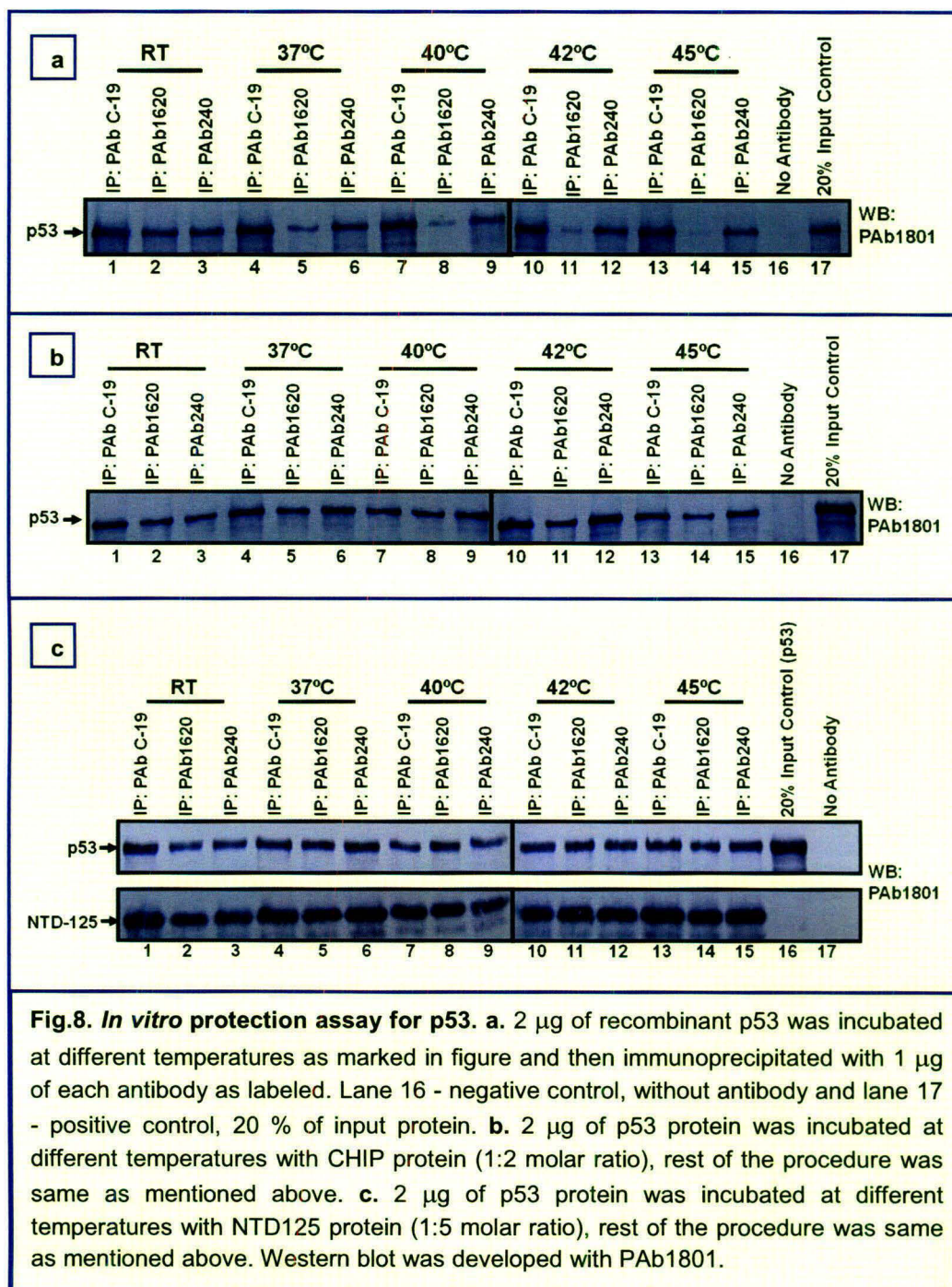
As p53 is one of the most sensitive and important cellular protein and loss of wild-type p53 function is probably the most common molecular abnormality in human neoplasm; it is important to restore its activity to check carcinogenesis. Wild type p53 stays in two different functional/conformational forms in normal growing cells and usually exists in equilibrium between active and latent form. The wild conformation or active form can be detected by PAb1620 (human origin) / PAb246 (murine origin), and mutant conformation or latent form by PAb240 antibodies.

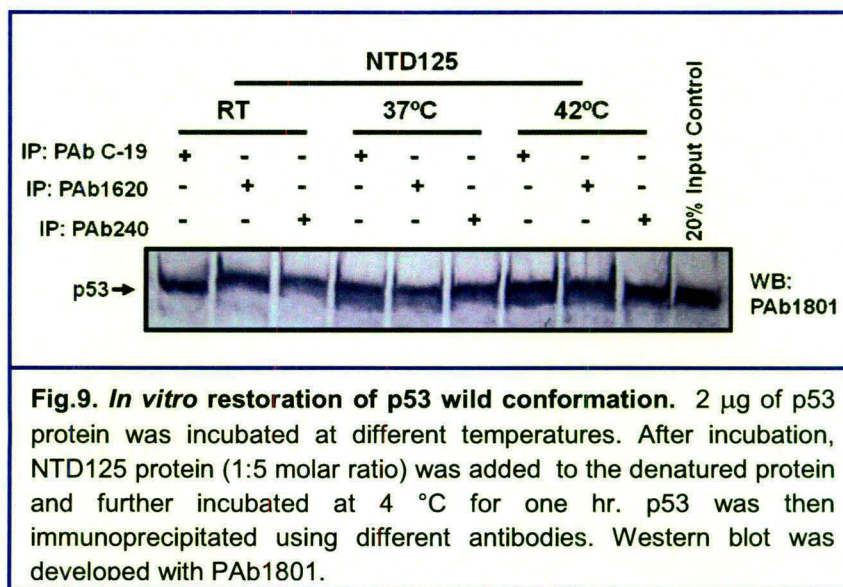
The approach of probing the alteration in p53 conformation using conformation specific antibodies was developed way back in early 1990s by two independent groups: Milner's and Lane's (Milner and Watson, 1990; Stephen and Lane, 1992). Only on the basis of antibody specificity, Milner and Watson identified the existence of two functionally different forms of p53 in normal and serum starved cells. They found that latent form was unable to bind p53 consensus site and did not function as transcription factor (Milner and Watson, 1990). Similar type of interchange of conformations was also observed in purified wild type p53 when subjected to heat stress. Recombinant p53 underwent transient conformational changes under heat stress; similar to that of misfolding caused by structural mutations (Zylicz *et al.*, 2001; Wang *et al.*, 2003).

We analyzed the effect of heat on bacterially expressed wild type p53 and possible role of NTD125 on p53 conformation at higher temperature. Therefore, we designed an experiment wherein, we incubated purified p53 at various temperatures i.e. RT, 37, 40, 42 and 45 °C, for 1 hr and then immunoprecipitated it using PAb C-19, PAb1620 and PAb240 antibodies. After precipitating with

protein-A agarose, followed by multiple washings, sample was eluted and resolved on SDS-PAGE followed by immunoblotting. Blot was developed using PAb1801 antibodies, which has an N-terminal specific epitope and thus, can detect p53 and NTD125 simultaneously. We performed the experiment using only p53 to check its heat sensitivity in relation to its conformation; p53 with CHIP for protection of p53 conformation at higher temperature and p53 with NTD125 to check the effect of NTD125 on p53 conformation. The blot clearly showed that as temperature rises, p53 loses its wild conformation and within an hour at 45 °C, wild conformation is completely lost (Fig. 8.a). This experiment evidently revealed the transition of wild type to mutant conformation of p53 upon heating. Further, we performed the similar experiment by mixing p53 either with NTD125 (1:5 molar ratio) or CHIP (1:2 molar ratio) before incubation at different temperatures. CHIP (a known chaperone of p53) was used as a positive control for protection, as it has been proved that CHIP protects wild phenotype of WT p53 under heat stress (Tripathi *et al.*, 2007).

In our experiment, CHIP chaperoned p53 and protected its PAb1620 binding conformation at higher temperature *in vitro* (Fig. 8.b). Immunoprecipitation together with NTD125 also showed the occurrence of PAb1620 interacting conformation of p53 at higher temperatures, even at 45 °C (Fig. 8.c) similar to CHIP. These results prove that NTD125 binds to p53 and helps it to remain in wild type conformation as other chaperones do. In addition, chaperones are capable of restoring the lost conformation of denatured proteins. So to verify the restoring function of NTD125, we added the NTD125 to the denatured p53 (1 hr at RT, 37 or 45 °C) and further incubated for 1 hr at 4 °C. Results exhibited the recovery of lost wild and mutant conformation of p53 (Fig. 9). Therefore, NTD125 was able to both protect and restore wild conformation of heat denatured recombinant p53. These results led us to explore a possible role of NTD125 as a chaperone.

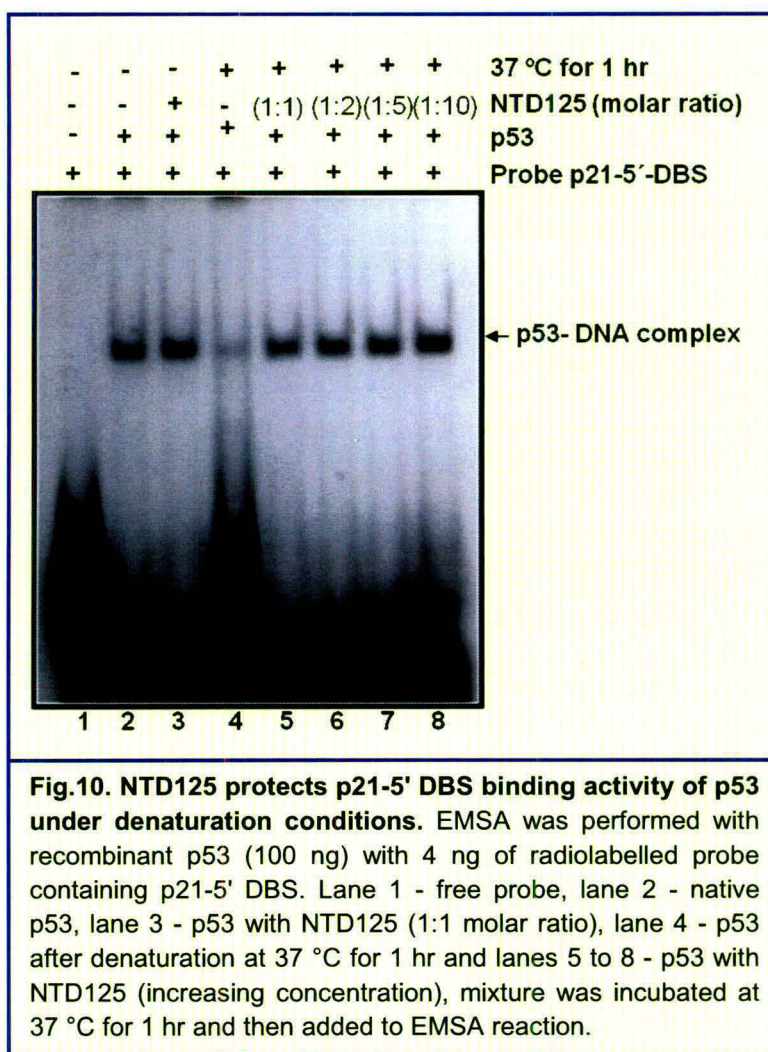




4. NTD125 protects and restores p53 DNA binding activity *in vitro*-

Chaperones are molecular machines within the cells which protect protein and RNA molecules during stress (e.g. heat stress or unfavorable conditions) and usually do so by providing structural stability during initial folding or later at higher structural level; thus maintaining activity of the molecule. It has been previously reported by our group that CHIP protected DNA binding activity of p53 under denaturing condition (37 °C for 1 hr) in dose dependent manner (Tripathi *et al.*, 2007). Being temperature sensitive, p53 loses its specific DNA binding activity even at 37 °C within 1 hr, most probably due to loss of wild conformation.

In order to determine whether NTD125 can also protect/restore the DBS binding activity of denatured p53, we performed EMSA with radiolabeled p21-5' p53 consensus binding site in the presence or absence of NTD125. In radiolabeled probe, we added native or denatured p53 (incubated at 37 °C for 1 hr) and p53 with NTD125 (increasing concentration) before heat treatment. We observed that NTD125 is able to protect p53 binding activity in dose dependent manner (Fig. 10). Further, to confirm restoration of p53 DNA binding activity, we first denatured the p53 and then added NTD125 to it followed by incubation at 4 °C for 1 hr. This mixture was then used for EMSA reaction; results showed that NTD125 could efficiently restore DNA binding activity of denatured p53 (Fig. 11).



When recombinant proteins are purified using a bacterial system, there are chances that some bacterial chaperones may get co-purified with the target protein. Due to over-expression, proteins can't properly fold and need to be chaperoned for proper structure, function and integrity. Even traces of any chaperone can reactivate the protein's activity. To rule out the presence of any Hsp90 homologue from *E. coli*, we grew bacterial culture in the presence of 5 μ M geldanamycin during the induction period. Geldanamycin is an inhibitor of p53 and Hsp90 interaction (Whitesell *et al.*, 1998). Subsequently, all purification steps and heat treatment were carried out in the presence of geldanamycin. Results show similar pattern of p53 restoration, even in presence of geldanamycin leading to the conclusion that the protection effect was solely due to NTD125 (Fig. 12).

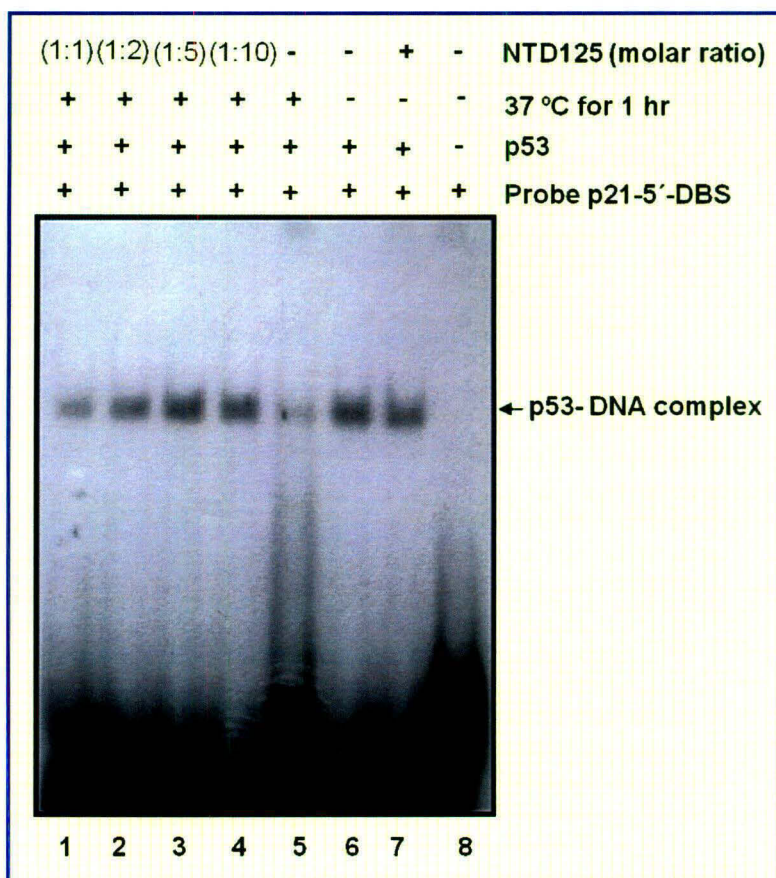
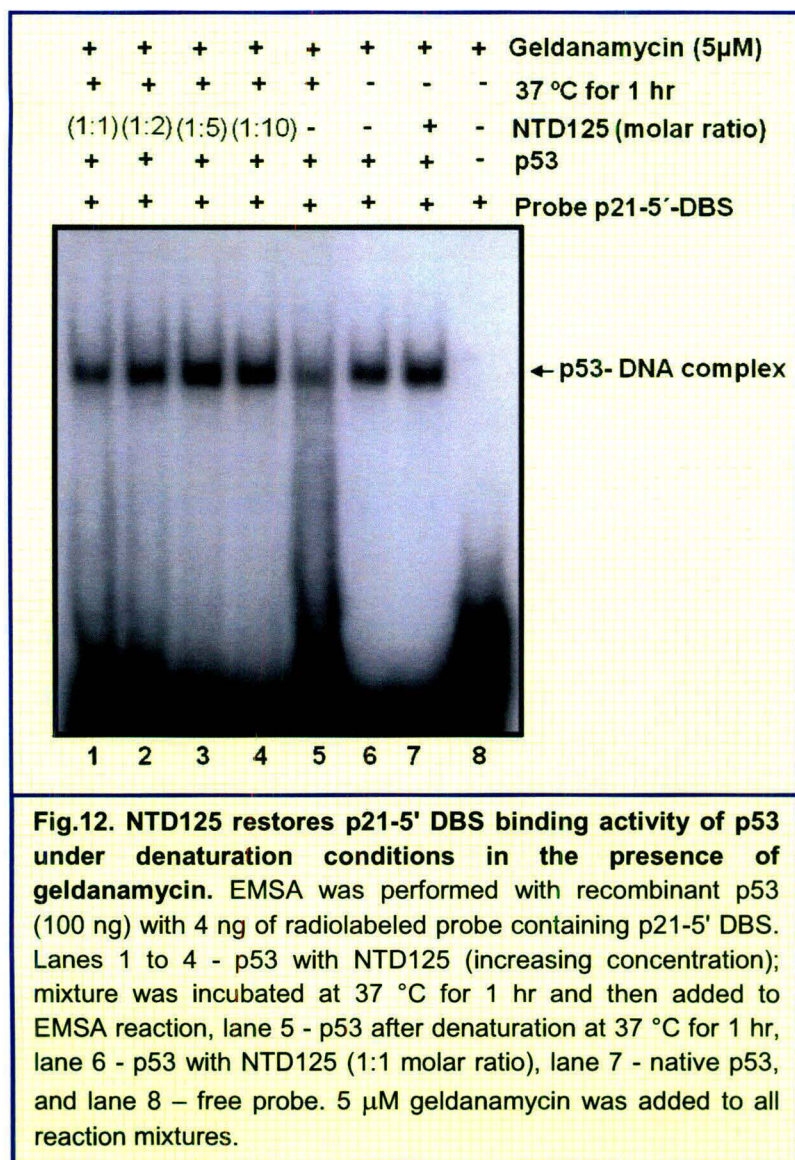
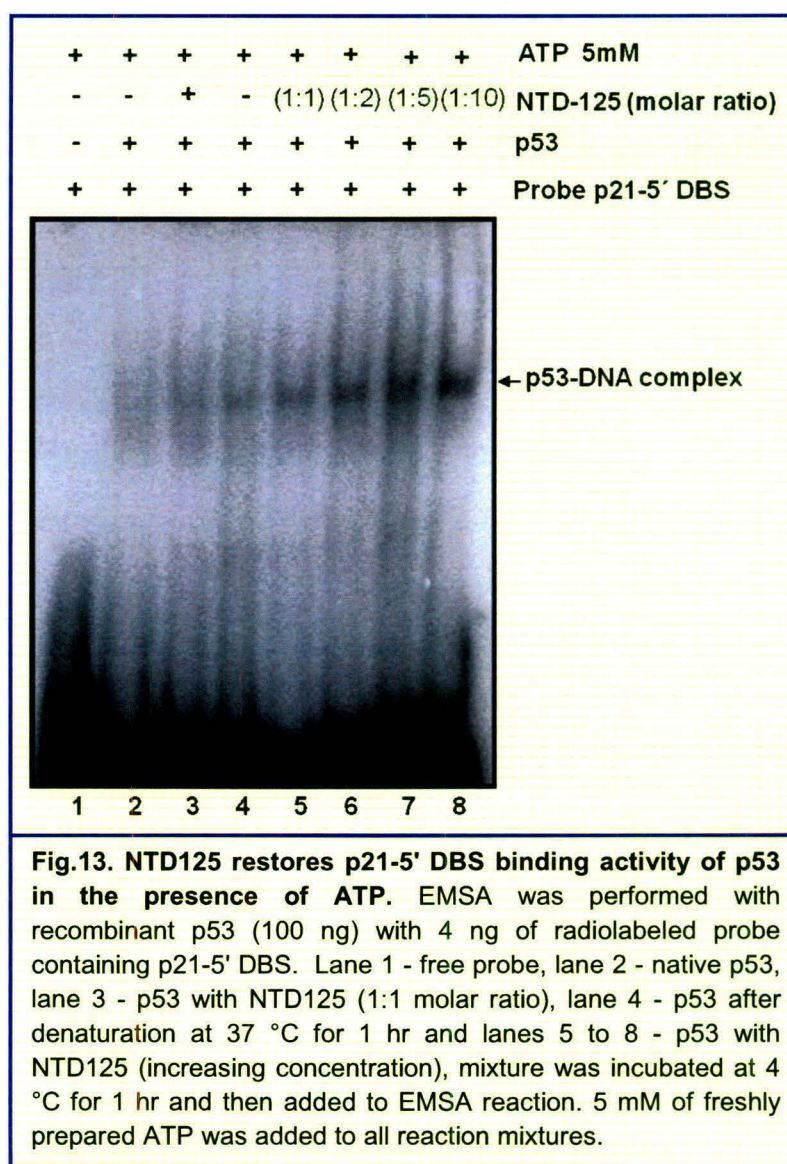


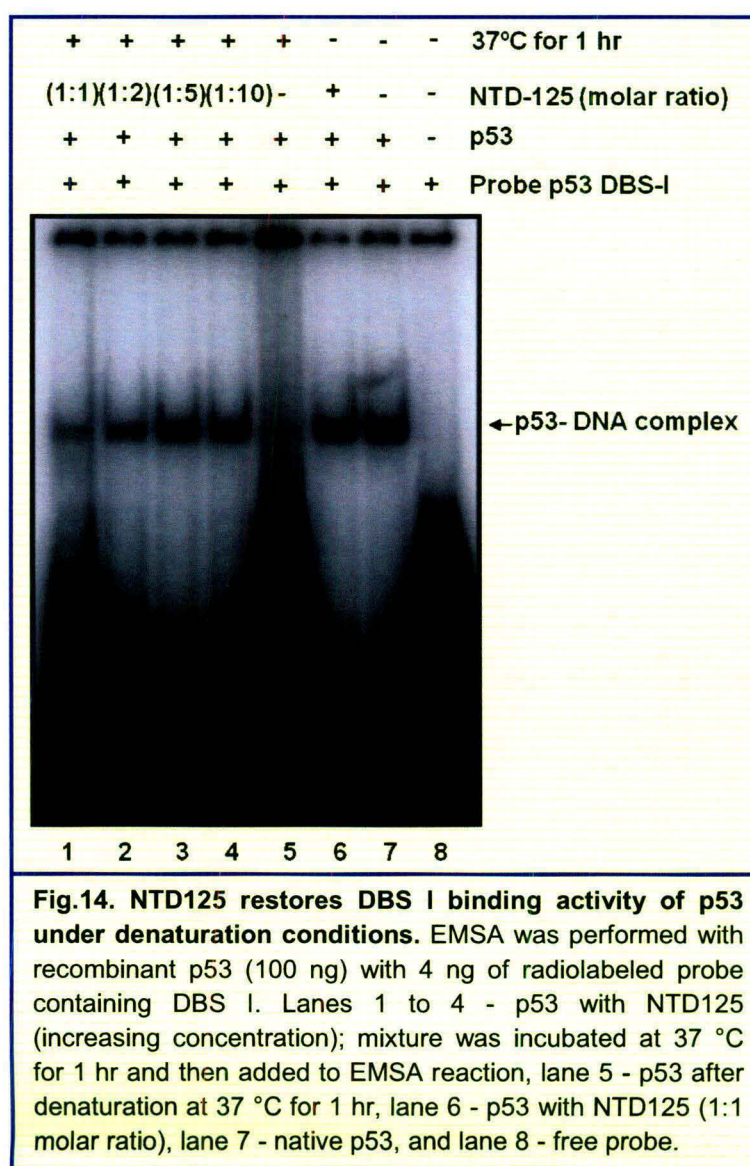
Fig.11. NTD125 restores p21-5' DBS binding activity of p53 under denaturation conditions. EMSA was performed with recombinant p53 (100 ng) with 4 ng of radiolabelled probe containing p21-5' DBS. Lane 1 - free probe, lane 2 - native p53, lane 3 - p53 with NTD125 (1:1 molar ratio), lane 4 - p53 after denaturation at 37 °C for 1 hr and lanes 5 to 8 - p53 with NTD125 (increasing concentration), NTD125 was added post denaturation step and incubated at 4 °C for 1 hr and then added to EMSA reaction.



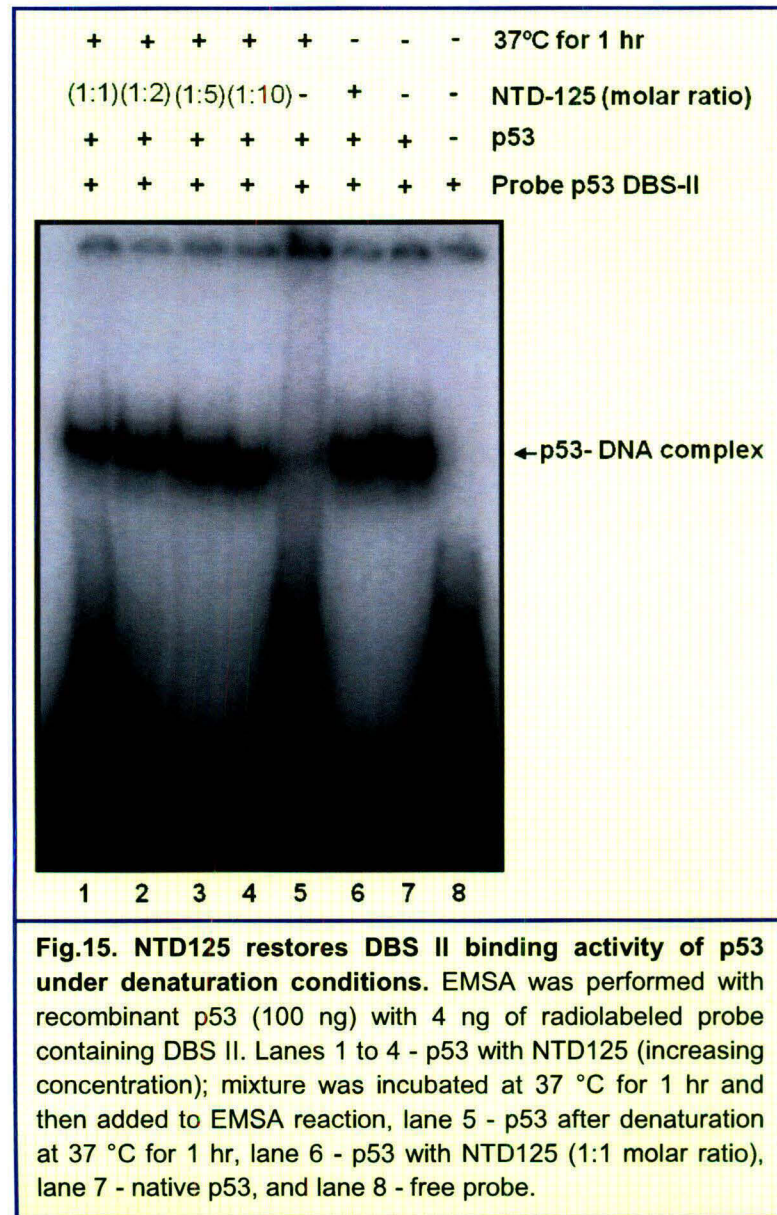
Heat stress is one of the stresses that can abort p53 DNA binding activity by altering its conformation, but there are other factors too which can inhibit p53 activity. While studying the role of ATP/ADP as a switch in regulation of p53-DNA complex; ATP was found to destabilize or abort the binding activity of p53 while ADP stabilizes/enhances the binding (Okorokov and Milner, 1999). Using ATP as inhibitor of p53-DNA binding along with heat denaturation, we observed the effect of NTD125 on p53 binding activity under this condition. NTD125 shows promising recovery of p53 binding activity, which was lost because of ATP (Fig. 13).

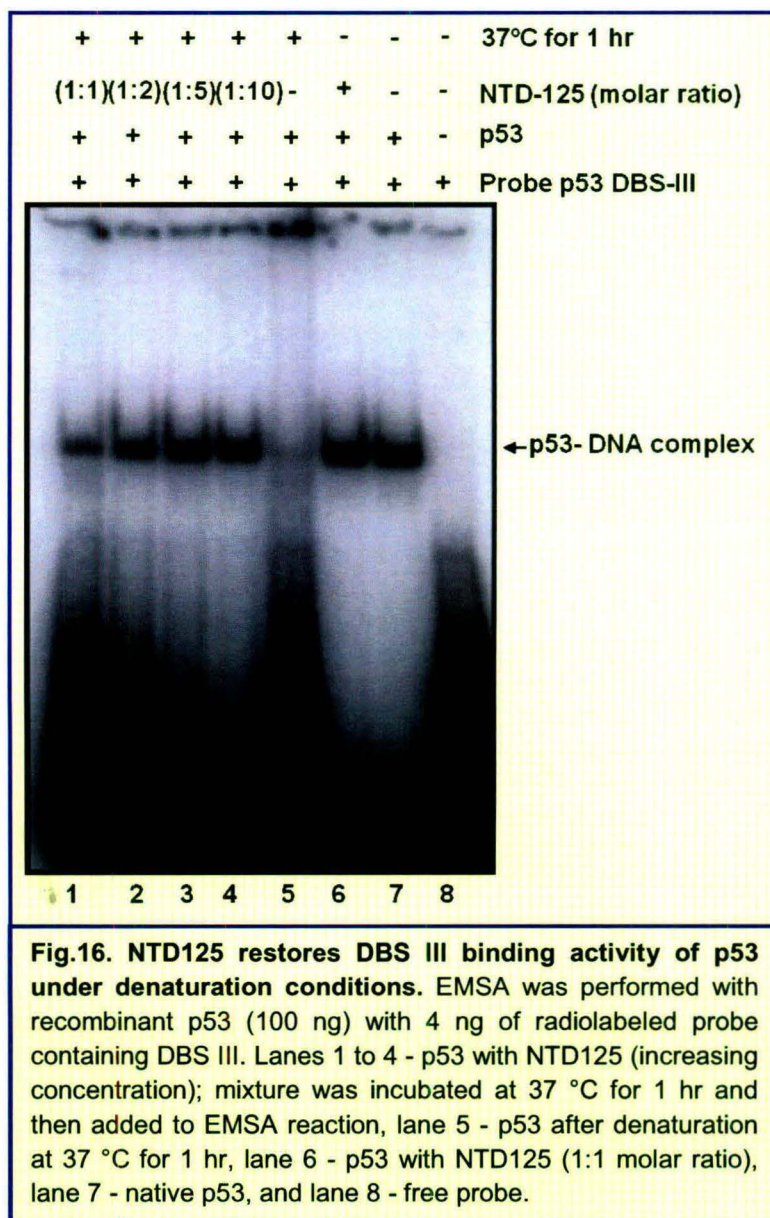


p21-5' DBS is one of the most commonly used site for evaluating p53 binding activity, because this is a full binding site, through which p53 upregulates p21, but there are thousands of predicted p53 binding sites within the human genome (Hoh *et al.*, 2002). Even there are three separate p53 consensus binding sites within p53 promoter through which p53 regulates its own expression (Akaury, 2003; Tripathi *et al.*, 2007). DBS I and DBS III are half sites whereas DBS II is a full consensus binding site. As we were interested in investigating the role of NTD125 in autoregulation of p53 gene, it was very important to establish the role of NTD125 on p53 binding to these DBSs. Thus, we performed EMSA using DBS I, DBS II and DBS III as a probe and reached to the conclusion that NTD125 can restore the DNA binding activity of wild-type p53 regardless of the kind of DBS it is binding



to (Fig. 14, 15 & 16). DBS II showed more prominent binding than DBS I and DBS III. p53 preferred to bind to DBS II, it being a full site. Taken together, these results gave us a clue to further study the effect of NTD125 on wild type p53, *in vivo* and to determine its consequences.





5. Cloning of NTD125, NTD93, NTD61 and NTD55 cDNA in pNHA1 vector-

Dissecting the role of NTD and its sub-regions in conformational regulation of p53, Xirodimas and Lane identified 20 amino acid residues (aa 101-120) in the core domain. This region was shown to be responsible for thermostable phenotype (Xirodimas and Lane, 1999). Similarly, we wanted to identify specific region (domain) responsible for chaperoning activity within 125 residues. For this, we assessed the transition of wild type to mutant phenotype or vice-versa in cultured cells expressing WT p53 with or without external HA-NTD125 or related constructs. Therefore, we cloned full length NTD125 and its deleted mutants NTD93, NTD61, and NTD55 encoding DNA (NTD125, NTD93, NTD61 and NTD55, respectively) in pNHA1-eukaryotic expression vector. pNHA1 plasmid contains a HA-tag at N-terminal of the cloning site, leading to respective HA-tagged constructs.

All NTD constructs were generated by PCR based directional cloning in pNHA1 vector at *XbaI/EcoRI* sites as shown in (Fig. 17). Briefly, pNHA1 vector was digested with *XbaI/EcoRI* restriction enzymes followed by CIP treatment. For insert, primers with *XbaI* (sense) or *EcoRI* (antisense) restriction site were synthesized and employed for PCR amplification of respective inserts from pNHA1-p53 plasmid. Amplified fragments were also digested with *XbaI/EcoRI* and gene cleaned. Subsequently, ligation was carried out at 1:5 :: vector: insert ratio. After transformation of the ligated mix, no colony was obtained in empty vector ligation and with insert, 12, 28, 19 and 11 colonies were obtained, respectively. 4 to 5 colonies from each set were screened by restriction digestion analysis and all were found to be positive for insert (Fig. 17).

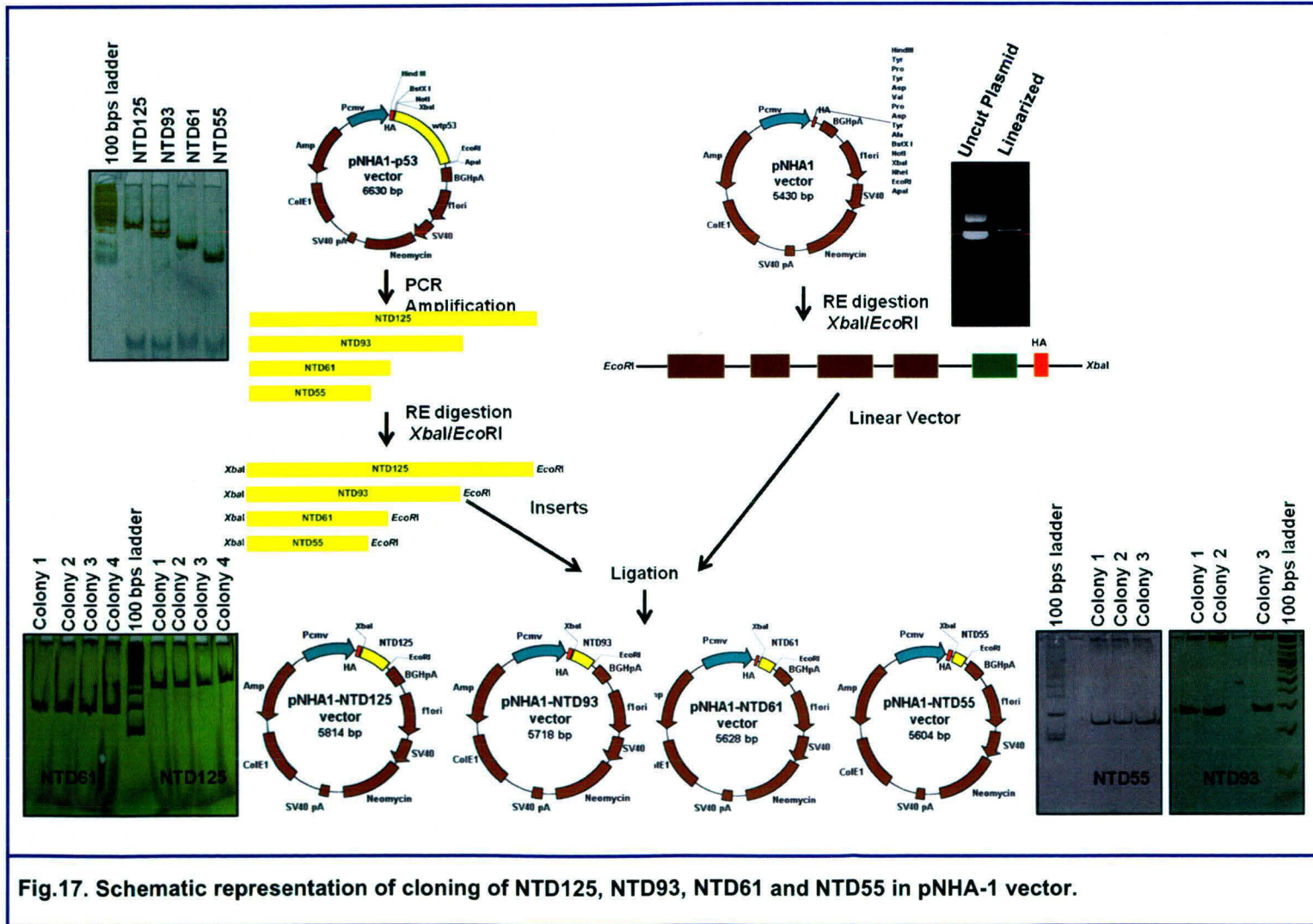
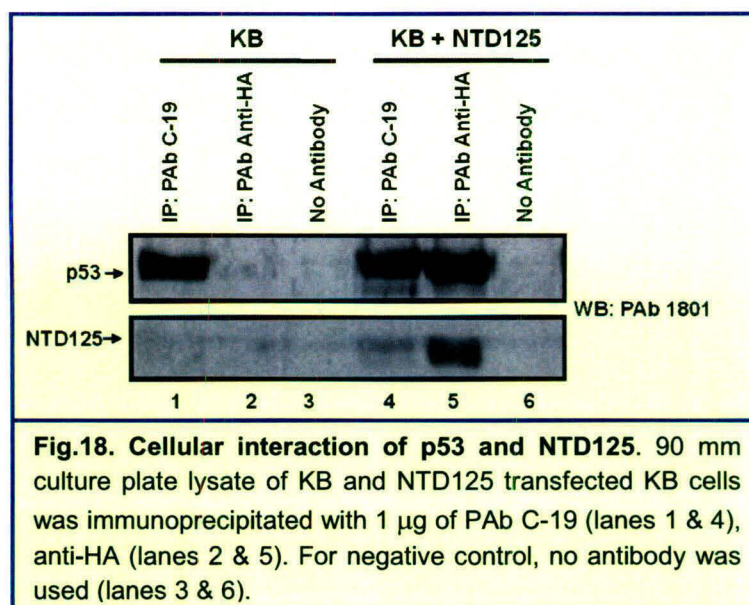


Fig.17. Schematic representation of cloning of NTD125, NTD93, NTD61 and NTD55 in pNHA-1 vector.

6. NTD125 interacts with p53 in cell-

We have shown that NTD125 interacted with p53 *in vitro*. The interaction between NTD (1-186) and CTD (187-393) in cells was shown (Okorokov *et al.*, 2006), and a low energy complex between CTD (361-382) and PRD (80-93) was predicted earlier (Kim *et al.*, 1999). We also wanted to know whether NTD125 could interact with WT p53 *in vivo*; in a complex cellular environment. Co-immunoprecipitation of p53 and NTD125 from pNHA1-NTD125 transfected KB cells using PAb C-19 and anti-HA antibodies, confirms the intermolecular interaction of both the proteins *in vivo*. Untransfected KB cells were used as negative control (Fig. 18). Here we observed that NTD125 precipitated to a lesser extent in comparison to p53 using PAb C-19 (lane 4), whereas more p53 was immunoprecipitated using anti-HA antibodies together with NTD125. This could be because not all the p53 molecules precipitated by PAb C-19 were in complex with NTD125. In contrast, all NTD125 molecules precipitated by anti-HA antibodies were occupying p53 molecules. In addition, competition between NTD125 and PAb C-19 might be responsible for such results because both interact within the C-terminus of p53. ELISA results also confirmed that NTD125 interacted within C-terminal region (CTD) of p53 (Sharma *et al.*, 2009).

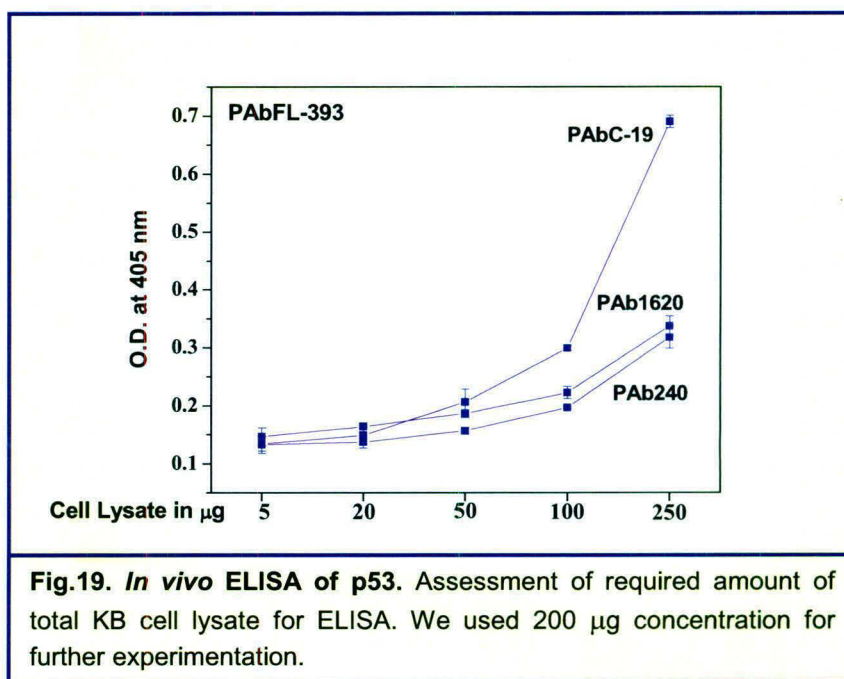


7. NTD125 also protects wild type conformation of endogenous p53 in cell-

The observations that NTD125 could restore p53 DNA binding activity even under denaturing conditions and was able to protect wild type phenotype of bacterially expressed p53 at higher temperature led us to investigate the *in vivo* consequences of p53 and NTD125 interaction on p53 conformation in cellular milieu. Wild type p53 exists in very low levels in normal growing cells and stays mostly in an inactive latent form. Its levels rise under stresses or unfavorable conditions (Levine, 1997). p53 has a short cellular half-life of ~30 mins however it increases to hrs during stress and DNA damage (Maltzman *et al.*, 1984). The increase in p53 level is necessary in response to stress and any damage caused to cells, so there exist multiple pathways to stabilize p53 in response to different forms of stress (Ashcroft *et al.*, 2000).

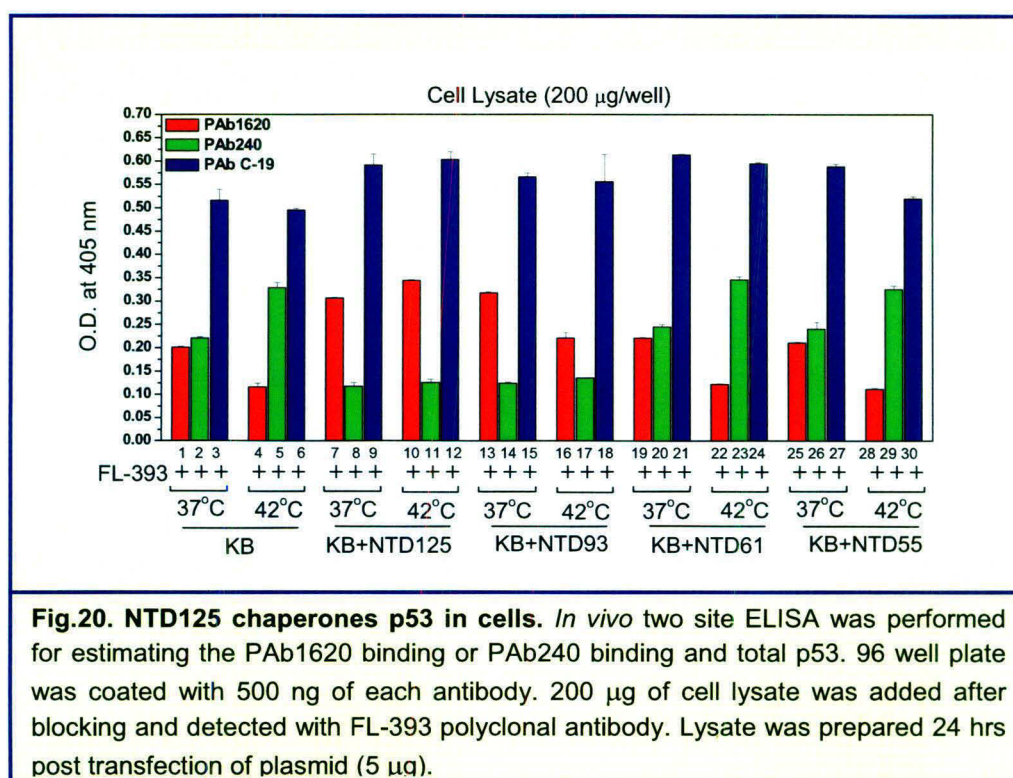
- i) Post translational modifications that activate p53 in response to stress e.g. DNA damage (Sakaguchi *et al.*, 1998); phosphorylation is the one of the most important post translational modifications that mostly occurs within p53-NTD. It also modulates the conformation of p53 to transcriptionally active form and allows the binding of proteins like p300, which help in transcriptional regulation (Grossman, 2001).
- ii) The conversion of latent form of p53 to active form by changing the conformation from mutant to wild-type; this process mostly involves molecular chaperones of cellular system and helps p53 to maintain wild type conformation even at higher temperatures and cause the nuclear translocation of p53 (Tripathi *et al.*, 2007; Wawrzynow *et al.*, 2007).
- iii) At the transcriptional level, upregulation of p53 gene and expression can yield higher levels of p53 protein.

In vivo two site ELISA is employed for estimating various conformation of p53 in cells (Liu *et al.*, 2001). We also used the technique and found that ~200 µg of cell lysate is most appropriate to compare between the different conformation (PAb1620 and PAb240 coated wells) in contrast to total p53 (PAb C-19 coated wells) in our system (Fig. 19). To assess the effect of NTD125 on p53 conformation in cells, we transfected pNHA1-NTD125 in KB cells having a



characteristic 1:1 ratio of wild phenotype and mutant phenotype of WT p53 under normal growing conditions. Under heat stress (42 °C for 70 mins) this equilibrium shifted towards PAb240 binding form; depleting PAb1620 binding form (Tripathi *et al.*, 2007). But, when NTD125 expressing cells were subjected to heat shock treatment for 70 mins, there was not only a total gain of PAb1620 binding form but also increase in total concentration of p53; at the same time, a decrease in the PAb240 binding form was evident through *in vivo* (two site) ELISA (Fig. 20).

This suggests that NTD125 favors PAb1620 conformation and can bind to p53 either before folding leading to more wild type conformation or binds to mutant conformation converting it to wild type. Function of NTD125 is similar to that of molecular chaperones in stabilizing p53 wild phenotype. Further, to locate region responsible for this chaperone like activity within NTD, different NTD deletion constructs (NTD93, NTD61 and NTD55) were expressed in KB cells, which were subjected to *in vivo* ELISA. Result yielded that even NTD93 retained PAb1620 stabilizing properties but this feature was only intact at 37 °C temperature. NTD93 could not stabilize p53 wild conformation as efficiently as NTD125 under heat shock condition. On the other hand, NTD61 and NTD55 completely lack chaperone-like stabilizing activity (Fig. 20).



Further, to re-confirm our finding, we also performed immunoprecipitation assay using conformational antibodies (PAb1620 and PAb240) utilizing KB cell lysate after transfecting different NTD constructs (NTD125 and deletion constructs). Cells were transfected with 5 µg of expression vectors and 24 hr post-transfection, processed for lysate preparation. Untransfected KB cells were utilized for internal controls. In immunoprecipitation, we found that NTD125 not only protected wild-type conformation but also promoted it both under normal and heat stress conditions in comparison to only KB cells. Simultaneously, NTD125 also suppressed mutant phenotype of endogenous p53 even under heat stress conditions. Although, NTD93 was capable of protecting wild-type conformation under normal conditions, it did not protect wild form under heat stress condition. NTD55 and NTD61 do not show any protection towards wild type conformation. Hence, only NTD125 was able to chaperone p53 at physiologically higher temperature (Fig. 21).

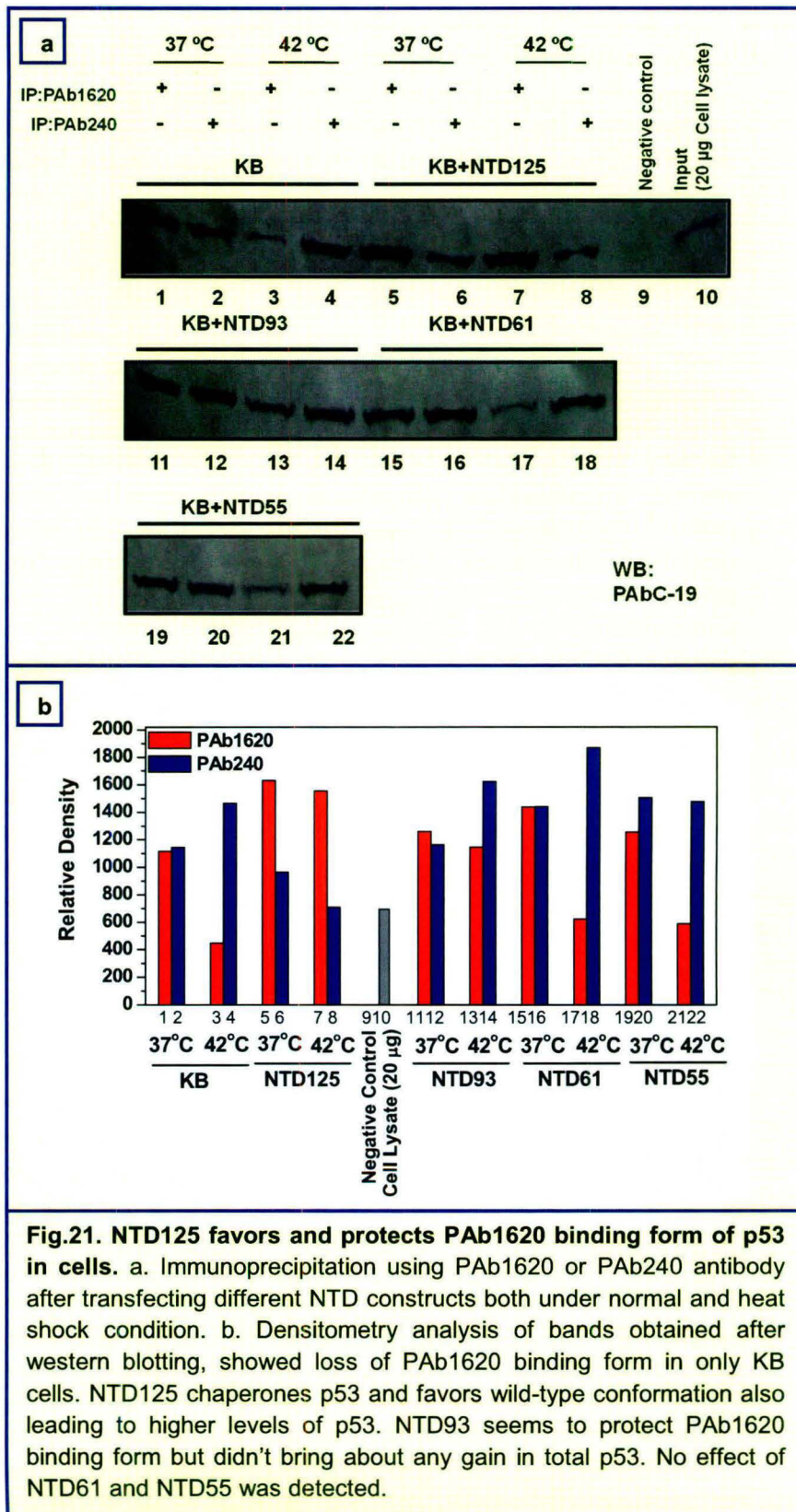


Fig.21. NTD125 favors and protects PAb1620 binding form of p53 in cells. a. Immunoprecipitation using PAb1620 or PAb240 antibody after transfecting different NTD constructs both under normal and heat shock condition. b. Densitometry analysis of bands obtained after western blotting, showed loss of PAb1620 binding form in only KB cells. NTD125 chaperones p53 and favors wild-type conformation also leading to higher levels of p53. NTD93 seems to protect PAb1620 binding form but didn't bring about any gain in total p53. No effect of NTD61 and NTD55 was detected.

8. NTD125 stabilizes p53 protein levels and quenches MDM2-

p53 protein level is tightly regulated inside cells; increasing levels of p53 protein are regulated through lengthening of its half life. The level of p53 and its activity in the cell depends on the cell's situation and extracellular stimuli. We employed western blotting for checking the p53 protein levels in transiently NTD125 expressing KB cells and KB cells that were stably expressing NTD125. Cells were lysed in RIPA buffer and protein was resolved on 12 % SDS-PAGE and western blotted on to nitro cellulose membrane. Blots were developed using anti-p53 (PAb1801) and anti-actin antibodies. In case of transient transfection, we noticed increase in p53 protein level in dose dependent manner and 5 μ g DNA transfection resulted in \sim 4 fold higher p53 level in comparison to untransfected cells (Fig. 22).

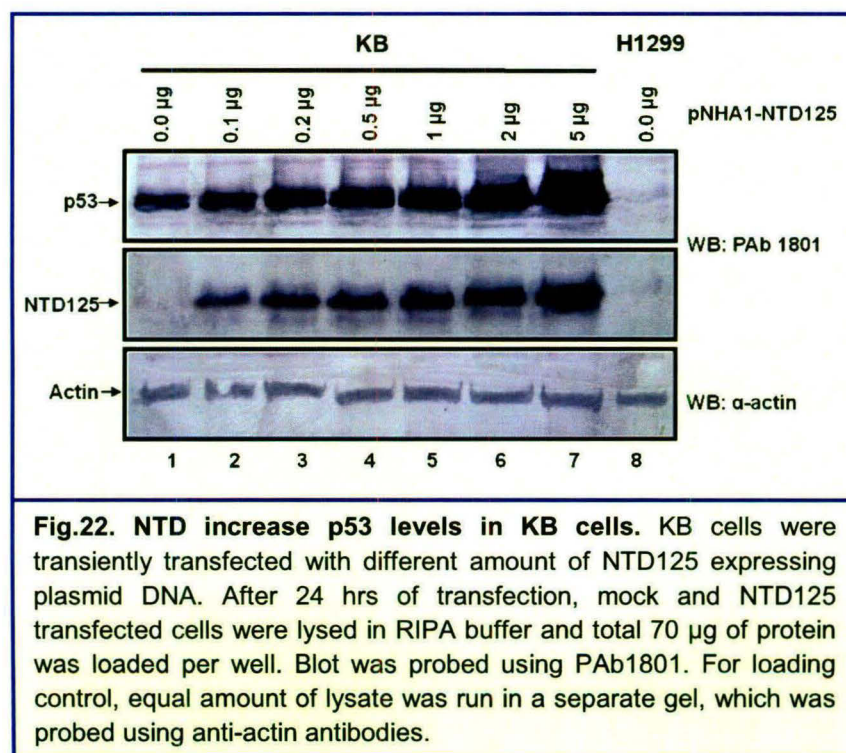
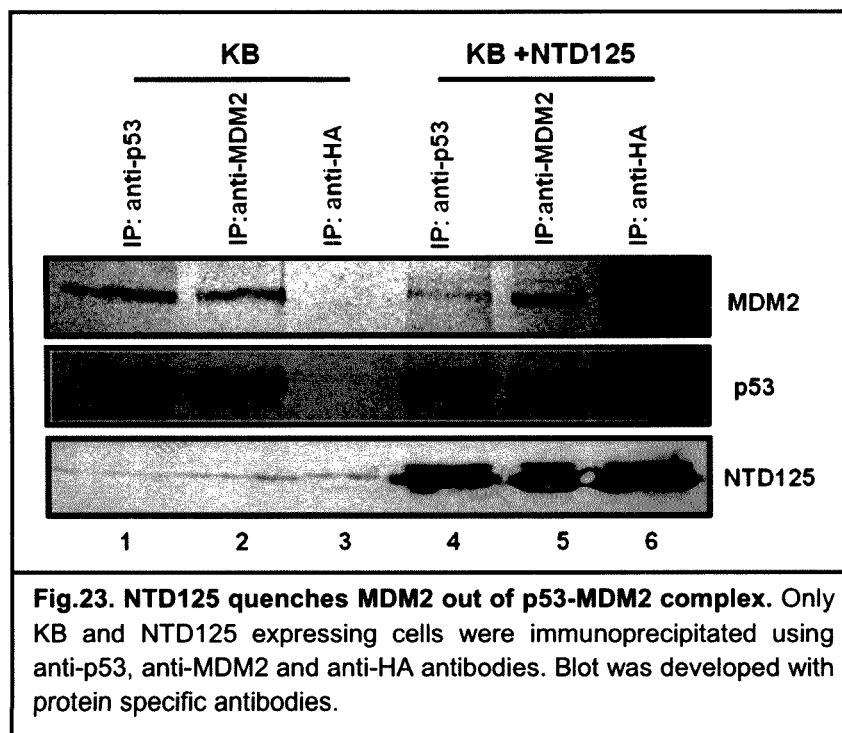


Fig.22. NTD increase p53 levels in KB cells. KB cells were transiently transfected with different amount of NTD125 expressing plasmid DNA. After 24 hrs of transfection, mock and NTD125 transfected cells were lysed in RIPA buffer and total 70 μ g of protein was loaded per well. Blot was probed using PAb1801. For loading control, equal amount of lysate was run in a separate gel, which was probed using anti-actin antibodies.

The regulation of p53 level and activity involves a multitude of cellular proteins. p53 activity and its stabilization are also highly governed through complex networks of post-translational modifications and cytoplasmic sequestration (Oren, 1999, Vogelstein *et al.*, 2000; Vousden and Lu, 2002; Bode and Dong, 2004). MDM2 is one of the prime transcriptional targets of p53 in cellular system and is known to regulate p53 level in feedback manner. While p53 upregulates

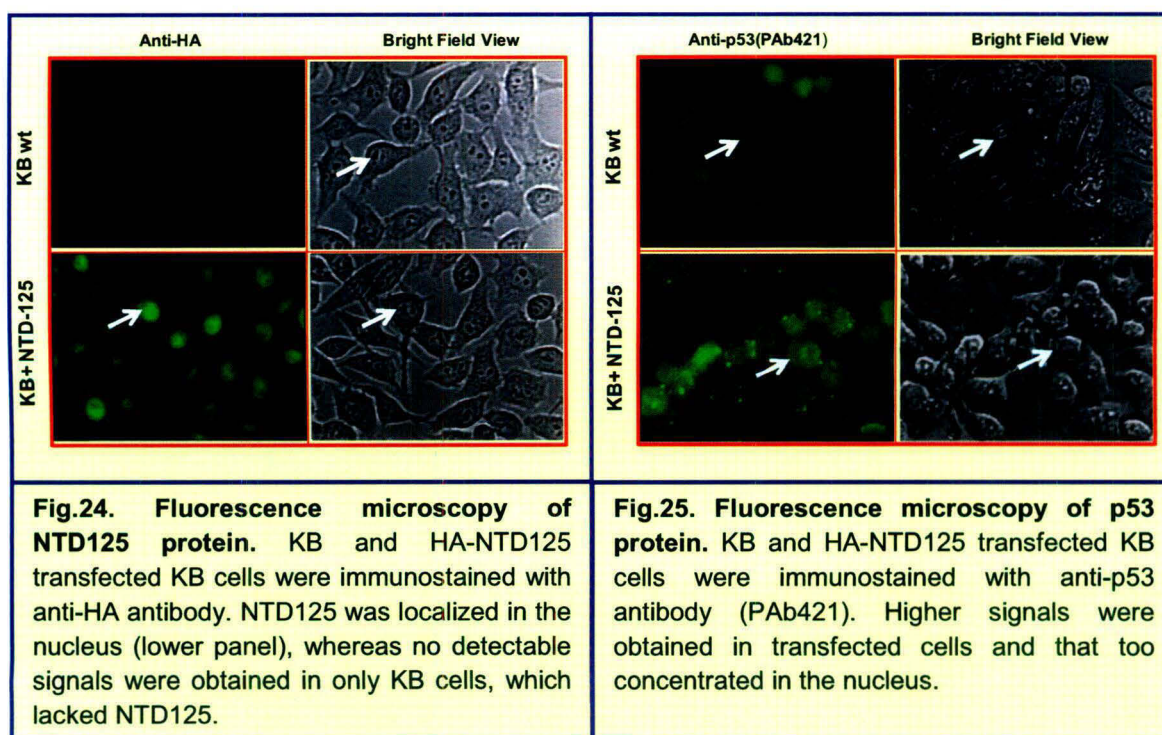
transcription of MDM2; MDM2 degrades p53 via ubiquitination (Zauberman *et al.*, 1995; Lahav, 2008). Recently, MDM2 was also reported to chaperone p53 (Wawrzynow *et al.*, 2007). As MDM2 plays crucial role in controlling p53 level and over-expression of MDM2 was reported to induce cancer by inhibiting p53 function by degrading it. It was very important to study the interaction of MDM2 with p53 and NTD125 simultaneously because NTD125 contains the MDM2 binding region of p53. For checking the same, we did immunoprecipitation from cell lysate using anti-p53, anti-MDM2 and anti-HA antibodies followed by developing the blot with p53, MDM2 and HA specific antibodies. Western blot showed the precipitation of MDM2 with p53 and vice-versa, whereas no band was observed in anti-HA antibodies lane. In NTD125 transfected cells, anti-p53 antibodies were not able to pull much MDM2 with p53 rather they pulled more NTD125 with it; similarly MDM2 pulled more NTD125 in comparison to p53 using anti-MDM2 antibodies. Whereas anti-HA antibodies pulled both p53 and MDM2 with NTD125 (Fig. 23). These results indicate that NTD125 quenched MDM2 from p53-MDM2 complex or vice-versa; thus not allowing two to interact at their natural strength. Therefore, NTD125 quenched MDM2 from the system and didn't allow MDM2 to degrade p53 efficiently, finally leading to higher levels of p53 in NTD125 expressing cells.



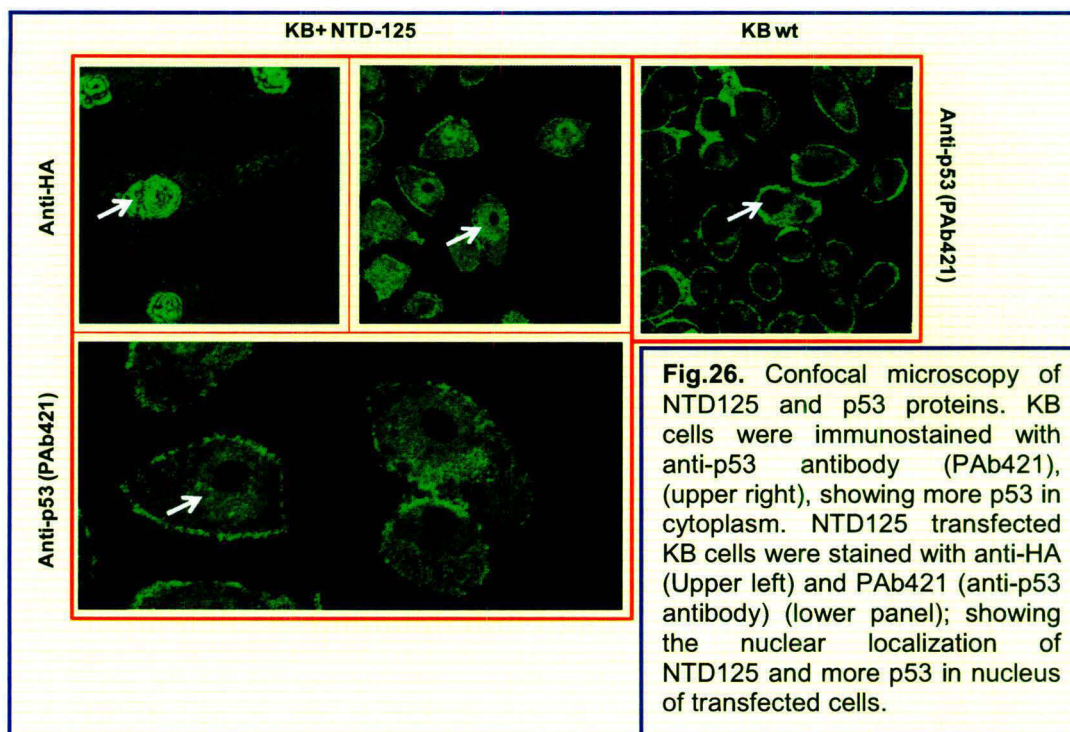
9. NTD125 localizes in the nucleus-

p53 is a phospho-nuclear protein and found to accumulate in the nucleus under stress conditions. Different pathways are reported for the translocation of p53 from cytoplasm to nucleus. Presence of nuclear localization signals in the C-terminus of p53 is one of the ways by which its translocation is regulated (Shaalsky *et al.*, 1990; Liang and Clarke, 2001). Other reports state the role of phosphorylation and other post-translational modifications (due to stress) in stabilization and nuclear export of active p53. The latent and active form based i.e. conformation dependent translocation of p53 from cytoplasm to nucleus has been recently proved; whereby wild-type active form resides in the nucleus (Wawrzynow *et al.*, 2007). However, in all these possible pathways, WT p53 is required except few mutants that can also accumulate in the nucleus.

To localize NTD125 inside the cell, we transfected HA-tagged NTD125 in to KB cells and after 24 hrs, cells were processed for immunofluorescence staining using anti-HA antibodies as primary and FITC-labeled anti-mouse antibodies as secondary antibodies. Immunofluorescence analysis clearly indicated the presence of NTD125 within the nucleus at higher levels than cytoplasm (Fig. 24).



Simultaneously, we also checked the localization of p53 protein in NTD125 expressing and control KB cells. Cells were immunostained using PAb421 as a primary and FITC-labeled anti-mouse antibodies as secondary antibodies. NTD125 expressing cells displayed more p53 signals in nucleus in comparison to only KB cells (Fig. 25). Confocal microscopic studies also showed the similar result (Fig. 26). These results showed that NTD125 mediated stabilization of wild phenotype of p53 led to the nuclear localization of p53. CHIP was identified as a

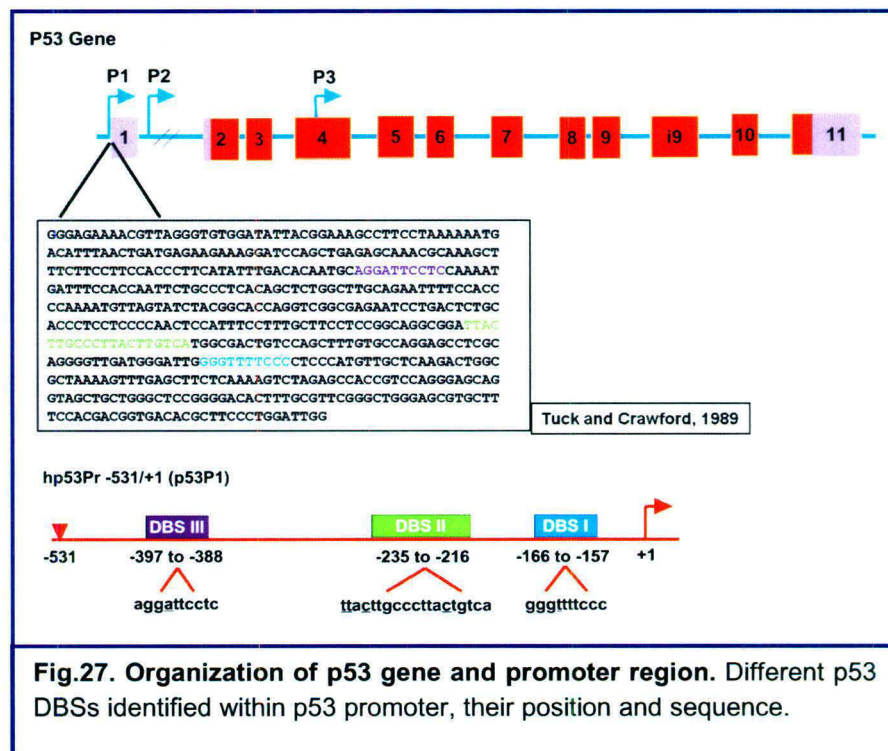


direct chaperone of p53 and specifically interacted with mutant conformation of p53 at physiologically higher temperature thereby converting it to wild type conformation; wild conformation helped p53 to remain in nucleus in higher levels (Tripathi *et al.*, 2007). Recent addition to p53-associated chaperones is MDM2; studies carried out with MDM2 also confirmed the presence of PAb1620 conformation in the nucleus (Wawrzynow *et al.*, 2007). Thus, NTD125 interaction could also initiate p53 nuclear translocation, however total amount of NTD125 localized in nucleus was much higher than p53. It may be possible that NTD125 could diffuse in to the nucleus passively; there are reports confirming that more than 60 kDa proteins can passively diffuse through the nuclear pore complex, in and out of nucleus (Wang and Brattain, 2007). Other possibilities also exist, whereby other p53-NTD interacting nuclear proteins can assist NTD125

translocation to nucleus. Thus, in NTD125 expressing cells, NTD125 localized in nucleus and initiated p53 nuclear transport.

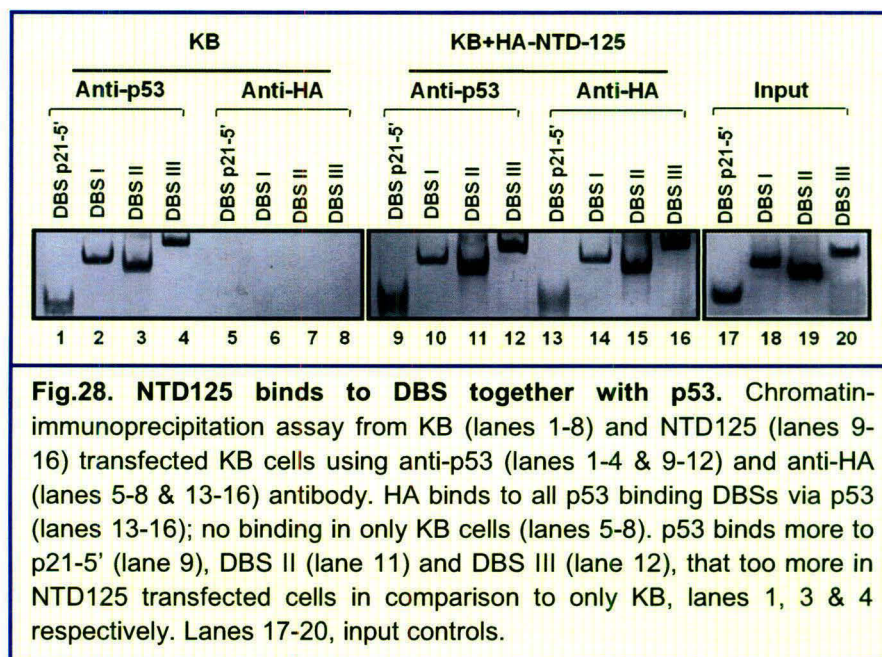
10. NTD125 activates p53 gene transcription-

p53 is a DNA sequence specific transcriptional factor and transactivates genes containing p53 response elements (REs) or consensus DNA-binding site/s (DBS). Three p53 DBSs were also identified within p53 promoter (DBS II; -216 to -235, class I whereas DBS I; -157 to -166 and DBS III; -388 to -397, class II) (Fig. 27) that independently control p53 expression (Tiwari, 2003). As NTD125 interacted with p53 and localized in the nucleus, we wanted to explore whether NTD125 can modulate p53 activity to transactivate its own expression by binding to these DBSs together with p53.



First, to determine the simultaneous promoter occupancy by p53 and NTD125 in genome, we performed chromatin-immunoprecipitation (ChIP) assay using both anti-p53 and anti-HA antibodies in KB and HA-NTD125 expressing KB cells. ChIP is the best way to identify direct/indirect protein-DNA interaction in native cellular conditions. Results clearly show the presence of NTD125 on all three p53 DBSs in NTD125 expressing cells together with p53 (Fig. 28). Data also revealed

that in NTD125 expressing cells, p53 differentially binds more to DBS II and DBS III, and less to DBS I along with NTD125. p21-5' DBS was taken as a positive control for p53 binding.



ChIP assay confirmed the presence of NTD125 on p53 binding sites within p53 promoter along with p53. NTD125 also promoted the PAb1620⁺ conformation of p53 in the cells and localized p53 in nucleus; therefore to ascertain a possible role of p53 conformations in differential DBS selection, we performed ChIP assay using conformational specific antibodies. Assay was done with normal, heat stressed and NTD125 expressing KB cells. Result showed the presence of more PAb1620 binding conformation on DBS II and DBS III in NTD125 expressing cells; even under heat stress conditions more PAb1620 form targeted to DBS II and DBS III in comparison to PAb240. However, no significant difference between the two antibodies was observed (Fig. 29). To our surprise, preferential selection of DBS III under heat shock condition seemed to be remarkable and could be interesting to explore it in more details. Thus, we wanted to discern how the differential DBS selection affects the expression of p53 gene.

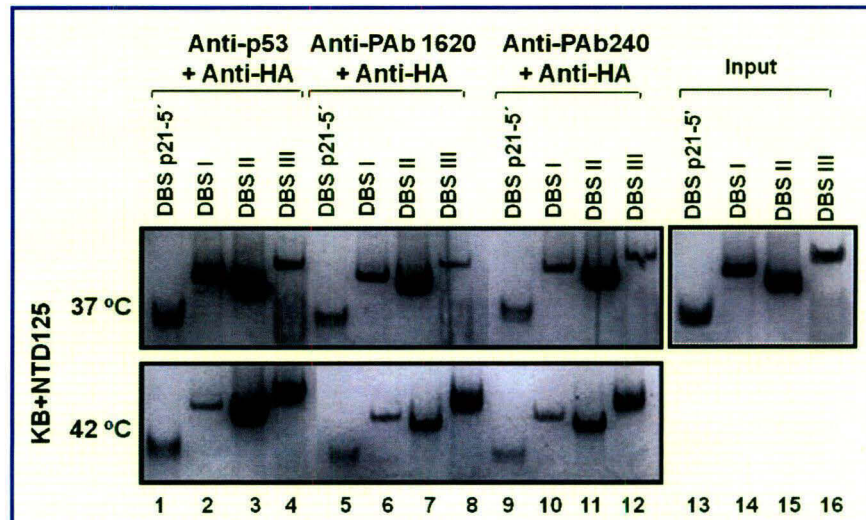


Fig.29. Differential DBS selection under heat stress conditions. ChIP assay shows that p53 preferentially binds more to DBS II and DBS III (lanes 3 & 4) under heat stress condition; upper panel vs lower panel, whereas less p53 binds to DBS I (lane 2, upper panel vs lower panel). Similarly PAB1620 and PAB240 binding forms show more binding with DBS III (lanes 8 & 12) after heat stress but no difference in binding specificities between PAB1620 and PAB240 binding forms (lanes 6 to 8 vs 9 to 12) could be detected. Lanes 13-16 input controls.

Earlier studies stated that p53 could repress and transactivate its own expression in cell type specific manner (Akhaury, 2003; Tripathi *et al.*, 2007) and there might exist a negative feedback regulation of wild-type p53 on its own synthesis

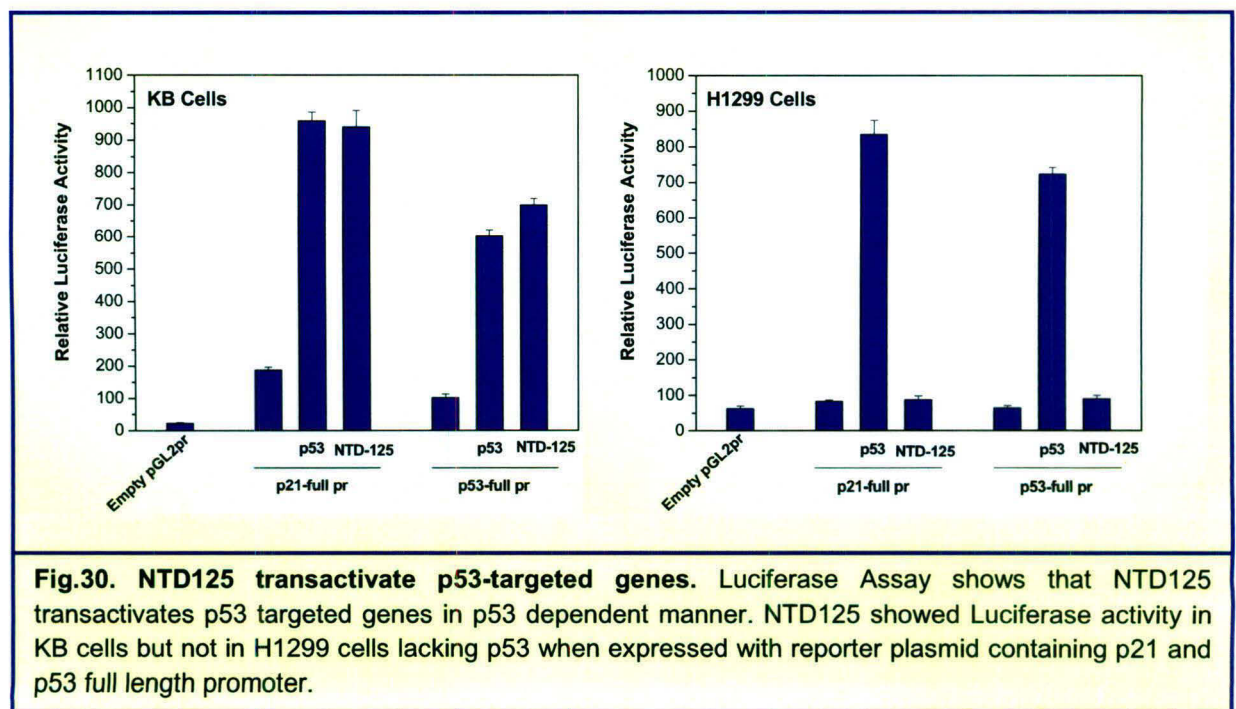
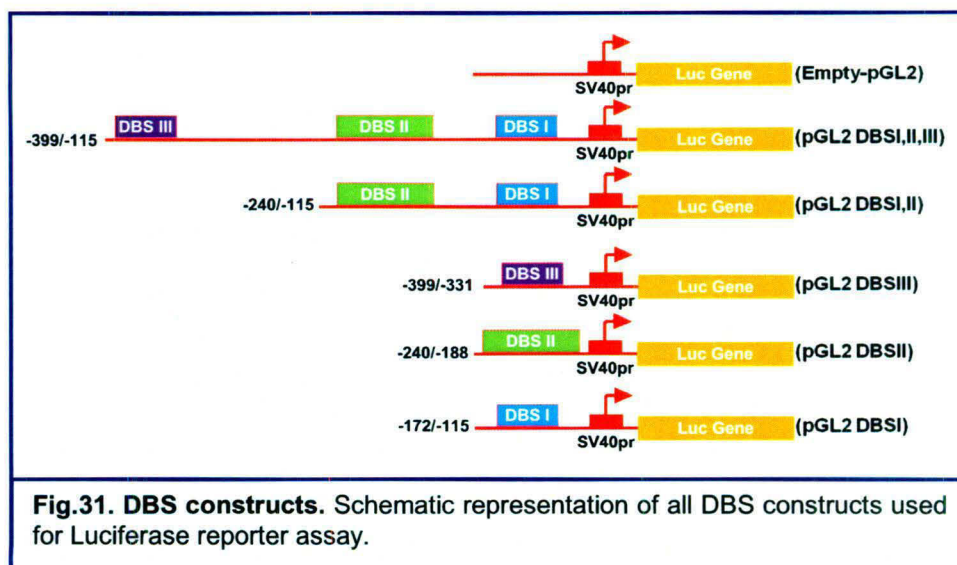


Fig.30. NTD125 transactivate p53-targeted genes. Luciferase Assay shows that NTD125 transactivates p53 targeted genes in p53 dependent manner. NTD125 showed Luciferase activity in KB cells but not in H1299 cells lacking p53 when expressed with reporter plasmid containing p21 and p53 full length promoter.

(Mosner, 1995). In addition, a recent study confirms p53 and p73 dependent p53 activation via DBS selection and supports the p53-mediated autoregulation of p53 transcription (Wang and El-Deiry, 2006). To determine the role of NTD125 in p53 mediated transcriptional regulation, we expressed NTD125 in KB cells (p53^{+/+}) and H-1299 cells (p53^{-/-}) together with constructs containing full-length promoter of p21 and p53 gene in a luciferase reporter vector. Results showed that NTD125 could transactivate p53-targeted genes in p53-dependent manner; NTD125 showed no luciferase activity in H1299 cells (Fig. 30).

Therefore, to probe the role of NTD125 in autoregulation of p53 expression by modulating p53 at DBS or through differential selection of DBSs; we used reporter based luciferase assay with individual sites and combination of these sites. DBS II and DBS III of p53 promoter were PCR amplified and cloned in pGL2-promoter vector at *Kpn*I and *Bgl*III restriction sites as shown in Fig. 31 (DBS I, DBS I,II and minimal promoter clones were reported earlier; Akhaury, 2003). Clones were screened by PCR amplification, restriction digestion analysis and subsequently confirmed by sequencing (Schematic diagram and chromatogram in Fig. 32 and 33). pGL2-promoter vector containing different regions i.e. pGL2-DBS I, pGL2-DBS II, pGL2-DBS III, pGL2-DBS I,II and pGL2-DBS I,II,III were transfected alone and with p53 or NTD125 expressing plasmids. DBS-I was found to repress the luciferase gene in p53 dependent manner (with p53 expression plasmid), showing the negative regulation whereas



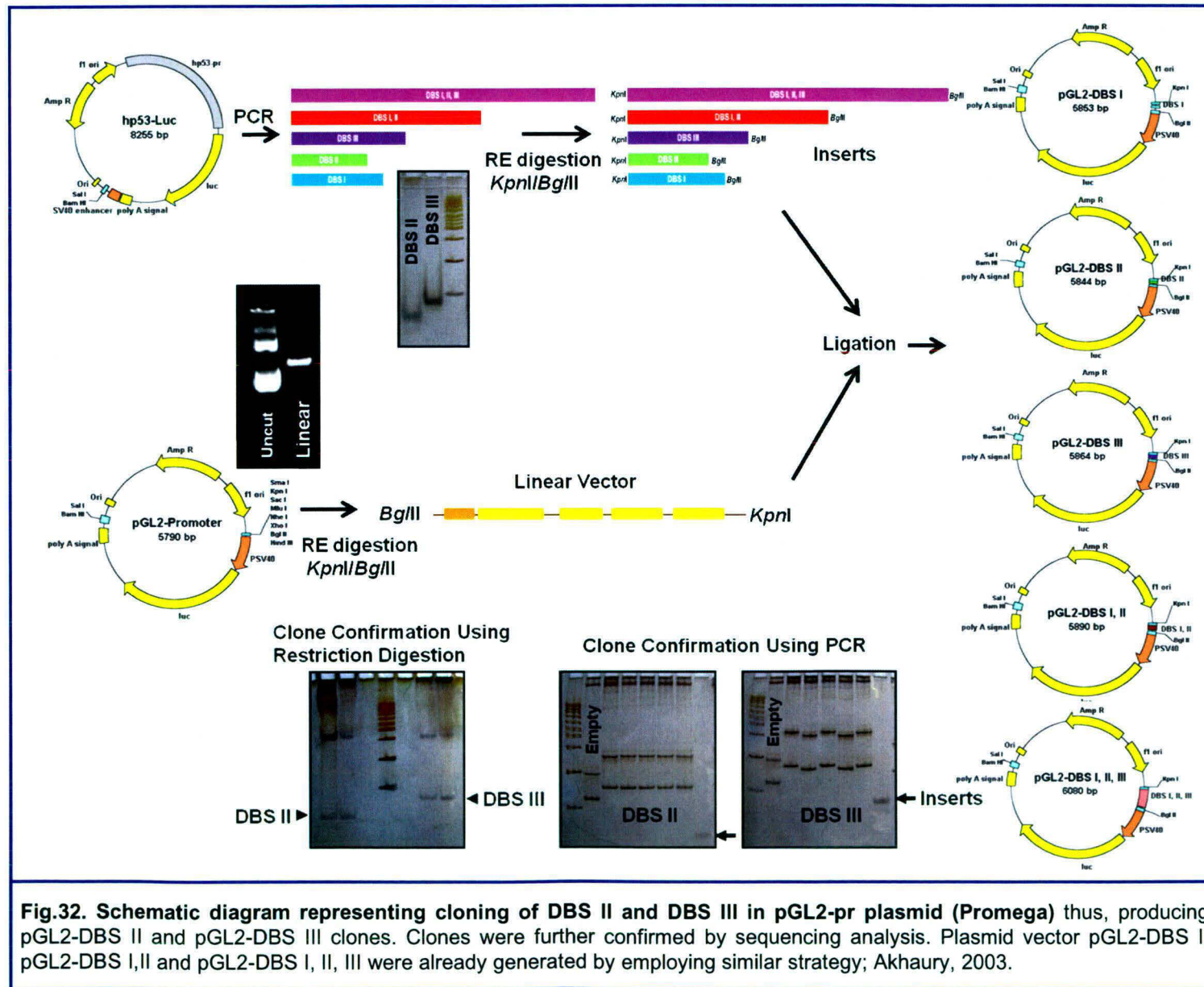


Fig.32. Schematic diagram representing cloning of DBS II and DBS III in pGL2-pr plasmid (Promega) thus, producing pGL2-DBS II and pGL2-DBS III clones. Clones were further confirmed by sequencing analysis. Plasmid vector pGL2-DBS I, pGL2-DBS I,II and pGL2-DBS I, II, III were already generated by employing similar strategy; Akhaury, 2003.

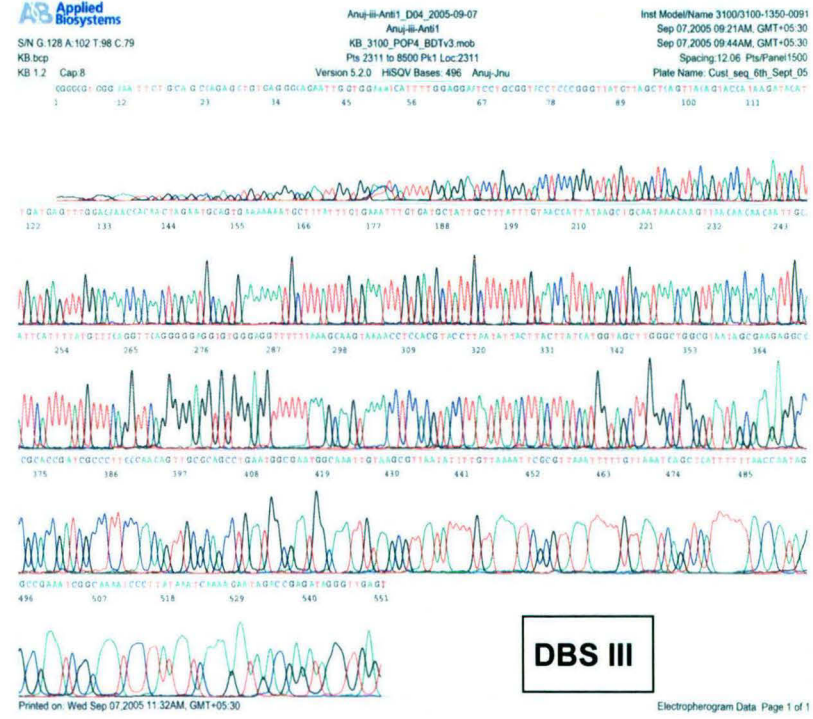
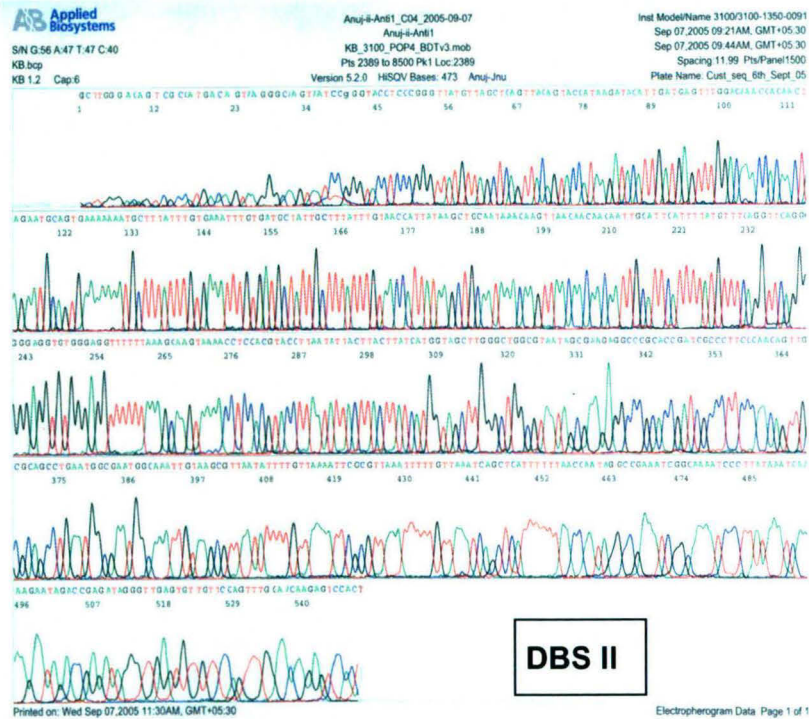
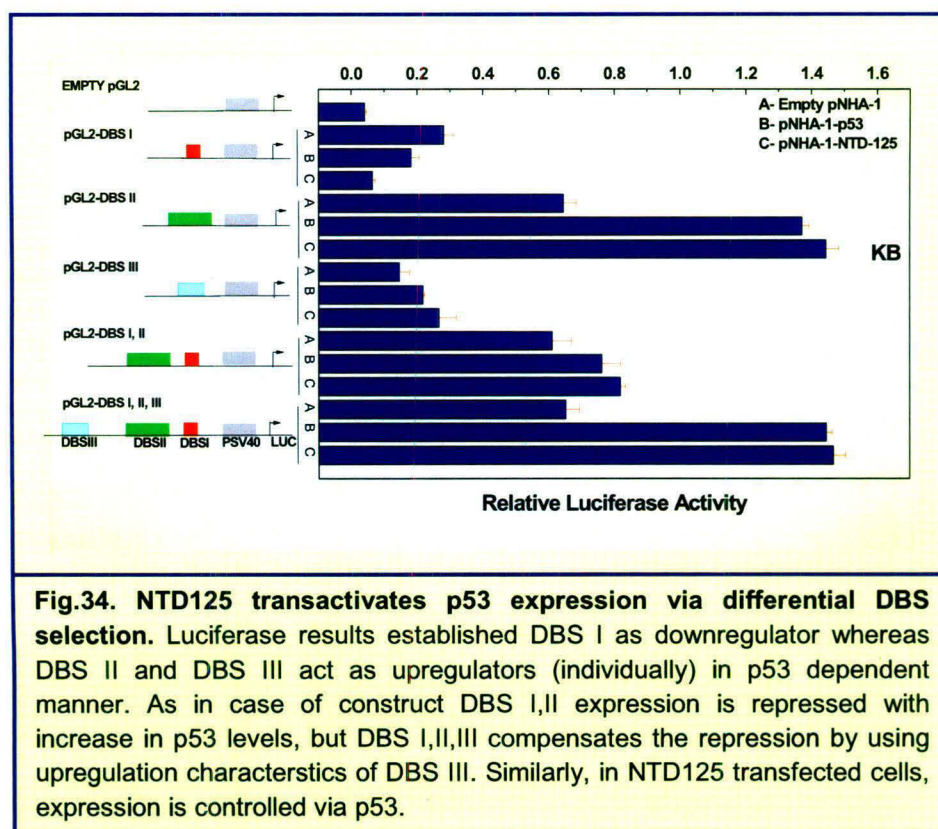


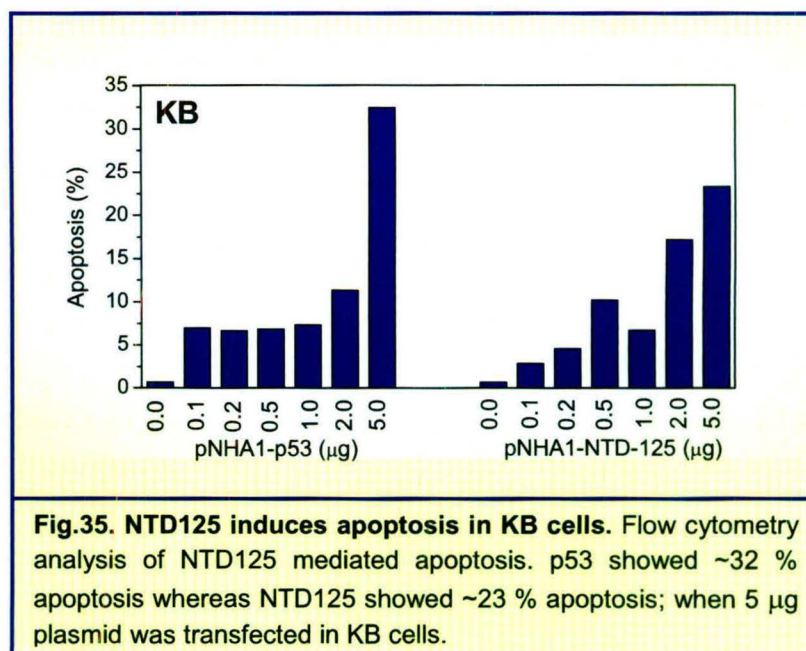
Fig.33. Chromatograms of sequences of pGL2-DBS II and pGL2-DBS III clones.

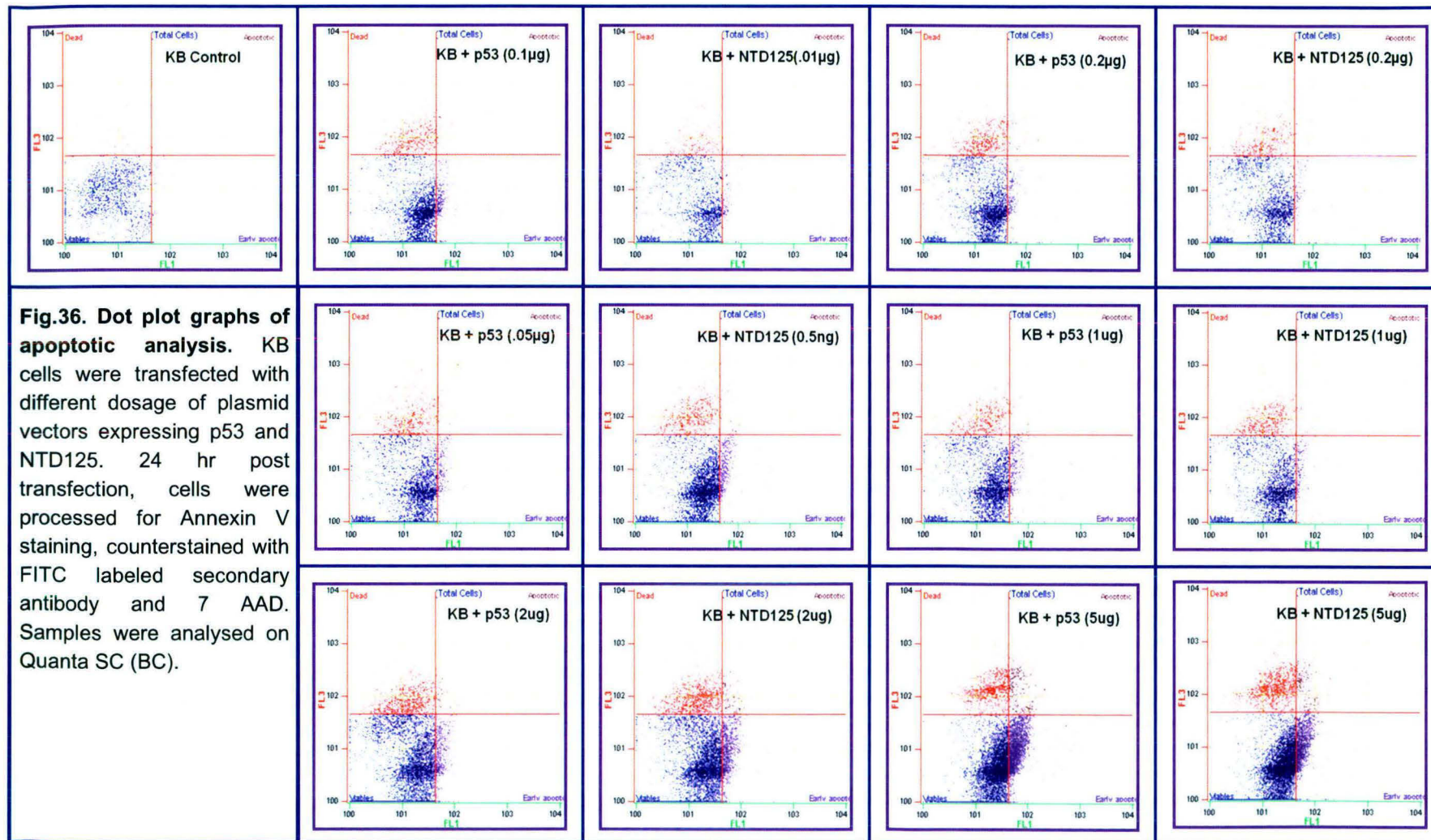
DBS II and DBS III upregulated luciferase gene. Results obtained from DBS I, II and DBS I,II,III constructs also followed the similar pattern establishing DBSI as a negative, and DBS II and DBS III as positive regulators of expression (Fig. 34). Construct having DBS I,II,III shows upregulation of p53 gene by p53. The combined effect of DBS II and DBS III prevails over the repression brought about by DBS I thus, resulted in net activation in combination. In a similar manner, KB cells transfected with only NTD125 showed the upregulation by DBS II and DBS III; and repression by DBS I (Fig. 34). NTD125 itself could not bind to DBS (Fig. 28) still it affected the expression in the manner p53 did (Fig. 30). We, therefore, conclude that NTD125 could upregulate p53 mediated gene expression of p53 gene through differential DBS selection. In this way, NTD125 stabilizes p53 and thus upregulates the expression of p53 by modulating p53 conformation and activity.



11. NTD125 induces apoptosis in KB cells-

So far, we can infer that NTD125 could stabilize p53 at protein level and can upregulate the transcription of p53 gene, thus resulting in higher levels of activated p53 in the cells. This led us to investigate outcome of such highly expressed p53 in the cells. As a cellular gatekeeper (Levine, 1997; Kinzler and Vogelstein, 1997), one of major roles of p53 is to check cellular stress and to induce apoptosis as a response (Hofseth *et al.*, 2004). Also, apoptosis is very important to check carcinogenesis. At times when stress generates severe and irreversible damage, p53 can initiate apoptosis thereby eliminating damaged cells/tissue. Studies with lower organisms have shown that p53 brings about cell death when subjected to genotoxic stress; whereas in higher organisms p53 activity is preferred for cell growth arrest (Derry *et al.*, 2001; Sogame *et al.*, 2003). For apoptosis analysis, we used Annexin V antibodies based flow cytometry approach. Briefly, experiential cells were stained using FITC labeled anti-Annexin V antibodies (Beckman Coulter), counter stained with 7-AAD (for dead nuclei) and analyzed using Quanta SC, Flow cytometer (Beckman Coulter). We noticed that transient expression of p53 and NTD125 induced apoptosis in KB cells in a dose dependent manner. Approximately ~32 % and ~23 % cell population showed apoptosis after transfecting 5 μ g of plasmid DNA of p53 and NTD125 expression vectors respectively (Fig. 35); dot plots of apoptotic analysis





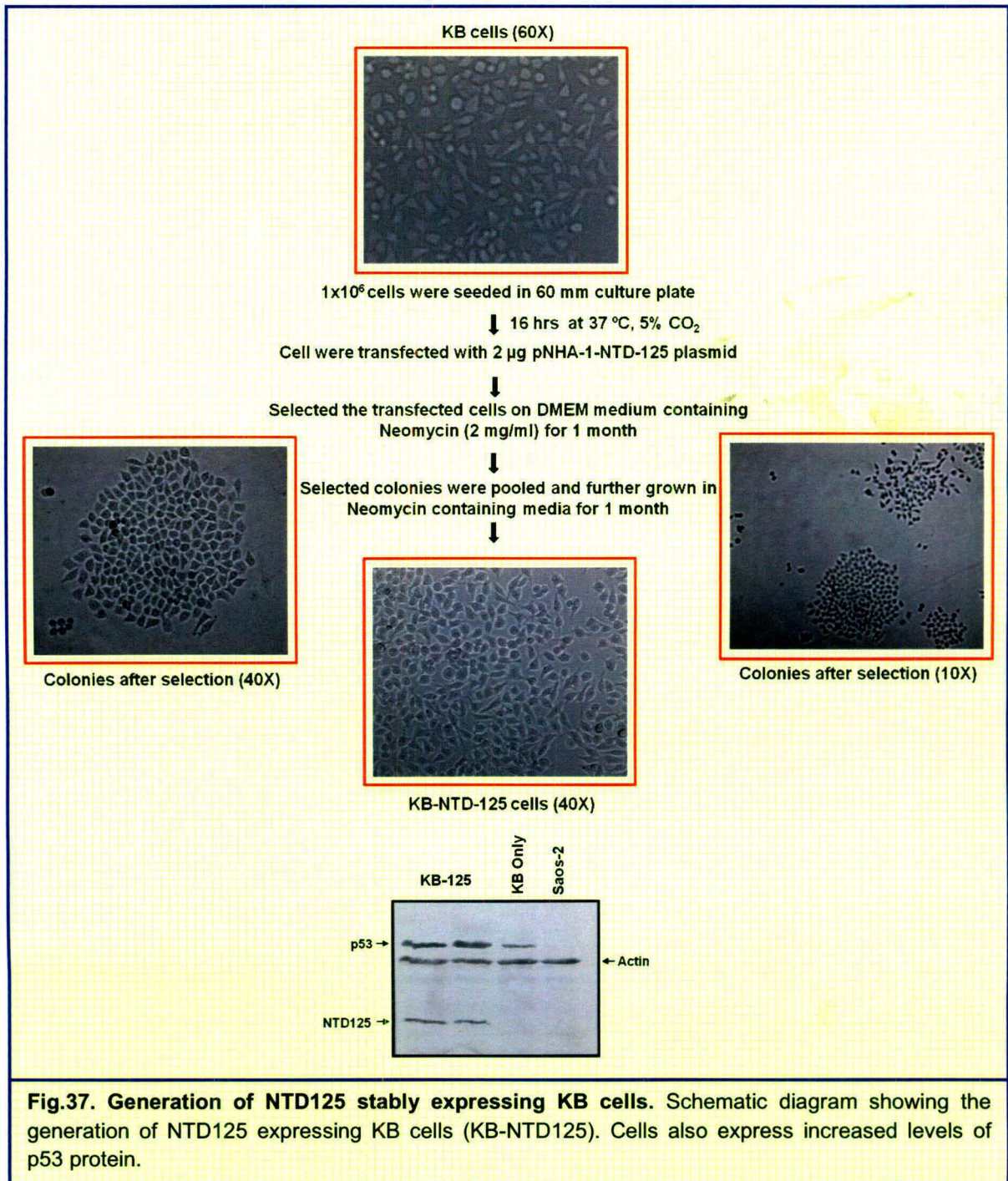
are given in Fig. 36. Thus, these results suggest that NTD125 can efficiently cause apoptosis in KB cells in a manner similar to that of p53. This is due to activation of p53 level by NTD125 so it actually brought about apoptosis via p53 only. High level of WT p53 protein was shown to induce apoptosis in cells (Ronen *et al.*, 1996).

12. NTD125 affects the gene expression profile of stably expressing NTD125 KB cells (KB-125)-

Transiently transfected NTD125 could stabilize, activate p53 protein within the cytoplasm and upregulate the expression of p53 gene. Thus, over-expressed, activated p53 also induced apoptosis in KB cells. Here, we only studied the effect of NTD125 expression on p53 whereas there are much more p53 regulated genes in the cellular system. Apoptosis data hinted that NTD125 had also upregulated some apoptotic genes. Therefore, to determine the effects of NTD125 on the expression pattern of whole genome we established stably expressing NTD125 KB cell line (KB-NTD125; Fig. 37) and performed its microarray analysis.

Briefly, we transfected KB cells with pNHA1-NTD125 plasmid and selected the cells on Neomycin (2 mg/ml) supplemented medium. Initially, cells started dying, but with regular selection pressure, after 4 weeks, we got ample number of colonies in the plates. The colonies thus obtained were pooled and continued to growing on selection medium. After 15 passages, we shifted the cells to normal growing medium. Thus, obtained cells (KB-125) were used for microarray analysis. Total RNA from fully-grown 90 mm culture plates of KB and KB-NTD125 cells was isolated and sent for Microarray analysis. Microarray and analysis were done by Ocimum Biosolutions (detailed report in Appendix-Microarray and analysis). As expected, at least 936 downregulated genes and 385 up-regulated genes were identified in KB-NTD125 cells (only 2 fold difference in expression were considered as significant).

Microarray analysis showed up-regulation of genes involved in cell communication, regulation of GTPase activity, positive regulation of enzyme activity and down-regulation of genes involved in response to stimulus,



development, regulation of cell growth, cell differentiation and response to stress and other biological processes in KB-NTD-125 cells in comparison to KB control cells.

Except this, genes involved in Nitrogen metabolism, 1- and 2-Methylnaphthalene degradation, gamma-Hexachlorocyclohexane degradation, apoptosis (NKKB-2, PRKAR1B), complement and coagulation cascades pathways were up-regulated whereas genes involved in Oxidative phosphorylation, purine metabolism, N-Glycan biosynthesis, MAPK signaling pathway, cytokine-cytokine receptor interaction, Cell adhesion molecules (CAMs), cell cycle, axon guidance and cell communication pathways were down-regulated in KB-NTD125 cells in comparison to control KB cells. Hoh *et al.* using p53MH algorithm, identified 2,583 genes in human having putative p53 binding sites; many of them are known targets of p53 mediated transcriptional regulation (Hoh *et al.*, 2002). Using their database (<http://linkage.rockefeller.edu/p53>), we identified 86 such down-regulated and 27 up-regulated genes in KB-NTD125 cells (Table. 4). This list includes many genes, which are either transcription factor or co-factor, so these genes could further directly or indirectly influence the expression of other genes. Total number of upregulated and downregulated genes is listed in Appendix section. These genes are very important in cellular processes and affect the normal growing properties of cells, which were evident during cell culture. For example, NTD125 expressing cells showed less adherent property and on trypsinization detached faster than control KB cells; NTD125 expressing cells showed more elongated shape in comparison to normal KB cells.

Down-regulated and up-regulated genes containing p53 DBS (Total Genes)-

	Down-regulated Genes	Fold Change KB-125/KB	Up-regulated Genes	Fold Change KB-125/KB
Biological Process/Pathways				
Signaling intermediate genes				
1	akap9	0.45000002	a2m	2.2259889
2	atm	0.17307694	trim29	2.2743363
3	bin1	0.2992126	btrc	3.3974361
4	capn3	0.25185186	Plcb4	3.0465114
5	col6a3	0.4	tulp1	3.1612904
6	ctnnd2	0.3382353	sh3gl3	3.1232874

7	ctsl	0.03571429	Srpk1	2.467742
8	dad1	0.00330033		
9	dnm1	0.14285715		
10	mageb2	0.1948052		
11	map4	0.46875		
12	ppm1d-wip1	0.18947369		
14	slc2a2	0.09392265		
15	socs3	0.49689442		
16	sod1	0.19694397		
17	sod2	0.4212963		
18	tcl1b	0.16666667		
19	timp1	0.28879312		
20	timp2	0.49418604		
Tumor suppressor/Apoptosis genes				
1	bnip3	0.4791667	tacc1	9.857142
2	gzma	0.05747126		
3	ing1	0.03092783		
4	mcl1	0.05113637		
5	rad51c	0.47859925		
6	birc5-survivin	0.4542762		
7	xrcc2	0.5		
8	cdc2l1-pitslre	0.03157895		
Transcription regulator genes				
1	ahr	0.08219178	Dnmt3l	2.2027028
2	cebpb	0.18181819	mitf	2.7999997
3	e2f2	0.09497207	tfec	2.1754386
4	gata4	0.34693876	Srebfl	2.6543212
5	hsf2	0.46363634		
6	lmo2	0.4657534		
7	nrl	0.16666667		
8	pax4	0.42553192		
9	pax5	0.10958903		
10	six4	0.2903226		
11	top1	0.4587156		
12	ubtf	0.02479339		
Protein kinase genes				
1	gak	0.35576925	Camk2a	2.0243902
2	musk	0.0877193	ttk	2.0497513
3	prkc	0.24358974	txk	2.467742
4	tlk2	0.29411766		

Growth factor and hormone genes				
1	bmp2	0.1724138	vegf	2.8857143
2	csf1	0.15315315	ctf1	2.32
3	efna2	0.37837836	rab7	3.6588233
4	egf	0.17721519		
5	ttr	0.15441176		
Membrane receptor genes				
1	ccr2	0.32710278	il8rb	2.122807
2	ltbr	0.45	tlr8	5.8999996
3	mc3r	0.4047619		
4	mertk	0.32484075		
5	notch4	0.1641791		
6	ret	0.3908046		
7	tlr3	0.48148146		
Protein phosphatase genes				
1	ppfia1	0.03571428		
2	ptpn13	0.02666667		
3	skip	0.4042553		
GDP/GTP binding genes				
1	gnb2	0.03292181	gna13	2.0649352
Lymphocyte signaling genes				
1	cd14	0.08928572	cd34	2.5806453
2	cd3g	0.13095239		
3	il18bp	0.10672854		
4	mica	0.32432434		
Neurobiology genes				
1	abcc8	0.4784483		
2	gabarap	0.25294116		
3	kcnk1	0.1026616		
4	nptx2	0.474359		
5	ntsr1	0.38356164		
6	hcrt	0.04471545		
Cell adhesion genes				
1	cdh12	0.35211268		
2	cdh1	0.04950495		
3	cdh3	0.00970874		
4	gjb6	0.09333333		

5	lamb1	0.02150538		
6	muc4	0.04026846		
7	itga2b	0.39175257		
Structural genes				
1	des	0.28070176	cald1	4.5652175
2	vim	0.36608863	Tubb1	2.7368422
Miscellaneous genes				
1	apoc3	0.33333334	ilf2	2.4
2	kl	0.2769231	hmox1	2.5094342
3	map2k3	0.09782609	Pten	4
4	p2rx1	0.1888112		
5	scn1a	0.14864865		
6	sirt7	0.41777778		
7	snrpb	0.19412725		
Total-	86 (936)		27 (385)	

Table.4. List of down-regulated and up-regulated genes containing p53 DBS. Listed genes have p53 response element as predicted by p53MH-algorithm (many of them are established targets of p53 transcriptional activity).

Discussion

In the present study, we showed that the amino-terminus domain of p53 (NTD125) can function as a chaperone and activate p53 both at the protein and gene levels. Reactivation of WT p53 activity is considered as a promising cure for cancer since loss of tumor suppressor activity of p53 is the most evident reason for neoplasm. Therefore, this study can be significant in understanding the p53 stability and the possible role of p53-NTD in its stabilization under heat stress condition. In most of the cancers, loss of p53 function either by mutations or by change in conformation leads to its inactivity (Wiman, 2006). Thus, research is focused on either reactivation of mutant p53 or activation of WT p53 as anti-cancer therapy. Chaperone such as CHIP was found to be associated with the mutant form of p53 under heat shock condition resulting in conversion to wild type conformation along with accumulation of p53 in the nucleus (Tripathi *et al.*, 2007). Studies show that Hsp90 is also required for both stabilization and reactivation of mutant p53 at the permissive temperature in cell lines that contain human tumor-derived temperature sensitive p53 mutants (Muller *et al.*, 2005). Our immunoprecipitation results both *in vitro* and *in vivo* conclusively showed the interaction between NTD125 and p53. Furthermore, NTD125 also stabilized the wild conformation of both bacterially expressed recombinant p53 and endogenous cellular p53 protein.

p53 is an important protein and functions as a hub of cell signaling; during the process it interacts with ample number of other proteins, which either influence p53 or get influenced by this interaction. Mostly, these interactions decide the fate of p53 stability and activity, like CBP/p300, PCAF, ATM, ATR, SUMO, MDM2 (Apella and Anderson, 2001; Wawrzynow *et al.*, 2007), CHIP (Tripathi *et al.*, 2007), HSP90, HSP70, co-chaperones (Zylicz *et al.*, 2001), and many more proteins. NTD125 was also able to chaperone p53 by interacting with it and stabilizing its conformation in native (active) form. Nevertheless, it binds to different forms of p53 regardless of its conformation and structure. We noticed that after heat treatments *in vitro*, wild conformation disappeared while loss of mutant conformation was also evident. After NTD125 addition, both the conformations were rescued; predominantly the wild conformation.

Temperature sensitivity for conformation is an intrinsic property of WT p53 and affects its activity (Hainaut *et al.*, 1995). Therefore, through heat treatment, p53 can be inactivated and the effect of any molecule or chemical on its activity can be checked either through its conformation specificity or by checking its DNA binding activity. EMSA was employed to check the DNA binding activity of p53 and incubation at 37 °C for 1 hr was enough to abolish the binding activity of purified protein. This also indicates the sensitivity of p53 towards factors like temperature and time that can affect its activity. We used freshly purified recombinant p53 for EMSA as it was observed that upon storage of protein for a longer period, its DNA binding activity was abolished. Addition of NTD125 both prior to and after denaturation step could protect DNA-binding activity of p53. Not only heat dependent, NTD125 was also able to protect p53-DNA binding against ATP dependent inhibition. ATP was shown to facilitate the release of p53 from target DNA (Okorokov and Milner, 1999) and subsequent studies showed that possible ATP binding site was localized within NTD and in core domain (Warnock and Raines, 2004). Most probably due to this reason, NTD125 in increasing concentration, binds to more ATP molecules from the mixture and doesn't allow this to directly affect p53. Though NTD125 showed physical interaction with p53 in immunoprecipitation analysis, we never noticed a super-shift band in EMSA after adding NTD125 to p53. It seems that NTD125 interacted with p53 and contained it in wild-DNA binding conformation, but this interaction was abolished either before or after DNA-p53 interaction. p53-CTD is basic in nature and also binds to DNA molecules non-specifically (Bayle *et al.*, 1995; Selivanova *et al.*, 1996); NTD125 also bind to p53 in C-ter region (Sharma *et al.*, 2009). There are possibilities that non-specific oligos (poly DI-DC) used in EMSA might have replaced the NTD125 out of p53-CTD although specific DNA-binding activity could not be altered by non-specific molecules.

NTD125 interaction assisted p53 for its structural stability under heat stress situation in a manner similar to chaperones. There are many reports, which show that loss of wild conformation of p53 results in loss of its transcriptional/DNA binding activity leading to failure of tumor suppressor function (Muller *et al.*, 2005). Genotypically WT p53 behaves as tumor suppressor in activating p53-

downstream genes (Sabapathy *et al.*, 1997). Conformational stabilization in case of p53 is very important and responsible for its transcriptional function. Both *in vitro* protection assay and EMSA results proved that NTD125 protected wild phenotype of p53 and thus, also rescued DNA binding activity. Further, experiments in cells (IPP and *in vivo* ELISA) also confirmed that NTD125 promoted wild phenotype of endogenous p53 both under physiological and heat stress condition. Similarly, small molecules have been identified which can convert mutant p53 to wild-type active conformation and are able to carry out p53 dependent apoptosis or cell cycle arrest. For example, PRIMA-I restores sequence specific DNA binding and active conformation of mutant p53 proteins *in vitro* and in cells (Bykov *et al.*, 2002).

Molecular chaperones are the potential regulators of p53 conformation. Hsp70, Hsp90, CHIP and MDM2 are shown to be involved in the conformational modulation of p53 at physiological and heat stress conditions. It has also been noted that post-translational modifications of p53 lead to the binding of co-chaperone like Pin1, a peptidyl prolyl isomerase (Zacchi *et al.*, 2002; Zheng *et al.*, 2002). This interaction of Pin1-p53 might have further stabilized p53 conformation and activated p53 transactivation function to act against stress.

NTD125 is natively unfolded, thermostable and possesses the chaperone like activity. Tompa and Csermely in a review on importance of unstructured regions in chaperones, quoted that unstructured regions are characteristics of most of RNA and protein chaperones and contain more than 40 % unstructured regions (Tompa and Csermely, 2004). In addition, small natively unfolded proteins were also shown to contain chaperoning properties (Bhattacharyya and Das, 1999). In most cases role of p53-NTD was studied either as an intact molecule within p53 or by deleting the NTD region, but we for the first time used NTD125 as an independent molecule and explored its *in vitro* and *in vivo* functions in relation to p53. Extensive studies have been carried out to find the role of NTD domain and its sub-domains in p53 stability and activity regulation. Earlier studies on NTD have contradicting results, some reported NTD to be essential for stabilization and activation of p53 activity (Cregan *et al.*, 2004), while others reported that NTD possesses allosteric, auto inhibitory function affecting DNA binding and

thermostability of protein (Hansen *et al.*, 1996). NTD is essential for transcriptional activation and drug induced apoptosis via WT p53 (Matas *et al.*, 2001), in contrast NTD deleted p53 isoform (Δ Np53) could also induce apoptosis and retains an intrinsic capacity to transactivate pro-apoptotic genes, in p53-null cells (Yin *et al.*, 2002). Our study with isolated NTD125 molecule exhibited that it retained some chaperone like characteristics and could efficiently stabilize p53 structure. WT p53 which otherwise loses its wild conformation under heat stress (*in vivo*) or at elevated temperature (*in vitro*) remains in its wild type conformation in the presence of NTD125. At the same time, NTD125 does not interfere with p53 DNA binding activity rather enhances it, whereas an earlier report indicated that peptide from the similar region 105-126 inhibits specific DNA binding activity and thus apoptotic activity of p53 (Protopopova and Selivanova, 2003).

Results showing that chaperone like activity resides in p53-NTD is very significant because p53 itself is a very sensitive protein as a whole. However, in this study, we used isolated NTD125 domain and it showed such chaperoning activity thereby stabilizing WT p53. As such, NTD125 is natively unstructured but most of small Heat Shock Proteins (sHSPs) are either devoid of secondary structure or less structured proteins with molecular mass of 12-43 kDa (Ganea, 2001). However, sHSPs interaction with their substrate and their mode of action is poorly defined yet they play significant role during stress and human disease (Macario and Conway de Macario, 2000; Sun and MacRae, 2005). Thus, it is very important to establish the function of p53-NTD, both at inter-molecular and intra-molecular levels.

We thought that possible mechanism for conformational rescue of p53 might be due to the interaction of NTD125 with basic-unstructured C-terminal domain (CTD) and CTD-NTD125 complex get exposed to the surface of the molecule facing more of environmental heat, without harming the sensitive core. However, NTD125 stabilizes wild conformation of p53 at physiological temperature; simultaneously it also restores the denatured conformation. These results clearly indicate that NTD125 interaction with p53 molecule maintains and stabilizes p53 native/active structure intact by providing chaperone like assistance. As wild

conformation is the DNA binding form of p53; in this way, NTD125 surely enhances DNA binding activity of p53. All our EMSA results clearly indicate the same. It was also proved earlier that protecting PAb1620 interacting, wild conformation of p53 results in increased DNA binding activity of p53 (Walerych *et al.*, 2004; Tripathi *et al.*, 2007; Wawrzynow *et al.*, 2007). One can question that *in vivo* there are plenty of other factors (chaperones) that could up-regulate and assist p53 for maintaining its function to deal with heat stress although mock transfected cells do not exhibit enhanced wild phenotype of p53; however other factors might be active in mock experiments too. Still the question remained whether NTD125 somehow recruited such chaperone molecules to p53 in cells because many of them are found to interact within NTD region. Nevertheless, *in vitro* data nullified the presence of any such factors involved, as these experiments involved only purified p53 and NTD125; thus, there exists no question of any external molecule's role in p53 stabilization by NTD125. Therefore, we concluded that the higher levels of p53 and conformational stabilization were solely due to NTD125 in NTD125 expressing cells. We also thought that NTD125 might be possibly keeping some kind of check on p53 DBS selection but EMSA using varied probes (from both class 1 and 2) yielded that it helped p53 DNA binding regardless of target sequence; otherwise size, sequence, symmetry, level of p53 etc. every factor matters in p53 DNA binding.

Both N- and C-terminal regions play significant role in p53 stability, activation, nuclear localization and DNA binding activity. CTD which is also an unstructured domain and basic in nature is a target of various regulatory modifications (phosphorylation, acetylation, methylation, ubiquitination, sumoylation etc.) that affect both stability and transcriptional activity of p53 (Bakalkin *et al.*, 1995; Takenaka *et al.*, 1995; Zotchev *et al.*, 2000; Wetzel and Berberich, 2001). CTD is also responsible for non-specific, sequence-independent, DNA binding particularly to non-linear DNA agents and negatively regulate p53 activity. According to earlier studies, modifications within CTD removes structural obstacles that prevent interaction of p53 with specific DNA elements and converts latent non-active p53 to DNA bound active form (Hupp *et al.*, 1993); whereas other studies employing ChIP assay contradicted this (Kaeser and Iggo, 2002;

Kaneshiro *et al.*, 2007). However, the activation of p53 using PAb421 prior to DNA binding confirms the alteration of molecule towards DNA binding form after quenching CTD (Takenaka *et al.*, 1995). Similarly peptide derived from CTD also restored the growth suppression function of mutant p53 through interacting with the core. (Selivanova *et al.*, 1997; 1999). But, how does NTD125 stabilize the p53 wild conformation is very important, it is possible that NTD125 interacts with p53 at CTD through its N-terminal (TAD region) and its C-terminal region (extended NTD) that is slightly structured might interact with core in order to stabilize its wild conformation.

Our results also confirmed that the interaction of NTD125 with CTD provided thermal stability and protected DNA binding activity of p53; these two qualities are comparable and must be complementary. Dimerization and tetramerization of p53 molecule is also very crucial prior to DNA interaction. It might be possible that NTD125 maintained p53 wild conformation, which favors dimerization/tetramerization and therefore DNA binding activity. The DNA binding activity of p53 can also be modulated by certain metabolites e.g. high concentration of ADP and dADP, which enhance DNA binding whereas ATP and GTP inhibit binding. Inhibition also occurs in case of increased level of TDP and NAD^+ . As the mechanism of ATP based inhibition is not yet established, research revealed that the possible binding of ATP molecule in NTD region could further destabilize p53 molecule and prohibit DNA binding. Our data also supports this theory and shows neutralization of high concentration of ATP by NTD125, thus re-establishing the lost DNA binding in the presence of NTD125.

We also explored the *in vivo* role of NTD125 on p53 and carried out our experiments in KB cells that express WT p53 in low levels. The level of p53 in KB could be detected by western blotting after loading ~80-100 μg cell lysate per well but using IP, it is easier to pull p53 out and analyze it. NTD125 expressing cells exhibited higher levels of p53 protein; level increased with the increase in dose of transfected DNA (pNHA1-NDT125). WT p53 is continuously expressed in the cells at a constant rate and is been degraded both via ubiquitin dependent and independent manner (Brooks and Gu, 2006; Asher *et al.*, 2006). Degradation of p53 via 26s proteasomes is initiated by a set of E3 type ubiquitin ligases (Cop1,

Pirh2, ARF-BP/MULE, CHIP, MDM2); out of which most important and most studied is MDM2. MDM2, itself is the product of p53-activated gene (Momand *et al.*, 1992; Oliner *et al.*, 1992; Haupt *et al.*, 1997; Leng *et al.*, 2003; Dornan *et al.*, 2004; Chen *et al.*, 2005; Shmueli and Oren, 2005). The feed back loop created between p53 and MDM2 plays major role in controlling cellular level of p53. MDM2 interacts within NTD (aa 18-22) of p53, ubiquitinates it at C-terminus finally leading to proteasomal degradation (Haupt *et al.*, 1997; Honda *et al.*, 1997).

Our co-immunoprecipitation data also showed the interruption of MDM2-p53 interaction by NTD125. Data showed that both NTD125 and p53 interact with MDM2 in NTD125 expressing cells but the p53-MDM2 interaction was far lesser in comparison to untransfected cells. Thus, we postulated that NTD125 interacted with MDM2; not allowing MDM2 to interact with and degrade p53 at a regular pace because NTD125 could compete with p53 to bind to MDM2. On the other hand, if a MDM2 protein molecule binds to the p53 molecule already in complex with NTD125 (it interacts within C-terminus); MDM2 will not be able to ubiquitinate target sites at C-terminus and degrade p53. Immunoprecipitation data was confusing and showing the presence of ternary complex among three molecules but precipitated proteins did not seem to be in equimolar ratio, therefore chances of exclusive interactions prevail. In the similar fashion, NTD125 could also provide protection against other proteins employed in p53 degradation. If any of them interacts within N-terminus of p53 or have ubiquitination site at C-terminus, their functions can be easily intercepted by NTD125.

We also performed ChIP assay and found that NTD125 is present upon DBSs together with p53 on the DBSs probed e.g. p21-5'-DBS, p53-DBS I, p53-DBS II and p53-DBS III. Further, we also noted that it helped p53 to differentially select DBS II and DBS III over DBS I in NTD125 expressing cells, which is quite surprising because NTD125 showed no effect on site selection in EMSA. In EMSA, we used different DBS from p21 and p53 promoter but noticed that p53 binds to different DBSs with almost equal intensity without any discrimination of being a full site or half site. Addition of NTD125 also did not change the p53

binding pattern. The differential site selection *in vivo* might be possible due to the involvement of some other factors that could co-occupy similar or nearby site within the region and hinder p53 binding at the same time. In particular, ChIP data does not represent information from a single cell rather millions of cells, which indicate that more cells are using DBS II and DBS III in comparison to DBS I, or in combinations.

We also analyzed the PAb1620 and PAb240 conformation on DBS but found that both the forms are able to recognize binding sites. This is against the active and latent theory for p53 activation, but earlier studies also showed the presence of both forms onto DNA binding sites in the nucleus (Halazonetis *et al.*, 1993). This might be due to the use of formaldehyde during cross-linking, which could have disrupted antibodies specificity for p53 molecule, or the situation may be much more complex than what we understand by now. But, data showed that more PAb1620 form bound to DBS II and DBS III, this hinted that activated p53 goes to these sites for activation of p53 gene. At the same time, luciferase assay results also confirmed that NTD125 upregulated p53 gene expression via DBS II and DBS III in p53 dependent manner. Combined results postulated that NTD125 guided more p53 to DBS II and DBS III sites, which are the activator sites. Results using only p53 in luciferase system confirmed that DBS II and DBS III are activator sites and DBS I is repressor.

In addition, stabilized, over-expressed p53 protein in NTD125 transfected cells also induced apoptosis in KB cells. Other molecules, which stabilize p53 wild-conformation, also induce apoptosis in p53 dependent manner. CBD3 can slow down the unfolding rate of the p53 core domain and rescue the conformation of unstable mutants of p53 (Friedler *et al.*, 2002 and 2003). It acts in a manner similar to chaperones by up-regulating WT p53, thus, inducing p53 targeted genes and partial restoration of apoptosis (Issaeva *et al.*, 2003). CP-31398 restores wild-type DNA binding conformation of mutant p53 thereby suppressing tumors *in vivo* (Foster *et al.*, 1999). Investigation of cell lines after exposure to CP-31398 revealed that most of the cells respond by undergoing apoptosis, while few exclusively undergo cell cycle arrest (Takimoto *et al.*, 2002). Other peptides derived from p53 C-terminal also enhanced radiation-induced apoptosis in human

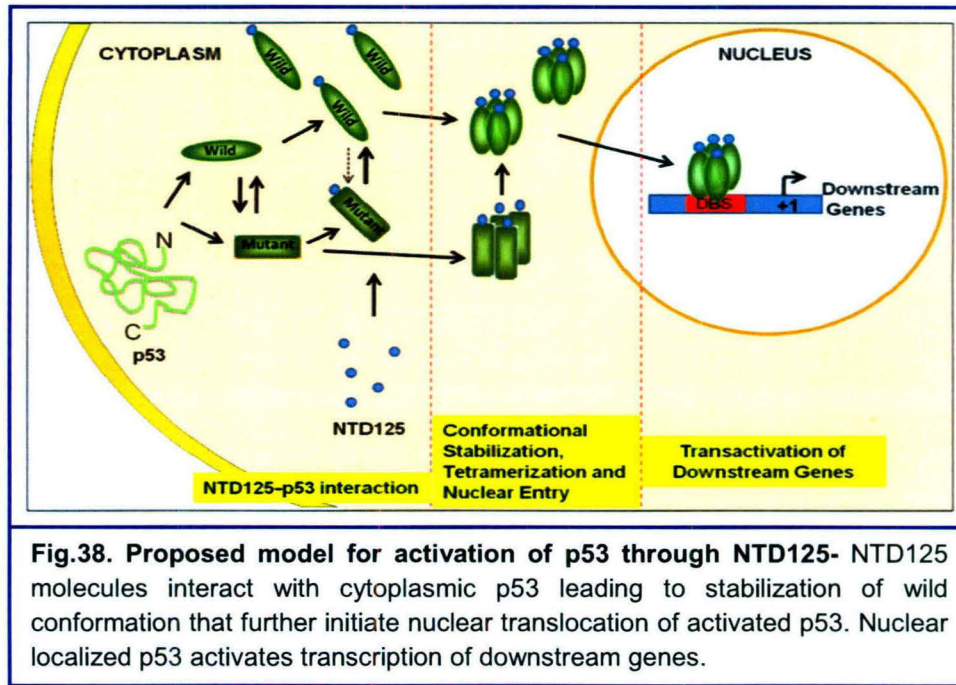
mutant p53 cancer cells (Ohnishi *et al.*, 2004). There are other molecules like MIRA-1 (Bykov *et al.*, 2005), RETRA (Kravchenko *et al.*, 2008) reported as potent anti-cancer drugs, that target p53 and brought about apoptosis in cells containing mutant p53 protein through converting it to active-wild form.

Lastly, our microarray studies with stably expressing NTD125 (KB-NTD125) cells showed that a number of genes were up-regulated and down-regulated together with those, which contained p53 target sites. Certain gene sets were able to up-regulate and down-regulate various biological process and pathways in NTD125 expressing KB cells. Although we witnessed apoptosis in transiently NTD125 transfected KB cells and observed heavy cell death during selection but after few passages, the stabilized cells started showing continuous growing properties.

Thus, we concluded that extended amino-terminus domain of p53 that is NTD125 can function as an inter-molecular chaperone of WT p53 both *in vitro* and in cells. We showed that NTD125 could protect the DNA binding native conformation of recombinant p53 in solution *in vitro*, even at higher temperatures. Further, NTD125 can interact with WT p53 and increase its level and wild phenotype in cells, can also co-migrates into nucleus and even assists p53 during transcriptional regulation. Results showed the role of NTD125 in auto-activation of p53 through differential DNA selection. We have also proposed a possible model for NTD125 mediated auto-activation of p53 in a synchronized manner (Fig. 38). Thus activated and over-expressed p53 in not only able to activate its own transcription but also activates other downstream genes related to apoptosis and other biological processes/pathways.

While, this study brings in notice a new function of p53-NTD region, yet a lot more remains to be explored. What actually happens in p53 and NTD125 interaction needs to be investigated at structural levels? This can give us better insight of chaperoning activity of NTD125 (which residues are involved in interaction and which are responsible for chaperoning activity). As NTD125 can activate p53 in KB cells by stabilizing wild conformation and induce apoptosis, we can also check its effects on cancer mutant specific cells. If NTD125 is able to

restore the activity of mutant p53, it may be used as a pharmacological molecule. Further, consequences of expression of NTD125 in cells (*in vivo*), both in transient and stable expression conditions need to be explored in details because amino-terminal region of p53 interacts with a lot more numbers of cellular proteins. Further, it also affects the expression of a large number of proteins in stably transfected cells, therefore its effect on overall gene profile demands study



with more precision in short and long term expression conditions because that may be both beneficiary and harmful as a whole.

Bibliography

- ❖ **Adams JM, Cory S. 1998.** The bcl-2 protein family: Arbiters of cell survival. *Science* **281**: 1322-1326.
- ❖ **Adimoolam S, Ford JM. 2002.** P53 and DNA damage-inducible expression of the xeroderma pigmentosum group c gene. *Proc Natl Acad Sci U S A* **99**: 12985-12990.
- ❖ **Akhaury P. 2003.** Heterogeneity of transcriptional activity of oral tumour associated p53 mutants. Ph.D. Thesis.
- ❖ **Ali A. 2008.** The role of p53 amino-terminal domain in regulating p53 conformation. Ph.D. Thesis.
- ❖ **Anzola M, Burgos JJ. 2003.** Hepatocellular carcinoma: Molecular interactions between hepatitis c virus and p53 in hepatocarcinogenesis. *Expert Rev Mol Med* **5**: 1-16.
- ❖ **Appella E, Anderson CW. 2001.** Post-translational modifications and activation of p53 by genotoxic stresses. *Eur J Biochem* **268**: 2764-2772.
- ❖ **Arias-Lopez C, Lazaro-Trueba I, Kerr P, Lord CJ, Dexter T, Irvani M, Ashworth A, Silva A. 2006.** P53 modulates homologous recombination by transcriptional regulation of the rad51 gene. *EMBO Rep* **7**: 219-224.
- ❖ **Ashcroft M, Taya Y, Vousden KH. 2000.** Stress signals utilize multiple pathways to stabilize p53. *Mol Cell Biol* **20**: 3224-3233.
- ❖ **Asher G, Shaul Y. 2006.** Ubiquitin-independent degradation: Lessons from the p53 model. *Isr Med Assoc J* **8**: 229-232.
- ❖ **Ashkenazi A, Dixit VM. 1998.** Death receptors: Signaling and modulation. *Science* **281**: 1305-1308.
- ❖ **Attardi LD, Reczek EE, Cosmas C, Demicco EG, McCurrach ME, Lowe SW, Jacks T. 2000.** Perp, an apoptosis-associated target of p53, is a novel member of the pmp-22/gas3 family. *Genes Dev* **14**: 704-718.
- ❖ **Avantaggiati ML, Ogryzko V, Gardner K, Giordano A, Levine AS, Kelly K. 1997.** Recruitment of p300/cbp in p53-dependent signal pathways. *Cell* **89**: 1175-1184.
- ❖ **Bakalkin G, Selivanova G, Yakovleva T, Kiseleva E, Kashuba E, Magnusson KP, Szekely L, Klein G, Terenius L, Wiman KG. 1995.** P53 binds single-stranded DNA ends through the c-terminal domain and internal DNA segments via the middle domain. *Nucleic Acids Res* **23**: 362-369.
- ❖ **Bannister AJ, Kouzarides T. 1996.** The cbp co-activator is a histone acetyltransferase. *Nature* **384**: 641-643.
- ❖ **Bayle JH, Elenbaas B, Levine AJ. 1995.** The carboxyl-terminal domain of the p53 protein regulates sequence-specific DNA binding through its nonspecific nucleic acid-binding activity. *Proc Natl Acad Sci U S A* **92**: 5729-5733.
- ❖ **Bell S, Klein C, Muller L, Hansen S, Buchner J. 2002.** P53 contains large unstructured regions in its native state. *J Mol Biol* **322**: 917-927.
- ❖ **Benchimol S, Lamb P, Crawford LV, Sheer D, Shows TB, Bruns GA, Peacock J. 1985.** Transformation associated p53 protein is encoded by a gene on human chromosome 17. *Somat Cell Mol Genet* **11**: 505-510.
- ❖ **Benchimol S, Matlashewski G, Crawford L. 1984.** The use of monoclonal antibodies for selection of a low-abundance mrna: P53. *Biochem Soc Trans* **12**: 708-711.
- ❖ **Bensaad K, Tsuruta A, Selak MA, Vidal MN, Nakano K, Bartrons R, Gottlieb E, Vousden KH. 2006.** Tigar, a p53-inducible regulator of glycolysis and apoptosis. *Cell* **126**: 107-120.
- ❖ **Bensaad K, Vousden KH. 2007.** P53: New roles in metabolism. *Trends Cell Biol* **17**: 286-291.
- ❖ **Beretta GL, Gatti L, Benedetti V, Perego P, Zunino F. 2008.** Small molecules targeting p53 to improve antitumor therapy. *Mini Rev Med Chem* **8**: 856-868.

- ❖ **Bhattacharyya J, Das KP. 1999.** Molecular chaperone-like properties of an unfolded protein, alpha(s)-casein. *J Biol Chem* **274**: 15505-15509.
- ❖ **Bian J, Sun Y. 1997.** Transcriptional activation by p53 of the human type iv collagenase (gelatinase a or matrix metalloproteinase 2) promoter. *Mol Cell Biol* **17**: 6330-6338.
- ❖ **Bochkareva E, Kaustov L, Ayed A, Yi GS, Lu Y, Pineda-Lucena A, Liao JC, Okorokov AL, Milner J, Arrowsmith CH, Bochkarev A. 2005.** Single-stranded DNA mimicry in the p53 transactivation domain interaction with replication protein a. *Proc Natl Acad Sci U S A* **102**: 15412-15417.
- ❖ **Bode AM, Dong Z. 2004.** Post-translational modification of p53 in tumorigenesis. *Nat Rev Cancer* **4**: 793-805.
- ❖ **Boggs K, Reisman D. 2006.** Increased p53 transcription prior to DNA synthesis is regulated through a novel regulatory element within the p53 promoter. *Oncogene* **25**: 555-565.
- ❖ **Boggs K, Reisman D. 2007.** C/ebpbeta participates in regulating transcription of the p53 gene in response to mitogen stimulation. *J Biol Chem* **282**: 7982-7990.
- ❖ **Botuyan MV, Momand J, Chen Y. 1997.** Solution conformation of an essential region of the p53 transactivation domain. *Fold Des* **2**: 331-342.
- ❖ **Bourdon JC, Fernandes K, Murray-Zmijewski F, Liu G, Diot A, Xirodimas DP, Saville MK, Lane DP. 2005.** P53 isoforms can regulate p53 transcriptional activity. *Genes Dev* **19**: 2122-2137.
- ❖ **Braithwaite AW, Royds JA, Jackson P. 2005.** The p53 story: Layers of complexity. *Carcinogenesis* **26**: 1161-1169.
- ❖ **Brooks CL, Gu W. 2006.** P53 ubiquitination: Mdm2 and beyond. *Mol Cell* **21**: 307-315.
- ❖ **Buckbinder L, Talbott R, Velasco-Miguel S, Takenaka I, Faha B, Seizinger BR, Kley N. 1995.** Induction of the growth inhibitor igf-binding protein 3 by p53. *Nature* **377**: 646-649.
- ❖ **Budanov AV, Sablina AA, Feinstein E, Koonin EV, Chumakov PM. 2004.** Regeneration of peroxiredoxins by p53-regulated sestrins, homologs of bacterial ahpD. *Science* **304**: 596-600.
- ❖ **Bullock AN, Henckel J, Fersht AR. 2000.** Quantitative analysis of residual folding and DNA binding in mutant p53 core domain: Definition of mutant states for rescue in cancer therapy. *Oncogene* **19**: 1245-1256.
- ❖ **Butler JS, Loh SN. 2003.** Structure, function, and aggregation of the zinc-free form of the p53 DNA binding domain. *Biochemistry* **42**: 2396-2403.
- ❖ **Bykov VJ, Issaeva N, Shilov A, Hultcrantz M, Pugacheva E, Chumakov P, Bergman J, Wiman KG, Selivanova G. 2002.** Restoration of the tumor suppressor function to mutant p53 by a low-molecular-weight compound. *Nat Med* **8**: 282-288.
- ❖ **Bykov VJ, Issaeva N, Zache N, Shilov A, Hultcrantz M, Bergman J, Selivanova G, Wiman KG. 2005.** Reactivation of mutant p53 and induction of apoptosis in human tumor cells by maleimide analogs. *J Biol Chem* **280**: 30384-30391.
- ❖ **Cain C, Miller S, Ahn J, Prives C. 2000.** The n terminus of p53 regulates its dissociation from DNA. *J Biol Chem* **275**: 39944-39953.
- ❖ **Campomenosi P, Monti P, Aprile A, Abbondandolo A, Frebourg T, Gold B, Crook T, Inga A, Resnick MA, Iggo R, Fronza G. 2001.** P53 mutants can often transactivate promoters containing a p21 but not bax or pig3 responsive elements. *Oncogene* **20**: 3573-3579.
- ❖ **Chan TA, Hermeking H, Lengauer C, Kinzler KW, Vogelstein B. 1999.** 14-3-3sigma is required to prevent mitotic catastrophe after DNA damage. *Nature* **401**: 616-620.

- ❖ **Chang C, Simmons DT, Martin MA, Mora PT. 1979.** Identification and partial characterization of new antigens from simian virus 40-transformed mouse cells. *J Virol* **31**: 463-471.
- ❖ **Chang J, Kim DH, Lee SW, Choi KY, Sung YC. 1995.** Transactivation ability of p53 transcriptional activation domain is directly related to the binding affinity to tata-binding protein. *J Biol Chem* **270**: 25014-25019.
- ❖ **Chen D, Kon N, Li M, Zhang W, Qin J, Gu W. 2005.** Arf-bp1/mule is a critical mediator of the arf tumor suppressor. *Cell* **121**: 1071-1083.
- ❖ **Chen J, Sadowski I. 2005.** Identification of the mismatch repair genes pms2 and mlh1 as p53 target genes by using serial analysis of binding elements. *Proc Natl Acad Sci U S A* **102**: 4813-4818.
- ❖ **Chen X, Ko LJ, Jayaraman L, Prives C. 1996.** P53 levels, functional domains, and DNA damage determine the extent of the apoptotic response of tumor cells. *Genes Dev* **10**: 2438-2451.
- ❖ **Chi SW, Lee SH, Kim DH, Ahn MJ, Kim JS, Woo JY, Torizawa T, Kainosho M, Han KH. 2005.** Structural details on mdm2-p53 interaction. *J Biol Chem* **280**: 38795-38802.
- ❖ **Cho Y, Gorina S, Jeffrey PD, Pavletich NP. 1994.** Crystal structure of a p53 tumor suppressor-DNA complex: Understanding tumorigenic mutations. *Science* **265**: 346-355.
- ❖ **Cistulli CA, Kaufmann WK. 1998.** P53-dependent signaling sustains DNA replication and enhances clonogenic survival in 254 nm ultraviolet-irradiated human fibroblasts. *Cancer Res* **58**: 1993-2002.
- ❖ **Clore GM, Ernst J, Clubb R, Omichinski JG, Kennedy WM, Sakaguchi K, Appella E, Gronenborn AM. 1995.** Refined solution structure of the oligomerization domain of the tumour suppressor p53. *Nat Struct Biol* **2**: 321-333.
- ❖ **Cory S, Adams JM. 2002.** The bcl2 family: Regulators of the cellular life-or-death switch. *Nat Rev Cancer* **2**: 647-656.
- ❖ **Cregan SP, Arbour NA, Maclaurin JG, Callaghan SM, Fortin A, Cheung EC, Guberman DS, Park DS, Slack RS. 2004.** P53 activation domain 1 is essential for puma upregulation and p53-mediated neuronal cell death. *J Neurosci* **24**: 10003-10012.
- ❖ **Dameron KM, Volpert OV, Tainsky MA, Bouck N. 1994.** Control of angiogenesis in fibroblasts by p53 regulation of thrombospondin-1. *Science* **265**: 1582-1584.
- ❖ **Dang CV, Lee WM. 1989.** Nuclear and nucleolar targeting sequences of c-erb-a, c-myc, n-myc, p53, hsp70, and hiv tat proteins. *J Biol Chem* **264**: 18019-18023.
- ❖ **Daniel NN, Korsmeyer SJ. 2004.** Cell death: Critical control points. *Cell* **116**: 205-219.
- ❖ **Dawson R, Muller L, Dehner A, Klein C, Kessler H, Buchner J. 2003.** The n-terminal domain of p53 is natively unfolded. *J Mol Biol* **332**: 1131-1141.
- ❖ **Deffie A, Wu H, Reinke V, Lozano G. 1993.** The tumor suppressor p53 regulates its own transcription. *Mol Cell Biol* **13**: 3415-3423.
- ❖ **Derry WB, Putzke AP, Rothman JH. 2001.** Caenorhabditis elegans p53: Role in apoptosis, meiosis, and stress resistance. *Science* **294**: 591-595.
- ❖ **Dignam JD. 1990.** Preparation of extracts from higher eukaryotes. *Methods Enzymol* **182**: 194-203.
- ❖ **Dornan D, Wertz I, Shimizu H, Arnott D, Frantz GD, Dowd P, O'Rourke K, Koeppen H, Dixit VM. 2004.** The ubiquitin ligase cop1 is a critical negative regulator of p53. *Nature* **429**: 86-92.
- ❖ **Dosztanyi Z, Csizmok V, Tompa P, Simon I. 2005.** Iupred: Web server for the prediction of intrinsically unstructured regions of proteins based on estimated energy content. *Bioinformatics* **21**: 3433-3434.

- ❖ **Dosztanyi Z, Csizmok V, Tompa P, Simon I. 2005.** The pairwise energy content estimated from amino acid composition discriminates between folded and intrinsically unstructured proteins. *J Mol Biol* **347**: 827-839.
- ❖ **el-Deiry WS. 1998.** Regulation of p53 downstream genes. *Semin Cancer Biol* **8**: 345-357.
- ❖ **el-Deiry WS, Kern SE, Pietenpol JA, Kinzler KW, Vogelstein B. 1992.** Definition of a consensus binding site for p53. *Nat Genet* **1**: 45-49.
- ❖ **el-Deiry WS, Tokino T, Velculescu VE, Levy DB, Parsons R, Trent JM, Lin D, Mercer WE, Kinzler KW, Vogelstein B. 1993.** Waf1, a potential mediator of p53 tumor suppression. *Cell* **75**: 817-825.
- ❖ **El-Mahdy MA, Hamada FM, Wani MA, Zhu Q, Wani AA. 2000.** P53-degradation by hpv-16 e6 preferentially affects the removal of cyclobutane pyrimidine dimers from non-transcribed strand and sensitizes mammary epithelial cells to uv-irradiation. *Mutat Res* **459**: 135-145.
- ❖ **Espinosa JM. 2008.** Mechanisms of regulatory diversity within the p53 transcriptional network. *Oncogene* **27**: 4013-4023.
- ❖ **Farmer G, Bargonetti J, Zhu H, Friedman P, Prywes R, Prives C. 1992.** Wild-type p53 activates transcription in vitro. *Nature* **358**: 83-86.
- ❖ **Fields S, Jang SK. 1990.** Presence of a potent transcription activating sequence in the p53 protein. *Science* **249**: 1046-1049.
- ❖ **Finlay CA, Hinds PW, Levine AJ. 1989.** The p53 proto-oncogene can act as a suppressor of transformation. *Cell* **57**: 1083-1093.
- ❖ **Finlay CA, Hinds PW, Tan TH, Eliyahu D, Oren M, Levine AJ. 1988.** Activating mutations for transformation by p53 produce a gene product that forms an hsc70-p53 complex with an altered half-life. *Mol Cell Biol* **8**: 531-539.
- ❖ **Fiscella M, Zhang H, Fan S, Sakaguchi K, Shen S, Mercer WE, Vande Woude GF, O'Connor PM, Appella E. 1997.** Wip1, a novel human protein phosphatase that is induced in response to ionizing radiation in a p53-dependent manner. *Proc Natl Acad Sci U S A* **94**: 6048-6053.
- ❖ **Ford JM, Hanawalt PC. 1995.** Li-fraumeni syndrome fibroblasts homozygous for p53 mutations are deficient in global DNA repair but exhibit normal transcription-coupled repair and enhanced uv resistance. *Proc Natl Acad Sci U S A* **92**: 8876-8880.
- ❖ **Foster BA, Coffey HA, Morin MJ, Rastinejad F. 1999.** Pharmacological rescue of mutant p53 conformation and function. *Science* **286**: 2507-2510.
- ❖ **Fourie AM, Hupp TR, Lane DP, Sang BC, Barbosa MS, Sambrook JF, Gething MJ. 1997.** Hsp70 binding sites in the tumor suppressor protein p53. *J Biol Chem* **272**: 19471-19479.
- ❖ **Fridman JS, Lowe SW. 2003.** Control of apoptosis by p53. *Oncogene* **22**: 9030-9040.
- ❖ **Friedler A, Hansson LO, Veprintsev DB, Freund SM, Rippin TM, Nikolova PV, Proctor MR, Rudiger S, Fersht AR. 2002.** A peptide that binds and stabilizes p53 core domain: Chaperone strategy for rescue of oncogenic mutants. *Proc Natl Acad Sci U S A* **99**: 937-942.
- ❖ **Friedler A, Veprintsev DB, Hansson LO, Fersht AR. 2003.** Kinetic instability of p53 core domain mutants: Implications for rescue by small molecules. *J Biol Chem* **278**: 24108-24112.
- ❖ **Fu M, Wang C, Li Z, Sakamaki T, Pestell RG. 2004.** Minireview: Cyclin d1: Normal and abnormal functions. *Endocrinology* **145**: 5439-5447.
- ❖ **Funk WD, Pak DT, Karas RH, Wright WE, Shay JW. 1992.** A transcriptionally active DNA-binding site for human p53 protein complexes. *Mol Cell Biol* **12**: 2866-2871.

- ❖ **Furlong EE, Rein T, Martin F. 1996.** Yy1 and nf1 both activate the human p53 promoter by alternatively binding to a composite element, and yy1 and ela cooperate to amplify p53 promoter activity. *Mol Cell Biol* **16**: 5933-5945.
- ❖ **Gaitonde SV, Riley JR, Qiao D, Martinez JD. 2000.** Conformational phenotype of p53 is linked to nuclear translocation. *Oncogene* **19**: 4042-4049.
- ❖ **Ganea E. 2001.** Chaperone-like activity of alpha-crystallin and other small heat shock proteins. *Curr Protein Pept Sci* **2**: 205-225.
- ❖ **Gannon JV, Greaves R, Iggo R, Lane DP. 1990.** Activating mutations in p53 produce a common conformational effect. A monoclonal antibody specific for the mutant form. *EMBO J* **9**: 1595-1602.
- ❖ **Gorina S, Pavletich NP. 1996.** Structure of the p53 tumor suppressor bound to the ankyrin and sh3 domains of 53bp2. *Science* **274**: 1001-1005.
- ❖ **Gostissa M, Hengstermann A, Fogal V, Sandy P, Schwarz SE, Scheffner M, Del Sal G. 1999.** Activation of p53 by conjugation to the ubiquitin-like protein sumo-1. *EMBO J* **18**: 6462-6471.
- ❖ **Grossman SR. 2001.** P300/cbp/p53 interaction and regulation of the p53 response. *Eur J Biochem* **268**: 2773-2778.
- ❖ **Gu W, Roeder RG. 1997.** Activation of p53 sequence-specific DNA binding by acetylation of the p53 c-terminal domain. *Cell* **90**: 595-606.
- ❖ **Gu W, Shi XL, Roeder RG. 1997.** Synergistic activation of transcription by cbp and p53. *Nature* **387**: 819-823.
- ❖ **Hainaut P, Butcher S, Milner J. 1995.** Temperature sensitivity for conformation is an intrinsic property of wild-type p53. *Br J Cancer* **71**: 227-231.
- ❖ **Hainaut P, Milner J. 1993.** Redox modulation of p53 conformation and sequence-specific DNA binding in vitro. *Cancer Res* **53**: 4469-4473.
- ❖ **Hainaut P, Rolley N, Davies M, Milner J. 1995.** Modulation by copper of p53 conformation and sequence-specific DNA binding: Role for cu(ii)/cu(i) redox mechanism. *Oncogene* **10**: 27-32.
- ❖ **Halazonetis TD, Davis LJ, Kandil AN. 1993.** Wild-type p53 adopts a 'mutant'-like conformation when bound to DNA. *EMBO J* **12**: 1021-1028.
- ❖ **Hansen S, Hupp TR, Lane DP. 1996.** Allosteric regulation of the thermostability and DNA binding activity of human p53 by specific interacting proteins. Crc cell transformation group. *J Biol Chem* **271**: 3917-3924.
- ❖ **Harper JW, Adami GR, Wei N, Keyomarsi K, Elledge SJ. 1993.** The p21 cdk-interacting protein cip1 is a potent inhibitor of g1 cyclin-dependent kinases. *Cell* **75**: 805-816.
- ❖ **Haupt Y, Maya R, Kazaz A, Oren M. 1997.** Mdm2 promotes the rapid degradation of p53. *Nature* **387**: 296-299.
- ❖ **Havre PA, Yuan J, Hedrick L, Cho KR, Glazer PM. 1995.** P53 inactivation by hpv16 e6 results in increased mutagenesis in human cells. *Cancer Res* **55**: 4420-4424.
- ❖ **Hearnnes JM, Mays DJ, Schavolt KL, Tang L, Jiang X, Pietenpol JA. 2005.** Chromatin immunoprecipitation-based screen to identify functional genomic binding sites for sequence-specific transactivators. *Mol Cell Biol* **25**: 10148-10158.
- ❖ **Hermeking H, Lengauer C, Polyak K, He TC, Zhang L, Thiagalingam S, Kinzler KW, Vogelstein B. 1997.** 14-3-3 sigma is a p53-regulated inhibitor of g2/m progression. *Mol Cell* **1**: 3-11.
- ❖ **Hinds PW, Finlay CA, Quartin RS, Baker SJ, Fearon ER, Vogelstein B, Levine AJ. 1990.** Mutant p53 DNA clones from human colon carcinomas cooperate with ras in transforming primary rat cells: A comparison of the "Hot spot" Mutant phenotypes. *Cell Growth Differ* **1**: 571-580.
- ❖ **Hofseth LJ, Hussain SP, Harris CC. 2004.** P53: 25 years after its discovery. *Trends Pharmacol Sci* **25**: 177-181.

- ❖ **Hoh J, Jin S, Parrado T, Edington J, Levine AJ, Ott J. 2002.** The p53mh algorithm and its application in detecting p53-responsive genes. *Proc Natl Acad Sci U S A* **99**: 8467-8472.
- ❖ **Honda R, Tanaka H, Yasuda H. 1997.** Oncoprotein mdm2 is a ubiquitin ligase e3 for tumor suppressor p53. *FEBS Lett* **420**: 25-27.
- ❖ **Horwitz J. 1992.** Alpha-crystallin can function as a molecular chaperone. *Proc Natl Acad Sci U S A* **89**: 10449-10453.
- ❖ **Hudson JM, Frade R, Bar-Eli M. 1995.** Wild-type p53 regulates its own transcription in a cell-type specific manner. *DNA Cell Biol* **14**: 759-766.
- ❖ **Hupp TR, Lane DP. 1994.** Allosteric activation of latent p53 tetramers. *Curr Biol* **4**: 865-875.
- ❖ **Hupp TR, Meek DW, Midgley CA, Lane DP. 1992.** Regulation of the specific DNA binding function of p53. *Cell* **71**: 875-886.
- ❖ **Hupp TR, Meek DW, Midgley CA, Lane DP. 1993.** Activation of the cryptic DNA binding function of mutant forms of p53. *Nucleic Acids Res* **21**: 3167-3174.
- ❖ **Hussain SP, Amstad P, He P, Robles A, Lupold S, Kaneko I, Ichimiya M, Sengupta S, Mechanic L, Okamura S, Hofseth LJ, Moake M, Nagashima M, Forrester KS, Harris CC. 2004.** P53-induced up-regulation of mnsod and gpx but not catalase increases oxidative stress and apoptosis. *Cancer Res* **64**: 2350-2356.
- ❖ **Hwang BJ, Ford JM, Hanawalt PC, Chu G. 1999.** Expression of the p48 xeroderma pigmentosum gene is p53-dependent and is involved in global genomic repair. *Proc Natl Acad Sci U S A* **96**: 424-428.
- ❖ **Inga A, Storici F, Darden TA, Resnick MA. 2002.** Differential transactivation by the p53 transcription factor is highly dependent on p53 level and promoter target sequence. *Mol Cell Biol* **22**: 8612-8625.
- ❖ **Inoue T, Wu L, Stuart J, Maki CG. 2005.** Control of p53 nuclear accumulation in stressed cells. *FEBS Lett* **579**: 4978-4984.
- ❖ **Isobe M, Emanuel BS, Givol D, Oren M, Croce CM. 1986.** Localization of gene for human p53 tumour antigen to band 17p13. *Nature* **320**: 84-85.
- ❖ **Issaeva N, Friedler A, Bozko P, Wiman KG, Fersht AR, Selivanova G. 2003.** Rescue of mutants of the tumor suppressor p53 in cancer cells by a designed peptide. *Proc Natl Acad Sci U S A* **100**: 13303-13307.
- ❖ **Iwabuchi K, Bartel PL, Li B, Marraccino R, Fields S. 1994.** Two cellular proteins that bind to wild-type but not mutant p53. *Proc Natl Acad Sci U S A* **91**: 6098-6102.
- ❖ **Iwabuchi K, Li B, Massa HF, Trask BJ, Date T, Fields S. 1998.** Stimulation of p53-mediated transcriptional activation by the p53-binding proteins, 53bp1 and 53bp2. *J Biol Chem* **273**: 26061-26068.
- ❖ **Jacobs WB, Govoni G, Ho D, Atwal JK, Barnabe-Heider F, Keyes WM, Mills AA, Miller FD, Kaplan DR. 2005.** P63 is an essential proapoptotic protein during neural development. *Neuron* **48**: 743-756.
- ❖ **Jeffrey PD, Gorina S, Pavletich NP. 1995.** Crystal structure of the tetramerization domain of the p53 tumor suppressor at 1.7 angstroms. *Science* **267**: 1498-1502.
- ❖ **Joerger AC, Fersht AR. 2008.** Structural biology of the tumor suppressor p53. *Annu Rev Biochem* **77**: 557-582.
- ❖ **Kaesler MD, Iggo RD. 2002.** Chromatin immunoprecipitation analysis fails to support the latency model for regulation of p53 DNA binding activity in vivo. *Proc Natl Acad Sci U S A* **99**: 95-100.
- ❖ **Kaneshiro K, Tsutsumi S, Tsuji S, Shirahige K, Aburatani H. 2007.** An integrated map of p53-binding sites and histone modification in the human encode regions. *Genomics* **89**: 178-188.

- ❖ **Kao CC, Yew PR, Berk AJ. 1990.** Domains required for in vitro association between the cellular p53 and the adenovirus 2 e1b 55k proteins. *Virology* **179**: 806-814.
- ❖ **Kastan MB, Zhan Q, el-Deiry WS, Carrier F, Jacks T, Walsh WV, Plunkett BS, Vogelstein B, Fornace AJ, Jr. 1992.** A mammalian cell cycle checkpoint pathway utilizing p53 and gadd45 is defective in ataxia-telangiectasia. *Cell* **71**: 587-597.
- ❖ **Kern SE, Kinzler KW, Bruskin A, Jarosz D, Friedman P, Prives C, Vogelstein B. 1991.** Identification of p53 as a sequence-specific DNA-binding protein. *Science* **252**: 1708-1711.
- ❖ **Kim E, Albrechtsen N, Deppert W. 1997.** DNA-conformation is an important determinant of sequence-specific DNA binding by tumor suppressor p53. *Oncogene* **15**: 857-869.
- ❖ **Kim E, Deppert W. 2006.** The versatile interactions of p53 with DNA: When flexibility serves specificity. *Cell Death Differ* **13**: 885-889.
- ❖ **Kim E, Rohaly G, Heinrichs S, Gimnopoulos D, Meissner H, Deppert W. 1999.** Influence of promoter DNA topology on sequence-specific DNA binding and transactivation by tumor suppressor p53. *Oncogene* **18**: 7310-7318.
- ❖ **Kimura T, Takeda S, Sagiya Y, Gotoh M, Nakamura Y, Arakawa H. 2003.** Impaired function of p53r2 in rrm2b-null mice causes severe renal failure through attenuation of dntp pools. *Nat Genet* **34**: 440-445.
- ❖ **Kinzler KW, Vogelstein B. 1997.** Cancer-susceptibility genes. Gatekeepers and caretakers. *Nature* **386**: 761, 763.
- ❖ **Komarova EA, Diatchenko L, Rokhlin OW, Hill JE, Wang ZJ, Krivokrysenko VI, Feinstein E, Gudkov AV. 1998.** Stress-induced secretion of growth inhibitors: A novel tumor suppressor function of p53. *Oncogene* **17**: 1089-1096.
- ❖ **Kravchenko JE, Ilyinskaya GV, Komarov PG, Agapova LS, Kochetkov DV, Strom E, Frolova EI, Kovriga I, Gudkov AV, Feinstein E, Chumakov PM. 2008.** Small-molecule retractor suppresses mutant p53-bearing cancer cells through a p73-dependent salvage pathway. *Proc Natl Acad Sci U S A* **105**: 6302-6307.
- ❖ **Kress M, May E, Cassingena R, May P. 1979.** Simian virus 40-transformed cells express new species of proteins precipitable by anti-simian virus 40 tumor serum. *J Virol* **31**: 472-483.
- ❖ **Kubbutat MH, Ludwig RL, Ashcroft M, Vousden KH. 1998.** Regulation of mdm2-directed degradation by the c terminus of p53. *Mol Cell Biol* **18**: 5690-5698.
- ❖ **Kunz C, Pebler S, Otte J, von der Ahe D. 1995.** Differential regulation of plasminogen activator and inhibitor gene transcription by the tumor suppressor p53. *Nucleic Acids Res* **23**: 3710-3717.
- ❖ **Kussie PH, Gorina S, Marechal V, Elenbaas B, Moreau J, Levine AJ, Pavletich NP. 1996.** Structure of the mdm2 oncoprotein bound to the p53 tumor suppressor transactivation domain. *Science* **274**: 948-953.
- ❖ **Kuwana T, Mackey MR, Perkins G, Ellisman MH, Latterich M, Schneider R, Green DR, Newmeyer DD. 2002.** Bid, bax, and lipids cooperate to form supramolecular openings in the outer mitochondrial membrane. *Cell* **111**: 331-342.
- ❖ **Lahav G. 2008.** Oscillations by the p53-mdm2 feedback loop. *Adv Exp Med Biol* **641**: 28-38.
- ❖ **Lambert PF, Kashanchi F, Radonovich MF, Shiekhattar R, Brady JN. 1998.** Phosphorylation of p53 serine 15 increases interaction with cbp. *J Biol Chem* **273**: 33048-33053.
- ❖ **Lane DP. 1992.** Cancer. P53, guardian of the genome. *Nature* **358**: 15-16.

- ❖ **Lane DP, Crawford LV. 1979.** T antigen is bound to a host protein in sv40-transformed cells. *Nature* **278**: 261-263.
- ❖ **Laptenko O, Prives C. 2006.** Transcriptional regulation by p53: One protein, many possibilities. *Cell Death Differ* **13**: 951-961.
- ❖ **Lee H, Mok KH, Muhandiram R, Park KH, Suk JE, Kim DH, Chang J, Sung YC, Choi KY, Han KH. 2000.** Local structural elements in the mostly unstructured transcriptional activation domain of human p53. *J Biol Chem* **275**: 29426-29432.
- ❖ **Leng RP, Lin Y, Ma W, Wu H, Lemmers B, Chung S, Parant JM, Lozano G, Hakem R, Benchimol S. 2003.** Pirh2, a p53-induced ubiquitin-protein ligase, promotes p53 degradation. *Cell* **112**: 779-791.
- ❖ **Levine AJ. 1997.** P53, the cellular gatekeeper for growth and division. *Cell* **88**: 323-331.
- ❖ **Levine AJ, Hu W, Feng Z. 2006.** The p53 pathway: What questions remain to be explored? *Cell Death Differ* **13**: 1027-1036.
- ❖ **Li X, Coffino P. 1996.** High-risk human papillomavirus e6 protein has two distinct binding sites within p53, of which only one determines degradation. *J Virol* **70**: 4509-4516.
- ❖ **Liang SH, Clarke MF. 2001.** Regulation of p53 localization. *Eur J Biochem* **268**: 2779-2783.
- ❖ **Lill NL, Grossman SR, Ginsberg D, DeCaprio J, Livingston DM. 1997.** Binding and modulation of p53 by p300/cbp coactivators. *Nature* **387**: 823-827.
- ❖ **Lin J, Chen J, Elenbaas B, Levine AJ. 1994.** Several hydrophobic amino acids in the p53 amino-terminal domain are required for transcriptional activation, binding to mdm-2 and the adenovirus 5 e1b 55-kd protein. *Genes Dev* **8**: 1235-1246.
- ❖ **Linzer DI, Levine AJ. 1979.** Characterization of a 54k dalton cellular sv40 tumor antigen present in sv40-transformed cells and uninfected embryonal carcinoma cells. *Cell* **17**: 43-52.
- ❖ **Liu G, Chen X. 2006.** DNA polymerase eta, the product of the xeroderma pigmentosum variant gene and a target of p53, modulates the DNA damage checkpoint and p53 activation. *Mol Cell Biol* **26**: 1398-1413.
- ❖ **Liu L, Scolnick DM, Trievel RC, Zhang HB, Marmorstein R, Halazonetis TD, Berger SL. 1999.** P53 sites acetylated in vitro by pcaf and p300 are acetylated in vivo in response to DNA damage. *Mol Cell Biol* **19**: 1202-1209.
- ❖ **Liu WL, Midgley C, Stephen C, Saville M, Lane DP. 2001.** Biological significance of a small highly conserved region in the n terminus of the p53 tumour suppressor protein. *J Mol Biol* **313**: 711-731.
- ❖ **Lu H, Levine AJ. 1995.** Human tafii31 protein is a transcriptional coactivator of the p53 protein. *Proc Natl Acad Sci U S A* **92**: 5154-5158.
- ❖ **Luo J, Li M, Tang Y, Laszkowska M, Roeder RG, Gu W. 2004.** Acetylation of p53 augments its site-specific DNA binding both in vitro and in vivo. *Proc Natl Acad Sci U S A* **101**: 2259-2264.
- ❖ **Ma B, Levine AJ. 2007.** Probing potential binding modes of the p53 tetramer to DNA based on the symmetries encoded in p53 response elements. *Nucleic Acids Res* **35**: 7733-7747.
- ❖ **Ma B, Pan Y, Zheng J, Levine AJ, Nussinov R. 2007.** Sequence analysis of p53 response-elements suggests multiple binding modes of the p53 tetramer to DNA targets. *Nucleic Acids Res* **35**: 2986-3001.
- ❖ **Macario AJ, Conway de Macario E. 2000.** Stress and molecular chaperones in disease. *Int J Clin Lab Res* **30**: 49-66.
- ❖ **Maltzman W, Czyzyk L. 1984.** Uv irradiation stimulates levels of p53 cellular tumor antigen in nontransformed mouse cells. *Mol Cell Biol* **4**: 1689-1694.

- ❖ **Mashimo T, Watabe M, Hirota S, Hosobe S, Miura K, Tegtmeyer PJ, Rinker-Shaeffer CW, Watabe K. 1998.** The expression of the kail gene, a tumor metastasis suppressor, is directly activated by p53. *Proc Natl Acad Sci U S A* **95**: 11307-11311.
- ❖ **Matas D, Sigal A, Stambolsky P, Milyavsky M, Weisz L, Schwartz D, Goldfinger N, Rotter V. 2001.** Integrity of the n-terminal transcription domain of p53 is required for mutant p53 interference with drug-induced apoptosis. *EMBO J* **20**: 4163-4172.
- ❖ **Matoba S, Kang JG, Patino WD, Wragg A, Boehm M, Gavrilova O, Hurley PJ, Bunz F, Hwang PM. 2006.** P53 regulates mitochondrial respiration. *Science* **312**: 1650-1653.
- ❖ **Matsumura I, Ellington AD. 1999.** In vitro evolution of thermostable p53 variants. *Protein Sci* **8**: 731-740.
- ❖ **McBride OW, Merry D, Givol D. 1986.** The gene for human p53 cellular tumor antigen is located on chromosome 17 short arm (17p13). *Proc Natl Acad Sci U S A* **83**: 130-134.
- ❖ **McKay BC, Chen F, Perumalswami CR, Zhang F, Ljungman M. 2000.** The tumor suppressor p53 can both stimulate and inhibit ultraviolet light-induced apoptosis. *Mol Biol Cell* **11**: 2543-2551.
- ❖ **Mercer WE, Avignolo C, Baserga R. 1984.** Role of the p53 protein in cell proliferation as studied by microinjection of monoclonal antibodies. *Mol Cell Biol* **4**: 276-281.
- ❖ **Milner J, Watson JV. 1990.** Addition of fresh medium induces cell cycle and conformation changes in p53, a tumour suppressor protein. *Oncogene* **5**: 1683-1690.
- ❖ **Mittl PR, Chene P, Grutter MG. 1998.** Crystallization and structure solution of p53 (residues 326-356) by molecular replacement using an nmr model as template. *Acta Crystallogr D Biol Crystallogr* **54**: 86-89.
- ❖ **Miyashita T, Reed JC. 1995.** Tumor suppressor p53 is a direct transcriptional activator of the human bax gene. *Cell* **80**: 293-299.
- ❖ **Momand J, Zambetti GP, Olson DC, George D, Levine AJ. 1992.** The mdm-2 oncogene product forms a complex with the p53 protein and inhibits p53-mediated transactivation. *Cell* **69**: 1237-1245.
- ❖ **Moroni MC, Hickman ES, Lazzerini Denchi E, Caprara G, Colli E, Cecconi F, Muller H, Helin K. 2001.** Apaf-1 is a transcriptional target for e2f and p53. *Nat Cell Biol* **3**: 552-558.
- ❖ **Mosner J, Mummenbrauer T, Bauer C, Sczakiel G, Grosse F, Deppert W. 1995.** Negative feedback regulation of wild-type p53 biosynthesis. *EMBO J* **14**: 4442-4449.
- ❖ **Muller M, Wilder S, Bannasch D, Israeli D, Lehlbach K, Li-Weber M, Friedman SL, Galle PR, Stremmel W, Oren M, Krammer PH. 1998.** P53 activates the cd95 (apo-1/fas) gene in response to DNA damage by anticancer drugs. *J Exp Med* **188**: 2033-2045.
- ❖ **Muller P, Ceskova P, Vojtesek B. 2005.** Hsp90 is essential for restoring cellular functions of temperature-sensitive p53 mutant protein but not for stabilization and activation of wild-type p53: Implications for cancer therapy. *J Biol Chem* **280**: 6682-6691.
- ❖ **Nagata S, Golstein P. 1995.** The fas death factor. *Science* **267**: 1449-1456.
- ❖ **Nakamura Y. 2004.** Isolation of p53-target genes and their functional analysis. *Cancer Sci* **95**: 7-11.
- ❖ **Nakano K, Vousden KH. 2001.** Puma, a novel proapoptotic gene, is induced by p53. *Mol Cell* **7**: 683-694.

- ❖ **Nie L, Sasaki M, Maki CG. 2007.** Regulation of p53 nuclear export through sequential changes in conformation and ubiquitination. *J Biol Chem* **282**: 14616-14625.
- ❖ **Nishimori H, Shiratsuchi T, Urano T, Kimura Y, Kiyono K, Tatsumi K, Yoshida S, Ono M, Kuwano M, Nakamura Y, Tokino T. 1997.** A novel brain-specific p53-target gene, bai1, containing thrombospondin type 1 repeats inhibits experimental angiogenesis. *Oncogene* **15**: 2145-2150.
- ❖ **Oda E, Ohki R, Murasawa H, Nemoto J, Shibue T, Yamashita T, Tokino T, Taniguchi T, Tanaka N. 2000.** Noxa, a bh3-only member of the bcl-2 family and candidate mediator of p53-induced apoptosis. *Science* **288**: 1053-1058.
- ❖ **Oda K, Arakawa H, Tanaka T, Matsuda K, Tanikawa C, Mori T, Nishimori H, Tamai K, Tokino T, Nakamura Y, Taya Y. 2000.** P53aip1, a potential mediator of p53-dependent apoptosis, and its regulation by ser-46-phosphorylated p53. *Cell* **102**: 849-862.
- ❖ **Ogryzko VV, Schiltz RL, Russanova V, Howard BH, Nakatani Y. 1996.** The transcriptional coactivators p300 and cbp are histone acetyltransferases. *Cell* **87**: 953-959.
- ❖ **Ohnishi K, Inaba H, Yasumoto J, Yuki K, Takahashi A, Ohnishi T. 2004.** C-terminal peptides of p53 molecules enhance radiation-induced apoptosis in human mutant p53 cancer cells. *Apoptosis* **9**: 591-597.
- ❖ **Okamoto K, Beach D. 1994.** Cyclin g is a transcriptional target of the p53 tumor suppressor protein. *EMBO J* **13**: 4816-4822.
- ❖ **Okorokov AL, Milner J. 1999.** An atp/adp-dependent molecular switch regulates the stability of p53-DNA complexes. *Mol Cell Biol* **19**: 7501-7510.
- ❖ **Okorokov AL, Sherman MB, Plisson C, Grinkevich V, Sigmundsson K, Selivanova G, Milner J, Orlova EV. 2006.** The structure of p53 tumour suppressor protein reveals the basis for its functional plasticity. *EMBO J* **25**: 5191-5200.
- ❖ **Oliner JD, Kinzler KW, Meltzer PS, George DL, Vogelstein B. 1992.** Amplification of a gene encoding a p53-associated protein in human sarcomas. *Nature* **358**: 80-83.
- ❖ **Oliner JD, Pietenpol JA, Thiagalingam S, Gyuris J, Kinzler KW, Vogelstein B. 1993.** Oncoprotein mdm2 conceals the activation domain of tumour suppressor p53. *Nature* **362**: 857-860.
- ❖ **Oren M. 1999.** Regulation of the p53 tumor suppressor protein. *J Biol Chem* **274**: 36031-36034.
- ❖ **Ozbun MA, Butel JS. 1995.** Tumor suppressor p53 mutations and breast cancer: A critical analysis. *Adv Cancer Res* **66**: 71-141.
- ❖ **Parada LF, Land H, Weinberg RA, Wolf D, Rotter V. 1984.** Cooperation between gene encoding p53 tumour antigen and ras in cellular transformation. *Nature* **312**: 649-651.
- ❖ **Park SM, Jung HY, Kim TD, Park JH, Yang CH, Kim J. 2002.** Distinct roles of the n-terminal-binding domain and the c-terminal-solubilizing domain of alpha-synuclein, a molecular chaperone. *J Biol Chem* **277**: 28512-28520.
- ❖ **Pavletich NP, Chambers KA, Pabo CO. 1993.** The DNA-binding domain of p53 contains the four conserved regions and the major mutation hot spots. *Genes Dev* **7**: 2556-2564.
- ❖ **Phan RT, Dalla-Favera R. 2004.** The bcl6 proto-oncogene suppresses p53 expression in germinal-centre b cells. *Nature* **432**: 635-639.
- ❖ **Pietenpol JA, Tokino T, Thiagalingam S, el-Deiry WS, Kinzler KW, Vogelstein B. 1994.** Sequence-specific transcriptional activation is essential for growth suppression by p53. *Proc Natl Acad Sci U S A* **91**: 1998-2002.
- ❖ **Pluquet O, Hainaut P. 2001.** Genotoxic and non-genotoxic pathways of p53 induction. *Cancer Lett* **174**: 1-15.

- ❖ **Polyak K, Xia Y, Zweier JL, Kinzler KW, Vogelstein B. 1997.** A model for p53-induced apoptosis. *Nature* **389**: 300-305.
- ❖ **Prives C, Hall PA. 1999.** The p53 pathway. *J Pathol* **187**: 112-126.
- ❖ **Protopopova M, Selivanova G. 2003.** Inhibition of p53 activity in vitro and in living cells by a synthetic peptide derived from its core domain. *Cell Cycle* **2**: 592-595.
- ❖ **Qian H, Wang T, Naumovski L, Lopez CD, Brachmann RK. 2002.** Groups of p53 target genes involved in specific p53 downstream effects cluster into different classes of DNA binding sites. *Oncogene* **21**: 7901-7911.
- ❖ **Rahman-Roblick R, Roblick UJ, Hellman U, Conrotto P, Liu T, Becker S, Hirschberg D, Jornvall H, Auer G, Wiman KG. 2007.** P53 targets identified by protein expression profiling. *Proc Natl Acad Sci U S A* **104**: 5401-5406.
- ❖ **Raman V, Martensen SA, Reisman D, Evron E, Odenwald WF, Jaffee E, Marks J, Sukumar S. 2000.** Compromised *hoxa5* function can limit p53 expression in human breast tumours. *Nature* **405**: 974-978.
- ❖ **Reisman D, Greenberg M, Rotter V. 1988.** Human p53 oncogene contains one promoter upstream of exon 1 and a second, stronger promoter within intron 1. *Proc Natl Acad Sci U S A* **85**: 5146-5150.
- ❖ **Rigacci S, Bucciantini M, Relini A, Pesce A, Gliozzi A, Berti A, Stefani M. 2008.** The (1-63) region of the p53 transactivation domain aggregates in vitro into cytotoxic amyloid assemblies. *Biophys J* **94**: 3635-3646.
- ❖ **Rodriguez MS, Desterro JM, Lain S, Midgley CA, Lane DP, Hay RT. 1999.** Sumo-1 modification activates the transcriptional response of p53. *EMBO J* **18**: 6455-6461.
- ❖ **Ronen D, Schwartz D, Teitz Y, Goldfinger N, Rotter V. 1996.** Induction of hl-60 cells to undergo apoptosis is determined by high levels of wild-type p53 protein whereas differentiation of the cells is mediated by lower p53 levels. *Cell Growth Differ* **7**: 21-30.
- ❖ **Roth J, Dobbstein M, Freedman DA, Shenk T, Levine AJ. 1998.** Nucleocytoplasmic shuttling of the hdm2 oncoprotein regulates the levels of the p53 protein via a pathway used by the human immunodeficiency virus rev protein. *EMBO J* **17**: 554-564.
- ❖ **Rotter V. 1983.** P53, a transformation-related cellular-encoded protein, can be used as a biochemical marker for the detection of primary mouse tumor cells. *Proc Natl Acad Sci U S A* **80**: 2613-2617.
- ❖ **Rouault JP, Falette N, Guehenneux F, Guillot C, Rimokh R, Wang Q, Berthet C, Moyret-Lalle C, Savatier P, Pain B, Shaw P, Berger R, Samarut J, Magaud JP, Ozturk M, Samarut C, Puisieux A. 1996.** Identification of *btg2*, an antiproliferative p53-dependent component of the DNA damage cellular response pathway. *Nat Genet* **14**: 482-486.
- ❖ **Sabapathy K, Klemm M, Jaenisch R, Wagner EF. 1997.** Regulation of es cell differentiation by functional and conformational modulation of p53. *EMBO J* **16**: 6217-6229.
- ❖ **Sakaguchi K, Herrera JE, Saito S, Miki T, Bustin M, Vassilev A, Anderson CW, Appella E. 1998.** DNA damage activates p53 through a phosphorylation-acetylation cascade. *Genes Dev* **12**: 2831-2841.
- ❖ **Sakaguchi K, Sakamoto H, Xie D, Erickson JW, Lewis MS, Anderson CW, Appella E. 1997.** Effect of phosphorylation on tetramerization of the tumor suppressor protein p53. *J Protein Chem* **16**: 553-556.
- ❖ **Sakamuro D, Sabbatini P, White E, Prendergast GC. 1997.** The polyproline region of p53 is required to activate apoptosis but not growth arrest. *Oncogene* **15**: 887-898.
- ❖ **Sambrook J, Fritsch EF, Maniatis T. 1989.** *Molecular cloning : A laboratory manual*. Cold Spring Harbor, N.Y.: Cold Spring Harbor Laboratory Press.

- ❖ **Sax JK, Fei P, Murphy ME, Bernhard E, Korsmeyer SJ, El-Deiry WS. 2002.** Bid regulation by p53 contributes to chemosensitivity. *Nat Cell Biol* **4**: 842-849.
- ❖ **Scherer SJ, Maier SM, Seifert M, Hanselmann RG, Zang KD, Muller-Hermelink HK, Angel P, Welter C, Scharl M. 2000.** P53 and c-jun functionally synergize in the regulation of the DNA repair gene hms2 in response to uv. *J Biol Chem* **275**: 37469-37473.
- ❖ **Selivanova G, Iotsova V, Kiseleva E, Strom M, Bakalkin G, Grafstrom RC, Wiman KG. 1996.** The single-stranded DNA end binding site of p53 coincides with the c-terminal regulatory region. *Nucleic Acids Res* **24**: 3560-3567.
- ❖ **Selivanova G, Iotsova V, Okan I, Fritsche M, Strom M, Groner B, Grafstrom RC, Wiman KG. 1997.** Restoration of the growth suppression function of mutant p53 by a synthetic peptide derived from the p53 c-terminal domain. *Nat Med* **3**: 632-638.
- ❖ **Selivanova G, Ryabchenko L, Jansson E, Iotsova V, Wiman KG. 1999.** Reactivation of mutant p53 through interaction of a c-terminal peptide with the core domain. *Mol Cell Biol* **19**: 3395-3402.
- ❖ **Sengupta S, Shimamoto A, Koshiji M, Pedoux R, Rusin M, Spillare EA, Shen JC, Huang LE, Lindor NM, Furuichi Y, Harris CC. 2005.** Tumor suppressor p53 represses transcription of recq4 helicase. *Oncogene* **24**: 1738-1748.
- ❖ **Seto E, Usheva A, Zambetti GP, Momand J, Horikoshi N, Weinmann R, Levine AJ, Shenk T. 1992.** Wild-type p53 binds to the tata-binding protein and represses transcription. *Proc Natl Acad Sci U S A* **89**: 12028-12032.
- ❖ **Shakke Z. 2007.** Quaternary structure of p53: The light at the end of the tunnel. *Proc Natl Acad Sci U S A* **104**: 12231-12232.
- ❖ **Sharma A, Khan AA, Gogna R, Singh AK, Pati U. 2009.** p53 amino-terminus region (1-125) stabilizes and restores heat denatured p53 wild phenotype. *PLoS ONE*: Submitted after revision.
- ❖ **Shaulsky G, Goldfinger N, Ben-Ze'ev A, Rotter V. 1990.** Nuclear accumulation of p53 protein is mediated by several nuclear localization signals and plays a role in tumorigenesis. *Mol Cell Biol* **10**: 6565-6577.
- ❖ **Shieh SY, Ikeda M, Taya Y, Prives C. 1997.** DNA damage-induced phosphorylation of p53 alleviates inhibition by mdm2. *Cell* **91**: 325-334.
- ❖ **Shimodaira H, Yoshioka-Yamashita A, Kolodner RD, Wang JY. 2003.** Interaction of mismatch repair protein pms2 and the p53-related transcription factor p73 in apoptosis response to cisplatin. *Proc Natl Acad Sci U S A* **100**: 2420-2425.
- ❖ **Shmueli A, Oren M. 2005.** Life, death, and ubiquitin: Taming the mule. *Cell* **121**: 963-965.
- ❖ **Skulachev VP. 1998.** Cytochrome c in the apoptotic and antioxidant cascades. *FEBS Lett* **423**: 275-280.
- ❖ **Smith ML, Chen IT, Zhan Q, O'Connor PM, Fornace AJ, Jr. 1995.** Involvement of the p53 tumor suppressor in repair of u.V.-type DNA damage. *Oncogene* **10**: 1053-1059.
- ❖ **Soengas MS, Alarcon RM, Yoshida H, Giaccia AJ, Hakem R, Mak TW, Lowe SW. 1999.** Apaf-1 and caspase-9 in p53-dependent apoptosis and tumor inhibition. *Science* **284**: 156-159.
- ❖ **Sogame N, Kim M, Abrams JM. 2003.** Drosophila p53 preserves genomic stability by regulating cell death. *Proc Natl Acad Sci U S A* **100**: 4696-4701.
- ❖ **Stephen CW, Lane DP. 1992.** Mutant conformation of p53. Precise epitope mapping using a filamentous phage epitope library. *J Mol Biol* **225**: 577-583.
- ❖ **Stommel JM, Marchenko ND, Jimenez GS, Moll UM, Hope TJ, Wahl GM. 1999.** A leucine-rich nuclear export signal in the p53 tetramerization domain: Regulation of subcellular localization and p53 activity by nes masking. *EMBO J* **18**: 1660-1672.

- ❖ **Stuart ET, Haffner R, Oren M, Gruss P. 1995.** Loss of p53 function through pax-mediated transcriptional repression. *EMBO J* **14**: 5638-5645.
- ❖ **Sun Y, MacRae TH. 2005.** The small heat shock proteins and their role in human disease. *FEBS J* **272**: 2613-2627.
- ❖ **Szak ST, Mays D, Pietenpol JA. 2001.** Kinetics of p53 binding to promoter sites in vivo. *Mol Cell Biol* **21**: 3375-3386.
- ❖ **Takahashi K, Sumimoto H, Suzuki K, Ono T. 1993.** Protein synthesis-dependent cytoplasmic translocation of p53 protein after serum stimulation of growth-arrested mcf-7 cells. *Mol Carcinog* **8**: 58-66.
- ❖ **Takenaka I, Morin F, Seizinger BR, Kley N. 1995.** Regulation of the sequence-specific DNA binding function of p53 by protein kinase c and protein phosphatases. *J Biol Chem* **270**: 5405-5411.
- ❖ **Takimoto R, El-Deiry WS. 2000.** Wild-type p53 transactivates the killer/dr5 gene through an intronic sequence-specific DNA-binding site. *Oncogene* **19**: 1735-1743.
- ❖ **Takimoto R, Wang W, Dicker DT, Rastinejad F, Lyssikatos J, el-Deiry WS. 2002.** The mutant p53-conformation modifying drug, cp-31398, can induce apoptosis of human cancer cells and can stabilize wild-type p53 protein. *Cancer Biol Ther* **1**: 47-55.
- ❖ **Tan T, Chu G. 2002.** P53 binds and activates the xeroderma pigmentosum ddb2 gene in humans but not mice. *Mol Cell Biol* **22**: 3247-3254.
- ❖ **Tan TH, Wallis J, Levine AJ. 1986.** Identification of the p53 protein domain involved in formation of the simian virus 40 large t-antigen-p53 protein complex. *J Virol* **59**: 574-583.
- ❖ **Tanaka H, Arakawa H, Yamaguchi T, Shiraishi K, Fukuda S, Matsui K, Takei Y, Nakamura Y. 2000.** A ribonucleotide reductase gene involved in a p53-dependent cell-cycle checkpoint for DNA damage. *Nature* **404**: 42-49.
- ❖ **Tang J, Qu LK, Zhang J, Wang W, Michaelson JS, Degenhardt YY, El-Deiry WS, Yang X. 2006.** Critical role for daxx in regulating mdm2. *Nat Cell Biol* **8**: 855-862.
- ❖ **Tao W, Levine AJ. 1999.** Nucleocytoplasmic shuttling of oncoprotein hdm2 is required for hdm2-mediated degradation of p53. *Proc Natl Acad Sci U S A* **96**: 3077-3080.
- ❖ **Tewari V. 2003.** p53 dependent activation and repression of tumour suppressor gene p53. Ph.D. Thesis.
- ❖ **Tokino T, Nakamura Y. 2000.** The role of p53-target genes in human cancer. *Crit Rev Oncol Hematol* **33**: 1-6.
- ❖ **Tompa P, Csermely P. 2004.** The role of structural disorder in the function of rna and protein chaperones. *FASEB J* **18**: 1169-1175.
- ❖ **Tripathi V, Ali A, Bhat R, Pati U. 2007.** Chip chaperones wild type p53 tumor suppressor protein. *J Biol Chem* **282**: 28441-28454.
- ❖ **Tuck SP, Crawford L. 1989.** Characterization of the human p53 gene promoter. *Mol Cell Biol* **9**: 2163-2172.
- ❖ **Van Meir EG, Polverini PJ, Chazin VR, Su Huang HJ, de Tribolet N, Cavenee WK. 1994.** Release of an inhibitor of angiogenesis upon induction of wild type p53 expression in glioblastoma cells. *Nat Genet* **8**: 171-176.
- ❖ **van Tuinen P, Rich DC, Summers KM, Ledbetter DH. 1987.** Regional mapping panel for human chromosome 17: Application to neurofibromatosis type 1. *Genomics* **1**: 374-381.
- ❖ **Velasco-Miguel S, Buckbinder L, Jean P, Gelbert L, Talbott R, Laidlaw J, Seizinger B, Kley N. 1999.** Pa26, a novel target of the p53 tumor suppressor and member of the gadd family of DNA damage and growth arrest inducible genes. *Oncogene* **18**: 127-137.

- ❖ **Venanzoni MC, Robinson LR, Hodge DR, Kola I, Seth A. 1996.** Ets1 and ets2 in p53 regulation: Spatial separation of ets binding sites (ebs) modulate protein: DNA interaction. *Oncogene* **12**: 1199-1204.
- ❖ **Veprintsev DB, Freund SM, Andreeva A, Rutledge SE, Tidow H, Canadillas JM, Blair CM, Fersht AR. 2006.** Core domain interactions in full-length p53 in solution. *Proc Natl Acad Sci U S A* **103**: 2115-2119.
- ❖ **Vogelstein B, Lane D, Levine AJ. 2000.** Surfing the p53 network. *Nature* **408**: 307-310.
- ❖ **Vousden KH. 2000.** P53: Death star. *Cell* **103**: 691-694.
- ❖ **Vousden KH, Lu X. 2002.** Live or let die: The cell's response to p53. *Nat Rev Cancer* **2**: 594-604.
- ❖ **Vousden KH, Woude GF. 2000.** The ins and outs of p53. *Nat Cell Biol* **2**: E178-180.
- ❖ **Walerych D, Kudla G, Gutkowska M, Wawrzynow B, Muller L, King FW, Helwak A, Boros J, Zylicz A, Zylicz M. 2004.** Hsp90 chaperones wild-type p53 tumor suppressor protein. *J Biol Chem* **279**: 48836-48845.
- ❖ **Walker KK, Levine AJ. 1996.** Identification of a novel p53 functional domain that is necessary for efficient growth suppression. *Proc Natl Acad Sci U S A* **93**: 15335-15340.
- ❖ **Wang C, Chen J. 2003.** Phosphorylation and hsp90 binding mediate heat shock stabilization of p53. *J Biol Chem* **278**: 2066-2071.
- ❖ **Wang P, Reed M, Wang Y, Mayr G, Stenger JE, Anderson ME, Schwedes JF, Tegtmeyer P. 1994.** P53 domains: Structure, oligomerization, and transformation. *Mol Cell Biol* **14**: 5182-5191.
- ❖ **Wang PL, Sait F, Winter G. 2001.** The 'wildtype' conformation of p53: Epitope mapping using hybrid proteins. *Oncogene* **20**: 2318-2324.
- ❖ **Wang R, Brattain MG. 2007.** The maximal size of protein to diffuse through the nuclear pore is larger than 60kda. *FEBS Lett* **581**: 3164-3170.
- ❖ **Wang S, El-Deiry WS. 2006.** P73 or p53 directly regulates human p53 transcription to maintain cell cycle checkpoints. *Cancer Res* **66**: 6982-6989.
- ❖ **Wang XW, Zhan Q, Coursen JD, Khan MA, Kontny HU, Yu L, Hollander MC, O'Connor PM, Fornace AJ, Jr., Harris CC. 1999.** Gadd45 induction of a g2/m cell cycle checkpoint. *Proc Natl Acad Sci U S A* **96**: 3706-3711.
- ❖ **Wang Y, Prives C. 1995.** Increased and altered DNA binding of human p53 by s and g2/m but not g1 cyclin-dependent kinases. *Nature* **376**: 88-91.
- ❖ **Warnock LJ, Raines SA. 2004.** Restoration of wild-type conformation to full-length and truncated p53 proteins: Specific effects of atp and adp. *Cancer Biol Ther* **3**: 634-637.
- ❖ **Wawrzynow B, Zylicz A, Wallace M, Hupp T, Zylicz M. 2007.** Mdm2 chaperones the p53 tumor suppressor. *J Biol Chem* **282**: 32603-32612.
- ❖ **Wei CL, Wu Q, Vega VB, Chiu KP, Ng P, Zhang T, Shahab A, Yong HC, Fu Y, Weng Z, Liu J, Zhao XD, Chew JL, Lee YL, Kuznetsov VA, Sung WK, Miller LD, Lim B, Liu ET, Yu Q, Ng HH, Ruan Y. 2006.** A global map of p53 transcription-factor binding sites in the human genome. *Cell* **124**: 207-219.
- ❖ **Weinberg RL, Veprintsev DB, Bycroft M, Fersht AR. 2005.** Comparative binding of p53 to its promoter and DNA recognition elements. *J Mol Biol* **348**: 589-596.
- ❖ **Wells M, Tidow H, Rutherford TJ, Markwick P, Jensen MR, Mylonas E, Svergun DI, Blackledge M, Fersht AR. 2008.** Structure of tumor suppressor p53 and its intrinsically disordered n-terminal transactivation domain. *Proc Natl Acad Sci U S A* **105**: 5762-5767.
- ❖ **Wetzel CC, Berberich SJ. 2001.** P53 binds to cisplatin-damaged DNA. *Biochim*

- ❖ **Whitesell L, Sutphin PD, Pulcini EJ, Martinez JD, Cook PH. 1998.** The physical association of multiple molecular chaperone proteins with mutant p53 is altered by geldanamycin, an hsp90-binding agent. *Mol Cell Biol* **18**: 1517-1524.
- ❖ **Wiman KG. 2006.** Strategies for therapeutic targeting of the p53 pathway in cancer. *Cell Death Differ* **13**: 921-926.
- ❖ **Woods DB, Vousden KH. 2001.** Regulation of p53 function. *Exp Cell Res* **264**: 56-66.
- ❖ **Wu GS, Burns TF, McDonald ER, 3rd, Jiang W, Meng R, Krantz ID, Kao G, Gan DD, Zhou JY, Muschel R, Hamilton SR, Spinner NB, Markowitz S, Wu G, el-Deiry WS. 1997.** Killer/dr5 is a DNA damage-inducible p53-regulated death receptor gene. *Nat Genet* **17**: 141-143.
- ❖ **Wu H, Lozano G. 1994.** Nf-kappa b activation of p53. A potential mechanism for suppressing cell growth in response to stress. *J Biol Chem* **269**: 20067-20074.
- ❖ **Wu X, Bayle JH, Olson D, Levine AJ. 1993.** The p53-mdm-2 autoregulatory feedback loop. *Genes Dev* **7**: 1126-1132.
- ❖ **Xirodimas DP, Lane DP. 1999.** Molecular evolution of the thermosensitive pab1620 epitope of human p53 by DNA shuffling. *J Biol Chem* **274**: 28042-28049.
- ❖ **Xu J, Morris GF. 1999.** P53-mediated regulation of proliferating cell nuclear antigen expression in cells exposed to ionizing radiation. *Mol Cell Biol* **19**: 12-20.
- ❖ **Yamabe Y, Shimamoto A, Goto M, Yokota J, Sugawara M, Furuichi Y. 1998.** Sp1-mediated transcription of the werner helicase gene is modulated by rb and p53. *Mol Cell Biol* **18**: 6191-6200.
- ❖ **Yan W, Chen X. 2006.** Gpx2, a direct target of p63, inhibits oxidative stress-induced apoptosis in a p53-dependent manner. *J Biol Chem* **281**: 7856-7862.
- ❖ **Yin Y, Stephen CW, Luciani MG, Fahraeus R. 2002.** P53 stability and activity is regulated by mdm2-mediated induction of alternative p53 translation products. *Nat Cell Biol* **4**: 462-467.
- ❖ **Yoon KA, Nakamura Y, Arakawa H. 2004.** Identification of aldh4 as a p53-inducible gene and its protective role in cellular stresses. *J Hum Genet* **49**: 134-140.
- ❖ **Yu J, Wang Z, Kinzler KW, Vogelstein B, Zhang L. 2003.** Puma mediates the apoptotic response to p53 in colorectal cancer cells. *Proc Natl Acad Sci U S A* **100**: 1931-1936.
- ❖ **Yu J, Zhang L, Hwang PM, Kinzler KW, Vogelstein B. 2001.** Puma induces the rapid apoptosis of colorectal cancer cells. *Mol Cell* **7**: 673-682.
- ❖ **Zacchi P, Gostissa M, Uchida T, Salvagno C, Avolio F, Volinia S, Ronai Z, Blandino G, Schneider C, Del Sal G. 2002.** The prolyl isomerase pin1 reveals a mechanism to control p53 functions after genotoxic insults. *Nature* **419**: 853-857.
- ❖ **Zauberman A, Flusberg D, Haupt Y, Barak Y, Oren M. 1995.** A functional p53-responsive intronic promoter is contained within the human mdm2 gene. *Nucleic Acids Res* **23**: 2584-2592.
- ❖ **Zhang Y, Xiong Y. 2001.** A p53 amino-terminal nuclear export signal inhibited by DNA damage-induced phosphorylation. *Science* **292**: 1910-1915.
- ❖ **Zheng H, You H, Zhou XZ, Murray SA, Uchida T, Wulf G, Gu L, Tang X, Lu KP, Xiao ZX. 2002.** The prolyl isomerase pin1 is a regulator of p53 in genotoxic response. *Nature* **419**: 849-853.
- ❖ **Zhu J, Chen X. 2000.** Mcg10, a novel p53 target gene that encodes a kh domain rna-binding protein, is capable of inducing apoptosis and cell cycle arrest in g(2)-m. *Mol Cell Biol* **20**: 5602-5618.
- ❖ **Zotchev SB, Protopopova M, Selivanova G. 2000.** P53 c-terminal interaction with DNA ends and gaps has opposing effect on specific DNA binding by the core. *Nucleic Acids Res* **28**: 4005-4012.

- ❖ **Zou Z, Gao C, Nagaich AK, Connell T, Saito S, Moul JW, Seth P, Appella E, Srivastava S. 2000.** P53 regulates the expression of the tumor suppressor gene maspin. *J Biol Chem* **275**: 6051-6054.
- ❖ **Zylicz M, King FW, Wawrzynow A. 2001.** Hsp70 interactions with the p53 tumour suppressor protein. *EMBO J* **20**: 4634-4638.

Appendix

1. PREPARATION OF BACTERIAL CULTURE MEDIA

Luria Bertani (LB) Broth

Dissolve 20 gms of LB powder in double distilled water. Sterilize the media by autoclaving for 20 mins at 15 lb/sq.in.

LB Agar

Dissolve 40 gms of LB agar powder in double distilled water. Sterilize the media by autoclaving for 20 mins at 15 lb/sq.in. Allow LB agar to cool and pour in 90 mm disposable petri plates (Tarsons) along with appropriate antibiotics and allow it to solidify.

2. ANTIBIOTICS SOLUTION

Ampicillin

Prepare 100 mg/ml stock in double distilled water and sterilize by filtration through 0.22 μ m filter. Store at -20°C .

Kanamycin

Prepare 50 mg/ml stock solution in double distilled water and sterilize by filtration through 0.22 μ m filter. Store at -20°C .

3. SOLUTIONS FOR PLASMID ISOLATION AND PURIFICATION

Solution I

50 mM	Glucose
25 mM	Tris-Cl (pH 8.0)
10 mM	EDTA

Prepare Solution I in batches of 100 ml, autoclave for 20 mins at 15 lb/sq.inch and store at 4°C .

Solution II

0.2 N	NaOH (freshly diluted from 10 N stock).
1 %	SDS

Solution III

5M Potassium acetate	60 ml
Glacial Acetic acid	11.5 ml
MQ H ₂ O	28.5 ml

The resulting solution is 3 M with respect to potassium and 5 M with respect to acetate. Autoclave at 15 lb/sq.inch for 20 mins. Store at 4 °C.

4. STOCK SOLUTION OF COMMONLY USED REAGENTS

10 M Ammonium Acetate

Dissolve 385.4 gm of Ammonium acetate in 150 ml of water. Make up the volume to 500 ml. Sterilize the solution by autoclaving for 15 mins at 121 °C/15 lb/sq. in.

1 M CaCl₂

Dissolve 147 gm of Calcium Chloride (CaCl₂.2H₂O) in 1 litre water and sterilize the solution by filtration with a 0.22-micron filter membrane.

1 M Dithiothreitol (DTT)

Dissolve 3.09 gm of Dithiothreitol in 20 ml of 0.01M Sodium acetate, pH 5.2 and store at -20 °C after filter sterilization with 0.22-micron filter.

0.5 M EDTA

Dissolve 186.1 gm of Na₂EDTA.2H₂O powder in 700 ml of water. Keep on shaking vigorously. Adjust pH to 8.0 with 10M NaOH. EDTA will not dissolve completely until the pH of solution reaches 8.0. Finally, add water to 1 litre and autoclave the solution.

70 % Ethanol

Mix 70 ml of pure ethanol and add 30 ml of sterile water to make up the total volume to 100 ml. Store it at 4 °C.

50 % Glycerol

Add 50 ml of glycerol to 50 ml of sterile water; mix thoroughly and sterilize by autoclaving.

1 M HEPES Buffer (pH 7.9, 8.0)

Dissolve 23.83 gm of solid HEPES salt into 80 ml of sterile water. Adjust the pH to the desired value using 1 M NaOH. Make up the final volume to 100 ml with water. Filter the solution with a 0.45 micron filter. The buffer should be stored at 4 °C.

1 M KCl

Dissolve 74.6 gm of Potassium Chloride in 1 litre of water and autoclave. Store at RT.

1 M MgCl₂

Dissolve 20.3 gm of Magnesium Chloride (Hexahydrate) dry powder and make up the total volume to 1 litre with water. Sterilize the solution by autoclaving.

5 M NaCl

Dissolve 292.2 gm of Sodium Chloride in 800 ml water and make up the total volume to 1 litre with water. Finally, sterilize the solution by autoclaving.

Nonidet P-40 (NP-40)

Make 10 % solution of NP-40 detergent in sterile water as a stock solution. This solution can be diluted as per requirement.

dNTP's Mix (dATP, dCTP, dGTP, dTTP)

Prepare 25 mM each dNTP in T₁₀E₁ buffer, pH 7.5. Combine all the four dNTP's at a final concentration of 2.5 mM each and store in small aliquots at -20 °C.

Phenol:Chloroform:Isoamyl alcohol

Mix 25 parts (v/v) Phenol (previously equilibrated in 150 mM NaCl/50 mM Tris-Cl, pH 7.5 and 1 mM EDTA) with 24 parts (v/v) Chloroform and 1 part (v/v) of Isoamyl alcohol. Store in a dark coloured glass bottle at 4 °C.

Protease Inhibitors

All the protease inhibitor solutions were made as 100 X concentration stock. They should be added to the pre-cooled solutions just before use. All the protease

inhibitor solutions are active for 3-4 weeks at a storage temperature of -20 °C.

The required concentration of the solutions is 1 X.

Leupeptin	100 µg/ml in water
Aprotinin	100 µg/ml in water
Trypsin Inhibitor	100 µg/ml in water

Salmon Sperm DNA (denatured)

Dissolve 100 mg Salmon Sperm DNA in 1 ml of water. Pass vigorously through a 18-gauge needle 20 times to shear the DNA. Place in boiling water bath for 10 mins and then chill it. Store at -20 °C in small aliquots.

Sephadex G-50 and G-25

Add 10 gm of Sephadex G-50/ G-25 powder to 160 ml of sterile water. Wash the swollen resin with sterile water several times to remove soluble dextran, which can create problems by precipitating during ethanol precipitation. Finally, autoclave (121 °C/15 lb/sq. inch for 15 mins) and store at room temperature.

1 M Tris (pH 6.8, 7.0, 7.2, 7.4, 8.0, 8.8, 9.5)

Dissolve 121.1 gm of Tris base in 800 ml of MQ H₂O. Adjust pH to desired value by adding concentrated HCl. Make up the final volume to 1 litre with water and sterilize by autoclaving

1.5 M Tris (pH 8.8)

Dissolve 181.65 gm of Tris base in 800 ml of MQ H₂O. Adjust pH to 8.8 by adding concentrated HCl. Make up the final volume to 1 litre with water and sterilize by autoclaving

Triton X-100 (v/v)

Add 10 ml of Triton X-100 detergent solution into 90 ml of water to make up the final volume to 100 ml to get a final concentration of 10 %.

3 M sodium acetate

Dissolve 204.5 gms of $C_2H_3O_2Na \cdot 3H_2O$ in 400 ml of MQ H_2O . Adjust the pH to 5.3 with glacial acetic acid. Make up the volume to 500 ml and autoclave.

10% Sodium Dodecyl Sulphate (SDS)

Dissolve 10 gms of electrophoresis grade SDS in 70 ml of MQ H_2O . Heat at 60 °C to dissolve and make up the volume to 100 ml.

Ethidium Bromide (10 mg/ml)

Dissolve 10 mg of ethidium bromide in 1 ml MQ H_2O . Store in a dark bottle.

30 % Acrylamide Stock

Dissolve 29 gms of acrylamide and 1 gm of bis acrylamide in 50 ml of MQ H_2O . Make up the Volume to 100 ml, filter the solution through Whatman no. 1 paper, degas and store in a dark bottle.

IPTG (1 M)

Dissolve 238 mg of IPTG in 1 ml of MQ H_2O . Filter sterilize and store at -20 °C.

Sodium Phosphate Monobasic (1 M)

Dissolve 138 gms of $NaH_2HPO_4 \cdot H_2O$ in 800 ml of MQ H_2O and make up the volume to 1 liter.

Sodium Phosphate Dibasic (1 M)

Dissolve 268 gms of $Na_2HPO_4 \cdot 7H_2O$ in 700 ml of MQ H_2O and make up the volume to 1 liter.

Ammonium persulfate (10 %)

To 1 gm of ammonium persulfate add 10 ml of MQ H_2O the solution may be stored for several weeks at 4 °C.

100mM Phenyl methyl sulfonyl fluoride (PMSF)

Dissolve 17.4 mg of PMSF in 1 ml of isopropanol. Aliquot the solution and store at -20 °C.

5. BUFFERS

Phosphate Buffered Saline (PBS)

Dissolve 8 gms of NaCl, 2 gms of KCl, 1.44 gms of Na₂HPO₄ and 0.2 gms of KH₂PO₄ in 800 ml of MQ H₂O. Adjust the pH to 7.4 with HCl. Make up the final volume to 1 liter and sterilize by autoclaving at 15 lb/ sq.in for 20 mins and store at room temperature.

SDS-PAGE electrophoresis buffer

Dissolve 3 gms of Tris base, 14.4 gms of glycine and 1 gm of SDS in 1 liter of MQ H₂O.

Electrode (Protein) transfer buffer

Dissolve 5.8 gms of Tris base, 2.9 gms of glycine and 0.33 gms of SDS in 0.5 liter of MQ H₂O. Add 200 ml of methanol and make up the final volume to 1 liter with MQ H₂O.

2X SDS-PAGE sample buffer

The composition of sample buffer is as follows

100mM	Tris-Cl (pH6.8)
200mM	DTT
4%	SDS
0.2%	Bromophenol blue
20%	Glycerol
10%	β-mercaptoethanol

Annealing Buffer

Tris, pH 7.4	60mM
MgCl ₂	10mM
DTT	5mM
Spermidine	1mM

5X EMSA buffer

Glycerol	20%
MgCl ₂	5mM
EDTA	2.5mM
DTT	2.5mM
NaCl	250mM
Tris-Cl pH 7.5	50mM

6X Gel Loading Buffer

Bromophenol blue	0.25 % (w/v)
Xylene cyanol FF	0.25 % (w/v)
Ficoll (Type 400)	15 % (w/v)

Add MQ H₂O to make up the total volume. Store at room temperature.

OR

Alternatively, the DNA loading dye can be made with following components:

Bromophenol blue	0.25 % (w/v)
Xylene cyanol FF	0.25 % (w/v)
Glycerol	30 % (v/v)

Add MQ H₂O to make up the total volume. Store at 4 °C.

50X TAE buffer

Tris Base	242 gm
Glacial acetic acid	57.1 ml
Na ₂ EDTA.2H ₂ O	37.2 gm

Add sterile water to make up the total volume to 1 litre.

10X TBE buffer

Tris base	107.8 gm
Boric acid	55 gm
Disodium EDTA.2H ₂ O	7.44 gm

Add sterile water to make up the total volume to 1 litre.

5X Tris glycine buffer

Tris base	15.1 gm
Glycine	72.0 gm
SDS	5.0 gm

Add MQ H₂O to make up the total volume to 1 litre.

10X T4 PNK buffer

Tris-Cl, pH 7.5	500 mM
MgCl ₂	100 mM
DTT	50 mM
BSA/Gelatin	0.5 mg/ml

6. BUFFERS FOR CHROMATIN IMMUNOPRECIPITATION**Lysis Buffer**

1.0 % SDS, 10 mM EDTA, 50 mM Tris-Cl, pH 8.1, 1 X Protease inhibitor cocktail

Dilution Buffer

1.0 % Triton X-100, 2 mM EDTA, 150 mM NaCl and 20 mM Tris-Cl, pH 8.1, 1 X Protease inhibitor cocktail

TSE I buffer

0.1 % SDS, 1 % Triton X -100, 2 mM EDTA, 20 mM Tris-Cl, pH 8.1 and 150 mM NaCl, 1 X Protease inhibitor cocktail

TSE II Buffer

0.1 %SDS, 1.0 % Triton X -100, 2 mM EDTA, 20 mM Tris-Cl, pH 8.1, and 500 mM NaCl, 1 X Protease inhibitor cocktail

Buffer III

0.25 M LiCl, 1.0 % NP-40, 1.0 % deoxycholate, 1.0 mM EDTA, and 10 mM Tris-Cl, pH 8.1

TE Buffer

20 mM Tris-Cl pH8.1 and 1 mM EDTA

Elution Buffer

1 % SDS and 0.1M NaHCO₃

7. BUFFERS FOR IMMUNOPRECIPITATION

NP-40 Buffer

20 mM Tris-Cl pH 7.4, 100 mM NaCl, 10 % Glycerol, 1.0 % NP-40 and 1mM EDTA, 1 X protease inhibitor cocktail.

RIPA Buffer

50 mM Tris-Cl pH 7.4, 150 mM NaCl, 1 % Triton X-100, 0.1 % SDS, 1 % sodium deoxycholate, 1 X protease inhibitor cocktail.

8. SOLUTIONS FOR IMMUNOFLUORESCENCE STAINING

4% paraformaldehyde Stock solution

4 gm paraformaldehyde (Sigma-Aldrich) was added to 100 ml 1X PBS and dissolved on moderate heat, while continuous stirring. Prepared solution was filtered and stored at 4 °C.

Washing Buffer

0.01 % BSA and 0.1 % sodium azide were dissolved in 1 X PBS and only cold solution was used for washing.

Permeabilizing Buffer

0.1 % Triton X-100 and 0.5 % Saponin dissolved in PBS and stored at 4 °C.

Blocking Buffer

1 % BSA dissolved in 1 X PBS.

Antibody Dilution Buffer

0.01 % Saponin, 1 % BSA and 0.1 % Sodium Azide (NaN₃) dissolved in 10 ml 1 X PBS and stored at 4 °C.

9. BUFFERS FOR PROTEIN PURIFICATION

Purification using Ni²⁺-NTA column

Native Lysis buffer (1 liter)

50 mM NaH₂PO₄; 6.90 g NaH₂PO₄ · H₂O (MW 137.99 g/mol)

300 mM NaCl; 17.54 g NaCl (MW 58.44 g/mol)

10 mM imidazole; 0.68 g imidazole (MW 68.08 g/mol)

Adjust pH to 8.0 using NaOH.

Wash buffer (1 liter)

50 mM NaH₂PO₄; 6.90 g NaH₂PO₄ · H₂O (MW 137.99 g/mol)

300 mM NaCl; 17.54 g NaCl (MW 58.44 g/mol)

20 mM imidazole; 1.36 g imidazole (MW 68.08 g/mol)

Adjust pH to 8.0 using NaOH.

Elution buffer (1 liter)

50 mM NaH₂PO₄; 6.90 g NaH₂PO₄ · H₂O (MW 137.99 g/mol)

300 mM NaCl; 17.54 g NaCl (MW 58.44 g/mol)

250 mM imidazole; 17.00 g imidazole (MW 68.08 g/mol)

Adjust pH to 8.0 using NaOH.

Purification with Glutathione Sepharose

Lysis Buffer

PBS

0.1 % Triton X-100

PMSF

Wash Buffer

PBS

0.1 % Triton X-100

Elution Buffer

Tris-Cl, pH-8.0

10-20 mM reduced Glutathione

10. BUFFERS FOR WESTERN BLOTTING

Buffer 3 (AP-Buffer for Western)

Tris-Cl, pH 9.5	0.1 M
NaCl	0.1 M
MgCl ₂	50 mM

Buffer 4

Take 15 ml of buffer 3 and add 66 µl of NBT along with 33 µl of BCIP from the stock solution. Buffer 4 should be prepared just before use and kept in falcon tube wrapped with aluminium foil.

11. SOLUTIONS FOR SILVER STAINING

Fixative A

Methanol	50 %
Acetic acid	10 %

Add MQ H₂O to make up the total volume.

Fixative B

Ethanol	10 %
Acetic acid	5 %

Add MQ H₂O to make up the total volume.

Oxidizer solution

Potassium dichromate	3.4 mM
Nitric Acid	3.2 mM

Staining Solution

Sliver nitrate	12 mM
----------------	-------

Developer

Sodium Carbonate	0.28 mM
Formaldehyde (Formalin)	75 µl (0.05%)

10 X Calf Intestinal Alkaline Phosphatase buffer

NaCl	500 mM
Tris-Cl, pH 7.9	100 mM
MgCl ₂	100 mM
DTT	10 mM

12. SDS-PAGE REAGENTS

Composition of resolving gel (12%) 10 ml

4.0 ml	30 % acrylamide solution
2.5 ml	1.5 M Tris-Cl, pH 8.8
3.3 ml	MQ H ₂ O
100 µl	10 % SDS
100 µl	10 % APS
10 µl	TEMED

Composition of stacking gel (5%) (5.0 ml)

0.83 ml	30 % acrylamide solution
0.68 ml	10 M Tris-Cl, pH 6.8
3.4 ml	MQ H ₂ O
50 µl	10 % SDS
50 µl	10 % APS
5 µl	TEMED

Staining solution

Dissolve 1 gm of coomassie blue in 450 ml of methanol. Add 100 ml of glacial acetic acid and make up the volume to 1 liter by double distilled water. Filter through Whatman no. 1 and store at room temperature.

Destaining solution

Add methanol: Water: Acetic Acid in the ratio of 45:45:10. Store at RT.

13. ANIMAL TISSUE CULTURE REAGENTS**Phosphate Buffered Saline**

9.85 gms of PBS (Sigma-Aldrich) was dissolved in 1000 ml autoclaved MQ water and was sterilized by filtering.

Dulbecco's modified Eagle's media (DMEM)

DMEM dry powder (Biological Industries) 13.4 gms (with 4.5 mg/l of D-Glucose)

Sodium bicarbonate	33.3mM.
Sodium pyruvate	1.0 mM
Penicillin	100 U/ml
Streptomycin	100 µg/ml

Above media components were dissolved in autoclaved MQ H₂O, pH was adjusted to 7.4 with the help of 1 N HCl and was sterilized by vacuum filtration with 0.22-micron filter assembly. For making complete media, FCS was added to the final concentration of 10 % before filter sterilization. Store the media at 4 °C.

Trypsin-EDTA (TE)

10 X stock of commercial trypsin-EDTA (Sigma-Aldrich) was diluted to 1X with phosphate buffer saline for trypsinization of adherent cells and stored at 4 °C.

Neomycin (G418)

200 mg of Neomycin (G418, Calbiochem) was dissolved in 1 ml of MQ water and filter sterilized and stored at 4 °C (Can be store in refrigerator up to 1 month).

Ocimum
Biosolutions
...enabling R&D™

**Microarray
DATA
ANALYSIS
REPORT**

Prepared by Ocimumbio Solutions

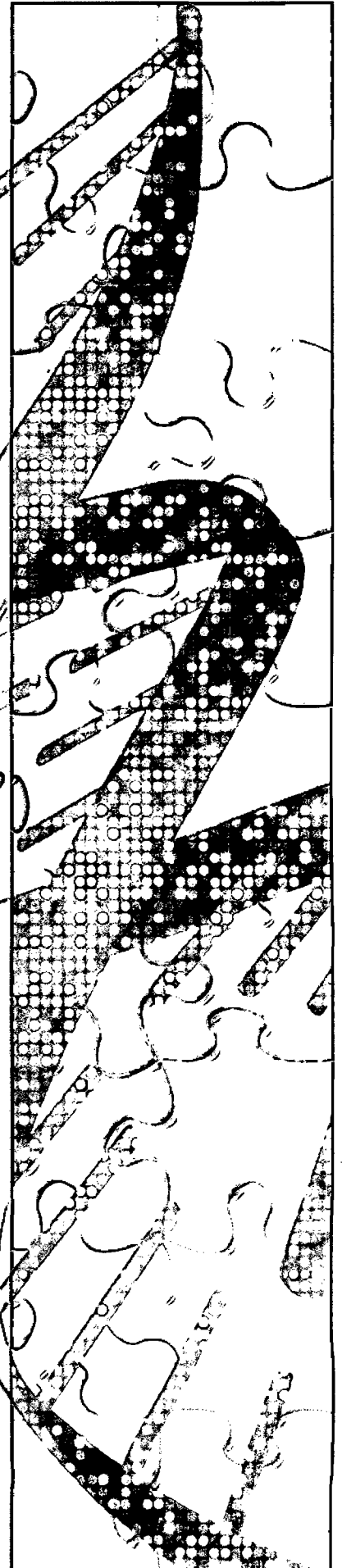




TABLE OF CONTENTS

1.0 Executive Summary.....2

2.0 Classification of Datasets3

3.0 Analysis Requirements.....3

4.0 Analysis Performed.....3

5.0 Results.....6



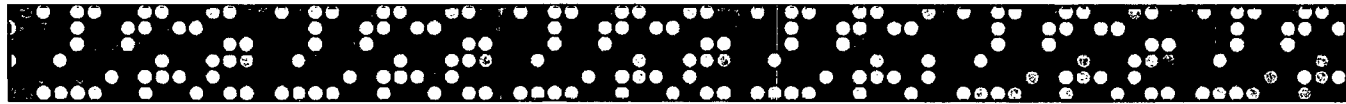

1.0 Executive Summary

This report presents the basic analysis of the data and discusses the types of analyses performed and our findings on the data sets.

This analysis was done using Genowiz™ our proprietary microarray and pathway analysis tool. Genowiz™ is a gene expression analysis and tracking tool that enables researchers to analyze microarray data in an intuitive and comprehensive bio-environment. It includes novel quantification matrices and algorithms that facilitate expression pattern analysis and give an insight into metabolic pathways. It offers an easy to use customizable interface and allows integration of biotools and laboratory information management system. Genowiz™ incorporates an entire army of analysis tools for the efficient analysis of microarray data.

Ocimum also provides analyses that are not required as a part of this study. A list of services provided in the microarray realm can be found at

http://www.ocimumbio.com/web/research_services/microarray_analysis.asp





2.0 Classification of Datasets

Data sets

- KB-125.
- KB (Wild Type).

3.0 Analysis Requirements

Identify Differentially regulated genes for:

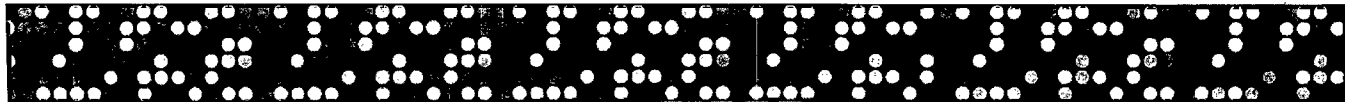
1. KB-125 Vs KB.

Analysis involves identification of up-and down-regulated genes and summarize biological processes associated with the gene lists.

4.0 Analysis Performed

Data has 40320 data-points (or probes). Data from empty spots and production control spots were filtered out. 39,400 genes were retained after initial filtering, which were used in further analysis using Genowiz™.

Data were analyzed to identify up-regulated and down-regulated genes in KB-125 sample when compared with KB(Wild Type) sample. These genes were further studied for biological significance using Gene Ontology terms and pathways.



A list of affected functions, processes , components and pathways has been reported.

Analysis process involved


1. Fold-change Analysis to identify differentially expressed genes.
2. Functional classification of differentially expressed genes.
3. Pathway analysis of differentially expressed genes.

- 1) **Fold-change Analysis to identify differentially expressed genes:** KB-125 sample was compared with KB (Wild Type) sample to find out differentially expressed genes. Genes with at least two-fold change in expression were considered as up-regulated or down-regulated.


<i>Treatment</i>	<i>Number of up regulated genes</i>	<i>Number of down regulated genes</i>
KB-125 Vs KB (Wild Type)	383	934

Table 1: Number of up regulated and down regulated genes in each treatment category

- 2) **Functional classification of differentially expressed genes:** To determine biological significance of differentially expressed genes, functional classification was performed using Gene Ontology. Gene Ontology reports along with z-score are provided in supplementary material for your reference. Numbers in parentheses indicate number of up-regulated/down-regulated genes and total number of genes (in uploaded data), present in that particular ontology respectively. Z-scores give statistical significance, indicating relative representation up-regulated/down-regulated genes in each function; higher the Z-score more significant is the result. (Please refer to supplementary material for details).



3) **Pathway analysis of differentially expressed genes:** To determine pathways associated with differentially expressed genes, pathway analysis was performed. Pathway reports are provided in supplementary material. Numbers in parentheses indicate number of up-regulated / down-regulated genes and total number of genes (in uploaded data), present in that particular pathway respectively. Statistically overrepresented pathways were identified using Fisher exact test, pathways with $p\text{-value} \leq 0.05$ are conventionally regarded as statistically significant and these statistically significant pathways for up- and downregulated genes are marked with blue color in Pathway_Analysis.xls (Please refer to supplementary material for details).





5.0 Results

Biological Process (Based on Gene Ontology based functional classification of differentially expressed genes):

Genes involved in cell communication, regulation of GTPase activity, positive regulation of enzyme activity are upregulated in KB-125 sample when compared to KB (wild type) sample.

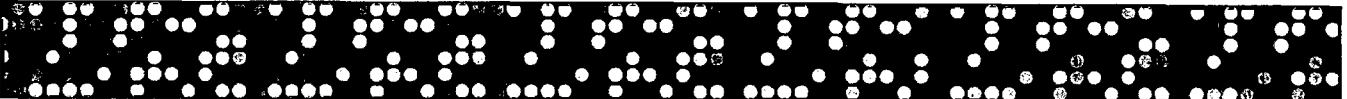
Genes involved in response to stimulus, development, regulation of cell growth, cell differentiation, response to stress are downregulated in KB-125 sample when compared to KB (wild type) sample.

Pathway Analysis:

Genes involved in Nitrogen metabolism, 1- and 2-Mthyl-naphthalene degradation, gamma-Hexachlorocyclohexane degradation, apoptosis (NKKB-2, PRKAR1B), complement and coagulation cascades pathways are some of the pathways which are upregulated in KB-125 sample when compared to KB (wild type) sample.

Genes involved in Oxidative phosphorylation, purine metabolism, N-Glycan biosynthesis, MAPK signaling pathway, cytokine-cytokine receptor interaction, Cell adhesion molecules (CAMs), cell cycle, axon guidance, cell communication pathways are some of the pathways which are downregulated in KB-125 sample when compared to KB (wild type) sample.

(Please refer to GO reports and Pathway report for performing further analysis).



Down-Regulated Genes

Gene Identifier	GenBank Accession	Gene Symbol	Expression Value		Fold Change	Gene Description
			KB (Wild Type)	KB-125	(KB-125/KB)	
obshum40K:A#00067	NM_020125	SLAMF8	3.75	1.54	0.41066664	SLAM family member 8
obshum40K:A#00078	NM_013308	GPR171	1.73	0.7	0.40462425	G protein-coupled receptor 171
obshum40K:A#00090	AY462284	CDK5RAP1	1	0.03	0.03	CDK5 regulatory subunit associated protein 1
obshum40K:A#00128	AC022536	IDI2	0.71	0.05	0.07042254	Homo sapiens chromosome 10 clone RP11-38M7, complete sequence
obshum40K:A#00175	D21209	PTPN13	2.03	0.79	0.38916257	protein tyrosine phosphatase, non-receptor type 13 (APO-1/CD95 (Fas)-associated phosphatase)
obshum40K:A#00601	NM_016571	GLULD1	1.84	0.75	0.4076087	glutamate-ammonia ligase (glutamine synthetase) domain containing 1
obshum40K:A#00845	AK022439	PGAP1	0.33	0.12	0.36363634	GPI deacylase
obshum40K:A#00975	BC029484	C9orf24	0.78	0.39	0.5	chromosome 9 open reading frame 24
obshum40K:A#01009	BC013985	PCQAP	2.28	0.98	0.42982456	PC2 (positive cofactor 2, multiprotein complex) glutamine/Q-rich-associated protein
obshum40K:A#01189	NM_017797	BTBD2	1.19	0.03	0.025210083	BTB (POZ) domain containing 2
obshum40K:A#01259	AF083116	PNMA3	7.85	1.24	0.15796179	paraneoplastic antigen MA3
obshum40K:A#01274	NM_004226	STK17B	1.74	0.28	0.16091955	serine/threonine kinase 17b (apoptosis-inducing)
obshum40K:A#01532	BC017197	MCL1	1.76	0.09	0.051136367	myeloid cell leukemia sequence 1 (BCL2-related)
obshum40K:A#01579	AL137704	DUSP4	3.39	1.17	0.3451327	dual specificity phosphatase 4
obshum40K:A#01661	NM_005108	XYLB	0.81	0.14	0.17283951	xylulokinase homolog (H. influenzae)
obshum40K:A#01891	BC014117	TBXAS1	3.69	0.99	0.2682927	thromboxane A synthase 1 (platelet, cytochrome P450, family 5, subfamily A)
obshum40K:A#01908	NM_014233	UBTF	1.21	0.03	0.024793386	upstream binding transcription factor, RNA polymerase I
obshum40K:A#01962	BC101485	RAD51C	2.57	1.23	0.47859925	RAD51 homolog C (S. cerevisiae)
obshum40K:A#02007	BC018115	TAF6	1.38	0.01	0.007246377	TAF6 RNA polymerase II, TATA box binding protein (TBP)-associated factor, 80kDa
obshum40K:A#02045	NM_005056	JARID1A	2.01	0.04	0.019900497	Jumonji, AT rich interactive domain 1A (RBBP2-like)
obshum40K:A#02062	NM_030579	CY5B	2.79	0.56	0.20071685	outer mitochondrial membrane cytochrome b5
obshum40K:A#02347	NM_018667	SMPD3	1.57	0.6	0.3821656	sphingomyelin phosphodiesterase 3, neutral membrane (neutral sphingomyelinase II)
obshum40K:A#02385	NM_021624	HRH4	1.72	0.54	0.3139535	histamine receptor H4
obshum40K:A#02419	NM_016943	TAS2R3	0.71	0.06	0.08450704	taste receptor, type 2, member 3
obshum40K:A#02432	NM_003620	PPM1D	0.95	0.18	0.18947369	protein phosphatase 1D magnesium-dependent, delta isoform
obshum40K:A#02480	AF083958	BNIP1	1.54	0.64	0.41558442	BCL2/adenovirus E1B 19kDa interacting protein 1
obshum40K:A#02597	BC032465	TCIRG1	1.1	0.53	0.48181814	T-cell, immune regulator 1, ATPase, H ⁺ transporting, lysosomal V0 protein a isoform 3
obshum40K:A#02646	NM_004160	PYY	0.66	0.15	0.22727273	peptide YY
obshum40K:A#02654	NM_002451	MTAP	0.89	0.17	0.19101124	methylthioadenosine phosphorylase

obshum40K:A#02668	AF252828		4.11	1.48	0.36009732	Homo sapiens chromosome 8 clone RP11-245A18 map q24.13, complete sequence
obshum40K:A#02670	NM_005834	TIMM17B	1.07	0.31	0.2897196	translocase of inner mitochondrial membrane 17 homolog B (yeast)
obshum40K:A#02699	AL592309	LOC767853	0.66	0.33	0.5	Human DNA sequence from clone RP11-293F5 on chromosome 1 Contains a novel gene, a novel pseudogene, a novel gene similar to heparan sulfate 6-O-sulfotransferase 1 (HS6ST1), a pseudogene similar to part of a novel gene, the gene for a hypothetical protein
obshum40K:A#02926	NM_000339	SLC12A3	0.78	0.39	0.5	solute carrier family 12 (sodium/chloride transporters), member 3
obshum40K:A#02933	NM_000955	PTGER1	0.5	0.23	0.46	prostaglandin E receptor 1 (subtype EP1), 42kDa
obshum40K:A#03023	AJ243297	RET	0.87	0.34	0.3908046	ret proto-oncogene (multiple endocrine neoplasia and medullary thyroid carcinoma 1, Hirschsprung disease)
obshum40K:A#03218	NM_001344	DAD1	6.06	0.02	0.00330033	defender against cell death 1
obshum40K:A#03390	AK056343	WDR4	1.52	0.72	0.47368422	WD repeat domain 4
obshum40K:A#03400	NM_001348	DAPK3	4.13	1.69	0.40920097	death-associated protein kinase 3
obshum40K:A#03413	NM_002203	ITGA2	0.97	0.38	0.39175257	integrin, alpha 2 (CD49B, alpha 2 subunit of VLA-2 receptor)
obshum40K:A#03422	BC034046	PPFIA1	3.92	0.14	0.035714284	protein tyrosine phosphatase, receptor type, f polypeptide (PTPRF), interacting protein (liprin), alpha 1
obshum40K:A#03439	NM_004761	RGL2	1.02	0.01	0.009803922	ral guanine nucleotide dissociation stimulator-like 2
obshum40K:A#03462	AL713657	COLEC12	3.83	0.93	0.24281985	collectin sub-family member 12
obshum40K:A#03528	NM_000412	HRG	0.68	0.08	0.11764705	histidine-rich glycoprotein
obshum40K:A#03557	NM_000040	APOC3	1.08	0.36	0.33333334	apolipoprotein C-III
obshum40K:A#03562	NM_014625	NPHS2	1.21	0.09	0.07438017	nephrosis 2, idiopathic, steroid-resistant (podocin)
obshum40K:A#03627	NM_014256	B3GNT3	0.79	0.05	0.06329114	UDP-GlcNAc:betaGal beta-1,3-N-acetylglucosaminyltransferase 3
obshum40K:A#03655	BC045631	TNRC6C	0.72	0.02	0.027777776	trinucleotide repeat containing 6C
obshum40K:A#03708	AY714054	AURKC	0.55	0.07	0.12727273	aurora kinase C
obshum40K:A#03811	NM_182627	WDR53	1.94	0.55	0.28350514	WD repeat domain 53
obshum40K:A#03829	NM_021733	TSKS	5.89	1.65	0.28013584	testis-specific kinase substrate
obshum40K:A#03872	NM_014748	SNX17	1.59	0.06	0.037735846	sorting nexin 17
obshum40K:A#03903	NM_006177	NRL	0.42	0.07	0.16666667	neural retina leucine zipper
obshum40K:A#03910	NM_006144	GZMA	0.87	0.05	0.057471264	granzyme A (granzyme 1, cytotoxic T-lymphocyte-associated serine esterase 3)
obshum40K:A#03932	NM_004091	E2F2	1.79	0.17	0.09497207	E2F transcription factor 2
obshum40K:A#03940	NM_001793	CDH3	1.03	0.01	0.009708738	cadherin 3, type 1, P-cadherin (placental)
obshum40K:A#04019	NM_007252	POU6F2	45.58	1.02	0.022378234	POU domain, class 6, transcription factor 2
obshum40K:A#04056	X60702	LTK	1.29	0.14	0.10852714	leukocyte tyrosine kinase
obshum40K:A#04134	BC028687	EXOSC10	3.2	0.2	0.0625	exosome component 10
obshum40K:A#04168	NM_004595	SMS	1.7	0.3	0.1764706	spermine synthase
obshum40K:A#04203	BX647500	COL6A3	0.85	0.34	0.4	collagen, type VI, alpha 3

obshum40K:A#04268	NM_003955	SOCS3	1.61	0.8	0.49689442	suppressor of cytokine signaling 3
obshum40K:A#04272	BC035422	SOD2	4.32	1.82	0.4212963	superoxide dismutase 2, mitochondrial
obshum40K:A#04313	NM_002531	NTSR1	5.11	1.96	0.38356164	neurotensin receptor 1 (high affinity)
obshum40K:A#04318	NM_001560	IL13RA1	1.05	0.07	0.06666667	interleukin 13 receptor, alpha 1
obshum40K:A#04322	NM_004557	NOTCH4	0.67	0.11	0.1641791	Notch homolog 4 (Drosophila)
obshum40K:A#04415	AK023479	CNNM2	0.64	0.1	0.15625	cyclin M2
obshum40K:A#04489	BC037272	CNNM3	1.19	0.55	0.46218488	cyclin M3
obshum40K:A#04545	NM_007009	ZBPB	1.18	0.12	0.10169492	zona pellucida binding protein
obshum40K:A#04572	NM_005255	GAK	1.04	0.37	0.35576925	cyclin G associated kinase
obshum40K:A#04623	NM_006343	MERTK	1.57	0.51	0.32484075	c-mer proto-oncogene tyrosine kinase
obshum40K:A#04706	NM_004533	MYBPC2	0.74	0.24	0.3243243	myosin binding protein C, fast type
obshum40K:A#04709	BC103688	DLX6	0.91	0.08	0.08791208	Homo sapiens distal-less homeobox 6, mRNA (cDNA clone MGC:125285 IMAGE:40000523), complete cds
obshum40K:A#04754	AL713697	BIN1	1.27	0.38	0.2992126	bridging integrator 1
obshum40K:A#04830	NM_004609	TCF15	1.18	0.11	0.093220346	transcription factor 15 (basic helix-loop-helix)
obshum40K:A#04914	NM_005194	CEBPB	1.1	0.2	0.18181819	CCAAT/enhancer binding protein (C/EBP), beta
obshum40K:A#04924	BC069331	ELA2A	6.9	3.21	0.46521738	elastase 2A
obshum40K:A#04952	U07664	HLXB9	0.63	0.27	0.42857146	homeo box HB9
obshum40K:A#04981	NM_000073	CD3G	0.84	0.11	0.13095239	CD3G antigen, gamma polypeptide (TiT3 complex)
obshum40K:A#05013	BC012120	NFIC	1.67	0.45	0.26946107	nuclear factor 1/C (CCAAT-binding transcription factor)
obshum40K:A#05037	AC022336	KALRN	1.07	0.53	0.49532706	Homo sapiens 3 BAC RP11-71H17 (Roswell Park Cancer Institute Human BAC Library) complete sequence
obshum40K:A#05048	NM_012466	TSPAN16	0.88	0.11	0.125	Homo sapiens tetraspanin 16 (TSPAN16), mRNA
obshum40K:A#05090	NM_006951	TAF5	0.52	0.15	0.28846157	TAF5 RNA polymerase II, TATA box binding protein (TBP)-associated factor, 100kDa
obshum40K:A#05202	BC033711	ATXN3	0.54	0.24	0.44444442	ataxin 3
obshum40K:A#05286	NM_133180	EPS8L1	0.55	0.21	0.38181818	EPS8-like 1
obshum40K:A#05313	NM_003742	ABCB11	24.1	0.45	0.018672198	ATP-binding cassette, sub-family B (MDR/TAP), member 11
obshum40K:A#05512	AY305384	ASAH1	0.35	0.16	0.45714286	N-acylsphingosine amidohydrolase (acid ceramidase) 1
obshum40K:A#05545	NM_002970	02/01/07	18.19	8.53	0.46893895	spermidine/spermine N1-acetyltransferase
obshum40K:A#05548	NM_000648	CCR2	0.78	0.39	0.5	chemokine (C-C motif) receptor 2
obshum40K:A#05562	NM_023918	TAS2R8	0.44	0.11	0.25	taste receptor, type 2, member 8
obshum40K:A#05566	BC084540	MARK2	1.24	0.05	0.04032258	MAP/microtubule affinity-regulating kinase 2
obshum40K:A#05567	BC021237	C2orf28	2.6	1.18	0.45384616	chromosome 2 open reading frame 28
obshum40K:A#05573	NM_019018	FAM105A	0.55	0.15	0.27272728	hypothetical protein FLJ11127
obshum40K:A#05592	AL021528	PAX7	5.98	2.99	0.5	Human DNA sequence from clone RP3-394P21 on chromosome 1p36.12-36.13 Contains the PAX7 gene for Paired box gene 7 and two

						CpG islands, complete sequence
obshum40K:A#05630	NM_016944	TAS2R4	1	0.18	0.18	taste receptor, type 2, member 4
obshum40K:A#05637	NM_005215	DCC	0.79	0.11	0.1392405	deleted in colorectal carcinoma
obshum40K:A#05785	NM_004061	CDH12	0.71	0.25	0.35211268	cadherin 12, type 2 (N-cadherin 2)
obshum40K:A#06010	NM_014906	PPM1E	0.94	0.02	0.021276595	protein phosphatase 1E (PP2C domain containing)
obshum40K:A#06070	NM_017420	SIX4	0.31	0.09	0.2903226	sine oculis homeobox homolog 4 (Drosophila)
obshum40K:A#06141	AC141077		10.24	3.88	0.37890628	Homo sapiens chromosome 16 clone RP11-799N4, complete sequence
obshum40K:A#06157	U79266	SAC3D1	6.11	2.3	0.37643206	Human clone 23627 mRNA, complete cds
obshum40K:A#06400	NM_015721	GEMIN4	1.45	0.08	0.05517241	gem (nuclear organelle) associated protein 4
obshum40K:A#06446	NM_016423	ZNF219	0.89	0.05	0.056179777	zinc finger protein 219
obshum40K:A#06528	NM_005813	PRKD3	1.01	0.07	0.06930693	protein kinase D3
obshum40K:A#06582	NM_012135	FAM50B	0.69	0.01	0.014492753	family with sequence similarity 50, member B
obshum40K:A#06628	XM_497965		2.36	0.1	0.042372882	similar to Ac2-210
obshum40K:A#06666	NM_018440	PAG1	0.64	0.06	0.09375	Homo sapiens phosphoprotein associated with glycosphingolipid microdomains 1 (PAG1), mRNA
obshum40K:A#06802	NM_006494	ERF	1.26	0.04	0.03174603	Ets2 repressor factor
obshum40K:A#06834	NM_014278	HSPA4L	1.11	0.05	0.045045044	heat shock 70kDa protein 4-like
obshum40K:A#06909	NM_022773	TMEM112	3.71	1.38	0.37196764	Homo sapiens hypothetical protein FLJ12681 (FLJ12681), mRNA
obshum40K:A#06942	NM_022055	KCNK12	2.24	0.17	0.07589286	potassium channel, subfamily K, member 12
obshum40K:A#06948	NM_022466	IKZF5	0.74	0.02	0.027027026	zinc finger protein, subfamily 1A, 5
obshum40K:A#06954	NM_007286	SYNPO	1.64	0.03	0.018292682	synaptopodin
obshum40K:A#06972	AF096771	MYLK	0.9	0.03	0.033333335	myosin, light polypeptide kinase
obshum40K:A#06982	NM_000932	PLCB3	0.92	0.02	0.021739129	phospholipase C, beta 3 (phosphatidylinositol-specific)
obshum40K:A#07042	CR597835	MAP2K3	0.92	0.09	0.097826086	full-length cDNA clone CS0DM014YD04 of Fetal liver of Homo sapiens (human)
obshum40K:A#07125	NM_005592	MUSK	0.57	0.05	0.0877193	muscle, skeletal, receptor tyrosine kinase
obshum40K:A#07182	BC020225	LOC220686	1.02	0.2	0.19607843	hypothetical protein LOC220686
obshum40K:A#07241	AF022375	VEGFA	1.19	0.45	0.37815124	vascular endothelial growth factor
obshum40K:A#07270	NM_024997	ATF7IP2	0.68	0.03	0.044117644	activating transcription factor 7 interacting protein 2
obshum40K:A#07308	AF414184	DAZ2	0.45	0.18	0.40000004	deleted in azoospermia 2
obshum40K:A#07313	NM_006083	IK	1.86	0.3	0.16129033	IK cytokine, down-regulator of HLA II
obshum40K:A#07370	AF279784	SLCO1A2	0.8	0.21	0.2625	solute carrier organic anion transporter family, member 1A2
obshum40K:A#07382	NM_000352	ABCC8	2.32	1.11	0.4784483	ATP-binding cassette, sub-family C (CFTR/MRP), member 8
obshum40K:A#07386	NM_001524	HCRT	2.46	0.11	0.044715445	hypocretin (orexin) neuropeptide precursor
obshum40K:A#07395	NM_019841	TRPV5	8.75	2.17	0.24800001	transient receptor potential cation channel, subfamily V, member 5
obshum40K:A#07449	NM_007345	ZNF236	5.55	1.9	0.34234232	zinc finger protein 236
obshum40K:A#07471	NM_022482	GZF1	2.41	1.06	0.439834	zinc finger protein 336

obshum40K:A#07474	NM_001963	EGF	1.58	0.28	0.17721519	epidermal growth factor (beta-urogastrone)
obshum40K:A#07602	NM_000051	ATM	0.52	0.09	0.17307694	ataxia telangiectasia mutated (includes complementation groups A, C and D)
obshum40K:A#07625	NM_016256	NAGPA	0.68	0.04	0.058823526	N-acetylglucosamine-1-phosphodiester alpha-N-acetylglucosaminidase
obshum40K:A#07634	NM_000139	MS4A2	1.48	0.73	0.49324325	membrane-spanning 4-domains, subfamily A, member 2 (Fc fragment of IgE, high affinity I, receptor for; beta polypeptide)
obshum40K:A#07664	NM_015986	CRLF3	1.83	0.62	0.3387978	cytokine receptor-like factor 3
obshum40K:A#07666	NM_001200	BMP2	0.87	0.15	0.1724138	bone morphogenetic protein 2
obshum40K:A#07708	X80289	PTPN13	0.75	0.02	0.026666665	protein tyrosine phosphatase, non-receptor type 13 (APO-1/CD95 (Fas)-associated phosphatase)
obshum40K:A#07722	NM_002501	NFIX	0.68	0.17	0.25	nuclear factor I/X (CCAAT-binding transcription factor)
obshum40K:A#07791	X91504	ARFRP1	1.08	0.03	0.027777776	ADP-ribosylation factor related protein 1
obshum40K:A#07803	NM_002763	PROX1	0.48	0.1	0.20833334	prospero-related homeobox 1
obshum40K:A#07808	NM_002195	INSL4	1.05	0.24	0.22857143	insulin-like 4 (placenta)
obshum40K:A#07811	NM_001927	DES	0.57	0.16	0.28070176	desmin
obshum40K:A#07924	NM_004829	NCR1	1.73	0.2	0.115606934	natural cytotoxicity triggering receptor 1
obshum40K:A#07956	NM_006256	PKN2	1.69	0.06	0.035502955	protein kinase N2
obshum40K:A#07983	BC019694	IHPK2	0.94	0.17	0.18085107	inositol hexaphosphate kinase 2
obshum40K:A#08073	NM_002364	MAGEB2	0.77	0.15	0.1948052	melanoma antigen family B, 2
obshum40K:A#08119	AJ488102	NAV2	0.62	0.07	0.11290322	neuron navigator 2
obshum40K:A#08148	NM_002245	KCNK1	2.63	0.27	0.102661595	potassium channel, subfamily K, member 1
obshum40K:A#08191	NM_004217	AURKB	2.83	0.33	0.116607785	aurora kinase B
obshum40K:A#08275	NM_006035	CDC42BPB	2.14	0.4	0.18691587	CDC42 binding protein kinase beta (DMPK-like)
obshum40K:A#08315	BC078144	SULT1A4	6.53	0.03	0.00459418	sulfotransferase family, cytosolic, 1A, phenol-preferring, member 3
obshum40K:A#08369	NM_001189	BAPX1	1.11	0.24	0.2162162	bagpipe homeobox homolog 1 (Drosophila)
obshum40K:A#08388	NM_016356	DCDC2	4.21	0.49	0.11638955	doublecortin domain containing 2
obshum40K:A#08396	NM_004776	B4GALT5	1.05	0.25	0.23809525	UDP-Gal:betaGlcNAc beta 1,4- galactosyltransferase, polypeptide 5
obshum40K:A#08427	NM_000340	SLC2A2	1.81	0.17	0.09392265	solute carrier family 2 (facilitated glucose transporter), member 2
obshum40K:A#08447	NM_002209	ITGAL	0.66	0.12	0.18181817	integrin, alpha L (antigen CD11A (p180), lymphocyte function-associated antigen 1; alpha polypeptide)
obshum40K:A#08529	NM_013392	NRBP1	0.62	0.01	0.016129032	nuclear receptor binding protein
obshum40K:A#08551	NM_016179	TRPC4	1.04	0.17	0.16346155	transient receptor potential cation channel, subfamily C, member 4
obshum40K:A#08590	Z23116	BCL2L1	1.58	0.21	0.13291138	BCL2-like 1
obshum40K:A#08627	NM_004782	SNAP29	2.41	0.36	0.1493776	synaptosomal-associated protein, 29kDa
obshum40K:A#08646	NM_007191	WIF1	0.74	0.07	0.09459459	WNT inhibitory factor 1
obshum40K:A#08658	NM_018460	ARHGAP15	0.68	0.21	0.30882353	Rho GTPase activating protein 15
obshum40K:A#08699	BC041075	TCL6	0.94	0.19	0.20212765	T-cell leukemia/lymphoma 6

obshum40K:A#08707	NM_005273	GNB2	2.43	0.08	0.03292181	guanine nucleotide binding protein (G protein), beta polypeptide 2
obshum40K:A#08801	NM_014450	SIT1	0.63	0.1	0.15873016	Homo sapiens signaling threshold regulating transmembrane adaptor 1 (SIT1), mRNA
obshum40K:A#08852	NM_004360	CDH1	1.01	0.05	0.04950495	cadherin 1, type 1, E-cadherin (epithelial)
obshum40K:A#08972	AF095791	TACC2	0.67	0.08	0.11940298	transforming, acidic coiled-coil containing protein 2
obshum40K:A#08980	NM_006783	GJB6	0.75	0.07	0.093333334	gap junction protein, beta 6 (connexin 30)
obshum40K:A#09118	NM_006344	CLEC10A	0.52	0.06	0.115384616	C-type lectin domain family 10, member A
obshum40K:A#09146	NM_005446	P2RXL1	1.43	0.27	0.1888112	purinergic receptor P2X-like 1, orphan receptor
obshum40K:A#09161	BC008021	GMPT2	1.06	0.27	0.254717	guanosine monophosphate reductase 2
obshum40K:A#09175	NM_007278	GABARAP	1.7	0.43	0.25294116	GABA(A) receptor-associated protein
obshum40K:A#09262	NM_006502	POLH	0.46	0.15	0.32608697	polymerase (DNA directed), eta
obshum40K:A#09370	BC064499	SSFA2	1.61	0.43	0.26708075	sperm specific antigen 2
obshum40K:A#09454	NM_001307	CLDN7	1.14	0.1	0.0877193	claudin 7
obshum40K:A#09463	NM_021727	FADS3	9.46	3.27	0.34566596	fatty acid desaturase 3
obshum40K:A#09485	NM_017727	FLJ20254	1.15	0.13	0.11304348	hypothetical protein FLJ20254
obshum40K:A#09515	NM_002291	LAMB1	6.51	0.14	0.021505376	laminin, beta 1
obshum40K:A#09611	NM_000258	MYL3	1.1	0.1	0.09090909	myosin, light polypeptide 3, alkali; ventricular, skeletal, slow
obshum40K:A#09621	NM_000591	CD14	1.12	0.1	0.08928572	CD14 antigen
obshum40K:A#09774	NM_002342	LTBR	2.6	1.17	0.45	lymphotoxin beta receptor (TNFR superfamily, member 3)
obshum40K:A#09785	NM_003380	VIM	5.19	1.9	0.36608863	vimentin
obshum40K:A#09814	NM_003901	SGPL1	1.77	0.44	0.24858758	sphingosine-1-phosphate lyase 1
obshum40K:A#09864	NM_030930	UNC93B1	6.46	0.77	0.119195044	unc-93 homolog B1 (C. elegans)
obshum40K:A#10098	NM_022072	NSUN3	1.02	0.1	0.09803922	NOL1/NOP2/Sun domain family, member 3
obshum40K:A#10181	NM_031948	PRSS27	1.47	0.1	0.06802721	Homo sapiens protease, serine 27 (PRSS27), mRNA
obshum40K:A#10273	NM_017849	TMEM127	1.06	0.28	0.26415095	hypothetical protein FLJ20507
obshum40K:A#10341	BC015757	DGUOK	1.03	0	0	deoxyguanosine kinase
obshum40K:A#10407	DQ246833	ND6	58.9	29.23	0.49626485	Homo sapiens isolate IND23 mitochondrion, complete genome
obshum40K:A#10585	NM_022370	ROBO3	0.49	0.15	0.30612245	roundabout, axon guidance receptor, homolog 3 (Drosophila)
obshum40K:A#10617	NM_020186	ACN9	1.14	0.37	0.32456142	ACN9 homolog (S. cerevisiae)
obshum40K:A#10734	AC154990		1.54	0.73	0.474026	Homo sapiens chromosome 9 clone fa1066, complete sequence
obshum40K:A#10805	NM_020175	DUS3L	1.9	0.16	0.08421052	Homo sapiens dihydrouridine synthase 3-like (S. cerevisiae) (DUS3L), mRNA
obshum40K:A#10952	NM_032564	DGAT2	16.64	4.5	0.2704327	diacylglycerol O-acyltransferase homolog 2 (mouse)
obshum40K:A#11087	NM_000184	HBG2	2.47	0.07	0.02834008	hemoglobin, gamma G
obshum40K:A#11654	NM_013274	POLL	0.92	0	0	polymerase (DNA directed), lambda
obshum40K:A#11680	NM_031484	MARVELD1	2.24	0.1	0.04464286	MARVEL domain containing 1
obshum40K:A#11729	NM_017577	GRAMD1C	0.33	0.04	0.12121212	Homo sapiens GRAM domain containing 1C (GRAMD1C), mRNA

obshum40K:A#11733	AF411456	TTC23	0.76	0.36	0.47368422	Homo sapiens proto-oncogene 8 mRNA, complete cds
obshum40K:A#11864	NM_006193	PAX4	0.94	0.4	0.42553192	paired box gene 4
obshum40K:A#11867	NM_000374	UROD	0.78	0.26	0.33333334	uroporphyrinogen decarboxylase
obshum40K:A#11907	NM_030784	GPR63	1.61	0.06	0.03726708	G protein-coupled receptor 63
obshum40K:A#12167	BC047673	APBA2BP	0.42	0.02	0.04761905	amyloid beta (A4) precursor protein-binding, family A, member 2 binding protein
obshum40K:A#12239	AF118081		3.79	1.69	0.4459103	Homo sapiens PRO1900 mRNA, complete cds
obshum40K:A#12256	NM_015492	C15orf39	2.3	1.06	0.46086955	Homo sapiens chromosome 15 open reading frame 39 (C15orf39), mRNA
obshum40K:A#12339	BC069742		2.03	0.91	0.4482759	Homo sapiens cDNA clone IMAGE:7262538, with apparent retained intron
obshum40K:A#12360	AF063595	B3GALT4	0.48	0.16	0.33333334	UDP-Gal:betaGlcNAc beta 1,3-galactosyltransferase, polypeptide 4
obshum40K:A#12441	AK021656	C17orf53	6.36	2.1	0.33018866	hypothetical protein MGC3130
obshum40K:A#12601	BC063850	DNM1	0.42	0.06	0.14285715	dynamin 1
obshum40K:A#12864	U80741		1.24	0.59	0.47580642	Homo sapiens CAGH44 mRNA, partial cds
obshum40K:A#12913	NM_001380	DOCK1	0.17	0.08	0.4705882	dedicator of cytokinesis 1
obshum40K:A#12957	NM_001013617	LOC541469	1.26	0.03	0.023809524	Homo sapiens hypothetical LOC541469 protein (LOC541469), mRNA
obshum40K:A#13149	AY870329	XRCC6	69.52	31.12	0.44764102	Homo sapiens thyroid autoantigen 70kDa (Ku antigen) (G22P1) gene, complete cds
obshum40K:A#13254	BC008026	MGC16025	0.83	0.03	0.036144577	hypothetical protein MGC16025
obshum40K:A#13496	AL354808	PSPC1	0.44	0.07	0.1590909	Human DNA sequence from clone RP11-523H24 on chromosome 13 Contains the 3' end of a novel gene, the gene for paraspeckle protein 1 (PSP1) (FLJ10955), two novel genes, a sialyltransferase 7D (SIAT7D) pseudogene, the 3' end of a variant of the ZNF237 gene
obshum40K:A#13511	NM_006612	KIF1C	1.95	0.06	0.030769229	kinesin family member 1C
obshum40K:A#13520	NM_015621	CCDC69	7.54	1.73	0.22944297	DKFZP434C171 protein
obshum40K:A#14506	NM_020768	KCTD16	0.64	0.17	0.265625	potassium channel tetramerisation domain containing 16
obshum40K:A#14531	NM_030795	STMN4	0.88	0.38	0.4318182	stathmin-like 4
obshum40K:A#14790	NM_006645	STARD10	4.77	1.51	0.31656185	START domain containing 10
obshum40K:A#15574	NM_017651	AHI1	0.88	0.36	0.40909094	Abelson helper integration site
obshum40K:A#15731	BC008058	PRKCZ	0.78	0.19	0.24358974	protein kinase C, zeta
obshum40K:A#15998	NM_005030	PLK1	1.88	0.04	0.021276595	polo-like kinase 1 (Drosophila)
obshum40K:A#16101	NR_001551	TTY12	0.09	0.03	0.33333333	testis-specific transcript, Y-linked 12
obshum40K:A#16137	NM_017828	COMMD4	3.7	0.02	0.005405405	COMM domain containing 4
obshum40K:A#16138	BC007366	C9orf70	1.1	0.54	0.4909091	chromosome 9 open reading frame 70
obshum40K:A#16216	NM_152743	C7orf27	0.51	0.02	0.039215688	chromosome 7 open reading frame 27
obshum40K:A#16219	XM_032571		0.48	0.14	0.2916667	KIAA0888 protein
obshum40K:A#16282	BC007796	FRMD5	0.96	0.04	0.041666668	Homo sapiens hypothetical protein MGC14161, mRNA (cDNA clone

						IMAGE:4111078), partial cds
obshum40K:A#16359	NM_031208	FAHD1	1.74	0.03	0.01724138	fumarylacetoacetate hydrolase domain containing 1
obshum40K:A#16387	NM_000030	AGXT	1.28	0.07	0.0546875	alanine-glyoxylate aminotransferase (oxalosis I; hyperoxaluria I; glycolicaciduria; serine-pyruvate aminotransferase)
obshum40K:A#16442	NM_022780	RMND5A	1.08	0.24	0.22222221	hypothetical protein FLJ13910
obshum40K:A#16518	NM_031481	SLC25A18	0.88	0.36	0.40909094	solute carrier family 25 (mitochondrial carrier), member 18
obshum40K:A#16606	AC110760	DKFZP564O0823	0.43	0.16	0.37209302	Homo sapiens BAC clone RP11-44F21 from 4, complete sequence
obshum40K:A#17054	AY775289	PRMT1	0.98	0.09	0.091836736	HMT1 hnRNP methyltransferase-like 2 (<i>S. cerevisiae</i>)
obshum40K:A#17087	NM_032109	OTP	1.09	0.28	0.25688073	orthopedia homolog (<i>Drosophila</i>)
obshum40K:A#17182	BC103831	PTHB1	0.59	0.24	0.40677968	Homo sapiens parathyroid hormone-responsive B1, transcript variant 2, mRNA (cDNA clone MGC:118917 IMAGE:40001794), complete cds
obshum40K:A#17549	BC093940	RNF19	0.64	0.28	0.4375	ring finger protein 19
obshum40K:A#17562	NM_032034	SLC4A11	1.54	0.65	0.42207792	solute carrier family 4, sodium bicarbonate transporter-like, member 11
obshum40K:A#17710	NM_001012271	BIRC5	27.01	12.27	0.4542762	baculoviral IAP repeat-containing 5 (survivin)
obshum40K:A#17800	BC071597	KIAA0286	0.61	0.05	0.08196721	KIAA0286 protein
obshum40K:A#17819	NM_022138	SMOC2	0.7	0.04	0.057142857	SPARC related modular calcium binding 2
obshum40K:A#17831	NM_052875	VPS26B	0.54	0.27	0.5	vacuolar protein sorting 26 homolog B (yeast)
obshum40K:A#17923	AC092597	ATP10D	0.57	0.02	0.03508772	Homo sapiens BAC clone RP11-100N21 from 4, complete sequence
obshum40K:A#17947	NM_024315	C7orf23	0.58	0.09	0.15517242	chromosome 7 open reading frame 23
obshum40K:A#18050	NM_032961	PCDH10	0.3	0.11	0.36666664	protocadherin 10
obshum40K:A#18074	BC015712	GFM2	0.92	0.06	0.06521739	G elongation factor, mitochondrial 2
obshum40K:A#18222	NM_025220	ADAM33	3.39	1.49	0.43952802	ADAM metallopeptidase domain 33
obshum40K:A#18278	NM_025163	PIGZ	0.55	0.27	0.4909091	SMP3 mannosyltransferase
obshum40K:A#18312	CR608401	CSH1	0.51	0.25	0.49019608	chorionic somatomammotropin hormone 1 (placental lactogen)
obshum40K:A#18654	BX936346	RPL10	0.97	0.04	0.041237112	Human DNA sequence from clone WI2-88778H2 on chromosome X Contains the 5' end of the FLNA gene for filamin A, alpha (actin binding protein 280), two artifact genes, the EMD gene for emerin (Emery-Dreifuss muscular dystrophy), a TEC gene, the 5' end of the
obshum40K:A#18757	NM_144770	RBM11	0.74	0.03	0.04054054	RNA binding motif protein 11
obshum40K:A#18787	U19727	MAP4	0.96	0.45	0.46875	microtubule-associated protein 4
obshum40K:A#18826	AL035652	TOP1	1.09	0.5	0.4587156	topoisomerase (DNA) I
obshum40K:A#18902	NM_014346	TBC1D22A	0.66	0.16	0.24242423	TBC1 domain family, member 22A
obshum40K:A#19184	NM_000055	BCHE	0.72	0.07	0.09722222	butyrylcholinesterase
obshum40K:A#19318	NM_032265	ZMYND15	1.67	0.8	0.47904193	zinc finger, MYND-type containing 15
obshum40K:A#19323	NM_015289	VPS39	0.16	0.01	0.0625	vacuolar protein sorting 39 (yeast)
obshum40K:A#19334	NM_053043	PRR8	1.13	0.55	0.4867257	Homo sapiens proline rich 8 (PRR8), mRNA
obshum40K:A#19403	NM_030623	SKIP	0.47	0.19	0.4042553	Homo sapiens SPHK1 (sphingosine kinase type 1) interacting protein (SKIP), mRNA

obshum40K:A#19424	AF119893		1.6	0.62	0.3875	Homo sapiens PRO2714 mRNA, complete cds
obshum40K:A#19565	NM_004735	LRRFIP1	1.77	0.18	0.10169492	leucine rich repeat (in FLII) interacting protein 1
obshum40K:A#19646	NM_031415	MLZE	0.85	0.04	0.04705882	melanoma-derived leucine zipper, extra-nuclear factor
obshum40K:A#20279	NM_152464	C17orf32	1.06	0.31	0.29245284	chromosome 17 open reading frame 32
obshum40K:A#20939	AC091821		0.71	0.2	0.28169015	Homo sapiens chromosome 5 clone CTC-325G23, complete sequence
obshum40K:A#21328	XM_496973	PLEKHA2	7.51	3.15	0.41944075	pleckstrin homology domain containing, family A (phosphoinositide binding specific) member 2
obshum40K:A#22048	NM_152996	ST6GALNAC3	0.43	0.16	0.37209302	ST6 (alpha-N-acetyl-neuraminyl-2,3-beta-galactosyl-1,3)-N-acetylgalactosaminide alpha-2,6-sialyltransferase 3
obshum40K:A#22426	NM_015261	NCAPD3	1.19	0.11	0.09243697	Homo sapiens KIAA0056 protein (hCAP-D3), mRNA
obshum40K:A#23313	AC015911	SLFN14	0.81	0.05	0.061728396	E2F transcription factor 3 pseudogene 1
obshum40K:A#24048	NM_032506	KIAA1841	1.16	0.22	0.18965517	KIAA1841 protein
obshum40K:A#24439	NM_052923	ZNF452	0.57	0.05	0.0877193	zinc finger protein 452
obshum40K:A#24508	NM_152647	C15orf33	0.58	0.12	0.20689656	Homo sapiens chromosome 15 open reading frame 33 (C15orf33), mRNA
obshum40K:A#25370	NM_004506	HSF2	1.9	0.92	0.48421055	heat shock transcription factor 2
obshum40K:A#25818	NM_006920	SCN1A	0.74	0.11	0.14864865	sodium channel, voltage-gated, type I, alpha
obshum40K:A#26302	XM_065166	KIAA1957	1.26	0.47	0.37301588	KIAA1957
obshum40K:A#26923	NM_182487	OLFML2A	0.81	0.33	0.40740743	olfactomedin-like 2A
obshum40K:A#28012	AL389889	C20orf83	0.47	0.18	0.38297874	chromosome 20 open reading frame 83
obshum40K:A#28145	AC090505		5.13	1.67	0.32553604	Homo sapiens 3 BAC RP11-152D21 (Roswell Park Cancer Institute Human BAC Library) complete sequence
obshum40K:A#29548	NM_054023	SCGB3A2	0.92	0.33	0.35869566	secretoglobin, family 3A, member 2
obshum40K:A#29664	NM_015480	PVRL3	0.6	0.06	0.099999994	poliovirus receptor-related 3
obshum40K:A#29674	AC009153	GLG1	2.82	0.29	0.10283688	Homo sapiens chromosome 16 clone RP11-572F4, complete sequence
obshum40K:A#29681	NM_032025	EIF2A	2.13	1.05	0.4929577	eukaryotic translation initiation factor (eIF) 2A
obshum40K:A#29696	NM_080743	SRrp35	0.86	0.43	0.5	serine-arginine repressor protein (35 kDa)
obshum40K:A#29742	NM_020782	KLHDC5	0.69	0.02	0.028985506	kelch domain containing 5
obshum40K:A#29821	AB058720	FRMPD3	1.43	0.71	0.4965035	KIAA1817 protein
obshum40K:A#29898	NM_183240	TMEM37	4.42	0.73	0.16515838	transmembrane protein 37
obshum40K:A#29944	BC017736	PIP5K3	0.63	0.23	0.36507937	phosphatidylinositol-3-phosphate/phosphatidylinositol 5-kinase, type III
obshum40K:A#29963	NM_033328	CAPZA3	1.35	0.13	0.09629629	capping protein (actin filament) muscle Z-line, alpha 3
obshum40K:A#29985	NM_020193	C11orf30	1.54	0.02	0.012987013	chromosome 11 open reading frame 30
obshum40K:A#30127	BC017187	RPS6KA5	0.56	0.28	0.5	ribosomal protein S6 kinase, 90kDa, polypeptide 5
obshum40K:A#30314	NM_014444	76P	4.26	1.69	0.3967136	gamma tubulin ring complex protein (76p gene)
obshum40K:A#30331	NM_014800	ELMO1	0.53	0	0	engulfment and cell motility 1 (ced-12 homolog, C. elegans)
obshum40K:A#30385	NM_015649	IRF2BP1	0.52	0.05	0.09615385	interferon regulatory factor 2 binding protein 1

obshum40K:A#30529	BC009701	PADI2	0.95	0.02	0.02105263	peptidyl arginine deiminase, type II
obshum40K:A#30658	NM_025209	EPC1	0.62	0.01	0.016129032	enhancer of polycomb homolog 1 (Drosophila)
obshum40K:A#30686	XM_291141		1.48	0.06	0.04054054	microtubule associated serine/threonine kinase family member 4
obshum40K:A#30696	NM_013320	HCFC2	0.6	0.3	0.5	host cell factor C2
obshum40K:A#30760	NM_022365	DNAJC1	0.68	0.19	0.27941176	DnaJ (Hsp40) homolog, subfamily C, member 1
obshum40K:A#30792	NM_005431	XRCC2	0.84	0.42	0.5	X-ray repair complementing defective repair in Chinese hamster cells 2
obshum40K:A#30795	AC012076	FLJ40411	0.71	0.2	0.28169015	leucine rich repeat (in FLII) interacting protein 1
obshum40K:A#30884	BC010240	CTSB	0.91	0.05	0.054945055	cathepsin B
obshum40K:A#30967	NM_021209	NLRC4	0.6	0.17	0.28333333	caspase recruitment domain family, member 12
obshum40K:A#30994	NM_145307	PLEKHK1	0.55	0.02	0.036363635	pleckstrin homology domain containing, family K member 1
obshum40K:A#31008	NM_020819	KIAA1411	0.58	0.01	0.01724138	KIAA1411
obshum40K:A#31061	BC024229	PTGER3	0.77	0.29	0.37662336	prostaglandin E receptor 3 (subtype EP3)
obshum40K:A#31075	BC100798	VGLL2	1.32	0.65	0.4924242	vestigial like 2 (Drosophila)
obshum40K:A#31147	AF395588	NSD1	0.6	0.27	0.45	nuclear receptor binding SET domain protein 1
obshum40K:A#31230	AF399620	OR3A3	1.99	0.34	0.17085427	olfactory receptor, family 3, subfamily A, member 3
obshum40K:A#31271	NM_000725	CACNB3	1.7	0.68	0.4	calcium channel, voltage-dependent, beta 3 subunit
obshum40K:A#31285	NM_013396	USP25	0.51	0.12	0.23529412	ubiquitin specific peptidase 25
obshum40K:A#31293	NM_005411	SFTPA1	0.77	0.17	0.22077923	surfactant, pulmonary-associated protein A1
obshum40K:A#31419	AL359771	PDPN	16.48	6.18	0.375	Human DNA sequence from clone CTA-520D8 on chromosome 1 Contains the 3' end of the gene for lung type-I cell membrane-associated glycoprotein (T1A-2), a novel gene, the 5' end of the PRDM2 gene for PR domain containing 2 with ZNF domain and a CpG island,
obshum40K:A#31575	Z84484	PNPLA1	0.66	0.06	0.090909086	ets variant gene 7 (TEL2 oncogene)
obshum40K:A#31582	Y19028	HOMER2	8.93	2.94	0.32922733	homer homolog 2 (Drosophila)
obshum40K:A#31626	NM_152933		0.77	0.06	0.077922076	protein phosphatase, EF-hand calcium binding domain 2
obshum40K:A#31871	NM_002802	PSMC1	1.19	0.22	0.18487394	proteasome (prosome, macropain) 26S subunit, ATPase, 1
obshum40K:A#32148	BC022967	WDR22	1.16	0.12	0.10344828	WD repeat domain 22
obshum40K:A#32203	AF022724	PHOX2A	3.87	1.8	0.4651163	paired-like (aristales) homeobox 2a
obshum40K:A#32385	NM_004506	HSF2	1.1	0.51	0.46363634	heat shock transcription factor 2
obshum40K:A#32530	NM_000208	INSR	0.65	0.02	0.03076923	insulin receptor
obshum40K:A#32795	BC042694	ATP5A1	0.97	0.47	0.48453608	ATP synthase, H+ transporting, mitochondrial F1 complex, alpha subunit, isoform 1, cardiac muscle
obshum40K:A#32846	BC013171		1.5	0.17	0.11333334	Homo sapiens cDNA clone MGC:17065 IMAGE:4344401, complete cds
obshum40K:A#32962	D63483	SCARF1	2.39	1.06	0.44351462	scavenger receptor class F, member 1
obshum40K:A#33948	NM_021138	TRAF2	0.41	0.19	0.46341464	TNF receptor-associated factor 2
obshum40K:A#34026	NM_001281	TBCB	0.93	0.21	0.22580644	cytoskeleton associated protein 1
obshum40K:A#34355	NM_004450	ERH	0.28	0.01	0.035714284	enhancer of rudimentary homolog (Drosophila)

obshum40K:A#35255	M26658		1.63	0.33	0.202454	Human testicular angiotensin converting enzyme mRNA (5' variant), complete cds
obshum40K:A#35376	NM_001469	XRCC6	3.84	0.61	0.15885417	Homo sapiens X-ray repair complementing defective repair in Chinese hamster cells 6 (Ku autoantigen, 70kDa) (XRCC6), mRNA
obshum40K:A#35861	NM_005788	PRMT3	0.85	0.34	0.4	HMT1 hnRNP methyltransferase-like 3 (<i>S. cerevisiae</i>)
obshum40K:A#36029	NM_014441	SIGLEC9	1.49	0.73	0.4899329	sialic acid binding Ig-like lectin 9
obshum40K:A#36067	NM_005775	SORBS3	1.28	0.02	0.015625	Homo sapiens sorbin and SH3 domain containing 3 (SORBS3), transcript variant 1, mRNA
obshum40K:A#36354	NM_016363	GP6	1.53	0.27	0.1764706	glycoprotein VI (platelet)
obshum40K:A#36503	AF467444	CTSL	0.84	0.03	0.035714287	cathepsin L
obshum40K:A#36581	AL078633	FLJ44790	1.64	0.67	0.4085366	proteasome (prosome, macropain) subunit, alpha type, 7
obshum40K:A#36609	NM_016219	MAN1B1	0.76	0.02	0.02631579	mannosidase, alpha, class 1B, member 1
obshum40K:A#37247	NM_003255	TIMP2	1.72	0.85	0.49418604	TIMP metalloproteinase inhibitor 2
obshum40K:A#37462	AL450468	CSF1	1.11	0.17	0.15315315	colony stimulating factor 1 (macrophage)
obshum40K:A#37517	NM_016734	PAX5	0.73	0.08	0.10958903	paired box gene 5 (B-cell lineage specific activator)
obshum40K:A#37558	BC051000	TCL1B	1.8	0.3	0.16666667	T-cell leukemia/lymphoma 1B
obshum40K:A#37870	NM_000901	NR3C2	0.82	0.02	0.024390243	nuclear receptor subfamily 3, group C, member 2
obshum40K:A#38113	NM_012073	CCT5	14.19	0.54	0.03805497	chaperonin containing TCP1, subunit 5 (epsilon)
obshum40K:A#38377	BC001439	ABI2	0.74	0.08	0.1081081	abl interactor 2
obshum40K:A#38630	BC006201	AP2B1	1.55	0.01	0.006451613	adaptor-related protein complex 2, beta 1 subunit
obshum40K:A#39251	AL137002	PCID2	4.09	1.31	0.32029337	coagulation factor VII (serum prothrombin conversion accelerator)
obshum40K:A#39767	NM_000367	TPMT	1.64	0.12	0.07317073	thiopurine S-methyltransferase
obshum40K:A#39960	BC009375	CDC2L1	0.95	0.03	0.031578947	cell division cycle 2-like 1 (PITSLRE proteins)
obshum40K:A#40017	AL022097	FARS2	1.31	0.07	0.053435117	phenylalanine-tRNA synthetase 2 (mitochondrial)
obshum40K:A#40196	XM_373343	LOC392447	3.46	0.05	0.014450867	similar to 60S ribosomal protein L32
obshum40K:A#40273	NM_000247	MICA	1.85	0.6	0.32432434	MHC class I polypeptide-related sequence A
obshum40K:A#40285	NM_001194	HCN2	4.88	1.55	0.31762293	hyperpolarization activated cyclic nucleotide-gated potassium channel 2
obshum40K:A#40378	NM_001332	CTNND2	0.68	0.23	0.3382353	catenin (cadherin-associated protein), delta 2 (neural plakophilin-related arm-repeat protein)
obshum40K:A#40910	NM_006644	HSPH1	0.81	0.29	0.3580247	heat shock 105kDa/110kDa protein 1
obshum40K:A#41015	AL353743	LOC548599	1	0.31	0.31	Human DNA sequence from clone RP11-213G2 on chromosome 9 Contains the 3' end of a pseudogene similar to part of a novel protein (DKFZp434D0917), a pseudogene similar to part of a novel protein (DKFZp434D0917), a novel gene, a prohibitin pseudogene (PHB),
obshum40K:A#41086	CR606710	IL18BP	4.31	0.46	0.10672854	full-length cDNA clone CS0DI022YN06 of Placenta Cot 25-normalized of Homo sapiens (human)
obshum40K:A#41367	XM_497700		0.65	0.23	0.35384616	similar to ribosomal protein L6
obshum40K:A#41521	AL133217	HSD17B7P2	0.63	0.09	0.14285715	hypothetical protein LOC158160

obshum40K:A#41557	NM_005537	ING1	0.97	0.03	0.030927833	inhibitor of growth family, member 1
obshum40K:A#41625	NM_003308	TSPY1	0.79	0.2	0.25316456	testis specific protein, Y-linked 1
obshum40K:A#41642	AY742712	SNRPB	6.13	1.19	0.19412725	small nuclear ribonucleoprotein polypeptides B and B1
obshum40K:A#41848	XM_498140		19.51	0.7	0.035879035	similar to ADP,ATP carrier protein, fibroblast isoform (ADP/ATP translocase 2) (Adenine nucleotide translocator 2) (ANT 2)
obshum40K:A#41874	BC107791	CAPN3	1.35	0.34	0.25185186	calpain 3, (p94)
obshum40K:A#41913	NM_005543	INSL3	1.89	0.61	0.32275134	insulin-like 3 (Leydig cell)
obshum40K:A#41942	L07772	CTSL1	1.69	0.2	0.11834319	cathepsin L-like 1
obshum40K:A#42101	XR_000076		66.31	8.28	0.12486804	ribosomal protein, large, P0 pseudogene 2
obshum40K:A#42125	BC018843	PPIA	47.46	0.41	0.008638854	peptidylprolyl isomerase A (cyclophilin A)
obshum40K:A#42205	NM_003254	TIMP1	4.64	1.34	0.28879312	TIMP metalloproteinase inhibitor 1
obshum40K:A#42303	DQ234083	HLA-A	11.8	0.38	0.032203387	Homo sapiens MHC class I antigen (HLA-A) gene, HLA-A*02new allele, exon 4 and partial cds
obshum40K:A#42347	BC007578	PPARD	2.51	0.09	0.035856575	peroxisome proliferative activated receptor, delta
obshum40K:A#42537	NM_000454	SOD1	5.89	1.16	0.19694397	superoxide dismutase 1, soluble (amyotrophic lateral sclerosis 1 (adult))
obshum40K:A#42580	XM_375632		0.66	0.19	0.28787878	similar to Serine/threonine protein phosphatase 5 (PP5) (Protein phosphatase T) (PP-T) (PPT)
obshum40K:A#42627	NM_005514	HLA-B	3.5	0.14	0.04	major histocompatibility complex, class I, B
obshum40K:A#42742	NM_004547	NDUFB4	1.36	0.19	0.13970588	NADH dehydrogenase (ubiquinone) 1 beta subcomplex, 4, 15kDa
obshum40K:A#42908	NM_005052	RAC3	0.53	0.06	0.11320755	ras-related C3 botulinum toxin substrate 3 (rho family, small GTP binding protein Rac3)
obshum40K:A#42946	NM_004474	FOXD2	1.31	0.05	0.038167942	forkhead box D2
obshum40K:A#42976	XM_060887	LOC128192	6.5	0.16	0.024615385	similar to peptidyl-Pro cis trans isomerase
obshum40K:A#43070	AF276292	KIR2DL4	1.2	0.05	0.041666664	killer cell immunoglobulin-like receptor, two domains, long cytoplasmic tail, 4
obshum40K:A#43105	NM_005514	HLA-B	5.42	0.23	0.042435426	major histocompatibility complex, class I, B
obshum40K:A#43237	AK000270	AKAP9	0.4	0.18	0.45000002	A kinase (PRKA) anchor protein (yotiao) 9
obshum40K:A#43259	NG_001334		0.77	0.32	0.41558442	Homo sapiens growth hormone locus (GH@) on chromosome 17
obshum40K:A#43473	BC002431	B4GALT2	3.56	0.07	0.019662922	UDP-Gal:betaGlcNAc beta 1,4- galactosyltransferase, polypeptide 2
obshum40K:A#43566	NR_001296	TRY6	0.86	0.05	0.058139537	trypsinogen C
obshum40K:A#43579	NM_002121	HLA-DPB1	0.67	0.13	0.19402984	major histocompatibility complex, class II, DP beta 1
obshum40K:A#43615	AY597812	KRTAP5-3	3.17	1.29	0.40694004	keratin associated protein 5-3
obshum40K:A#43973	NM_152247	CPT1B	1.2	0.06	0.049999997	carnitine palmitoyltransferase 1B (muscle) [Homo sapiens]
obshum40K:A#44055	NM_000096	CP	0.99	0.09	0.09090909	ceruloplasmin (ferroxidase)
obshum40K:A#44253	AF058803	MUC4	1.49	0.06	0.040268455	mucin 4, tracheobronchial
obshum40K:A#44260	AJ277481	ILK-2	0.46	0.07	0.1521739	integrin-linked kinase-2
obshum40K:A#44393	BC046110	FBXO3	0.7	0.14	0.2	F-box protein 3
obshum40K:A#44416	NM_000924	PDE1B	22.5	8.2	0.36444443	phosphodiesterase 1B, calmodulin-dependent

obshum40K:A#44586	AL109804	HSPA12B	1.01	0.32	0.31683168	cell division cycle 25B
obshum40K:A#44703	CR749236	FOXP2	0.61	0.09	0.14754099	Homo sapiens mRNA; cDNA DKFZp686H1726 (from clone DKFZp686H1726)
obshum40K:A#44732	XM_291314		0.96	0.23	0.23958334	F-box protein 10
obshum40K:A#44762	AB115176		1.27	0.59	0.46456692	Homo sapiens RNA transcript, HERV-W env, isolate:CWE18-3
obshum40K:A#44812	NM_001621	AHR	0.73	0.06	0.08219178	aryl hydrocarbon receptor
obshum40K:A#44862	AL161898	KL	0.65	0.18	0.2769231	klotho
obshum40K:A#44886	AF190464	NR5A2	0.72	0.13	0.18055554	nuclear receptor subfamily 5, group A, member 2
obshum40K:A#44976	AJ438986		1.73	0.22	0.12716763	homeo box C13
obshum40K:B#00062	U92817		1.78	0.81	0.4550562	Homo sapiens unnamed HERV-H protein mRNA, complete cds
obshum40K:B#00172	AL122094	C6orf26	1.36	0.68	0.5	mutS homolog 5 (E. coli)
obshum40K:B#00278	AC093825		1.53	0.61	0.39869282	Homo sapiens BAC clone RP11-389O4 from 4, complete sequence
obshum40K:B#01276	NM_006260	DNAJC3	0.97	0.38	0.39175257	DnaJ (Hsp40) homolog, subfamily C, member 3
obshum40K:B#03499	AC004673		0.55	0.27	0.4909091	Homo sapiens X BAC GSHB-590J15 (Genome Systems Human BAC library) complete sequence
obshum40K:B#09006	AP000901	ZC3H12C	6.54	2.11	0.32262996	Homo sapiens genomic DNA, chromosome 11 clone:RP11-686G14, complete sequence
obshum40K:B#09880	NG_002496	EIF2S2P	0.9	0.13	0.14444444	eukaryotic translation initiation factor 2, subunit 2 beta, pseudogene
obshum40K:B#10182	AC015911	SLFN14	0.63	0.3	0.4761905	Homo sapiens chromosome 17, clone RP11-1094M14, complete sequence
obshum40K:B#10247	AL160035		1.21	0.53	0.4380165	Human DNA sequence from clone RP11-545M8 on chromosome 13 Contains a novel pseudogene similar to HSPC123, a ribosomal protein S21 (RPS21) pseudogene and a ribosomal protein S20 (RPS20) pseudogene, complete sequence
obshum40K:B#10269	NR_001288	LOC260341	1.18	0.06	0.05084746	processed pseudogene mtTFA 1
obshum40K:B#10279	AL359741		0.7	0.24	0.34285715	Human DNA sequence from clone RP11-161P17 on chromosome 13 Contains a novel pseudogene, complete sequence
obshum40K:B#10359	AC023271		1.07	0.35	0.32710278	Homo sapiens BAC clone RP11-96E8 from 2, complete sequence
obshum40K:B#10372	NM_153834	GPR112	1.08	0.54	0.5	G protein-coupled receptor 112
obshum40K:B#10969	AL136146	LDLRAD3	0.93	0.43	0.4623656	Human DNA sequence from clone RP5-916O11 on chromosome 11p12-13, complete sequence
obshum40K:B#10999	NM_152608	C1orf55	1.02	0.46	0.4509804	chromosome 1 open reading frame 55
obshum40K:B#11100	AL109682	LOC145678	0.88	0.4	0.45454547	hypothetical protein LOC145678
obshum40K:B#11114	AP001751	SNF1LK	0.75	0.23	0.30666667	Homo sapiens genomic DNA, chromosome 21q, section 95/105
obshum40K:B#11122	AC092121		0.95	0.44	0.4631579	Homo sapiens chromosome 16 clone RP11-102D18, complete sequence
obshum40K:B#11153	AK021711		1.57	0.75	0.477707	Homo sapiens cDNA FLJ11649 fis, clone HEMBA1004429
obshum40K:B#11162	AP001982		0.79	0.36	0.4556962	Homo sapiens genomic DNA, chromosome 11q, clone:RP11-344F5, complete sequence

obshum40K:B#11168	AL512783	CAMK1D	1.69	0.52	0.3076923	Human DNA sequence from clone RP11-462F15 on chromosome 10 Contains the 3' end of the gene for CamKI-like protein kinase (CKLiK) (LOC221042 LOC283070), complete sequence
obshum40K:B#11171	NM_174893	C17orf49	0.85	0.41	0.4823529	hypothetical protein MGC49942
obshum40K:B#11180	AC063979		0.85	0.38	0.4470588	Homo sapiens chromosome 5 clone RP11-474H20, complete sequence
obshum40K:B#11181	NM_181745	GPR120	5.51	2.36	0.42831212	G protein-coupled receptor 120
obshum40K:B#11195	AC074121	NPTX2	0.78	0.37	0.474359	Homo sapiens BAC clone RP11-725M1 from 7, complete sequence
obshum40K:B#11201	AF130116		1.02	0.44	0.43137255	Homo sapiens clone FLC0461 PRO2812 mRNA, complete cds
obshum40K:B#11208	AC093484	SNORD65	0.67	0.3	0.4477612	Homo sapiens chromosome , clone RP11-138I1, complete sequence
obshum40K:B#11223	AL611962	RP11-45J16.2	0.94	0.44	0.4680851	Human DNA sequence from clone RP11-45J16 on chromosome 1 Contains a pseudogene similar to flavin-containing monooxygenase proteins and the gene for a novel protein similar to flavin-containing monooxygenase proteins, complete sequence
obshum40K:B#11303	BC049840	POLDIP3	1.35	0.05	0.037037037	polymerase (DNA-directed), delta interacting protein 3
obshum40K:B#11474	AC009410		1.06	0.2	0.18867926	Homo sapiens BAC clone RP11-335M11 from 2, complete sequence
obshum40K:B#11667	AC104070	TLR3	0.81	0.39	0.48148146	Homo sapiens BAC clone RP11-279K24 from 4, complete sequence
obshum40K:B#11685	AC011676	SLC45A4	0.94	0.41	0.43617022	Homo sapiens chromosome , clone RP11-10J21, complete sequence
obshum40K:B#11688	AC069061		7.51	2.17	0.28894806	Homo sapiens chromosome 17, clone RP11-260A9, complete sequence
obshum40K:B#11694	NG_004324	OR51F4P	2.21	1.09	0.49321267	olfactory receptor, family 51, subfamily F, member 4 pseudogene
obshum40K:B#11765	AY972819	OR4F4	0.6	0.11	0.18333332	olfactory receptor, family 4, subfamily F, member 4
obshum40K:B#11774	AL159999	LOC780815	1.16	0.49	0.42241383	Human DNA sequence from clone RP11-8I8 on chromosome 9 Contains a phosphoribosylaminoimidazole carboxylase (PAICS) pseudogene and the 3' end of one variant of the ROR2 gene for receptor tyrosine kinase-like orphan receptor 2, complete sequence
obshum40K:B#11826	XM_373714		2.64	0.23	0.08712121	hypothetical LOC388338
obshum40K:B#11870	AL031073	MAGEC2	0.85	0.41	0.4823529	Human DNA sequence from clone RP1-142F18 on chromosome Xq26.3-27.2 Contains the MAGEE1 gene for melanoma antigen, family E 1, a melanoma antigen, family E 1(MAGEE1) pseudogene, and a CpG island, complete sequence
obshum40K:B#11871	AL442067	MBNL2	0.52	0.26	0.5	Human DNA sequence from clone RP11-128N14 on chromosome 13 Contains the 3' end of the gene for muscleblind-like protein (MBLL39), the RAP2A gene for a member of the RAS oncogene family and a CpG island, complete sequence
obshum40K:B#11881	XM_376372	LOC134121	0.95	0.37	0.3894737	hypothetical protein LOC134121
obshum40K:B#11895	NM_001012977	RP11-493K23.3	1.04	0.38	0.36538464	hypothetical protein LOC340529
obshum40K:B#11913	AF272976	KLHL5	0.46	0.2	0.4347826	kelch-like 5 (Drosophila)
obshum40K:B#11968	AC079866	SRGAP1	1.11	0.46	0.4144144	Homo sapiens 12 BAC RP11-274J7 (Roswell Park Cancer Institute Human BAC Library) complete sequence
obshum40K:B#12009	Z72006		1.04	0.5	0.48076925	Human DNA sequence from clone LL22NC03-69F4 on chromosome 22,

						complete sequence
obshum40K:B#12285	Z70273		0.58	0.22	0.37931034	Human DNA sequence from clone LL0XNC01-116E7 on chromosome X Contains an E74-like factor 2 (ELF2) pseudogene, a novel gene, the 5' end of a novel gene, a solute carrier family 25 (mitochondrial oxodicycarboxylate carrier) member 21 (SLC25A21) pseudogene and
obshum40K:B#12293	AC092584		0.59	0.26	0.44067797	Homo sapiens BAC clone RP11-20H7 from 2, complete sequence
obshum40K:B#12302	NG_002647	VN1R8P	0.75	0.33	0.44000003	vomeronasal 1 receptor 8 pseudogene
obshum40K:B#12320	AJ250907	RPS21	1.11	0.53	0.47747743	ribosomal protein S21
obshum40K:B#12378	AP001793	RAB12	0.91	0.44	0.48351645	Homo sapiens genomic DNA, chromosome 18 clone:RP11-661O13, complete sequence
obshum40K:B#12727	XM_291028		0.49	0.19	0.3877551	coiled-coil domain containing 39
obshum40K:B#12738	NM_002745	MAPK1	1.92	0.67	0.34895834	mitogen-activated protein kinase 1
obshum40K:B#12793	AC005330	EFNA2	0.74	0.28	0.37837836	Homo sapiens chromosome 19, cosmid R34047 and overlapping PCR product, complete sequence
obshum40K:B#12811	AC008854	RGS7BP	1.66	0.74	0.44578314	Homo sapiens chromosome 5 clone CTD-2177J2, complete sequence
obshum40K:B#12824	NM_181719	TMCO4	1.36	0.67	0.49264705	transmembrane and coiled-coil domains 4
obshum40K:B#12836	NM_152748	KIAA1324L	0.63	0.24	0.3809524	KIAA1324-like
obshum40K:B#12863	AL451050	POU2F1	1.77	0.75	0.42372882	Human DNA sequence from clone RP11-277B15 on chromosome 1 Contains a ribosomal protein S17 (RPS17) pseudogene, a novel gene, the 5' end of the POU2F1 gene for POU domain class 2 transcription factor 1 and a CpG island, complete sequence
obshum40K:B#12882	AC104062		0.88	0.09	0.102272734	Homo sapiens BAC clone RP11-11I23 from 4, complete sequence
obshum40K:B#13001	AL135998	FLJ38964	0.35	0.15	0.42857146	Human chromosome 14 DNA sequence BAC R-137H15 of library RPCI-11 from chromosome 14 of Homo sapiens (Human), complete sequence
obshum40K:B#13011	AC018793		0.77	0.31	0.40259743	Homo sapiens chromosome 11, clone RP11-437G21, complete sequence
obshum40K:B#13020	AC092691		1.21	0.37	0.30578512	Homo sapiens 3q BAC RP11-768G7 (Roswell Park Cancer Institute Human BAC Library) complete sequence
obshum40K:B#13072	XM_499155		1.14	0.45	0.39473683	hypothetical gene supported by AK091930
obshum40K:B#13087	AK123061	NEK10	0.67	0.31	0.46268657	NIMA (never in mitosis gene a)- related kinase 10
obshum40K:B#13240	NM_207514	FLJ20186	0.9	0.06	0.06666667	hypothetical protein FLJ20186
obshum40K:B#13291	AL833655		1.09	0.05	0.04587156	Homo sapiens mRNA; cDNA DKFZp667O0320 (from clone DKFZp667O0320)
obshum40K:B#13294	AC129471		0.72	0.1	0.13888888	Homo sapiens chromosome 5 clone RP11-352J21, complete sequence
obshum40K:B#13642	NM_032283	ZDHHC18	1.01	0.47	0.46534654	zinc finger, DHHC-type containing 18
obshum40K:B#13665	AC023644	LOC646486	1.12	0.45	0.4017857	Homo sapiens chromosome 8, clone RP11-257P3, complete sequence
obshum40K:B#13677	AL137457	SRGAP3	1.42	0.49	0.34507045	SLIT-ROBO Rho GTPase activating protein 3
obshum40K:B#13697	NM_178509	STXBP4	1.08	0.42	0.38888887	syntaxin binding protein 4
obshum40K:B#13702	AC006116	ZNF583	1.07	0.49	0.45794392	Homo sapiens chromosome 19, BAC CIT-B-393i15 (BC301323),

						complete sequence
obshum40K:B#13728	AK095766	LOC284023	1	0.47	0.47	hypothetical protein LOC284023
obshum40K:B#13817	AL031073	MAGEC2	1.36	0.63	0.4632353	Human DNA sequence from clone RP1-142F18 on chromosome Xq26.3-27.2 Contains the MAGEE1 gene for melanoma antigen, family E 1, a melanoma antigen, family E 1(MAGEE1) pseudogene, and a CpG island, complete sequence
obshum40K:B#13833	NM_032285	MGC3207	12.38	5.95	0.4806139	hypothetical protein MGC3207
obshum40K:B#13868	AL080285		0.68	0.34	0.5	Human DNA sequence from clone RP3-344J20 on chromosome 6q16.1-16.3 Contains an arginase, type II (ARG2) pseudogene and a peroxiredoxin 2 (thiol-specific antioxidant 1, natural killer-enhancing factor B, thioredoxin-dependent peroxide reductase 1, thiol-sp
obshum40K:B#13980	AL138997		0.57	0.24	0.42105263	Human DNA sequence from clone RP11-10023 on chromosome 13 Contains a hepatocyte nuclear factor 4 alpha (HNF4A) pseudogene, complete sequence
obshum40K:B#14466	AC117502	YEATS4	0.74	0.27	0.3648649	Homo sapiens 12 BAC RP11-159A18 (Roswell Park Cancer Institute Human BAC Library) complete sequence
obshum40K:B#14562	NM_207420	SLC2A7	0.95	0.35	0.36842105	solute carrier family 2 (facilitated glucose transporter), member 7
obshum40K:B#14649	AC023881		0.71	0.32	0.45070422	Homo sapiens BAC clone RP11-108C2 from 2, complete sequence
obshum40K:B#14652	NM_014631	SH3PXD2A	0.22	0.11	0.5	SH3 multiple domains 1
obshum40K:B#14680	AL117351	GCLM	0.53	0.25	0.47169814	Human DNA sequence from clone RP5-837O21 on chromosome 1p22 Contains the 5' end of the GCLM gene for glutamate-cysteine ligase modifier subunit, a pseudogene similar to part of NADH dehydrogenase 4 (MTND4), a NADH dehydrogenase 3 (MTND3) pseudogene, a cyt
obshum40K:B#14684	NM_030911	CDADC1	0.57	0.24	0.42105263	cytidine and dCMP deaminase domain containing 1
obshum40K:B#14700	AK092508		1.79	0.45	0.25139666	Homo sapiens cDNA FLJ35189 fis, clone PLACE6016210
obshum40K:B#14734	AL159973	RFXAP	16.11	0.5	0.031036623	Human DNA sequence from clone RP11-197L7 on chromosome 13q13.1-13.3 Contains a novel gene similar to binder of Arl Two (Bart1), the RFXAP gene for regulatory factor X-associated protein and a CpG island, complete sequence
obshum40K:B#14759	NM_006772	SYNGAP1	3.73	0.96	0.25737265	synaptic Ras GTPase activating protein 1 homolog (rat)
obshum40K:B#14761	BC007399		3.17	1.08	0.340694	Homo sapiens cDNA clone IMAGE:3836116, partial cds
obshum40K:B#14961	AC132216	LMO2	0.73	0.34	0.4657534	Homo sapiens chromosome 11, clone RP13-786C16, complete sequence
obshum40K:B#15039	NM_001003693	C6orf21	0.83	0.36	0.43373495	chromosome 6 open reading frame 21
obshum40K:B#15070	BX648674	FLJ46481	0.88	0.38	0.4318182	FLJ46481 protein
obshum40K:B#15162	NM_001004698	OR2W5	0.91	0.07	0.07692307	olfactory receptor, family 2, subfamily W, member 5
obshum40K:B#15216	XM_378703		1.09	0.16	0.14678898	hypothetical gene supported by AK129994
obshum40K:B#15530	NM_054104	OR6C3	0.77	0.35	0.45454547	olfactory receptor, family 6, subfamily C, member 3
obshum40K:B#15551	XM_371480		0.81	0.36	0.44444445	similar to tudor domain containing 6 protein
obshum40K:B#15555	AL451127		0.94	0.39	0.4148936	Human DNA sequence from clone RP11-12817 on chromosome 9

						Contains a novel gene, complete sequence
obshum40K:B#15564	AL162274	BNIP3	0.48	0.23	0.4791667	Human DNA sequence from clone RP11-45A17 on chromosome 10 Contains the BNIP3 gene for BCL2/adenovirus E1B 19kD-interacting protein 3, the 5' end of a novel gene, possible ortholog of mouse RIKEN cDNA 6330417G02 gene and CpG islands, complete sequence
obshum40K:B#15582	AK021967		0.82	0.39	0.47560975	Homo sapiens cDNA FLJ11905 fis, clone HEMBB1000050
obshum40K:B#15610	XM_378750		0.76	0.38	0.5	chromosome 18 open reading frame 49
obshum40K:B#15635	BC010502	KRAS	0.92	0.43	0.4673913	v-Ki-ras2 Kirsten rat sarcoma viral oncogene homolog
obshum40K:B#15654	AC099058	MAG11	0.86	0.17	0.19767442	Homo sapiens chromosome 3 clone RP11-714G12, complete sequence
obshum40K:B#15666	CR624559	ALG1	0.44	0.18	0.40909094	full-length cDNA clone CS0DD001YN12 of Neuroblastoma Cot 50-normalized of Homo sapiens (human)
obshum40K:B#15773	AC008981		0.83	0.19	0.22891566	Homo sapiens chromosome 19 clone LLNL-F_162A4, complete sequence
obshum40K:B#16155	NM_207118	GTF2H5	0.55	0.27	0.4909091	general transcription factor IIH, polypeptide 5
obshum40K:B#16157	CR625363	LHX9	0.92	0.4	0.4347826	LIM homeobox 9
obshum40K:B#16166	AC091134		3.16	1.51	0.47784808	Homo sapiens chromosome 17, clone RP11-646F1, complete sequence
obshum40K:B#16171	AL355852	FAM123B	0.78	0.3	0.38461542	Human DNA sequence from clone RP11-403E24 on chromosome X Contains gene FLJ39827 and a CpG island, complete sequence
obshum40K:B#16175	NM_024783	AGBL2	5.96	2.59	0.43456376	ATP/GTP binding protein-like 2
obshum40K:B#16182	AK021878	LOC284017	1.09	0.44	0.40366971	hypothetical protein LOC284017
obshum40K:B#16195	AL137797	DMBX1	0.48	0.18	0.37500003	Human DNA sequence from clone RP5-1109J22 on chromosome 1 Contains three novel genes, the OTX3 gene for orthodenticle homolog 3 (Drosophila) and a CpG island, complete sequence
obshum40K:B#16292	AC092685	ZNF92	1.63	0.52	0.3190184	Homo sapiens BAC clone RP11-746P2 from 7, complete sequence
obshum40K:B#16574	NM_002052	GATA4	0.49	0.17	0.34693876	GATA binding protein 4
obshum40K:B#16673	AC145213		0.55	0.26	0.47272724	Homo sapiens fosmid clone XXFOS-800837B7 from 7, complete sequence
obshum40K:B#16688	AL353708	TOR1AIP1	1.79	0.86	0.48044693	Human DNA sequence from clone RP11-533E19 on chromosome 1 Contains the 5' ends of two novel genes, two novel genes and a laminin receptor 1 (ribosomal protein SA, 67kDa) (LAMR1) pseudogene, complete sequence
obshum40K:B#16758	AL611933		0.59	0.2	0.33898306	Human DNA sequence from clone RP11-374C13 on chromosome 1 Contains a eukaryotic translation elongation factor 1 delta (guanine nucleotide exchange protein) (EEF1D) pseudogene, complete sequence
obshum40K:B#16807	AC015524		2.69	0.95	0.35315984	Homo sapiens chromosome 18, clone RP11-202D1, complete sequence
obshum40K:B#16811	AL359851		1.31	0.62	0.47328246	Human DNA sequence from clone RP13-192B19 on chromosome Xq24-25 Contains a translationally-controlled 1 tumor protein (TPT1) pseudogene, complete sequence
obshum40K:B#16836	AL513007	RNF12	18.14	5.65	0.3114664	Human DNA sequence from clone CTD-2530H13 on chromosome X Contains the RNF12 gene for ring finger protein 12, a cytoplasmic

						poly(A) binding protein (PABPC) pseudogene and a CpG island, complete sequence
obshum40K:B#16866	AC090051	ALDH1L2	0.76	0.34	0.44736844	Homo sapiens 12q BAC RP11-467E3 (Roswell Park Cancer Institute Human BAC Library) complete sequence
obshum40K:B#16874	AL160394	RFC3	1.02	0.06	0.05882353	Human DNA sequence from clone RP11-218I21 on chromosome 13 Contains a voltage dependent anion channel protein pseudogene, complete sequence
obshum40K:B#16909	AC108078	UGT2B24P	0.68	0.28	0.4117647	Homo sapiens BAC clone RP11-790I12 from 4, complete sequence
obshum40K:B#17213	AK123258	C6orf105	0.62	0.27	0.43548387	chromosome 6 open reading frame 105
obshum40K:B#17610	AL139824	MC3R	1.68	0.68	0.4047619	Human DNA sequence from clone RP11-380D15 on chromosome 20 Contains the MC3R gene for melanocortin 3 receptor, a zinc finger pseudogene and a novel gene, complete sequence
obshum40K:B#17625	AL359920		1.87	0.73	0.39037433	Human DNA sequence from clone RP11-359P14 on chromosome 13 Contains a novel gene and a TAR DNA binding protein (TARDBP) pseudogene, the 5' UTR of a novel gene (FLJ21007) and 2 CpG islands, complete sequence
obshum40K:B#17646	AC011355	MGC21644	1.47	0.63	0.4285714	Homo sapiens chromosome 5 clone CTC-354H18, complete sequence
obshum40K:B#17876	AC093928	DNHD2	1.89	0.59	0.3121693	Homo sapiens chromosome 3 clone RP11-241K3, complete sequence
obshum40K:B#17889	AC011146	CNBD1	0.75	0.2	0.26666668	Homo sapiens chromosome 8, clone RP11-2F15, complete sequence
obshum40K:B#18107	AL121995	HSD3B1	1.79	0.69	0.38547486	Human DNA sequence from clone RP5-920G3 on chromosome 1p12-13.3 Contains the 3' end of a hydroxy-delta-5-steroid dehydrogenase 3 beta- and steroid delta-isomerase family (HSD3B) pseudogene, two glyceraldehyde-3-phosphate dehydrogenase (GAPD) pseudogenes, similar to Hypothetical protein MGC67567
obshum40K:B#18116	XM_377445		0.54	0.22	0.4074074	
obshum40K:B#18125	NG_002302	OR1R1P	0.94	0.46	0.4893617	olfactory receptor, family 1, subfamily R, member 1 pseudogene
obshum40K:B#18133	AC090137		1.19	0.41	0.3445378	Homo sapiens chromosome 8, clone RP11-56A10, complete sequence
obshum40K:B#18145	AL109624		1.1	0.52	0.47272724	Human DNA sequence from clone RP1-61M11 on chromosome 11p13 Contains STSs and GSSs, complete sequence
obshum40K:B#18169	NM_173468	MOBK1A	0.74	0.36	0.4864865	MOB1, Mps One Binder kinase activator-like 1A (yeast)
obshum40K:B#18326	AP000445	GLYAT	1.46	0.65	0.44520545	Homo sapiens genomic DNA, chromosome 11q, clone:CMB9-78H16, complete sequences
obshum40K:B#18379	BC043201		2.01	0.97	0.48258707	Homo sapiens cDNA clone IMAGE:5294578
obshum40K:B#18401	NM_001010870	TDRD6	0.92	0.33	0.35869566	tudor domain containing 6
obshum40K:B#18403	XM_290948		0.51	0.15	0.29411766	similar to Hypothetical protein DJ845O24.1
obshum40K:B#18453	XM_373815		0.79	0.35	0.44303796	similar to General transcription factor II-I (GTFII-I) (TFII-I) (Bruton tyrosine kinase-associated protein-135) (BTK-associated protein-135) (BAP-135)
obshum40K:B#18468	NM_207375	CLEC2A	0.84	0.38	0.45238096	C-type lectin domain family 2, member A
obshum40K:B#18528	NM_001017931	PAGE3	0.74	0.3	0.4054054	P antigen family, member 3 (prostate associated)

obshum40K:B#18555	AL450426	OR13D2P	1.59	0.3	0.18867925	Human DNA sequence from clone RP11-317C20 on chromosome 9 Contains five novel olfactory (seven transmembrane helix) receptor genes, a pseudogene similar to part of novel olfactory (seven transmembrane helix) receptor and a CpG island, complete sequence
obshum40K:B#18633	AC131159	WSB2	1.13	0.31	0.27433628	Homo sapiens 12 BAC RP11-33N14 (Roswell Park Cancer Institute Human BAC Library) complete sequence
obshum40K:B#18636	NM_173462	PAPLN	2.32	0.9	0.38793105	papilin, proteoglycan-like sulfated glycoprotein
obshum40K:B#18640	BC010081	MAN2C1	0.86	0.35	0.40697673	mannosidase, alpha, class 2C, member 1
obshum40K:B#18645	AC021660	OR5K2	1.39	0.61	0.43884894	Homo sapiens 3 BAC RP11-227H4 (Roswell Park Cancer Institute Human BAC Library) complete sequence
obshum40K:B#18648	AF364863		0.95	0.4	0.42105263	Homo sapiens metastasis-related protein (WCL1) mRNA, complete cds
obshum40K:B#18676	DQ246833	ND6	151.93	52.13	0.34311858	Homo sapiens isolate IND23 mitochondrion, complete genome
obshum40K:B#18701	NM_004241	JMJD1C	0.79	0.39	0.49367085	jumonji domain containing 1C
obshum40K:B#18731	BC067351	GUSBP1	1.92	0.86	0.4479167	hypothetical protein LOC153561
obshum40K:B#18990	NG_004681	IFNWP12	1.58	0.68	0.43037975	interferon omega pseudogene 12
obshum40K:B#19087	AC024577	ADCY2	0.73	0.33	0.4520548	Homo sapiens chromosome 5 clone CTD-2346M20, complete sequence
obshum40K:B#19107	AC091214	TMTC2	1.24	0.51	0.41129032	Homo sapiens 12q BAC RP11-13F9 (Roswell Park Cancer Institute Human BAC Library) complete sequence
obshum40K:B#19118	XM_294093	ZFP57	2.02	0.95	0.47029704	zinc finger protein 57 homolog (mouse)
obshum40K:B#19121	AC027020	PRKXP1	1.16	0.55	0.47413796	Homo sapiens chromosome 15, clone RP11-526I2, complete sequence
obshum40K:B#19128	AC007922	HRH4	1.67	0.43	0.25748503	Homo sapiens chromosome 18, clone RP11-178F10, complete sequence
obshum40K:B#19871	AC073585	LOC399815	0.92	0.43	0.4673913	Homo sapiens chromosome 10 clone RP11-564D11, complete sequence
obshum40K:B#19882	AC005249		0.75	0.33	0.44000003	Homo sapiens BAC clone GS1-115J1 from 7, complete sequence
obshum40K:B#19884	AF130342		1.12	0.49	0.4375	Homo sapiens chromosome 8, complete sequence
obshum40K:B#19885	AC017063		0.83	0.36	0.43373495	Homo sapiens BAC clone RP11-354H17 from 4, complete sequence
obshum40K:B#19925	AC025287	TERF2IP	1.55	0.32	0.20645161	Homo sapiens chromosome 16 clone RP11-490B18, complete sequence
obshum40K:B#19976	AF202964		0.7	0.34	0.4857143	Homo sapiens chromosome 8 clone XX-77L18 map q21.3, complete sequence
obshum40K:B#19995	AC092366	HSPB3	0.59	0.15	0.25423732	Homo sapiens chromosome 5 clone RP11-461C13, complete sequence
obshum40K:B#20026	AC103925	DKFZp434B1231	0.89	0.25	0.28089887	Homo sapiens chromosome 1 clone RP11-567E21, complete sequence
obshum40K:B#20099	AC141057		0.93	0.46	0.49462366	Homo sapiens chromosome 16 clone RP11-1023K5, complete sequence
obshum40K:B#20102	NG_002375	OPHN1P1	1.5	0.64	0.42666665	Homo sapiens oligophrenin 1 pseudogene 1 (OPHN1P1) on chromosome 22
obshum40K:B#20107	AF399449	OR4H6P	0.53	0.26	0.49056605	olfactory receptor, family 4, subfamily H, member 6 pseudogene
obshum40K:B#20116	AC034214	TAS2R1	0.96	0.36	0.37500003	Homo sapiens chromosome 5 clone CTD-2001E22, complete sequence
obshum40K:B#20175	AC020918		1.45	0.2	0.13793103	Homo sapiens chromosome 5 clone CTD-2020C3, complete sequence
obshum40K:B#20196	AC134043	FLJ31951	2.05	0.97	0.47317076	Homo sapiens chromosome 5 clone RP11-175K6, complete sequence
obshum40K:B#20209	AL512622	STK32C	0.54	0.25	0.46296296	Human DNA sequence from clone RP11-140A10 on chromosome 10

						Contains the 3' end of the gene for protein kinase (PKE), the 3' end of a novel gene, possible ortholog of mouse RIKEN cDNA 6330417G02 gene, a novel gene (LOC282973), the DPYSL4 gene for dihydrop
obshum40K:B#20216	AC010546		0.54	0.15	0.2777778	Homo sapiens chromosome 16 clone RP11-50021, complete sequence
obshum40K:B#20244	AL031010	IYD	0.43	0.17	0.39534885	Human DNA sequence from clone RP3-422F24 on chromosome 6q24.1-25.2 Contains the C6orf71 gene and a signal sequence receptor, alpha (translocon-associated protein alpha) (SSR1) (TRAPA) pseudogene, complete sequence
obshum40K:B#20317	AC104343		0.55	0.27	0.4909091	Homo sapiens chromosome 8, clone RP11-822K17, complete sequence
obshum40K:B#20321	XM_374141		0.59	0.28	0.4745763	hypothetical LOC389332
obshum40K:B#20562	AL121973	FLJ41841	0.73	0.32	0.43835613	Human DNA sequence from clone RP3-401O12 on chromosome 6p11.2-21.1, complete sequence
obshum40K:B#20564	XM_371397	LOC388795	2.95	1.45	0.49152544	similar to hypothetical protein FLJ33620
obshum40K:B#20784	AC008080	FLJ20712	0.77	0.33	0.42857146	Homo sapiens clone RP11-89N17 from 7p14-15, complete sequence
obshum40K:B#20787	AC018509		1.36	0.68	0.5	Homo sapiens chromosome 10 clone RP11-307B23, complete sequence
obshum40K:B#20807	AC134043	FLJ31951	0.45	0.2	0.44444448	Homo sapiens chromosome 5 clone RP11-175K6, complete sequence
obshum40K:B#21031	AL034451		0.7	0.35	0.5	Human DNA sequence from clone RP1-191E19 on chromosome 6q23.2-24.2, complete sequence
obshum40K:B#21085	AL589787	C10orf90	1.03	0.4	0.38834953	Human DNA sequence from clone RP11-422P15 on chromosome 10 Contans the 5' end of the ADAM12 gene for a disintegrin and metalloproteinase domain 12 (meltrin alpha) (MCMP, MLTN, MLTNA, MCMPMltna), a novel gene, the 3' end of a novel gene and a CpG island, c
obshum40K:B#21171	AC093627	MGC70863	0.86	0.43	0.5	Homo sapiens BAC clone RP11-90P13 from 7, complete sequence
obshum40K:B#21190	AC004028		0.54	0.23	0.4259259	Homo sapiens PAC clone RP4-800B9 from 7, complete sequence
obshum40K:B#21282	AL445985	PCOTH	0.76	0.28	0.36842105	Human DNA sequence from clone RP11-45B20 on chromosome 13, complete sequence
obshum40K:B#21507	Z98743		0.54	0.25	0.46296296	Human DNA sequence from clone RP1-181C9 on chromosome 22q13.2-13.33, complete sequence
obshum40K:B#21512	AC008669	SNX24	0.48	0.2	0.4166667	Homo sapiens chromosome 5 clone CTB-36H16, complete sequence
obshum40K:B#21733	XM_498890		1.12	0.54	0.48214287	LOC440850
obshum40K:B#21735	AL121890	C20orf30	1.15	0.48	0.4173913	Human DNA sequence from clone RP5-1116H23 on chromosome 20 Contains the 5' end of the SLC23A2 gene for solute carrier family 23 (nucleobase transporters) member 2, the 3' end of the C20orf30 gene for HSPC274 protein, an RPS21 (ribosomal protein S21) pseud
obshum40K:B#21739	AC092128		1.35	0.61	0.45185184	Homo sapiens chromosome 16 clone RP11-133M24, complete sequence
obshum40K:B#21745	AL137026	CXCL12	1.4	0.58	0.41428572	Human DNA sequence from clone RP11-20J15 on chromosome 10 Contains CXCL12 gene for chemokine (C-X-C motif) ligand 12 (stromal cell-derived factor 1), two putative transcripts and two putative CpG islands, complete sequence

obshum40K:B#21825	AK055918	FLJ31356	0.72	0.33	0.45833334	hypothetical protein FLJ31356
obshum40K:B#21986	AL359757	FAM123A	0.47	0.22	0.4680851	Human DNA sequence from clone RP11-16519 on chromosome 13q12.11-12.3 Contains the PABPC3 gene for poly(A) binding protein, cytoplasmic 3, the gene for a novel protein (FLJ30487), a pseudogene similar to part of 60S ribosomal protein L23a (RPL23A), 4 novel
obshum40K:B#21994	XM_371632	FLJ36157	1.25	0.39	0.31199998	FLJ36157 protein
obshum40K:B#22021	AK057309		1.72	0.44	0.25581396	Homo sapiens cDNA FLJ32747 fis, clone TESTI2001518
obshum40K:B#22072	AL050333	IBTK	0.52	0.2	0.3846154	Human DNA sequence from clone RP1-93K22 on chromosome 6q14.1-15.3 Contains the gene for a novel BTB/POZ domain containing protein (KIAA1417) and a CpG island, complete sequence
obshum40K:B#22079	AC078980		2.3	0.48	0.20869565	Homo sapiens 3q BAC RP11-424I3 (Roswell Park Cancer Institute Human BAC Library) complete sequence
obshum40K:B#22112	AC011841	LOC644257	6.23	0.64	0.10272873	Homo sapiens chromosome 17, clone RP11-272E10, complete sequence
obshum40K:B#22283	AC004674	ATXN3L	0.75	0.07	0.093333334	Homo sapiens X BAC GSHB-600G8 (Genome Systems Human BAC library) complete sequence
obshum40K:B#22288	XM_374070		1.89	0.09	0.04761905	hypothetical LOC389188
obshum40K:B#22366	AC112195		1.62	0.64	0.39506173	Homo sapiens chromosome 5 clone RP11-436K21, complete sequence
obshum40K:B#22452	AC007384	LHFPL3	4.12	1.6	0.38834953	Homo sapiens BAC clone RP11-325F22 from 7, complete sequence
obshum40K:B#22911	AL590325		2.68	0.44	0.1641791	Human DNA sequence from clone RP11-85L21 on chromosome Xq25-26.3 Contains a nucleolin (NCL) pseudogene, a zinc finger family pseudogene, three novel genes, the 3' end of a novel gene and a CpG island, complete sequence
obshum40K:B#23185	AC020611	SRGAP1	0.83	0.31	0.373494	Homo sapiens 12 BAC RP11-1029F8 (Roswell Park Cancer Institute Human BAC Library) complete sequence
obshum40K:B#23271	AC015711	THSD4	1.23	0.5	0.40650406	Homo sapiens, clone RP11-47G3, complete sequence
obshum40K:B#23334	AC090810	PXMP3	0.71	0.3	0.42253524	Homo sapiens chromosome 8, clone RP11-48J8, complete sequence
obshum40K:B#23462	NM_001012970	Clorf100	0.51	0.22	0.43137255	chromosome 1 open reading frame 100
obshum40K:B#23498	AL139331	FOXP4	0.67	0.28	0.41791043	Human DNA sequence from clone RP11-328M4 on chromosome 6 Contains a novel gene, the FOXP4 gene for forkhead box P4 and five CpG islands, complete sequence
obshum40K:B#23628	NG_004225	OR52B1P	0.84	0.32	0.3809524	olfactory receptor, family 52, subfamily B, member 1 pseudogene
obshum40K:B#23741	AC104037		0.43	0.2	0.4651163	Homo sapiens chromosome 8, clone RP11-692P18, complete sequence
obshum40K:B#23778	AC021316	OTUD7A	0.85	0.36	0.42352942	Homo sapiens chromosome 15, clone RP11-11J16, complete sequence
obshum40K:B#24230	NM_001004712	OR4K14	0.5	0.24	0.48	olfactory receptor, family 4, subfamily K, member 14
obshum40K:B#24506	AK056600	LOC441178	1.44	0.3	0.20833333	hypothetical LOC441178
obshum40K:B#24662	AL139158	POU3F1	0.66	0.26	0.39393938	Human DNA sequence from clone RP5-884C9 on chromosome 1p34.1-35.3, complete sequence
obshum40K:B#24831	BC028978		2.18	1.08	0.49541286	Homo sapiens, clone IMAGE:3919084, mRNA
obshum40K:B#24904	NM_198152	UTS2D	1.46	0.49	0.33561644	urotensin 2 domain containing

obshum40K:B#24920	AK056484	LOC441204	0.6	0.27	0.45	hypothetical protein LOC340281
obshum40K:B#24975	AC099061		0.79	0.36	0.4556962	Homo sapiens chromosome 1 clone RP11-105D8, complete sequence
obshum40K:B#25438	AL034412	MIRN222	1.55	0.77	0.4967742	Human DNA sequence from clone RP6-99M1 on chromosome Xp11.1-11.4 Contains a novel pseudogene (GL004), complete sequence
obshum40K:B#25475	NM_016929	CLIC5	1.2	0.56	0.46666664	chloride intracellular channel 5
obshum40K:B#25503	AK023628	LOC199725	0.76	0.34	0.44736844	hypothetical protein LOC199725
obshum40K:B#25505	AC108174		0.67	0.24	0.35820892	Homo sapiens chromosome 5 clone RP11-78C3, complete sequence
obshum40K:B#25563	AC020708		0.59	0.19	0.3220339	Homo sapiens BAC clone RP11-425B17 from 4, complete sequence
obshum40K:B#25577	AC022882	OR8K1	0.66	0.32	0.48484847	Homo sapiens chromosome 11, clone RP11-444K7, complete sequence
obshum40K:B#25585	AC011401	NDFIP1	0.65	0.3	0.4615385	Homo sapiens chromosome 5 clone CTB-35K5, complete sequence
obshum40K:B#26251	XM_093839		1.89	0.7	0.37037036	furry homolog-like (Drosophila)
obshum40K:B#26483	NM_199050	C21orf25	0.55	0.16	0.29090908	chromosome 21 open reading frame 25
obshum40K:B#26523	NM_198449	EMB	0.69	0.17	0.24637681	embigin homolog (mouse)
obshum40K:B#26895	AC118457		0.82	0.38	0.46341464	Homo sapiens chromosome 5 clone CTD-251511, complete sequence
obshum40K:B#27281	BC104458	TEPP	0.78	0.36	0.4615385	testis/prostate/placenta-expressed protein, isoform 2
obshum40K:B#27318	AL031670	FTLL1	0.92	0.42	0.45652172	Human DNA sequence from clone RP4-681N20 on chromosome 20p12.1-13 Contains the 3' end of the PANK2 gene the Pantothenate kinase 2 (Hallervorden-Spatz syndrome), RNF24 gene for ring finger protein 24, a FTL (ferritin light polypeptide) pseudogene and two C
obshum40K:B#27383	AC003085		0.67	0.18	0.26865673	Homo sapiens BAC clone CTB-94H21 from 7, complete sequence
obshum40K:B#27418	XM_085236		0.55	0.25	0.45454544	hypothetical LOC145788
obshum40K:B#27494	BX647680		1.02	0.46	0.4509804	Homo sapiens genomic DNA; cDNA DKFZp686G12112 (from clone DKFZp686G12112)
obshum40K:B#27578	AC073578		2.11	0.89	0.42180097	Homo sapiens 12 BAC RP11-897M7 (Roswell Park Cancer Institute Human BAC Library) complete sequence
obshum40K:B#27591	XM_376423		0.78	0.33	0.42307696	hypothetical gene supported by AK126569
obshum40K:B#27593	XM_170950		1.82	0.58	0.3186813	OTU domain containing 3
obshum40K:B#27611	AK090412	LOC375010	5.41	2.13	0.39371538	hypothetical LOC375010
obshum40K:B#27960	XM_114611		1.41	0.55	0.39007095	hypothetical protein KIAA1833
obshum40K:B#27979	Z85996	CPNE5	0.68	0.34	0.5	Human DNA sequence from clone RP3-431A14 on chromosome 6p21 Contains the CDKN1A gene for cyclin-dependent kinase inhibitor 1A, the gene for a novel protein similar to ras family protein, the gene for a novel copine-like protein (KIA1599), a galanin recept
obshum40K:B#28050	BC045796	LOC150383	1.27	0.51	0.4015748	similar to RIKEN cDNA 2210021J22
obshum40K:B#28273	NM_152573	RASEF	0.64	0.29	0.453125	RAS and EF-hand domain containing
obshum40K:B#28503	NM_001037225	LOC283129	0.82	0.19	0.23170732	hypothetical protein LOC283129
obshum40K:B#28529	AC020679		0.65	0.28	0.43076923	Homo sapiens, clone RP11-11H9, complete sequence
obshum40K:B#29239	AL691515		0.68	0.26	0.38235292	Human DNA sequence from clone RP11-316I3 on chromosome 1

						Contains two novel genes, complete sequence
obshum40K:B#29259	AC095038		1.08	0.51	0.4722222	Homo sapiens BAC clone RP11-10F11 from 7, complete sequence
obshum40K:B#29288	AL031943		0.52	0.18	0.3461539	Human DNA sequence from clone RP1-223B1 on chromosome 6p24.1-25.3 Contains the 3' end of a putative novel gene, complete sequence
obshum40K:B#29326	NM_198468	C6orf167	1.29	0.45	0.3488372	chromosome 6 open reading frame 167
obshum40K:B#29345	XM_379716		1.08	0.3	0.2777778	hypothetical gene supported by AK057746
obshum40K:B#29394	XM_373974		1.52	0.62	0.40789473	hypothetical LOC388924
obshum40K:B#29404	AL359382		0.5	0.25	0.5	Human DNA sequence from clone RP11-631F7 on chromosome 6 Contains the 3' part of a novel gene, a novel gene and a CpG island, complete sequence
obshum40K:B#29408	AC108210	TMEM33	5.15	2.54	0.49320388	Homo sapiens BAC clone RP11-457P14 from 4, complete sequence
obshum40K:B#29467	AF011889	CXorf40A	0.95	0.46	0.48421055	Human Xq28 cosmids U126G1, U142F2, U69B6, U145C10, U169A5, U84H1, U24D12, U80A7, U153E6, L35485, and R7-163A8 containing iduronate 2-sulfatase gene and pseudogene, complete sequence
obshum40K:B#29471	AC114958		1.12	0.56	0.5	Homo sapiens chromosome 5 clone RP11-167O18, complete sequence
obshum40K:B#29739	NM_001004743	OR5M9	0.48	0.21	0.4375	olfactory receptor, family 5, subfamily M, member 9
obshum40K:B#29789	AC004082	PCLO	0.97	0.44	0.45360824	Homo sapiens PAC clone RP5-897G10 from 7q11.23-q21.1, complete sequence
obshum40K:B#30309	AC093600	CLRN2	0.66	0.33	0.5	Homo sapiens BAC clone RP11-333E5 from 4, complete sequence
obshum40K:B#30319	NM_001003745	OR10A3	1.83	0.9	0.49180326	olfactory receptor, family 10, subfamily A, member 3
obshum40K:B#30339	NM_000918	P4HB	16.68	4.9	0.29376498	procollagen-proline, 2-oxoglutarate 4-dioxygenase (proline 4-hydroxylase), beta polypeptide (protein disulfide isomerase-associated 1)
obshum40K:B#30351	BC032837	FLJ23861	0.88	0.39	0.4431818	hypothetical protein FLJ23861
obshum40K:B#30439	AY142148		1.88	0.84	0.4468085	Homo sapiens hypothetical protein HGRHSV1 (HGRHSV1) mRNA, complete cds
obshum40K:B#30936	AF289592	SLC43A2	9.86	4.41	0.44726166	solute carrier family 43, member 2
obshum40K:B#31281	NG_004229	OR51A10P	0.63	0.26	0.4126984	olfactory receptor, family 51, subfamily A, member 10 pseudogene
obshum40K:B#31295	XM_064190	HSF5	0.91	0.28	0.3076923	hypothetical protein FLJ40311
obshum40K:B#31334	BC037341	GALNTL4	1.25	0.5	0.4	UDP-N-acetyl-alpha-D-galactosamine:polypeptide N-acetylgalactosaminyltransferase-like 4
obshum40K:B#31370	AC138356	BRF2	0.78	0.27	0.3461539	Homo sapiens chromosome 8, clone RP11-863K10, complete sequence
obshum40K:B#31380	CR625367	HERPUD1	2.69	1.18	0.4386617	homocysteine-inducible, endoplasmic reticulum stress-inducible, ubiquitin-like domain member 1
obshum40K:B#31421	BC020434	OSGIN1	1.53	0.59	0.3856209	pregnancy-induced growth inhibitor
obshum40K:B#31435	AK022687	MLL3	0.65	0.28	0.43076923	myeloid/lymphoid or mixed-lineage leukemia 3
obshum40K:B#31436	BC031469	LOC554207	1.1	0.49	0.44545454	hypothetical LOC554207
obshum40K:B#31457	AY358722	OLFM3	0.63	0.22	0.34920636	olfactomedin 3
obshum40K:B#31482	NM_152715	TBCEL	0.97	0.46	0.4742268	leucine rich repeat containing 35

obshum40K:B#31747	NM_138342	LOC89944	0.92	0.42	0.45652172	hypothetical protein BC008326
obshum40K:B#31757	NM_139278	LGI3	0.64	0.2	0.3125	leucine-rich repeat LGI family, member 3
obshum40K:B#31777	NM_152547	BTNL9	0.72	0.3	0.41666666	butyrophilin-like 9
obshum40K:B#31783	NM_017678	FAM55D	0.62	0.25	0.4032258	family with sequence similarity 55, member D
obshum40K:B#31803	NM_152423	MUM1L1	1.46	0.62	0.42465752	melanoma associated antigen (mutated) 1-like 1
obshum40K:B#31842	NM_033084	FANCD2	0.34	0.12	0.35294116	Fanconi anemia, complementation group D2
obshum40K:B#31997	NM_152440	FLJ32549	0.9	0.39	0.43333334	hypothetical protein FLJ32549
obshum40K:B#32017	AK057741	C10orf6	2.39	1.11	0.46443513	chromosome 10 open reading frame 6
obshum40K:B#32061	NM_173081	ARMC3	0.98	0.43	0.4387755	armadillo repeat containing 3
obshum40K:B#32066	NM_031479	INHBE	0.64	0.24	0.375	inhibin, beta E
obshum40K:B#32069	NM_152495	CNIH3	0.9	0.38	0.42222223	cornichon homolog 3 (Drosophila)
obshum40K:B#32175	NM_020666	CLK4	1.32	0.64	0.48484847	CDC-like kinase 4
obshum40K:B#32249	NM_015571	SENPA6	1.3	0.08	0.06153846	SUMO1/sentrin specific peptidase 6
obshum40K:B#32253	NM_052996	PRDM7	0.92	0.03	0.032608695	PR domain containing 7
obshum40K:B#32339	DQ246833	ND6	18.96	6.38	0.3364979	Homo sapiens isolate IND23 mitochondrion, complete genome
obshum40K:B#32374	BC001719	ASB6	0.64	0.08	0.125	ankyrin repeat and SOCS box-containing 6
obshum40K:B#32378	NM_033085	FATE1	0.46	0.19	0.41304347	fetal and adult testis expressed 1
obshum40K:B#32394	NM_033504	TMEM54	5.83	1.97	0.33790737	transmembrane protein 54
obshum40K:B#32395	NM_014839	LPPR4	0.69	0.16	0.23188405	plasticity related gene 1
obshum40K:B#32398	NM_012429	SEC14L2	7.08	2.23	0.31497175	SEC14-like 2 (S. cerevisiae)
obshum40K:B#32406	NM_017676	ZH2C2	0.66	0.28	0.4242424	hypothetical protein FLJ20125
obshum40K:B#32485	NM_032356	LSMD1	1.79	0.81	0.45251396	hypothetical protein MGC14151
obshum40K:B#32689	AF258566	UBE1	1.43	0.13	0.09090909	ubiquitin-activating enzyme E1 (A1S9T and BN75 temperature sensitivity complementing)
obshum40K:B#32691	NM_023037	FRY	0.59	0.25	0.42372882	hypothetical protein CG003
obshum40K:B#32700	NM_139166	ABRA	0.42	0.14	0.33333334	striated muscle activator of Rho-dependent signaling
obshum40K:B#32705	NM_015853	LOC51035	1	0.38	0.38	unknown protein LOC51035
obshum40K:B#32712	NM_024713	C15orf29	0.63	0.3	0.4761905	chromosome 15 open reading frame 29
obshum40K:B#32719	NM_024779	PIP5K2C	1.36	0.57	0.41911763	phosphatidylinositol-4-phosphate 5-kinase, type II, gamma
obshum40K:B#32733	BX647449	CECR2	0.91	0.44	0.48351645	cat eye syndrome chromosome region, candidate 2
obshum40K:B#33027	NM_032270	*LRRC8C	0.72	0.31	0.43055555	leucine rich repeat containing 8 family, member C
obshum40K:B#33042	AB051446	KIAA1659	0.63	0.25	0.3968254	KIAA1659 protein
obshum40K:B#33061	NM_144615	TMIGD2	12.29	3.74	0.30431244	hypothetical protein MGC23244
obshum40K:B#33065	NM_023011	UPF3A	0.95	0.45	0.4736842	UPF3 regulator of nonsense transcripts homolog A (yeast)
obshum40K:B#33169	NM_145807	LOC126147	1.47	0.65	0.44217685	hypothetical protein BC018697
obshum40K:B#33175	NM_080818	OXGR1	0.94	0.44	0.4680851	oxoglutarate (alpha-ketoglutarate) receptor 1
obshum40K:B#33297	XM_374769		1.04	0.52	0.5	hypothetical LOC439951 protein

obshum40K:B#33352	NM_201269	ZNF644	0.66	0.31	0.46969697	zinc finger protein 644
obshum40K:B#33360	NR_001278	CYP2B7P1	1.53	0.74	0.48366013	cytochrome P450, family 2, subfamily B, polypeptide 7 pseudogene 1
obshum40K:B#33363	AC072028	TRPC1	0.58	0.05	0.0862069	Homo sapiens 3 BAC RP11-190C21 (Roswell Park Cancer Institute Human BAC Library) complete sequence
obshum40K:B#33366	NM_052886	MAL2	0.57	0.27	0.47368422	mal, T-cell differentiation protein 2
obshum40K:B#33429	NM_178826	TMEM16D	0.62	0.08	0.12903225	transmembrane protein 16D
obshum40K:B#33484	AC004079	LOC442290	1.81	0.66	0.36464092	Homo sapiens PAC clone RP1-167F23 from 7, complete sequence
obshum40K:B#33656	AC104333	LQK1	0.9	0.43	0.4777778	Homo sapiens chromosome 1 clone RP11-348H3, complete sequence
obshum40K:B#33659	NM_207316	UNQ846	1.76	0.86	0.48863637	SRSR846
obshum40K:B#33661	NM_138290	RPIB9	0.96	0.48	0.5	Rap2-binding protein 9
obshum40K:B#33664	NM_057175	NARG1	0.86	0.43	0.5	NMDA receptor regulated 1
obshum40K:B#33679	NM_145061	C13orf3	1.04	0.52	0.5	chromosome 13 open reading frame 3
obshum40K:B#33686	NM_152403	EGFLAM	0.36	0.15	0.41666666	hypothetical protein FLJ39155
obshum40K:B#33696	NM_153365	FLJ90013	0.36	0.17	0.4722222	hypothetical protein FLJ90013
obshum40K:B#33698	NM_152772	TCP11L2	0.5	0.25	0.5	t-complex 11 (mouse) like 2
obshum40K:B#33811	NM_015239	AGTPBP1	0.91	0.37	0.4065934	ATP/GTP binding protein 1
obshum40K:B#33975	NM_033107	GTPBP10	1.01	0.43	0.4257426	hypothetical protein
obshum40K:B#33982	NM_006939	SOS2	0.95	0.39	0.4105263	son of sevenless homolog 2 (Drosophila)
obshum40K:B#33984	NM_173630	RTTN	0.92	0.41	0.44565216	rotatin
obshum40K:B#34003	BC021180	HMGB4	0.83	0.26	0.31325302	high-mobility group box 4
obshum40K:B#34073	NM_001001964	OR2T11	3.65	1.57	0.43013698	olfactory receptor, family 2, subfamily T, member 11
obshum40K:B#34280	NM_173549	C8orf47	1.19	0.56	0.4705882	chromosome 8 open reading frame 47
obshum40K:B#34285	NM_058172	ANTXR2	0.96	0.31	0.3229167	anthrax toxin receptor 2
obshum40K:B#34289	BC024030	FBXO32	0.79	0.33	0.4177215	F-box protein 32
obshum40K:B#34296	NM_032243	TXNDC2	1.43	0.42	0.2937063	thioredoxin domain containing 2 (spermatozoa)
obshum40K:B#34303	CR623610	ALG10	0.46	0.2	0.4347826	full-length cDNA clone CS0DK002YI20 of HeLa cells Cot 25-normalized of Homo sapiens (human)
obshum40K:B#34381	BC032136	C9orf23	1.87	0.67	0.35828876	chromosome 9 open reading frame 23
obshum40K:B#34418	NM_031281	FCRL5	1.23	0.6	0.4878049	Fc receptor-like 5
obshum40K:B#34482	NM_018527	NARG1L	0.88	0.36	0.40909094	NMDA receptor regulated 1-like
obshum40K:B#34523	NM_174938	FRMD3	20.07	1.18	0.05879422	FERM domain containing 3
obshum40K:B#34599	NM_174912	FAAH2	0.79	0.32	0.40506327	hypothetical protein FLJ31204
obshum40K:B#34609	NM_139248	LIPH	0.64	0.23	0.359375	lipase, member H
obshum40K:B#34614	CR933659	SOCS4	1.44	0.72	0.5	suppressor of cytokine signaling 4
obshum40K:B#34665	NM_020796	SEMA6A	1.44	0.72	0.5	sema domain, transmembrane domain (TM), and cytoplasmic domain, (semaphorin) 6A
obshum40K:B#34730	NM_177967	PHGDHL1	1.12	0.34	0.30357143	phosphoglycerate dehydrogenase like 1

obshum40K:B#34767	NM_145115	ZNF498	7.94	2.49	0.313602	zinc finger protein 498
obshum40K:B#34923	NM_032276	RHBDD1	2.36	1.05	0.44491526	hypothetical protein LOC84236
obshum40K:B#34932	NM_021733	TSKS	1.89	0.87	0.46031746	testis-specific kinase substrate
obshum40K:B#34938	NM_016538	SIRT7	2.25	0.94	0.41777778	sirtuin (silent mating type information regulation 2 homolog) 7 (S. cerevisiae)
obshum40K:B#34946	NM_018462	C3orf10	2.13	0.94	0.44131452	chromosome 3 open reading frame 10
obshum40K:B#35009	NM_053054	CATSPER1	1.96	0.61	0.3112245	cation channel, sperm associated 1
obshum40K:B#35019	NM_024677	NSUN7	0.97	0.31	0.31958762	hypothetical protein FLJ14001
obshum40K:B#35275	AC006313	OR5C1	2.37	1.04	0.43881857	Homo sapiens chromosome 9, clone hRPK.465_F_21, complete sequence
obshum40K:B#35280	NM_152653	UBE2E2	0.42	0.21	0.5	ubiquitin-conjugating enzyme E2E 2 (UBC4/5 homolog, yeast)
obshum40K:B#35303	NM_022899	ACTR8	0.55	0.26	0.47272724	ARP8 actin-related protein 8 homolog (yeast)
obshum40K:B#35317	NM_015493	ANKRD25	0.45	0.2	0.44444448	ankyrin repeat domain 25
obshum40K:B#35420	NM_152333	SLC25A29	0.42	0.2	0.4761905	solute carrier family 25, member 29
obshum40K:B#35465	AC134028	ARIH2	0.69	0.34	0.49275362	Homo sapiens 3 BAC RP11-316M24 (Roswell Park Cancer Institute Human BAC Library) complete sequence
obshum40K:B#35491	NM_024838	THNSL1	0.62	0.24	0.38709676	threonine synthase-like 1 (bacterial)
obshum40K:B#35584	BC025420	C1QDC1	0.76	0.38	0.5	C1q domain containing 1
obshum40K:B#35591	NM_152612	CCDC116	0.4	0.12	0.29999998	hypothetical protein FLJ36046
obshum40K:B#35597	NM_152667	NANP	1.23	0.41	0.3333333	haloacid dehalogenase-like hydrolase domain containing 4
obshum40K:B#35604	NM_012206	HAVCR1	1.33	0.52	0.3909774	hepatitis A virus cellular receptor 1
obshum40K:B#35608	NM_173798	ZCCHC12	0.53	0.26	0.49056605	zinc finger, CCHC domain containing 12
obshum40K:B#35616	BC051707	GPRASP2	0.43	0.03	0.06976744	G protein-coupled receptor associated sorting protein 2
obshum40K:B#35621	NM_015652	C10orf12	0.8	0.32	0.39999998	chromosome 10 open reading frame 12
obshum40K:B#35634	NM_015602	TOR1AIP1	0.51	0.22	0.43137255	torsin A interacting protein 1
obshum40K:B#35660	BC038460	KIAA1641	5.34	1.81	0.3389513	KIAA1641
obshum40K:B#35672	NM_017921	NPLOC4	1.05	0.44	0.41904762	nuclear protein localization 4
obshum40K:B#35914	NM_139015	UNQ1887	1.58	0.72	0.4556962	signal peptide peptidase 3
obshum40K:B#35923	NM_020123	TM9SF3	1.34	0.54	0.40298507	SM-11044 binding protein
obshum40K:B#35930	NM_153338	GGT6	1.68	0.7	0.4166667	gamma-glutamyltransferase 6 homolog (rat)
obshum40K:B#35956	NM_017883	WDR13	4.34	2.09	0.4815668	WD repeat domain 13
obshum40K:B#36026	NM_080872	UNC5D	0.74	0.36	0.4864865	unc-5 homolog D (C. elegans)
obshum40K:B#36246	NM_130441	CLEC4C	0.58	0.27	0.46551728	C-type lectin domain family 4, member C
obshum40K:B#36267	NM_020194	C2orf33	1.78	0.75	0.42134833	chromosome 2 open reading frame 33
obshum40K:B#36491	S87083	CD8B	2.43	1.18	0.4855967	CD8 antigen, beta polypeptide 1 (p37)
obshum40K:B#36562	NM_015113	ZZEF1	0.67	0.27	0.40298507	zinc finger, ZZ-type with EF-hand domain 1
obshum40K:B#36567	AY092767	LDHD	1.13	0.52	0.46017697	lactate dehydrogenase D

obshum40K:B#36571	NM_032621	BEX2	2.12	0.96	0.4528302	brain expressed X-linked 2
obshum40K:B#36577	AK023392	CXYorf2	1.04	0.45	0.43269232	chromosome X and Y open reading frame 2
obshum40K:B#36586	NM_019091	PLEKHA3	0.86	0.34	0.39534885	pleckstrin homology domain containing, family A (phosphoinositide binding specific) member 3
obshum40K:B#36587	NM_017512	ENOSF1	0.78	0.36	0.4615385	enolase superfamily member 1
obshum40K:B#36842	AC128673		12.43	4.72	0.37972644	Homo sapiens BAC clone RP11-1195P3 from UL, complete sequence
obshum40K:B#36884	AF533251	ZNF396	0.86	0.39	0.45348835	zinc finger protein 396
obshum40K:B#36896	NM_032750	ABHD14B	1.56	0.68	0.43589747	hypothetical protein MGC15429
obshum40K:B#36907	NM_174943	C14orf178	0.46	0.23	0.5	hypothetical protein FLJ25976
obshum40K:B#37177	NM_001007530	CDRT15	1.25	0.55	0.44	Homo sapiens CDRT15 protein (CDRT15), mRNA
obshum40K:B#37190	NM_030624	KLHL15	0.72	0.33	0.45833334	kelch-like 15 (Drosophila)
obshum40K:B#37191	AJ505028		0.5	0.22	0.44	Homo sapiens ERMAP gene for erythroid membrane-associated protein, exons 2-3, Sc:-1,-2,-3 allele
obshum40K:B#37196	NM_053023	ZFP91	4.11	1.85	0.45012164	zinc finger protein 91 homolog (mouse)
obshum40K:B#37208	NM_018235	CNDP2	0.53	0.2	0.37735853	CNDP dipeptidase 2 (metallopeptidase M20 family)
obshum40K:B#37226	NM_138461	TM4SF19	1.24	0.54	0.43548387	transmembrane 4 L six family member 19
obshum40K:B#37232	NM_152791	ZNF555	0.58	0.17	0.29310346	zinc finger protein 555
obshum40K:B#37238	NM_020954	KIAA1618	0.47	0.2	0.42553192	KIAA1618
obshum40K:B#37241	NM_018334	LRRN3	0.65	0.32	0.4923077	leucine rich repeat neuronal 3
obshum40K:B#37252	NM_016448	DTL	8.28	4.11	0.49637684	denticleless homolog (Drosophila)
obshum40K:B#37264	NM_001029888	FAM24A	1.34	0.3	0.2238806	family with sequence similarity 24, member A
obshum40K:B#37368	NM_017711	GDPD2	0.53	0.23	0.4339623	glycerophosphodiester phosphodiesterase domain containing 2
obshum40K:B#37472	BC018833	MRS2L	0.36	0.15	0.41666666	MRS2-like, magnesium homeostasis factor (S. cerevisiae)
obshum40K:B#37478	NM_152259	*C15orf42	1.39	0.54	0.38848922	chromosome 15 open reading frame 42
obshum40K:B#37482	NM_020183	ARNTL2	0.8	0.37	0.4625	aryl hydrocarbon receptor nuclear translocator-like 2
obshum40K:B#37493	BC028395	EXOC6	1.29	0.63	0.48837212	exocyst complex component 6
obshum40K:B#37513	NM_033161	SURF4	1.39	0.66	0.47482017	surfeit 4
obshum40K:B#37524	NM_052841	TSSK3	0.85	0.36	0.42352942	testis-specific serine kinase 3
obshum40K:B#37543	NM_178583	WDFY3	0.92	0.38	0.41304347	WD repeat and FYVE domain containing 3
obshum40K:B#37672	AC093420	C1orf210	1.66	0.69	0.41566265	Homo sapiens chromosome 1 clone RP11-282K6, complete sequence
obshum40K:B#37688	BC105284		1.3	0.44	0.33846155	Homo sapiens cDNA clone IMAGE:6614723
obshum40K:B#37788	XM_059832	LOC136288	0.5	0.19	0.38	hypothetical protein LOC136288
obshum40K:B#37794	AK001063	YEATS2	8.96	2.58	0.28794643	YEATS domain containing 2
obshum40K:B#37800	NM_033064	ATCAY	1.21	0.59	0.48760328	ataxia, cerebellar, Cayman type (caytaxin)
obshum40K:B#37805	BX648703	BRD9	0.67	0.33	0.49253732	bromodomain containing 9
obshum40K:B#37810	NM_015493	ANKRD25	0.48	0.22	0.45833334	ankyrin repeat domain 25
obshum40K:B#37817	NM_019598	KLK12	0.74	0.3	0.4054054	kallikrein 12

obshum40K:B#37854	NM_024857	C17orf41	0.57	0.19	0.33333334	chromosome 17 open reading frame 41
obshum40K:B#37921	NM_153444	OR5P2	1.26	0.59	0.46825394	olfactory receptor, family 5, subfamily P, member 2
obshum40K:B#37924	NM_032046	TMPRSS13	1.21	0.44	0.36363634	transmembrane protease, serine 13
obshum40K:B#37984	AY033611		9.69	4.74	0.48916408	Homo sapiens placenta immunoregulatory factor PLIF mRNA, complete cds
obshum40K:B#37989	NM_145256	LRRC25	0.31	0.15	0.48387098	leucine rich repeat containing 25
obshum40K:B#37996	NM_153703	PODN	0.51	0.2	0.39215687	podocan
obshum40K:B#38094	NM_016652	CRNKL1	0.48	0.19	0.39583334	Crn, crooked neck-like 1 (Drosophila)
obshum40K:B#38099	NM_152531	C3orf21	0.51	0.22	0.43137255	chromosome 3 open reading frame 21
obshum40K:B#38101	AF338650	PDZD2	1.21	0.4	0.3305785	PDZ domain containing 3
obshum40K:B#38116	AF421375	LOC440264	8.09	3.4	0.42027193	similar to p40
obshum40K:B#38181	AK096171	SLC24A4	1.36	0.17	0.125	solute carrier family 24 (sodium/potassium/calcium exchanger), member 4
obshum40K:B#38185	NM_001002907	OR8K1	0.48	0.16	0.33333334	olfactory receptor, family 8, subfamily K, member 1
obshum40K:B#38417	AY359015	FKBP7	0.51	0.23	0.4509804	FK506 binding protein 7
obshum40K:B#38432	NM_144577	CCDC114	2.32	1.15	0.49568966	hypothetical protein FLJ32926
obshum40K:B#38435	NM_031288	ZNHIT4	1	0.49	0.49	zinc finger, HIT type 4
obshum40K:B#38441	NM_138335	GNPDA2	0.38	0.13	0.34210527	glucosamine-6-phosphate deaminase 2
obshum40K:B#38442	NM_022840	METTL4	0.81	0.22	0.27160493	methyltransferase like 4
obshum40K:B#38490	NM_138775	ALKBH8	0.92	0.39	0.42391303	hypothetical protein BC015183
obshum40K:B#38517	NM_052896	CSMD2	0.46	0.15	0.32608697	CUB and Sushi multiple domains 2
obshum40K:B#38664	NM_203454	APOBEC4	1.29	0.5	0.3875969	apolipoprotein B mRNA editing enzyme, catalytic polypeptide-like 4 (putative)
obshum40K:B#38681	NG_002601	UGT1A13P	2.69	1.04	0.38661706	Homo sapiens UDP glucuronosyltransferase 1 family, polypeptide A cluster (UGT1A@) on chromosome 2
obshum40K:B#38693	AF182414	TMBIM4	0.58	0.04	0.06896552	transmembrane BAX inhibitor motif containing 4
obshum40K:B#38731	AL021453	RP5-821D11.2	1.15	0.54	0.46956524	Human DNA sequence from clone RP5-821D11 on chromosome 22q12.3-13.1, complete sequence
obshum40K:B#38758	BC000978	QRICH1	0.39	0.14	0.35897437	hypothetical protein LOC54870
obshum40K:B#38759	NM_152381	CMYA3	0.61	0.25	0.40983605	cardiomyopathy associated 3
obshum40K:B#38775	CR626440	SERHL	0.69	0.32	0.4637681	full-length cDNA clone CS0DI048YG01 of Placenta Cot 25-normalized of Homo sapiens (human)
obshum40K:B#38819	NM_138295	PKD1L1	0.55	0.21	0.38181818	polycystic kidney disease 1 like 1
obshum40K:B#39075	NM_173352	KRT78	8.5	3.28	0.38588235	keratin 5b
obshum40K:B#39080	NM_144688	FLJ32658	2.28	0.03	0.013157895	hypothetical protein FLJ32658
obshum40K:B#39122	NM_176782	C1orf179	0.84	0.35	0.4166667	chromosome 1 open reading frame 179
obshum40K:B#39126	NM_032578	MYPN	0.37	0.18	0.4864865	myopalladin
obshum40K:B#39189	NM_145804	ABTB2	0.63	0.22	0.34920636	ankyrin repeat and BTB (POZ) domain containing 2

obshum40K:B#39195	BC016838	CPVL	0.52	0.14	0.26923078	carboxypeptidase, vitellogenic-like
obshum40K:B#39331	XM_372198		1.6	0.52	0.325	hypothetical protein MGC17403
obshum40K:B#39416	AC109133	ELOVL7	0.72	0.23	0.31944445	Homo sapiens chromosome 5 clone RP11-109B6, complete sequence
obshum40K:B#39428	AL031685	KRT18P4	0.76	0.33	0.43421054	Human DNA sequence from clone RP5-963K23 on chromosome 20q13.11-13.2 Contains the KRT18P4 gene for keratin 18 pseudogene 4, a Cytoskeletal 18 (Cytokeratin 18, CK18, CYK18)) pseudogene, the ZNF313 gene for zinc finger protein 313, the SPATA2 gene for sperm
obshum40K:B#39462	NM_206902	RTN2	0.57	0.2	0.3508772	reticulon 2
obshum40K:B#39476	AL833338	C12orf50	3.86	1.55	0.4015544	hypothetical protein FLJ35821
obshum40K:B#39477	AC092107		1.82	0.73	0.4010989	Homo sapiens BAC clone RP11-755J8 from UL, complete sequence
obshum40K:B#39574	AF017104		3.21	1.41	0.43925232	Homo sapiens chromosome 7 common fragile site, complete sequence
obshum40K:B#39599	AC091134		1.18	0.05	0.042372882	Homo sapiens chromosome 17, clone RP11-646F1, complete sequence
obshum40K:B#39665	AF196864	BPESC1	0.85	0.37	0.43529412	Homo sapiens putative BPES syndrome breakpoint region protein gene, complete cds
obshum40K:B#39751	NM_024560	FLJ21963	0.66	0.19	0.28787878	FLJ21963 protein
obshum40K:B#39775	NG_003015	HSP90AB3P	14.48	6.49	0.44820443	heat shock 90kDa protein 1, beta pseudogene 1
obshum40K:B#39941	AK074651	IGHA1	0.37	0.15	0.4054054	hypothetical protein MGC27165
obshum40K:B#40147	AB012130	SLC4A7	2.66	0.52	0.1954887	solute carrier family 4, sodium bicarbonate cotransporter, member 7
obshum40K:B#40151	XM_499030		1.5	0.6	0.4	LOC441139
obshum40K:B#40166	NG_005042	DEFT1P	0.57	0.11	0.19298245	defensin, theta 1 pseudogene
obshum40K:B#40206	NM_194251	GPR151	0.22	0.04	0.18181817	G protein-coupled receptor 151
obshum40K:B#40269	AL096862		2.97	1.2	0.40404043	Human DNA sequence from clone RP4-744A17 on chromosome 20 Contains STSs and GSSs, complete sequence
obshum40K:B#40271	AC092846		6.23	1.97	0.31621188	Homo sapiens BAC clone RP11-617A17 from 4, complete sequence
obshum40K:B#40281	AF421375	LOC440264	11.49	4.22	0.3672759	similar to p40
obshum40K:B#40307	AL163300	UBE2G2	1.29	0.63	0.48837212	Homo sapiens chromosome 21 segment HS21C100
obshum40K:B#40313	AL358394	LOC338579	2.62	1.25	0.47709927	Human DNA sequence from clone RP11-445N18 on chromosome 10 Contains four novel genes, the 5' end of a novel gene, a Ras suppressor protein 1 pseudogene, a pseudogene similar to part of cubilin (intrinsic factor-cobalamin receptor, CUBN), the 5' end of a
obshum40K:B#40321	BC063432	TRA@	1.57	0.76	0.4840764	T cell receptor alpha locus
obshum40K:B#40410	BC051790	STX17	2.26	1	0.44247788	syntaxin 17
obshum40K:B#40444	AC138069	CCR2	1.07	0.35	0.32710278	Homo sapiens chromosome 3 clone RP13-546I2, complete sequence
obshum40K:B#40452	NM_032041	NCALD	0.82	0.26	0.31707317	neurocalcin delta
obshum40K:B#40528	AF116715		28.25	14.01	0.4959292	Homo sapiens PRO2829 mRNA, complete cds
obshum40K:B#40698	NM_020344	SLC24A2	0.66	0.01	0.015151515	solute carrier family 24 (sodium/potassium/calcium exchanger), member 2
obshum40K:B#40763	AL160231	GARNL1	0.53	0.03	0.056603774	Human chromosome 14 DNA sequence BAC R-355C3 of library RPCI-

						11 from chromosome 14 of Homo sapiens (Human), complete sequence
obshum40K:B#40901	NM_001033515	LOC389833	1.78	0.79	0.44382024	similar to hypothetical protein MGC27019
obshum40K:B#40921	AC117379	C3orf58	0.65	0.28	0.43076923	Homo sapiens 3 BAC RP11-392C7 (Roswell Park Cancer Institute Human BAC Library) complete sequence
obshum40K:B#40990	AB007940	RABGAP1L	0.74	0.08	0.1081081	RAB GTPase activating protein 1-like
obshum40K:B#41091	NM_001029882	AHDC1	1.12	0.49	0.4375	AT hook, DNA binding motif, containing 1
obshum40K:B#41177	NM_006852	TLK2	0.17	0.05	0.29411766	tousled-like kinase 2
obshum40K:B#41184	NM_003546	HIST1H4L	1.39	0.65	0.4676259	histone 1, H4l
obshum40K:B#41196	XM_497382		2.23	0.97	0.4349776	similar to Glyceraldehyde 3-phosphate dehydrogenase, liver (GAPDH)
obshum40K:B#41226	NM_145214	TRIM11	0.1	0.04	0.39999998	tripartite motif-containing 11
obshum40K:B#41401	NM_145200	CABP4	1.1	0.37	0.33636364	calcium binding protein 4
obshum40K:B#41441	BC105968	ZNF777	0.96	0.46	0.4791667	KIAA1285 protein
obshum40K:B#41446	XM_370603		1.12	0.31	0.2767857	similar to hypothetical protein SB153 isoform 1
obshum40K:B#41495	NM_018083	ZNF358	6.51	3.05	0.46850997	zinc finger protein 358
obshum40K:B#41581	M22198	TRDV1	0.9	0.37	0.41111112	T cell receptor delta variable 1
obshum40K:B#41622	NM_018382		0.79	0.37	0.46835443	hypothetical protein FLJ11292
obshum40K:B#41683	NM_003523	HIST1H2BE	1.17	0.53	0.45299146	histone 1, H2be
obshum40K:B#41840	AE000658	TRAV1-1	0.7	0.31	0.44285715	Homo sapiens T-cell receptor alpha delta locus from bases 1 to 250529 (section 1 of 5) of the Complete Nucleotide Sequence
obshum40K:B#41860	NM_194249	DND1	0.52	0.19	0.36538464	dead end homolog 1 (zebrafish)
obshum40K:B#41870	AL132822	C20orf197	1.24	0.47	0.37903225	Human DNA sequence from clone RP5-1017F8 on chromosome 20 Contains a novel gene, part of a novel gene (LOC284757) and a CpG island, complete sequence
obshum40K:B#41988	AC021851		0.64	0.3	0.46875003	Homo sapiens BAC clone RP11-438L19 from 2, complete sequence
obshum40K:B#41995	BC022958	C9orf97	0.75	0.32	0.42666665	chromosome 9 open reading frame 97
obshum40K:B#41999	M11518	TTR	1.36	0.21	0.15441176	transthyretin (prealbumin, amyloidosis type I)
obshum40K:B#42004	AF337549	DYX1C1	0.68	0.3	0.44117647	dyslexia susceptibility 1 candidate 1
obshum40K:B#42016	BC040594	ZNF92	0.51	0.21	0.4117647	zinc finger protein 92 (HTF12)
obshum40K:B#42027	U38980	PMS2L11	0.46	0.16	0.34782606	postmeiotic segregation increased 2-like 11
obshum40K:B#42061	XM_498333	LOC442427	0.97	0.46	0.4742268	similar to chromosome 15 open reading frame 2
obshum40K:B#42087	AF533251	ZNF396	5.35	2.39	0.446729	zinc finger protein 396
obshum40K:B#42109	AC104826		2.99	1.49	0.49832776	Homo sapiens BAC clone RP11-775M3 from 4, complete sequence
obshum40K:B#42154	BC012108	LOC440700	9.53	4.18	0.4386149	carbonic anhydrase XIV (CA14) pseudogene
obshum40K:B#42208	AY305871		3.2	0.1	0.03125	Homo sapiens migration-inducing protein 6 (MIG6) mRNA, complete cds
obshum40K:B#42270	NM_148896	NPB	2.52	1.09	0.4325397	neuropeptide B
obshum40K:B#42498	AL163636	OR6S1	0.67	0.3	0.4477612	Human chromosome 14 DNA sequence BAC R-903H12 of library RPCI-11 from chromosome 14 of Homo sapiens (Human), complete

						sequence
obshum40K:B#42516	AC018362	LOC645106	0.49	0.01	0.020408163	Homo sapiens chromosome 15 clone RP11-265N6 map 15q15, complete sequence
obshum40K:B#42549	NM_152287	ZNF276	0.73	0.17	0.2328767	zinc finger protein 276 homolog (mouse)
obshum40K:B#42610	AP004607	TRIM64	0.51	0.11	0.21568628	Homo sapiens genomic DNA, chromosome 11 clone:RP11-529A4, complete sequence
obshum40K:B#43018	AY894583	NBPF14	0.73	0.29	0.39726025	Homo sapiens clone HSA8 NBPF gene, partial cds
obshum40K:B#43025	DQ100915		0.73	0.32	0.43835613	Homo sapiens isolate P131H immunoglobulin heavy chain variable region (IGHV3-23) mRNA, IGHV3-23*01 allele, partial cds
obshum40K:B#43035	BC050316	LOC253805	0.54	0.23	0.4259259	hypothetical protein LOC253805
obshum40K:B#43131	AC068473	FLJ25715	0.34	0.09	0.2647059	Homo sapiens chromosome 18, clone RP11-567M16, complete sequence
obshum40K:B#43140	AC093259	GCNT4	1.81	0.24	0.13259669	Homo sapiens chromosome 5 clone RP11-229C3, complete sequence
obshum40K:B#43179	NM_152261	C12orf23	0.79	0.1	0.12658228	hypothetical protein MGC17943
obshum40K:B#43207	AF027159		0.93	0.34	0.3655914	Homo sapiens immunoglobulin gamma heavy chain (T6J/g) mRNA, complete cds
obshum40K:B#43219	AL592047		0.84	0.42	0.5	Human DNA sequence from clone RP11-506C15 on chromosome 9 Contains a NADH dehydrogenase 2 (MTND2) pseudogene, complete sequence
obshum40K:B#43396	AY532914		1.4	0.51	0.3642857	Homo sapiens TCR beta chain (TRBV11-3) mRNA, TRBV11-3*01 allele, complete cds
obshum40K:B#43446	BC018744	DZIP1	0.8	0.04	0.049999997	DAZ interacting protein 1
obshum40K:B#43625	AC012331		0.89	0.39	0.43820223	Homo sapiens chromosome 22 clone b41c4 map 22q11, complete sequence
obshum40K:B#43682	XM_499277		0.57	0.28	0.49122807	similar to T-cell receptor gamma chain C region PT-gamma-1/2
obshum40K:B#43743	NM_053002	MED12L	1.86	0.7	0.37634408	mediator of RNA polymerase II transcription, subunit 12 homolog (yeast)-like
obshum40K:B#43762	BC035720	RP5-821D11.2	0.9	0.37	0.41111112	similar to mouse meiosis defective 1 gene
obshum40K:B#43776	NM_031407	HUWE1	1.28	0.36	0.28125003	HECT, UBA and WWE domain containing 1
obshum40K:B#43796	NM_001010872	FAM83B	0.55	0.2	0.36363637	chromosome 6 open reading frame 143
obshum40K:B#44015	AF007192		2.33	0.59	0.2532189	Homo sapiens SIB 297 intestinal mucin (MUC3) mRNA, partial cds
obshum40K:B#44068	AL137267	PLCB1	0.93	0.39	0.41935483	phospholipase C, beta 1 (phosphoinositide-specific)
obshum40K:B#44069	AJ580094	ATP11C	0.66	0.15	0.22727273	ATPase, Class VI, type 11C
obshum40K:B#44074	XM_062871	LOC643677	0.55	0.24	0.4363636	hypothetical protein FLJ40176
obshum40K:B#44075	NM_018714	COG1	0.91	0.45	0.49450547	component of oligomeric golgi complex 1
obshum40K:B#44088	NM_001004298	C10orf90	0.34	0.16	0.4705882	chromosome 10 open reading frame 90
obshum40K:B#44089	NM_020354	ENTPD7	0.96	0.43	0.4479167	ectonucleoside triphosphate diphosphohydrolase 7
obshum40K:B#44093	NM_003494	DYSF	1.39	0.21	0.15107913	dysferlin, limb girdle muscular dystrophy 2B (autosomal recessive)
obshum40K:B#44096	XM_059929	LOC137886	0.46	0.08	0.17391303	hypothetical protein LOC137886

obshum40K:B#44177	NM_014963	SBNO2	1.22	0.57	0.4672131	KIAA0963
obshum40K:B#44214	AK090476	NLRC3	5.86	2.39	0.40784985	NOD3 protein
obshum40K:B#44328	AL137798	MGC12760	0.74	0.31	0.4189189	Human DNA sequence from clone RP5-1182A14 on chromosome 1 Contains the 5' end of a novel gene, a novel gene, a macrophage stimulating 1 (hepatocyte growth factor-like)(MST1) pseudogene and three CpG islands, complete sequence
obshum40K:B#44365	AF480924		0.64	0.32	0.5	Homo sapiens rabbit endogenous retrovirus H, complete sequence
obshum40K:B#44495	NM_017934	PHIP	1.66	0.55	0.33132532	pleckstrin homology domain interacting protein
obshum40K:B#44506	AF548113	OFCC1	0.44	0.11	0.25	orofacial cleft 1 candidate 1
obshum40K:B#44509	NM_175898	C15orf37	1.6	0.7	0.4375	chromosome 15 open reading frame 37
obshum40K:B#44511	NM_015196	KIAA0922	0.61	0.3	0.4918033	KIAA0922 protein
obshum40K:B#44514	NM_207379	FLJ42486	0.86	0.31	0.3604651	FLJ42486 protein
obshum40K:B#44515	BC030258	C14orf28	0.76	0.38	0.5	chromosome 14 open reading frame 28
obshum40K:B#44536	BC012130	AZII	1.05	0.49	0.4666667	5-azacytidine induced 1
obshum40K:B#44840	NM_138477	CDAN1	0.88	0.17	0.19318183	congenital dyserythropoietic anemia, type I
obshum40K:B#44991	BC036825	SLC7A8	5.28	1.37	0.2594697	solute carrier family 7 (cationic amino acid transporter, y+ system), member 8

Up-Regulated Genes

Gene Identifier	GenBank Accession	Gene Symbol	Expression Value		Fold Change	Gene Description
			KB (Wild Type)	KB 125	(KB 125/KB)	
obshum40K:A#00279	NM_005063	SCD	0.79	1.59	2.012658	stearoyl-CoA desaturase (delta-9-desaturase)
obshum40K:A#00543	NM_016525	UBAP1	0.1	0.63	6.2999997	ubiquitin associated protein 1
obshum40K:A#00565	NM_006465	ARID3B	0.15	0.43	2.8666666	AT rich interactive domain 3B (BRIGHT-like)
obshum40K:A#00573	BC065243	MITF	0.3	0.84	2.7999997	microphthalmia-associated transcription factor
obshum40K:A#01163	NM_000291	PGK1	6.6	71.09	10.771212	phosphoglycerate kinase 1
obshum40K:A#01200	BX648680	PLCB4	0.43	1.31	3.0465114	phospholipase C, beta 4
obshum40K:A#01349	NM_020346	SLC17A6	0.33	0.75	2.2727273	solute carrier family 17 (sodium-dependent inorganic phosphate cotransporter), member 6
obshum40K:A#01370	NM_015679	TRUB2	0.02	1.01	50.5	TruB pseudouridine (psi) synthase homolog 2 (E. coli)
obshum40K:A#01374	NM_004280	EEF1E1	1.41	3.43	2.432624	eukaryotic translation elongation factor 1 epsilon 1
obshum40K:A#01448	NM_014604	TAX1BP3	0.09	0.69	7.6666665	Tax1 (human T-cell leukemia virus type I) binding protein 3
obshum40K:A#01563	BC067840	LLGL2	0.57	1.41	2.473684	lethal giant larvae homolog 2 (Drosophila)
obshum40K:A#01662	NM_007375	TARDBP	0.38	2.11	5.5526314	TAR DNA binding protein
obshum40K:A#01728	NM_012320	LYPLA3	1.28	18.47	14.4296875	lysophospholipase 3 (lysosomal phospholipase A2)
obshum40K:A#01843	BC029125	FPRL1	0.25	0.67	2.68	formyl peptide receptor-like 1
obshum40K:A#02056	NM_139204	EPS8L1	1.56	4.2	2.6923077	EPS8-like 1
obshum40K:A#02129	NM_016567	BCCIP	2.84	14.18	4.992958	BRCA2 and CDKN1A interacting protein
obshum40K:A#02136	BC104038	MBNL2	0.24	0.85	3.5416667	muscleblind-like 2 (Drosophila)
obshum40K:A#02284	NM_004758	BZRAP1	0.24	0.67	2.7916667	benzodiazepine receptor (peripheral) associated protein 1
obshum40K:A#02446	NM_007238	PXMP4	0.71	2.1	2.9577465	peroxisomal membrane protein 4, 24kDa
obshum40K:A#02713	NM_022103	ZNF667	0.08	0.57	7.125	Homo sapiens zinc finger protein 667 (ZNF667), mRNA
obshum40K:A#02845	NM_002502	NFKB2	2.31	5.75	2.4891775	nuclear factor of kappa light polypeptide gene enhancer in B-cells 2 (p49/p100)
obshum40K:A#03118	NM_016339	RAPGEFL1	0.31	0.78	2.516129	Rap guanine nucleotide exchange factor (GEF)-like 1
obshum40K:A#03140	AF305836	DIO3OS	1.3	2.97	2.2846155	deiodinase, iodothyronine, type III opposite strand
obshum40K:A#03258	NM_001216	CA9	1.96	4.01	2.0459185	carbonic anhydrase IX
obshum40K:A#03299	NM_000242	MBL2	0.89	4.29	4.820225	mannose-binding lectin (protein C) 2, soluble (opsonic defect)
obshum40K:A#03399	NM_006541	TXNL2	1.8	8.2	4.5555553	thioredoxin-like 2
obshum40K:A#03848	NM_016401	C11orf73	0.03	7.3	243.33334	hypothetical protein HSPC138
obshum40K:A#03878	NM_006061	CRISP3	0.03	0.57	19	cysteine-rich secretory protein 3
obshum40K:A#04011	AK023591	SVEP1	0.2	1.08	5.4	Homo sapiens cDNA FLJ13529 fis, clone PLACE1006157, weakly similar to E-SELECTIN PRECURSOR
obshum40K:A#04043	BC074772	ZNF322A	0.64	1.75	2.734375	zinc finger protein 322A
obshum40K:A#04195	BC035816	SUPT3H	0.53	1.94	3.6603777	suppressor of Ty 3 homolog (S. cerevisiae)

obshum40K:A#04290	BC041569	FOXK2	0.72	1.8	2.4999998	forkhead box K2
obshum40K:A#04303	NM_006815	TMED2	0.05	0.87	17.4	Homo sapiens transmembrane emp24 domain trafficking protein 2 (TMED2), mRNA
obshum40K:A#04639	NM_002693	POLG	1.12	2.75	2.455357	polymerase (DNA directed), gamma
obshum40K:A#05005	BC023621	SREBF1	0.81	2.15	2.6543212	sterol regulatory element binding transcription factor 1
obshum40K:A#05014	NM_015898	ZBTB7A	0.19	0.64	3.368421	Homo sapiens zinc finger and BTB domain containing 7A (ZBTB7A), mRNA
obshum40K:A#05155	NM_012101	TRIM29	1.13	2.57	2.2743363	tripartite motif-containing 29
obshum40K:A#05159	BC013327	KCNJ15	0.09	0.69	7.6666665	potassium inwardly-rectifying channel, subfamily J, member 15
obshum40K:A#05160	NM_007368	RASA3	0.04	0.53	13.25	RAS p21 protein activator 3
obshum40K:A#05208	AL832827	MTERFD3	0.06	1.24	20.6666668	Homo sapiens mRNA; cDNA DKFZp667I1824 (from clone DKFZp667I1824)
obshum40K:A#05511	NM_017600	GOLGA2L1	0.06	0.68	11.333334	hypothetical protein DKFZp434M0331
obshum40K:A#05518	NM_014859	KIAA0672	0.01	0.72	72.00001	KIAA0672 gene product
obshum40K:A#05613	NM_000481	AMT	0.05	0.59	11.799999	aminomethyltransferase (glycine cleavage system protein T)
obshum40K:A#06027	AY591530	A2M	1.77	3.94	2.2259889	alpha-2-macroglobulin
obshum40K:A#06101	BC034246	EFS	0.43	1.19	2.767442	embryonal Fyn-associated substrate
obshum40K:A#06151	BC018961	HNRPDL	12.87	30.75	2.3892775	heterogeneous nuclear ribonucleoprotein D-like
obshum40K:A#06259	NM_005513	GTF2E1	0.21	0.47	2.2380953	general transcription factor IIE, polypeptide 1, alpha 56kDa
obshum40K:A#06305	NM_014760	TATDN2	0.23	0.78	3.3913043	TatD DNase domain containing 2
obshum40K:A#06437	NM_016217	HECA	0.2	0.42	2.1	headcase homolog (Drosophila)
obshum40K:A#06547	X66610	ENO1B	0.65	4.16	6.4	enolase alpha, lung-specific
obshum40K:A#07198	AF194032	DNMT3L	0.74	1.63	2.2027028	DNA (cytosine-5-)-methyltransferase 3-like
obshum40K:A#07422	BC107155	GTF2A1	0.16	0.38	2.375	general transcription factor IIA, 1, 19/37kDa
obshum40K:A#07553	BC041945	SLC27A6	0.89	2.09	2.3483145	solute carrier family 27 (fatty acid transporter), member 6
obshum40K:A#07834	NM_016472	C14orf129	0.19	0.89	4.6842103	chromosome 14 open reading frame 129
obshum40K:A#07848	NM_018469	TEX2	0.06	0.77	12.833333	uncharacterized hypothalamus protein HT008
obshum40K:A#07922	NM_014384	ACAD8	0.66	3.15	4.772727	acyl-Coenzyme A dehydrogenase family, member 8
obshum40K:A#08126	NM_001052	SSTR4	0.11	1.15	10.454545	somatostatin receptor 4
obshum40K:A#08305	NM_016039	C14orf166	0.02	2.61	130.5	chromosome 14 open reading frame 166
obshum40K:A#08343	X55958	ALPPL2	9.03	18.25	2.021041	alkaline phosphatase, placental-like 2
obshum40K:A#08344	NM_001744	CAMK4	0.59	2.03	3.4406781	calcium/calmodulin-dependent protein kinase IV
obshum40K:A#08471	NM_002133	HMOX1	0.53	1.33	2.5094342	heme oxygenase (decycling) 1
obshum40K:A#08483	NM_024899	CEP76	0.11	1.19	10.818182	Homo sapiens centrosomal protein 76kDa (CEP76), mRNA
obshum40K:A#08489	NM_018330	KIAA1598	0.09	1.19	13.222222	KIAA1598
obshum40K:A#08665	AK027467	ARID1A	0.33	2.55	7.7272725	AT rich interactive domain 1A (SWI-like)
obshum40K:A#08680	NM_015993	PLLP	0.15	1.07	7.133333	Homo sapiens transmembrane 4 superfamily member 11 (plasmolipin)

						(TM4SF11), mRNA
obshum40K:A#08689	BC028722	ACCN2	0.84	2.65	3.154762	Homo sapiens cDNA clone IMAGE:4799069, with apparent retained intron
obshum40K:A#08778	BC025661	GLS2	0.32	0.92	2.875	glutaminase 2 (liver, mitochondrial)
obshum40K:A#09203	NM_017734	PALMD	0.51	1.54	3.0196078	palmdelphin
obshum40K:A#09426	NM_013264	DDX25	0.47	1.03	2.1914892	DEAD (Asp-Glu-Ala-Asp) box polypeptide 25
obshum40K:A#09448	NM_002108	HAL	0.28	0.6	2.1428573	histidine ammonia-lyase
obshum40K:A#09451	NM_006520	DYNLT3	1.13	2.34	2.0707965	Homo sapiens dynein, light chain, Tctex-type 3 (DYNLT3), mRNA
obshum40K:A#09746	NM_019599	TAS2R1	0.86	3.11	3.616279	taste receptor, type 2, member 1
obshum40K:A#10102	NM_030773	TUBB1	0.19	0.52	2.7368422	tubulin, beta 1
obshum40K:A#10114	NM_032856	WDR73	0.92	2.05	2.2282608	Homo sapiens WD repeat domain 73 (WDR73), mRNA
obshum40K:A#10404	CR624391	UBL7	1.27	2.74	2.1574802	full-length cDNA clone CSODN005YG12 of Adult brain of Homo sapiens (human)
obshum40K:A#10451	NM_032837	FAM104A	0.63	1.56	2.4761903	hypothetical protein FLJ14775
obshum40K:A#10634	BC101075	TLR8	0.1	0.59	5.8999996	toll-like receptor 8
obshum40K:A#10645	NM_015208	ANKRD12	0.12	0.99	8.25	ankyrin repeat domain 12
obshum40K:A#11073	NM_016458	C8orf30A	0.93	2.48	2.6666667	Homo sapiens chromosome 8 open reading frame 30A (C8orf30A), mRNA
obshum40K:A#11165	NM_033105	DNAJC5B	0.3	2.93	9.7666666	DnaJ (Hsp40) homolog, subfamily C, member 5 beta
obshum40K:A#11395	NM_031903	MRPL32	0.26	0.67	2.5769231	mitochondrial ribosomal protein L32
obshum40K:A#11404	NM_014750	DLG7	0.04	0.83	20.75	discs, large homolog 7 (Drosophila)
obshum40K:A#11528	NM_170601	SIAE	0.32	2.02	6.3125	Homo sapiens sialic acid acetyltransferase (SIAE), mRNA
obshum40K:A#11625	NM_003441	ZNF141	0.34	1.13	3.3235295	zinc finger protein 141 (clone pHZ-44)
obshum40K:A#11633	NM_004637	RAB7	0.85	3.11	3.6588233	RAB7, member RAS oncogene family
obshum40K:A#11884	BC009755	ADPRHL1	0.09	1.45	16.111111	Homo sapiens ADP-ribosylhydrolase like 1, transcript variant 2, mRNA (cDNA clone MGC:11146 IMAGE:3838063), complete cds
obshum40K:A#11937	NM_152522	ARL6IP6	0.08	1.53	19.125	ADP-ribosylation-like factor 6 interacting protein 6
obshum40K:A#12203	BC040564	NY-SAR-48	1.41	3.55	2.5177305	sarcoma antigen NY-SAR-48
obshum40K:A#12774	NM_004515	ILF2	0.25	0.6	2.4	interleukin enhancer binding factor 2, 45kDa
obshum40K:A#12932	NM_000175	GPI	13.68	30.54	2.2324562	glucose phosphate isomerase
obshum40K:A#13175	NM_014570	ARFGAP3	0.04	0.92	23	ADP-ribosylation factor GTPase activating protein 3
obshum40K:A#13512	NM_152699	SENP5	0.04	1.14	28.5	SUMO1/sentrin specific peptidase 5
obshum40K:A#13972	AL121845	ZBTB46	0.04	7.41	185.25	Human DNA sequence from clone RP4-583P15 on chromosome 20 Contains the 3' end of the TNFRSF6B gene for member 6 (decoy) of tumor necrosis factor receptor, the ARFRP1 gene for ADP-ribosylation factor related protein 1, the gene for a novel protein (KIAA184
obshum40K:A#14108	NM_018462	C3orf10	0.34	0.83	2.4411764	chromosome 3 open reading frame 10
obshum40K:A#14365	AF118082	TRSPAP1	0.29	0.79	2.724138	Homo sapiens PRO1902 mRNA, complete cds

obshum40K:A#14406	NM_020850	RANBP10	3.56	7.45	2.0926967	RAN binding protein 10
obshum40K:A#14453	NM_020947	KIAA1609	0.81	1.69	2.0864198	KIAA1609 protein
obshum40K:A#14564	X60152	ZNF2	0.02	0.41	20.5	zinc finger protein 2
obshum40K:A#14755	BC005133	TRPT1	0.85	1.79	2.1058822	Homo sapiens tRNA phosphotransferase 1, transcript variant 2, mRNA (cDNA clone MGC:11134 IMAGE:3836683), complete cds
obshum40K:A#15093	AF152305	PCDHA1	0.17	0.66	3.882353	protocadherin alpha 1
obshum40K:A#15245	NM_020751	COG6	0.23	0.48	2.0869565	component of oligomeric golgi complex 6
obshum40K:A#15260	X71745		0.03	1	33.333336	H.sapiens COL4A5 gene, exon 51
obshum40K:A#15591	NM_032344	NUDT22	0.01	0.95	95	Homo sapiens nudix (nucleoside diphosphate linked moiety X)-type motif 22 (NUDT22), mRNA
obshum40K:A#15807	NM_031442	TMEM47	0.02	1.08	54.000004	Homo sapiens transmembrane protein 47 (TMEM47), mRNA
obshum40K:A#15897	NM_032148	SLC41A2	0.43	1.4	3.2558138	solute carrier family 41, member 2
obshum40K:A#16132	BC029083	KIAA0859	0.65	2.18	3.3538463	KIAA0859
obshum40K:A#16616	NM_003540	HIST1H4F	0.01	0.56	56	histone 1, H4f
obshum40K:A#16747	NM_032933	C18orf45	0.05	1.47	29.4	chromosome 18 open reading frame 45
obshum40K:A#16753	NM_001030005	CPLX3	0.08	0.53	6.625	Homo sapiens complexin 3 (CPLX3), mRNA
obshum40K:A#17196	NM_032193	RNASEH2C	0.03	0.09	3.0000002	AYP1 protein
obshum40K:A#17378	Y14153	BTRC	0.78	2.65	3.3974361	beta-transducin repeat containing
obshum40K:A#17494	NM_020699	GATAD2B	0.49	1.28	2.6122448	Homo sapiens GATA zinc finger domain containing 2B (GATAD2B), mRNA
obshum40K:A#17874	NM_031485	GRWD1	0.23	0.46	2	glutamate-rich WD repeat containing 1
obshum40K:A#17888	NM_018659	CYTL1	0.24	0.92	3.8333335	cytokine-like 1
obshum40K:A#18229	NM_152660	FAM76A	0.27	0.85	3.148148	Homo sapiens family with sequence similarity 76, member A (FAM76A), mRNA
obshum40K:A#18891	NM_138768	MYEOV	0.01	0.96	96	myeloma overexpressed gene (in a subset of t(11;14) positive multiple myelomas)
obshum40K:A#18983	BC009254	FRAS1	0.29	0.64	2.2068965	Fraser syndrome 1
obshum40K:A#19303	NM_052925	LENG8	0.44	2	4.5454545	leukocyte receptor cluster (LRC) member 8
obshum40K:A#19631	AF161533	HSPC048	0.06	0.65	10.8333333	HSPC048 protein
obshum40K:A#19790	XM_499358		0.55	1.28	2.3272727	similar to hypothetical protein
obshum40K:A#21841	NM_173830	C6orf182	0.67	1.98	2.9552238	chromosome 6 open reading frame 182
obshum40K:A#21856	BC013224	ASS1	32.5	65.69	2.021231	argininosuccinate synthetase
obshum40K:A#22642	NR_002161	LOC401630	0.11	0.99	9	LOC401630
obshum40K:A#27247	NM_153704	TMEM67	0.3	1.9	6.3333333	Homo sapiens transmembrane protein 67 (TMEM67), mRNA
obshum40K:A#28666	AC009784		0.33	0.93	2.8181818	Homo sapiens clone RP11-277F10 from 7q31, complete sequence
obshum40K:A#29732	NM_024050	C19orf58	0.11	0.99	9	Homo sapiens DDA1 (DDA1), mRNA
obshum40K:A#29869	NM_022373	HERPUD2	0.43	0.86	2	hypothetical protein FLJ22313
obshum40K:A#29971	NM_138342	LOC89944	0.21	0.98	4.666667	hypothetical protein BC008326

obshum40K:A#30035	NM_019096	GTPBP2	0.53	1.41	2.6603775	GTP binding protein 2
obshum40K:A#30053	NM_152613	WBP2NL	0.04	0.43	10.75	Homo sapiens hypothetical protein MGC26816 (MGC26816), mRNA
obshum40K:A#30221	NM_144660	SAMD8	0.05	0.32	6.3999996	sterile alpha motif domain containing 8
obshum40K:A#30404	NM_032482	DOT1L	0.06	0.46	7.666667	DOT1-like, histone H3 methyltransferase (<i>S. cerevisiae</i>)
obshum40K:A#30547	NM_021908	ST7	0.17	0.64	3.7647057	suppression of tumorigenicity 7
obshum40K:A#30580	NM_023071	SPATS2	0.84	1.88	2.2380953	spermatogenesis associated, serine-rich 2
obshum40K:A#30712	NM_004651	USP11	0.74	1.76	2.3783784	ubiquitin specific peptidase 11
obshum40K:A#30823	NM_014367	C3orf28	5.68	11.9	2.0950704	growth and transformation-dependent protein
obshum40K:A#31004	NM_017735	TTC27	0.07	0.63	9	hypothetical protein FLJ20272
obshum40K:A#31010	NM_138443	CCDC5	0.19	0.46	2.4210527	coiled-coil domain containing 5 (spindle associated)
obshum40K:A#31037	NM_000314	PTEN	0.59	2.36	4	phosphatase and tensin homolog (mutated in multiple advanced cancers 1)
obshum40K:A#31304	NM_021870	FGG	0.78	1.62	2.0769231	fibrinogen gamma chain
obshum40K:A#31505	NM_006283	TACC1	0.07	0.69	9.857142	transforming, acidic coiled-coil containing protein 1
obshum40K:A#31859	AC096551	TFEC	0.57	1.24	2.1754386	transcription factor EC
obshum40K:A#31996	NM_001557	IL8RB	0.57	1.21	2.122807	interleukin 8 receptor, beta
obshum40K:A#32029	NM_002563	P2RY1	0.11	1.93	17.545454	purinergic receptor P2Y, G-protein coupled, 1
obshum40K:A#32257	NM_001025109	CD34	0.93	2.4	2.5806453	CD34 antigen
obshum40K:A#33533	NM_004312	ARR3	0.16	0.74	4.625	arrestin 3, retinal (X-arrestin)
obshum40K:A#33658	AL589644	RREB1	0.66	1.48	2.2424242	ras responsive element binding protein 1
obshum40K:A#33858	NM_003874	CD84	1.25	2.58	2.064	CD84 antigen (leukocyte antigen)
obshum40K:A#34411	Z99128	SRPK1	3.72	9.18	2.467742	SFRS protein kinase 1
obshum40K:A#35642	NM_003328	TXK	0.27	0.85	3.148148	TXK tyrosine kinase
obshum40K:A#35821	NG_005083	TPSB2	1.18	8.18	6.932204	Homo sapiens tryptase gene cluster (TPS@) on chromosome 16
obshum40K:A#36024	NM_003631	PARG	0.35	0.81	2.3142858	poly (ADP-ribose) glycohydrolase
obshum40K:A#38231	M83216	CALD1	1.61	7.35	4.5652175	caldesmon 1
obshum40K:A#38354	NM_002935	RNASE3	0.63	1.37	2.1746032	ribonuclease, RNase A family, 3 (eosinophil cationic protein)
obshum40K:A#39008	AF120268	COP2	1.7	8.48	4.988235	COP9 constitutive photomorphogenic homolog subunit 2 (<i>Arabidopsis</i>)
obshum40K:A#40995	AY766116	VEGFA	0.35	1.01	2.8857143	vascular endothelial growth factor
obshum40K:A#41020	NM_001330	CTF1	0.75	1.74	2.32	cardiotrophin 1
obshum40K:A#42363	NM_003043	SLC6A6	0.04	0.08	2	solute carrier family 6 (neurotransmitter transporter, taurine), member 6
obshum40K:A#42382	NM_005993	TBCD	0.62	1.77	2.8548386	tubulin-specific chaperone d
obshum40K:A#42618	NM_021103	TMSB10	2.03	6.32	3.1133006	thymosin, beta 10
obshum40K:A#42896	AC010186	LOC374443	0.23	0.74	3.2173913	Homo sapiens 12p12-21.3-21.8 BAC RP11-705C15 (Roswell Park Cancer Institute Human BAC Library) complete sequence
obshum40K:A#43116	AL356423	CYCSP35	2.44	10.95	4.4877048	serine/threonine kinase 24 (STE20 homolog, yeast)
obshum40K:A#43383	BC019059	SP110	2.31	5.54	2.3982685	SP110 nuclear body protein

obshum40K:A#43443	BC019014	RPLP0	28.62	58.71	2.0513625	ribosomal protein, large, P0
obshum40K:A#43791	NM_002473	MYH9	0.84	3.48	4.142857	myosin, heavy polypeptide 9, non-muscle
obshum40K:A#43965	NM_003127	SPTAN1	0.23	1.12	4.869565	spectrin, alpha, non-erythrocytic 1 (alpha-fodrin)
obshum40K:A#44354	NM_002735	PRKAR1B	0.23	2.11	9.173912	protein kinase, cAMP-dependent, regulatory, type I, beta
obshum40K:A#44685	NM_007037	ADAMTS8	0.36	1.29	3.583333	ADAM metalloproteinase with thrombospondin type 1 motif, 8
obshum40K:B#04569	NM_005124	NUP153	0.22	0.79	3.5909092	nucleoporin 153kDa
obshum40K:B#09912	AK021678		0.75	1.73	2.3066666	Homo sapiens cDNA FLJ11616 fis, clone HEMBA1004038
obshum40K:B#10132	NM_198508	FLJ44186	1.14	3.21	2.8157895	FLJ44186 protein
obshum40K:B#10200	XM_380008	SCRL	0.48	1.25	2.6041667	similar to Opioid binding protein/cell adhesion molecule precursor (OBCAM) (Opioid-binding cell adhesion molecule) (OPCML)
obshum40K:B#10268	NM_032933	C18orf45	0.76	1.71	2.25	chromosome 18 open reading frame 45
obshum40K:B#10503	AL596218	CD55	0.13	1.72	13.23077	Human DNA sequence from clone RP11-6J21 on chromosome 1 Contains a complement component 4 binding protein pseudogene, a novel gene and the 3' end of the DAF gene for decay accelerating factor for complement (CD55 Cromer blood group system), complete seque
obshum40K:B#11086	AC026412		0.18	0.73	4.0555553	Homo sapiens chromosome 5 clone CTD-2012J19, complete sequence
obshum40K:B#11117	AL354868		0.44	0.93	2.1136365	Human DNA sequence from clone RP11-339A7 on chromosome 6 Contains a ribosomal protein L21 (RPL21) pseudogene, complete sequence
obshum40K:B#11355	XM_496617		0.04	0.83	20.75	similar to CAVP-target protein (CAVPT)
obshum40K:B#11557	AC046136		0.79	1.96	2.4810126	Homo sapiens 3 BAC RP11-190P13 (Roswell Park Cancer Institute Human BAC Library) complete sequence
obshum40K:B#11569	AC010891	RBMY2NP	0.84	2.49	2.9642859	Homo sapiens BAC clone RP11-453C1 from Y, complete sequence
obshum40K:B#11704	AC105020	SH3PX3	1.1	3.45	3.1363635	Homo sapiens chromosome 15, clone CTD-2026K11, complete sequence
obshum40K:B#11786	NM_178516	EXOC3L	0.72	1.59	2.2083333	hypothetical protein LOC283849
obshum40K:B#11822	AC011453	MIRN519A2	0.07	0.64	9.142857	Homo sapiens chromosome 19 clone CTC-339O9, complete sequence
obshum40K:B#11899	AL356387	C1orf88	0.71	1.73	2.4366198	Human DNA sequence from clone RP5-1125M8 on chromosome 1p13.1-13.3 Contains the 3' end of the gene for eosinophil chemotactic cytokine (CHIA), a novel gene, a novel gene, a Glycosyl hydrolase family 18 pseudogene, a likely ortholog of mouse hypoxia induc
obshum40K:B#11912	AF235103	ZNF517	0.76	1.75	2.3026316	Homo sapiens chromosome 8 multiple clones map q24.3, complete sequence
obshum40K:B#12290	AC114689	LOC643542	0.79	1.67	2.113924	Homo sapiens chromosome 18, clone RP11-638L3, complete sequence
obshum40K:B#12581	AP000805	FAT3	0.79	1.81	2.2911391	Homo sapiens genomic DNA, chromosome 11q clone:RP11-698L23, complete sequence
obshum40K:B#12664	NM_001004304	ZNF740	0.57	1.33	2.3333335	hypothetical protein LOC283337
obshum40K:B#12716	AL138875	CAB39L	0.31	0.93	3	Human DNA sequence from clone RP11-103J18 on chromosome 13 Contains the 3' end of a novel gene (FLJ12577), the gene for protein

						kinase NYD-SP15 and a CpG island, complete sequence
obshum40K:B#13152	AC021021		0.05	0.85	17	Homo sapiens BAC clone RP11-557N1 from 2, complete sequence
obshum40K:B#13381	NG_000844	ALOX12P1	0.9	2.2	2.4444447	arachidonate 12-lipoxygenase pseudogene 1
obshum40K:B#13538	XM_375838	TATDN3	1.03	2.11	2.0485437	TatD DNase domain containing 3
obshum40K:B#14049	AL158073		0.88	2.61	2.965909	Human DNA sequence from clone RP11-323A7 on chromosome 9 Contains a cell division cycle associated 7 (JPO1, FLJ14722) (CDCA7) pseudogene, complete sequence
obshum40K:B#14329	AL157387	ANKRD30A	0.4	1.02	2.55	Human DNA sequence from clone RP11-20F24 on chromosome 10p11.21-12.1 Contains the 3' end of the NY-BR-1 gene for breast cancer antigen NY-BR-1, two novel genes, a pseudogene similar to part of ATP8A2 (ATPase, aminophospholipid transporter-like, Class I, t
obshum40K:B#14488	NM_003179	SYP	0.25	1.52	6.08	synaptophysin
obshum40K:B#14796	XM_377555	LOC401934	1.5	6.35	4.233333	similar to RIKEN cDNA 5830442J12
obshum40K:B#14817	AC093638	LOC136242	0.71	2.19	3.0845072	Homo sapiens BAC clone RP11-250J16 from 7, complete sequence
obshum40K:B#14830	AC109780	KNG1	0.68	1.69	2.485294	Homo sapiens 3 BAC RP11-795A2 (Roswell Park Cancer Institute Human BAC Library) complete sequence
obshum40K:B#14857	NM_001025357	LOC441376	0.9	3.95	4.388889	AARD protein
obshum40K:B#15165	NG_004832	LOC387364	0.84	1.91	2.2738097	Homo sapiens chromosome Y inverted repeat IR2, centromeric (IR2@) on chromosome Y
obshum40K:B#15518	NM_001013691	LOC401898	1.1	3.8	3.4545453	similar to hypothetical protein FLJ38281
obshum40K:B#15818	AK023954		0.54	1.57	2.9074073	Homo sapiens cDNA FLJ13892 fis, clone THYRO1001656, moderately similar to Homo sapiens Leman coiled-coil protein (LCCP) mRNA
obshum40K:B#15860	AL033519	TULP1	0.31	0.98	3.1612904	Human DNA sequence from clone RP3-340B19 on chromosome 6p21.2-21.3 Contains the TULP1 gene for tubby like protein 1, a novel gene, ribosomal protein S15A (RPS15A) and L36 (RPL36) pseudogenes, the 3' end of the FKBP5 gene for FK506 binding protein 5 (FKBP5)
obshum40K:B#16104	AC105760	LOC93463	0.29	1.18	4.0689654	Homo sapiens BAC clone RP11-346I14 from 2, complete sequence
obshum40K:B#16278	XM_370756	KIAA1305	0.34	1.01	2.9705882	KIAA1305
obshum40K:B#16397	AF372624		0.13	0.31	2.3846154	Homo sapiens PEBP-like protein (HSP714) mRNA, partial cds
obshum40K:B#16400	AC009522	MRPL2P1	0.29	0.64	2.2068965	Homo sapiens 12 BAC RP11-591N1 (Roswell Park Cancer Institute Human BAC Library) complete sequence
obshum40K:B#16496	BX119919	DHRXS	0.37	0.78	2.108108	Human DNA sequence from clone RP11-987D21 on chromosome X, complete sequence
obshum40K:B#16504	AL121939	PRSS35	0.51	1.05	2.0588236	Human DNA sequence from clone RP1-223E3 on chromosome 6q13-15 Contains the gene for a novel protein similar to serine protease 23 (PRSS23, ZSIG13), complete sequence
obshum40K:B#16604	AL031009	CRAMP1L	1.01	2.09	2.0693069	Human DNA sequence from clone LA16c-431H6 on chromosome 16 Contains a novel gene with some homology to mouse HN1 (Hematological and Neurological expressed sequence 1) downstream of

						a putative CpG island. Contains ESTs and GSSs, complete sequence
obshum40K:B#16996	AL030996	FERP	1.38	4.82	3.4927537	Human DNA sequence from clone RP5-1189B24 on chromosome Xq25-26.3 Contains the 3' end of the THOC2 gene for THO complex 2, a NADH dehydrogenase (ubiquinone) 1 alpha subcomplex, 4, 9kDa (NDUFA4) pseudogene, a tubulin beta 4 (TUBB4) pseudogene and a fer (fp)
obshum40K:B#17276	AL354980	AQP10	0.58	1.21	2.086207	Human DNA sequence from clone RP11-137P24 on chromosome 1 Contains the gene for HS1 binding protein (HAX1) and the 5' end of the AQP10 gene for aquaporin 10, complete sequence
obshum40K:B#17338	AL021917	BTN2A3	0.38	0.83	2.1842105	Human DNA sequence from clone RP1-45P21 on chromosome 6p21.3-22.2 Contains the H4FA gene for H4 histone family member A, a histone H3 pseudogene, the BTN3A2, BTN2A2, BTN3A1, BTN2A3 and BTN3A3 genes for butyrophilins 3A1, 2 and 3 and 2A2 and 3. Contains ES
obshum40K:B#17364	NM_198512	DGAT2L6	0.56	1.47	2.625	diacylglycerol O-acyltransferase 2 like 6
obshum40K:B#17535	AC090574	PRDM14	0.85	2.24	2.635294	Homo sapiens chromosome 8, clone RP11-449M6, complete sequence
obshum40K:B#18027	AC060764	MRPL15	0.98	2.92	2.9795918	Homo sapiens chromosome 8, clone RP11-626A5, complete sequence
obshum40K:B#18065	AC099654	ZNF479	1.24	2.52	2.032258	Homo sapiens BAC clone RP11-1217F2 from 7, complete sequence
obshum40K:B#18272	AL136128	IBRDC1	0.85	1.96	2.3058822	Human DNA sequence from clone RP1-84N20 on chromosome 6 Contains a novel gene, the 5' end of the TPD52L1 gene encoding two variants of tumor protein D52-like 1 protein and two CpG islands, complete sequence
obshum40K:B#18380	NG_004135		0.53	1.58	2.9811323	olfactory receptor, family 4, subfamily E, member 1 pseudogene
obshum40K:B#18460	AL592438	TRPM3	0.63	1.35	2.1428573	Human DNA sequence from clone RP11-187G6 on chromosome 9, complete sequence
obshum40K:B#18818	AC040160	LOC653319	0.21	0.93	4.4285717	Homo sapiens chromosome 16 clone CTC-277H1, complete sequence
obshum40K:B#18950	AC069020	ANXA2P3	0.51	1.02	2	Homo sapiens chromosome 10 clone RP11-165K20, complete sequence
obshum40K:B#19587	AC106806		0.96	2.15	2.2395835	Homo sapiens chromosome 5 clone RP11-510I6, complete sequence
obshum40K:B#19841	NM_006572	GNA13	0.77	1.59	2.0649352	guanine nucleotide binding protein (G protein), alpha 13
obshum40K:B#19855	AC087500	UNQ5783	0.66	1.51	2.2878788	Homo sapiens chromosome 17, clone RP11-333E1, complete sequence
obshum40K:B#20046	AC013733	LOC442060	0.03	1.11	37	Homo sapiens BAC clone RP11-553I15 from 2, complete sequence
obshum40K:B#20058	AP000478		1.06	2.71	2.556604	Homo sapiens genomic DNA, chromosome 11 clone:CMB9-14E22, complete sequence
obshum40K:B#20458	AC022033		0.01	1.29	129	Homo sapiens chromosome 8, clone RP11-214C21, complete sequence
obshum40K:B#20571	AL096821	C14orf177	0.19	0.42	2.2105262	Human chromosome 14 DNA sequence BAC R-677J5 of library RPCI-11 from chromosome 14 of Homo sapiens (Human), complete sequence
obshum40K:B#20721	AL391383	CSNK1A1L	0.58	1.46	2.5172415	Human DNA sequence from clone RP11-532O21 on chromosome 13 Contains the 5' of the gene for transcription factor (p38 interacting protein) (P38IP) (tumor rejection antigen), the gene for a novel protein similar to casein kinase I alpha 1 CSNK1A1 and a CpG

obshum40K:B#20735	AC074281	FAM9B	0.75	1.67	2.2266667	Homo sapiens X BAC RP11-66N5 (Roswell Park Cancer Institute Human BAC Library) complete sequence
obshum40K:B#20769	AC009806	PARVA	0.87	2.19	2.5172415	Homo sapiens chromosome 11, clone RP11-51B23, complete sequence
obshum40K:B#20777	AC139476		0.67	1.78	2.6567163	Homo sapiens chromosome 16 clone RP11-341P6, complete sequence
obshum40K:B#20823	BX664730		0.18	0.43	2.3888888	Human DNA sequence from clone RP11-118H15 on chromosome 9 Contains a novel gene, complete sequence
obshum40K:B#20880	AC104961	ZNF521	0.65	1.41	2.1692307	Homo sapiens chromosome 18, clone RP11-958F21, complete sequence
obshum40K:B#20896	AL137518	DKFZp566F0947	0.47	0.94	2	hypothetical gene DKFZp566F0947
obshum40K:B#20940	AL138691	SOX1	0.62	1.25	2.016129	Human DNA sequence from clone RP11-310D8 on chromosome 13 Contains the SOX1 gene for SRY (sex determining region Y)-box 1 protein and 7 CpG islands, complete sequence
obshum40K:B#20945	NG_002403	PGBD3P4	0.66	1.38	2.090909	piggyBac transposable element derived 3 pseudogene 4
obshum40K:B#21232	AL080313		0.61	1.29	2.114754	Human DNA sequence from clone RP3-448I9 on chromosome 6 Contains two novel genes, complete sequence
obshum40K:B#21239	AC016968		0.99	2.03	2.050505	Homo sapiens 3 BAC RP11-59J16 (Roswell Park Cancer Institute Human BAC Library) complete sequence
obshum40K:B#21267	AL022326	SNORD83B	0.88	2.53	2.875	Human DNA sequence from clone RP3-333H23 on chromosome 22q12.1-12.3 Contains the (possibly alternatively spliced) RPL3 gene for 60S Ribosomal Protein L3 and the threefold alternatively spliced gene for Synaptogyrin 1A, 1B and 1C (SYNGR1A, SYBGRIB, SYNGR1C)
obshum40K:B#21567	AC097262		0.11	0.79	7.1818185	Homo sapiens X BAC RP11-268G12 (Roswell Park Cancer Institute Human BAC Library) complete sequence
obshum40K:B#21902	AC122710	POLS	0.72	1.65	2.2916665	Homo sapiens chromosome 5 clone RP11-332J15, complete sequence
obshum40K:B#21903	AC018890	LOC440926	0.44	1.18	2.681818	Homo sapiens BAC clone RP11-493G24 from 2, complete sequence
obshum40K:B#21961	AC012506	KBTBD9	1.03	2.09	2.0291262	Homo sapiens BAC clone RP11-498O22 from 2, complete sequence
obshum40K:B#22180	AC019193	FLJ30277	2.17	4.42	2.0368664	Homo sapiens BAC clone RP11-335L23 from 4, complete sequence
obshum40K:B#22184	AC026782		0.9	1.88	2.088889	Homo sapiens chromosome 5 clone CTD-2015A6, complete sequence
obshum40K:B#22298	AC018992	ZHX1	0.95	2.34	2.463158	Homo sapiens chromosome 8, clone RP11-468O2, complete sequence
obshum40K:B#22390	AC025483	SH3GL3	0.73	2.28	3.1232874	Homo sapiens chromosome 15, clone RP11-398I10, complete sequence
obshum40K:B#22399	AC023794	SMUG1	0.71	1.86	2.6197183	Homo sapiens 12 BAC RP11-834C11 (Roswell Park Cancer Institute Human BAC Library) complete sequence
obshum40K:B#23075	XM_379089		0.64	2	3.125	hypothetical LOC400951
obshum40K:B#24240	AC018804	LOC112714	0.12	0.25	2.0833335	Homo sapiens BAC clone RP11-397H17 from 2, complete sequence
obshum40K:B#25179	AC026318	DHX30	0.31	1.68	5.4193544	Homo sapiens 3 BAC RP11-59D2 (Roswell Park Cancer Institute Human BAC Library) complete sequence
obshum40K:B#25201	AL035069		0.32	0.98	3.0625002	Human DNA sequence from clone RP3-404P13 on chromosome 22q13.2-13.13 Contains GSSs, complete sequence
obshum40K:B#25484	NM_001013403	RP11-35F15.2	0.17	1.01	5.9411764	hypothetical LOC347487

obshum40K:B#25508	AL353195	PDX1	1.17	2.84	2.4273505	Human DNA sequence from clone RP11-328P22 on chromosome 13, complete sequence
obshum40K:B#25677	AL356957	LOC647569	1.2	3.04	2.5333333	Human DNA sequence from clone RP11-403113 on chromosome 1 Contains the 5' end of a novel pseudogene, a profilin 1 (PFN1) pseudogene, six novel genes and a novel pseudogene, complete sequence
obshum40K:B#25950	XM_498831		0.52	1.05	2.0192308	LOC440722
obshum40K:B#26023	NM_001002915	IGFL2	0.67	2.2	3.283582	insulin growth factor-like family member 2
obshum40K:B#26578	AF064859	PCBP2P1	0.69	1.63	2.3623188	Homo sapiens chromosome 21q22.3 PAC 141B3, complete sequence, containing ribosomal protein homologue pseudogene L23a
obshum40K:B#26886	AL360267		0.43	1.22	2.8372092	Human DNA sequence from clone RP11-342C20 on chromosome 13 Contains a RNA-binding protein LIN-28 pseudogene, a novel gene and the 3' end of a novel gene, complete sequence
obshum40K:B#27021	AC002038		0.38	1.17	3.0789473	Homo sapiens chromosome 2 clone 101B6 map 2p11, complete sequence
obshum40K:B#27461	AL162394		1.29	5.67	4.395349	Human DNA sequence from clone RP11-547C13 on chromosome 9 Contains a novel gene, complete sequence
obshum40K:B#27501	AK057056	C20orf117	0.5	1.5	3	chromosome 20 open reading frame 117
obshum40K:B#29697	BC030812	ADAMTS4	0.3	1.63	5.433333	ADAM metalloproteinase with thrombospondin type 1 motif, 4
obshum40K:B#30167	NM_198547		0.87	2.16	2.4827588	chromosome 1 open reading frame 175
obshum40K:B#30261	NM_175067	TAAR6	1.18	32.12	27.220339	trace amine associated receptor 6
obshum40K:B#30896	AK090798	PHF20	0.15	0.96	6.3999996	PHD finger protein 20
obshum40K:B#31208	NM_152481	TMEM162	0.88	2.5	2.840909	hypothetical protein FLJ25660
obshum40K:B#31384	NM_017733	PIGG	0.87	1.85	2.1264367	GPI7 protein
obshum40K:B#31774	NM_001004746	OR5T2	0.51	2.05	4.019608	olfactory receptor, family 5, subfamily T, member 2
obshum40K:B#32013	NR_002314	FLJ40434	0.57	2.81	4.9298244	hypothetical FLJ40434
obshum40K:B#32044	NM_018060	IARS2	4.33	10.19	2.3533487	isoleucine-tRNA synthetase 2, mitochondrial
obshum40K:B#32309	NM_001018059	LOC440348	1.49	3.29	2.2080536	similar to nuclear pore complex interacting protein
obshum40K:B#32311	BC036784	RASGEF1B	0.8	2.7	3.375	RasGEF domain family, member 1B
obshum40K:B#32585	NM_002376	MARK3	0.57	1.32	2.3157897	MAP/microtubule affinity-regulating kinase 3
obshum40K:B#32774	NM_012276	LILRA4	0.03	0.73	24.333334	leukocyte immunoglobulin-like receptor, subfamily A (with TM domain), member 4
obshum40K:B#32997	AC074032	LASS5	0.73	2.48	3.3972602	Homo sapiens 12 BAC RP4-60503 (Roswell Park Cancer Institute Human BAC Library) complete sequence
obshum40K:B#33162	AL159168	ZNF483	0.17	0.46	2.7058823	Human DNA sequence from clone RP11-401H23 on chromosome 9 Contains the 3' end of a novel gene (KIAA0368), the gene for KIAA1962 protein similar to zinc finger protein HIT-10 and a CpG island, complete sequence
obshum40K:B#33200	AC118138	LOC653375	2	4.73	2.365	Homo sapiens BAC clone RP11-451K15 from 7, complete sequence

obshum40K:B#33239	NM_153685	C12orf53	0.68	14.68	21.588236	hypothetical protein DKFZp547D2210
obshum40K:B#33270	BC037988	MICALL2	0.58	1.3	2.2413793	MICAL-like 2
obshum40K:B#33325	NM_052819	CARD14	3.05	6.15	2.0163934	caspase recruitment domain family, member 14
obshum40K:B#33638	BC040049	FAM112A	0.09	1.08	12	chromosome 20 open reading frame 65
obshum40K:B#33728	NM_018227	UBE1L2	0.62	1.51	2.435484	hypothetical protein FLJ10808
obshum40K:B#34054	AK092526	GYLTL1B	0.39	1.2	3.0769234	glycosyltransferase-like 1B
obshum40K:B#34704	XM_499586		0.41	2.23	5.4390244	hypothetical gene supported by NM_175889
obshum40K:B#35028	BC040457	CAMK2A	1.64	3.32	2.0243902	calcium/calmodulin-dependent protein kinase (CaM kinase) II alpha
obshum40K:B#35116	BC008723	ASNS	4.01	11.97	2.9850373	asparagine synthetase
obshum40K:B#35234	AK095610	LRTM2	2.74	7.45	2.718978	Homo sapiens cDNA FLJ38291 fis, clone FCBBF3009069, weakly similar to Homo sapiens HT017 mRNA
obshum40K:B#35270	AK058066	LOC643923	0.32	0.98	3.0625002	Homo sapiens cDNA FLJ25337 fis, clone TST00714
obshum40K:B#35313	NM_207318	CXorf39	0.39	1.52	3.897436	chromosome X open reading frame 39
obshum40K:B#35347	DQ058016	ERVK6	0.74	2.02	2.7297297	endogenous retroviral sequence K, 6
obshum40K:B#35606	NM_138276	C6orf25	0.26	0.91	3.5000002	chromosome 6 open reading frame 25
obshum40K:B#35740	NM_001013658	LOC390667	0.01	1.47	147	similar to Neuronal pentraxin II precursor (NP-II) (NP2)
obshum40K:B#35886	NM_015677	SH3YL1	1.01	2.16	2.138614	SH3 domain containing, Ysc84-like 1 (<i>S. cerevisiae</i>)
obshum40K:B#36022	AC124068	KIAA1794	0.02	2.41	120.50001	Homo sapiens chromosome 15, clone RP11-217B1, complete sequence
obshum40K:B#36058	NM_022362	MMS19L	1.82	3.69	2.0274725	MMS19-like (MET18 homolog, <i>S. cerevisiae</i>)
obshum40K:B#36092	NM_024322	CENPO	0.62	1.38	2.2258065	hypothetical protein MGC11266
obshum40K:B#36505	BC034569	ZNF337	0.34	0.94	2.764706	zinc finger protein 337
obshum40K:B#36686	AK098692	C4orf28	0.54	1.26	2.3333333	hypothetical protein MGC29898
obshum40K:B#36859	NM_182594	ZNF454	0.04	0.96	24	zinc finger protein 454
obshum40K:B#37319	NM_152689	MGC9712	0.67	2	2.9850745	hypothetical protein MGC9712
obshum40K:B#37349	AF274944		0.85	1.8	2.117647	Homo sapiens PNAS-19 mRNA, complete cds
obshum40K:B#37350	BC013885	EPB41L1	0.39	1.01	2.5897436	erythrocyte membrane protein band 4.1-like 1
obshum40K:B#37363	BC034978	2'-PDE	0.73	1.51	2.0684931	2'-phosphodiesterase
obshum40K:B#37412	NM_138347	ZNF551	0.5	1.06	2.12	zinc finger protein 551
obshum40K:B#37561	NM_173551	ANKS6	0.1	0.5	5	sterile alpha motif domain containing 6
obshum40K:B#37563	NM_153451	ORAOV1	0.05	0.25	5	oral cancer overexpressed 1
obshum40K:B#37596	NM_152308	C16orf75	0.65	1.41	2.1692307	hypothetical protein MGC24665
obshum40K:B#37649	NM_052947	ALPK2	0.59	1.42	2.4067798	alpha-kinase 2
obshum40K:B#37665	NM_152352	C18orf19	0.39	0.92	2.3589745	chromosome 18 open reading frame 19
obshum40K:B#37943	NM_018060	IARS2	0.51	1.04	2.0392156	isoleucine-tRNA synthetase 2, mitochondrial
obshum40K:B#37960	NM_021937	EEFSEC	0.01	2.04	204	eukaryotic elongation factor, selenocysteine-tRNA-specific
obshum40K:B#37962	NM_133638	ADAMTS19	0.02	0.13	6.5	ADAM metalloproteinase with thrombospondin type 1 motif, 19
obshum40K:B#37999	NM_144997	FLCN	0.53	1.06	2	folliculin

obshum40K:B#38037	NM_032333	C10orf58	1.34	3.47	2.5895522	chromosome 10 open reading frame 58
obshum40K:B#38123	BC034580	SLC44A5	0.72	1.52	2.111111	solute carrier family 44, member 5
obshum40K:B#38300	AJ431725	C10orf4	0.42	0.86	2.047619	chromosome 10 open reading frame 4
obshum40K:B#38411	NM_144668	WDR66	0.64	1.8	2.8125	WD repeat domain 66
obshum40K:B#38495	NM_001010845	LOC123876	0.3	0.93	3.1	hypothetical protein LOC123876
obshum40K:B#38533	NM_080866	SLC22A9	0.58	1.65	2.8448277	solute carrier family 22 (organic anion/cation transporter), member 9
obshum40K:B#38539	NM_181885	RXFP4	0.24	1.36	5.666667	relaxin 3 receptor 2
obshum40K:B#38550	NM_001004726	OR4X1	1.07	4.74	4.429906	olfactory receptor, family 4, subfamily X, member 1
obshum40K:B#38579	NM_206891	DIP2A	0.71	1.65	2.3239436	chromosome 21 open reading frame 106
obshum40K:B#38598	NM_025182	KIAA1539	0.02	0.16	8	KIAA1539
obshum40K:B#38841	NM_016070	MRPS23	1.12	2.97	2.6517856	mitochondrial ribosomal protein S23
obshum40K:B#38871	NM_020750	XPO5	0.12	1.46	12.166667	exportin 5
obshum40K:B#38880	NM_144686	TMC4	0.23	0.48	2.0869565	transmembrane channel-like 4
obshum40K:B#39022	NM_031407	HUWE1	0.98	2.14	2.1836736	HECT, UBA and WWE domain containing 1
obshum40K:B#39255	AL713757	SF4	0.07	0.25	3.5714285	splicing factor 4
obshum40K:B#39264	NM_020933	ZNF317	0.66	1.89	2.8636363	zinc finger protein 317
obshum40K:B#39388	BC039540	RELL1	0.18	1.4	7.777777	Homo sapiens mRNA similar to expressed sequence AA536743 (cDNA clone MGC:50583 IMAGE:5748847), complete cds
obshum40K:B#39504	XM_371645		0.7	1.51	2.1571429	similar to 40S ribosomal protein S10
obshum40K:B#39516	U66061	TRY7	0.72	1.79	2.486111	Human germline T-cell receptor beta chain TCRBV17S1A1T, TCRBV2S1, TCRBV10S1P, TCRBV29S1P, TCRBV19S1P, TCRBV15S1, TCRBV11S1A1T, HVB relic, TCRBV28S1P, TCRBV34S1, TCRBV14S1, TCRBV3S1, TCRBV4S1A1T, TRY4, TRY5, TRY6, TRY7, TRY8, TCRBD1, TCRBJ1S1, TCRBJ1S2, TC
obshum40K:B#39621	NM_058188	C21orf67	0.08	1.47	18.375	chromosome 21 open reading frame 67
obshum40K:B#39687	NM_021018	HIST1H3F	0.19	0.54	2.8421054	histone 1, H3f
obshum40K:B#39692	AC113389		0.72	2.13	2.9583335	Homo sapiens chromosome 5 clone RP11-35A11, complete sequence
obshum40K:B#39773	Z92545	LOC654480	3.89	9.35	2.403599	Human DNA sequence from clone RP1-50A13 on chromosome Xp11-21 Contains a pseudogene similar to part of ribosomal protein S4, X-linked (RPS4X) and an ATP synthase, H ⁺ transporting, mitochondrial F0 complex, subunit c (subunit 9), isoform 1 (ATP5G1) pseudog
obshum40K:B#39798	NM_020152	C21orf7	0.75	3.27	4.36	chromosome 21 open reading frame 7
obshum40K:B#39812	BC020202	MGC3771	2.56	5.56	2.171875	hypothetical protein MGC3771
obshum40K:B#39979	AL133475	TTK	4.02	8.24	2.0497513	Human DNA sequence from clone RP3-357D13 on chromosome 6 Contains the 5' end of the ELOVL4 gene for elongation of very long chain fatty acids (FEN1/ELo2, SUR4/ELo3, yeast)-like 4, a GAPD (glyceraldehyde-3-phosphate dehydrogenase) pseudogene, an RPL35A (60

obshum40K:B#40070	NM_022153	C10orf54	0.75	3.41	4.5466666	chromosome 10 open reading frame 54
obshum40K:B#40177	AJ271736	LOC727856	0.52	1.31	2.5192308	Homo sapiens Xq pseudoautosomal region; segment 2/2
obshum40K:B#40238	NM_152472		0.03	0.08	2.6666667	zinc finger protein 578
obshum40K:B#40239	AF026564		0.03	0.07	2.3333335	Homo sapiens RNA binding protein II (RBMII) gene, complete cds
obshum40K:B#40268	NM_181776	SLC36A2	0.34	0.85	2.5	solute carrier family 36 (proton/amino acid symporter), member 2
obshum40K:B#40291	NM_002273	KRT8	0.74	2.66	3.5945947	keratin 8
obshum40K:B#40504	NG_003107	SLC25A6P1	0.37	1.3	3.5135133	solute carrier family 25 (mitochondrial carrier; adenine nucleotide translocator), member 6, pseudogene 1
obshum40K:B#40618	XM_498163		0.86	1.82	2.1162791	similar to SPCPB16A4.07c
obshum40K:B#40738	NM_133263	PPARGC1B	0.21	1.5	7.1428576	peroxisome proliferative activated receptor, gamma, coactivator 1, beta
obshum40K:B#40804	AP003120	GRM5	5.15	11.22	2.1786408	Homo sapiens genomic DNA, chromosome 11 clone:RP11-657K20, complete sequence
obshum40K:B#40998	AL713651	ITM2C	1.36	4.1	3.014706	integral membrane protein 2C
obshum40K:B#41173	NM_173620	HEXDC	0.03	0.06	2	hypothetical protein FLJ23825
obshum40K:B#41569	AF469043		0.31	1.75	5.645161	Homo sapiens hepatocellular carcinoma-associated antigen HCA25a mRNA, complete cds
obshum40K:B#41694	AC068880	SH2D4A	1.02	12.8	12.54902	Homo sapiens chromosome 8, clone RP11-618M23, complete sequence
obshum40K:B#41726	AC011825	RNF125	0.61	1.36	2.2295082	Homo sapiens chromosome 18, clone RP11-53I6, complete sequence
obshum40K:B#41729	NM_014023	WDR37	0.52	1.12	2.1538463	WD repeat domain 37
obshum40K:B#41780	AC007225	LOC388272	0.5	1.3	2.6	Homo sapiens chromosome 16 clone RPCI-11_480G7, complete sequence
obshum40K:B#41810	XM_497908		0.65	1.84	2.8307693	similar to UBF transcription factor, short form - rat
obshum40K:B#42072	BC030092		0.56	1.12	2	Homo sapiens cDNA clone IMAGE:4794631
obshum40K:B#42197	NM_001031618	MGC119295	0.76	2.65	3.4868422	similar to Williams-Beuren syndrome critical region protein 19
obshum40K:B#42213	AC108676	ATP13A3	2.33	5.16	2.2145922	Homo sapiens 3 BAC RP11-384A12 (Roswell Park Cancer Institute Human BAC Library) complete sequence
obshum40K:B#42227	AY671782		0.38	1.38	3.631579	Homo sapiens clone pCmnZ4 immunoglobulin mu heavy chain-like mRNA, partial sequence
obshum40K:B#42229	NM_032175	UTP15	0.25	1.44	5.76	UTP15, U3 small nucleolar ribonucleoprotein, homolog (yeast)
obshum40K:B#42331	M99685	IGHV4-55	0.88	2.03	2.3068182	immunoglobulin heavy variable 4-55
obshum40K:B#42430	AF318327		0.05	0.1	2	Homo sapiens pp12708 mRNA, complete cds
obshum40K:B#42853	AP005241		1.53	3.19	2.0849674	Homo sapiens genomic DNA, chromosome 18 clone:RP11-502P1, complete sequence
obshum40K:B#42858	AC106807		0.76	1.76	2.3157895	Homo sapiens chromosome 5 clone RP11-513C4, complete sequence
obshum40K:B#42911	AL022395	FBXL4	0.41	0.95	2.317073	Human DNA sequence from clone RP1-273N12 on chromosome 6q16.1-16.3 Contains the FBXL4 gene for F-box and leucine-rich repeat protein 4 and the POU3F2 gene for POU domain class 3 transcription factor 2 and a CpG island, complete sequence

obshum40K:B#42965	NM_203393	LOC389458	0.89	2	2.247191	hypothetical gene supported by BC031661
obshum40K:B#42972	NM_172341	PSENE1	2.08	4.41	2.1201923	presenilin enhancer 2 homolog (C. elegans)
obshum40K:B#43055	XM_210581		0.62	1.41	2.2741935	claudin 22
obshum40K:B#43113	BC071812	COX18	0.02	0.04	2	mitochondrial COX18
obshum40K:B#43244	NM_001013618	CTA-246H3.1	0.48	0.96	2	similar to omega protein
obshum40K:B#43403	AL663074	SH2D5	11.03	22.18	2.0108795	Human DNA sequence from clone RP5-930J4 on chromosome 1 Contains the 5' end of the KIF17 gene for kinesin family member 17, three novel genes, the 3' end of gene HP1-BP74 and two CpG islands, complete sequence
obshum40K:B#43563	AE000661	TRAJ46	0.1	0.55	5.5	Homo sapiens T-cell receptor alpha delta locus from bases 752679 to 1000555 (section 4 of 5) of the Complete Nucleotide Sequence
obshum40K:B#43680	AE000659	MGC40069	0.36	1.3	3.611111	Homo sapiens T-cell receptor alpha delta locus from bases 250472 to 501670 (section 2 of 5) of the Complete Nucleotide Sequence
obshum40K:B#43787	NM_015296	DOCK9	0.2	0.74	3.7	dedicator of cytokinesis 9
obshum40K:B#44033	NM_052843	OBSCN	1.42	3.38	2.380282	obscurin, cytoskeletal calmodulin and titin-interacting RhoGEF
obshum40K:B#44820	AL513327	FLJ25476	0.54	1.35	2.5	Human DNA sequence from clone RP11-415J8 on chromosome 1 Contains the gene for a novel protein (FLJ35476), the gene for a novel protein similar to ABO family protein, two novel genes, the PHC2 gene for polyhomeotic-like 2 (Drosophila) and two CpG islands,
obshum40K:B#44830	NM_007001	SLC35D2	0.99	10.71	10.818182	solute carrier family 35, member D2
obshum40K:B#44990	NM_207645	LOC399947	2.79	6.64	2.3799284	similar to expressed sequence AI593442
obshum40K:B#45002	NM_182501	MTERFD2	0.43	0.9	2.093023	MTERF domain containing 2

Publications

p53 amino-terminus region (1-125) stabilizes and restores heat denatured p53 wild phenotype

Anuj Kumar Sharma, Amjad Ali Khan, Rajan Gogna, Amir Kumar Singh and Uttam Pati*

School of Biotechnology, Jawaharlal Nehru University, New Delhi-110067

*E-mail: uttamsbt@gmail.com; uttam@mail.jnu.ac.in

Abstract

Background- The intrinsically disordered N-ter domain (NTD) of p53 encompasses approximately hundred amino acids that contain a transactivation domain (1-73) and a proline-rich domain (64-92) and is responsible for transactivation function and apoptosis. It also possesses an auto-inhibitory function as its removal results in remarkable reduction in dissociation of p53 from DNA.

Principle Findings- In this report, we have discovered that p53-NTD spanning amino acid residues 1-125 (NTD125) interacted with WT p53 and stabilized its wild type conformation under physiological and elevated temperatures, both *in vitro* and in cellular systems. NTD125 prevented irreversible thermal aggregation of heat denatured p53, enhanced p21-5'-DBS binding and further restored DBS binding activity of heat-denatured p53, *in vitro*, in a dose-dependent manner. *In vivo* ELISA and immunoprecipitation analysis of NTD125-transfected cells revealed that NTD125 shifted equilibrium from p53 mutant to wild type under heat stress conditions. Further, NTD125 initiated nuclear translocation of cytoplasmic p53 in transcriptionally active state in order to activate p53 downstream genes such as p21, Bax, PUMA, Noxa and SUMO.

Conclusion/Significance- Here, we showed that a novel chaperone-like activity resides in p53-N-ter region. Study might have significance in understanding the role of p53-NTD in its stabilization, conformational activation and apoptosis under heat-stress conditions.

Introduction

The tumor suppressor p53 protein is a transactivator that contains an independent regulatory N-ter domain (NTD) of approximately hundred amino acids (aa) affecting its activity and thermostability [1, 2]. There is substantial lack of structural and biophysical information on N-ter domain; in particular, this domain appears to be completely disordered with the typical features of the natively unfolded protein [3]. p53-NTD contains a transactivation domain (TAD, spanning amino acid residues 1-73) that alters transcription of genes controlling cell cycle arrest, proliferation and apoptosis [4, 5], and a proline rich domain (PRD, spanning aa residues 63-92) that plays role in drug induced, p53 mediated apoptosis [6] and influenced the ability of central domain to bind to

DNA [7]. It was proposed that TAD is composed of rapidly equilibrating conformers, one quasi-globular and the other relatively open, this intrinsically disordered domain with a tendency for helical structure in the TAD1 (aa residues 18-25) becomes helical on binding to MDM2 [8]. p53-NTD also possesses an auto-inhibitory function that controls the dissociation of p53 from DNA binding site (DBS) as the removal of 96 aa residues exhibits a remarkable reduction in dissociation from DNA [9] and the deletion of 40 aa residues changes the stability of p53 at 4 °C [2]. A 20 aa region spanning aa 101-120 was shown responsible for thermostable phenotype of human p53, that could partially protect the PAB1620⁺ conformation of tumor-derived p53 mutant from thermal unfolding [10]. An additional negative

regulatory region of p53 sequence-specific DNA binding was identified in proline rich region spanning aa residues 80-93, furthermore, synthetic peptides from this region (aa 80-93) are able to activate p53 DNA binding activity *in vitro* [11]. A peptide derived from p53-N-ter region (aa residues 105-126) inhibited p53 DNA binding and interfered with p53 DNA binding that was activated by PAb421 antibodies [12]. The activation of DNA binding function of p53 is not synonymous with protection of thermal denaturation; however, these functions may be used in cells to control the physiological activities [13]. Further, NTD is essential for the activity of WT p53 in apoptosis [14] including p53-mediated neuronal cell death [15]. On the contrary, a p53 natural isoform, that was deleted of 40 aa in NTD domain (Δ Np53); was identified in mammalian cells lines and in normal cells was shown to be tumorigenic and deficient in transactivation of MDM2 and p21 genes [16]. This isoform didn't form complex with MDM2 and failed to accumulate in response to DNA damage.

Heat denaturation of WT p53 and a majority of amino acid substitutions in p53 that occur in tumor destabilize the native DNA-binding conformation of core domain [17]. As NTD (1-73) is responsible for transactivation, it is interesting that through this portion of the molecule the sequence specific DNA binding of p53 must be stabilized. *In vivo*, this could result in reduced dissociation and increased association of p53 under conditions requiring the activation of specific genes for specific function. The cryoelectron microscopy study of full length p53 protein, that claimed to represent the *in vivo* nature of p53 oligomerization, reveals that aa 1-100 of N-ter of one monomer appears to abut the last aa 323-393 of C-ter of the partner in the dimer forming N/C nodes [18]. As intrinsically disordered segments of chaperones such as α -synuclein and casein become ordered due to reciprocal entropy transfer by contacting mis-folded part of the substrate [19-21], we explored whether disordered p53-NTD might possess chaperone-like activity and have any role in stabilizing DBS-binding conformation of WT p53.

In this report, we have discovered a novel function of NTD125 that binds to WT p53, stabilizes and restores its wild type conformation *in vitro* both at physiological and elevated temperatures. In cells, NTD125 stabilized and activated cytoplasmic p53 in initiating its nuclear translocation that led to activation of p53 downstream genes. Exogenously supplied NTD125 thus possessed a chaperone-like activity that activated p53 and could be of significance in restoring p53 mutant phenotype in cells under stress.

Results

NTD125 exhibited thermostability and physically interacted with p53

Highly purified recombinant p53 and NTD125 proteins were utilized for studying their stability and interaction. The thermal denaturation curve, as it was recorded at 280 nm in a UV-visible spectrophotometer, showed that NTD125 started to melt at a higher temperature (~50 °C) than WT p53 (~35 °C) (Fig. 1a). When the CD spectra of NTD125 was compared with that of WT p53 (data not shown), NTD125 was shown to be natively unstructured although it possessed some residual secondary structure as its conformational change at higher temperature (95 °C) was completely reversible on cooling it down to RT (Fig. 1b). These results confirmed the thermostable nature of NTD125. Earlier studies with amino-terminus domain containing 1-99 aa residues also showed NTD as natively unstructured at physiological conditions and thermostable [3, 22]. The interaction between NTD125 and p53 was further analyzed by CD (far UV range from 200 to 260 nm) at different temperatures (37 °C – 45 °C). The spectra of mixtures, that showed loss of signal intensity and was of similar pattern at different temperatures, was significantly different from the theoretical sum of individual spectra of NTD125 and p53; and the interaction between the proteins was not affected by temperature change (Fig. 1c, i-iv). It is widely reported in literature that if two proteins do not interact with each other, no structural change would result so the theoretical and experimental spectra would be identical. However, if the two proteins do interact substantially, conformational change in their structure would be detected and in this case, theoretical and experimental spectra would be substantially different. As it was shown in Fig. 1c, when p53 and NTD125 were combined at different temperatures, they interacted to produce evidence of a structural change. The same figure also presented individual spectra of p53 and NTD125. As significant structural changes had occurred due to probable interaction between these two peptides, we noticed the difference between spectra of mixtures and the theoretical sum of individual spectra. This observation led us to conclude that there was physical interaction between NTD125 and this interaction might further have stabilized p53 at higher temperatures (Fig. 1c, i-iv). Further, the interaction between p53 and NTD125 was studied by enzyme linked immunosorbent assay (ELISA). 0.5 μ g of either BSA, CHIP or NTD125 protein was plated per well onto which p53 (in increasing concentration) was added, followed by detection with anti-p53 antibody (PAb C-19). NTD125 showed interaction

with p53 in ELISA too (lanes 18-25). BSA (lanes 2-8) and CHIP (lane 10-16) were taken as negative and positive controls respectively (Fig. 2a). We then analyzed this interaction by immunoprecipitation (IPP) assay at room temperature using various p53 antibodies, PAb C-19 (specific for p53-C terminus), PAb1620 (specific for wild type p53) and PAb240 (specific for denatured/mutant p53); NTD125 was shown to bind to both p53 wild and mutant conformation with equal intensity (Fig. 2b). Again ELISA showed that NTD125 interacts with p53 and with C-ter domain (CTD) of p53 revealing that NTD125 interacts with p53 in C-terminus region (Fig. 2c). The interaction between NTD (1-186) and CTD (187-393) in cells was shown [18], and a low energy complex between CTD (361-382) and PRD (80-93) was predicted earlier [23]. The thermostable nature of NTD125 and its interaction with p53 led us to analyze whether it could stabilize p53 wild type conformation and DNA binding activity at elevated temperatures.

In vitro stabilization of p53 wild type conformation at higher temperature by NTD125

We monitored the transition of wild type p53 conformation in to the mutant phenotype at elevated temperatures utilizing p53 conformation specific antibodies (PAb1620 and PAb240) by IPP and ELISA. The recombinant p53 preparation contained both wild and mutant phenotype at ~1:1 ratio; shown by IPP with conformation-specific antibodies PAb1620 (wild specific) and PAb240 (mutant specific) at RT (Fig. 3a, panel 1, lanes 2 & 3). The recombinant preparation was separately heated at 37 °C, 40 °C, 42 °C and 45 °C and the heated mixture was immunoprecipitated either with PAb1620, PAb240 or PAb C-19 antibodies. When p53 was heated sequentially from 37 °C to 45 °C, the PAb1620 form was lost (Fig. 3a, panel-1, lanes 2, 5, 8, 11, & 14). The loss of wild type (PAb1620) form was progressive with the rise in temperature; the loss of wild type conformation at 37 °C and 40 °C was about 80 % whereas there was a total loss of this conformation at 45 °C within 1 hr (Fig. 3a). When NTD125 (1:5 molar ratio) was added prior to denaturation, there was no loss of wild type (PAb1620) (Fig. 3a, panel-2, lanes 2, 5, 8, 11, & 14, see arrow). In the presence of CHIP (1:2 molar ratio), a known chaperone of p53, the wild type (PAb1620) form was not lost (Fig. 3a, panel-3). This suggests that NTD125 showed chaperone-like function in stabilizing wild type conformation (PAb1620). In a parallel experiment, p53 was first heated to denaturation for 1 h at 37 °C followed by addition of NTD125 (Fig. 3b). In a similar manner, no loss of PAb1620 form was noticed thus confirming the

chaperone-like activity of NTD125. This observation was further confirmed by sandwich ELISA in which conformational antibodies PAb1620 (wild type specific) and PAb240 (mutant specific) were plated, onto which heat-denatured p53 (incubated with or without NTD125) was added. After washing the unbound protein, bound wild and mutant phenotypes were probed with either FL-393 (polyclonal antibodies against full length p53) or PAb C-19 (p53 C-ter specific antibodies); PAb C-19 was preferred when NTD125 was added into the mixture. Similar results were obtained by ELISA experiment (Fig. 3c & d) in which addition of NTD125 resulted in an increase in wild type form (PAb1620) (Fig. 3d, compare lanes 5, 7; 9, 11; 13, 15; 17, 19) and decrease in mutant form (PAb240). The result was more prominent in IPP experiment (Fig. 3a, b) than ELISA. Thus, NTD125 shifted the equilibrium from the mutant to wild type and behaved as a chaperone-like peptide.

NTD125 prevented irreversible thermal aggregation of p53

HSP90 [24], CHIP [25] were earlier shown to suppress p53 aggregation and catalyze disaggregation at elevated temperatures. As NTD125 was shown to bind to p53 and stabilized the wild conformation at elevated temperatures, we asked whether NTD125 could prevent aggregation of thermally denatured p53. p53 alone and with NTD125 (1:2 and 1:5 molar ratio) were incubated at 37 °C and 45 °C and the thermal aggregation kinetics was recorded by measuring light scattering in a fluorescence spectrophotometer. As WT p53 aggregated and reached a plateau after 40 min at 37 °C and after 10 min at 45 °C, addition of NTD125 in two molar excess prevented aggregation by approximately 75% both at 37 °C and 45 °C (Fig. 4a) whereas addition of five molar excess of NTD125 suppressed aggregation completely (Fig. 4b), thus suggesting that NTD125 stabilized p53 in shifting the equilibrium from the mutant to the wild type.

NTD125 protected and restored DNA binding of heat-denatured p53

In order to check the role of NTD125 upon DNA binding activity of p53, electrophoretic mobility shift assay (EMSA) was employed with or without NTD125 (in an increasing concentration), both under normal and denaturing conditions. p21-5'-DBS was radio-labeled and was mixed with recombinant p53 and DNA competitor for EMSA analysis either in the presence or absence of PAb421 antibodies (for super shift) and/or purified recombinant NTD125. An enhancement of DBS binding was observed after addition of NTD125 (0.5, 1.0, 1.5, and 2.0 µg) in the

reaction mixture (Fig. 5a, lanes 4, 5, 6 & 7). After heating p53 at 37 °C for 1 hr no binding was observed (Fig. 5b, lane 4) as most of the p53 was in mutant conformation, lacking DNA binding activity. Addition of NTD125 prior to denaturation step (1:1 to 1:10 molar ratio) resulted in complete restoration of DBS binding at 10 molar excess (Fig. 5b, lanes 5-8). HSP90 and CHIP were earlier shown to chaperone WT p53 [24, 25], the EMSA was repeated in the presence of HSP90 inhibitor geldanamycin and after utilizing bacterially expressed p53 that was passed through anti-CHIP and anti-HSP90 antibodies column (to terminate the role of any CHIP and HSP90 like homolog from bacterial system); similar results were obtained (Fig. 5c). In a parallel experiment, p53 was first denatured followed by the addition of NTD125 (Fig. 5d). Identical results were obtained thus suggesting that NTD125 restored p53 wild form and might have chaperone-like activity. In addition, we have utilized KB (p53^{+/+}) nuclear extract (NE) to check the effect of NTD125 on native WT p53. NE was first heated to denaturation in order to lose DBS binding and addition of NTD125 post denaturation resulted in restoration of DBS binding (Fig. 6a). Further, DNA-protein ELISA was utilized in order to study the interaction between biotinylated p21-5'-DBS and p53 in which either His-p53 or GST-p53 was used. Strong p53-DBS binding was detected with GST-p53 in comparison to His-p53 and both denatured GST-p53 and His-p53 failed to bind to DBS. Incubation of p53 with recombinant NTD125 prior to denaturation step resulted in protection of DBS binding by ~60% (Fig. 6b & c), thus supporting the EMSA data described above. These results thus confirmed that exogenous NTD125 stabilized p53 native conformation and facilitated p21-5'-DBS binding. Although a direct physical association through IPP was observed between NTD125 and p53 wild as well as mutant phenotype; the binding (super shift due to NTD125) was not detectable in EMSA in the presence of DBS suggesting that NTD125 might bind to WT p53 transiently in order to modulate its conformation prior to DNA interaction.

Stabilization of p53 wild phenotype in cytoplasm and nuclear translocation of activated WT p53 by NTD125

The restoration of p53 wild type conformation by NTD125 in EMSA led us to ask whether p53 could be stabilized by NTD125 in cells. We found that in KB cells, over-expression of HA-NTD brought a rise in p53 level and there was cellular interaction between NTD125 and endogenous p53 (data not shown). A negatively charged peptide based chaperone strategy to rescue p53 mutant conformation was reported to raise and stabilize p53

level [26] although no reasonable mechanism was proposed. We discovered that, in KB cells, exogenous NTD125 stabilized p53 wild conformation and reduced the mutant phenotype both under physiological and elevated temperature (Fig. 7a & b). In order to identify the minimal region that was responsible for the observed chaperone-like function, we further expressed HA-tagged NTD125 and its deletion constructs (NTD93, NTD61, and NTD55) in KB cells and utilized the whole cell extract (WCE) for *in vivo* ELISA and IPP utilizing conformation specific antibodies (PAb1620/ PAb240). *In vivo* ELISA, at 37 °C, showed that the ratio of p53 wild type (PAb1620) and mutant (PAb240) was ~1:1 (Fig. 7a, lanes 1 & 2). At 42 °C, the mutant was higher than wild type (Fig. 7a, lanes 4 & 5). In the cells that were transfected with NTD125, the trend was reversed. The wild type was higher than the mutant form both at 37 °C and 42 °C (Fig. 7a, lanes 7, 8 and 10, 11). Similar results were obtained by IPP experiment both at 37 °C and 42 °C. At 37 °C, the protein bands of wild type and mutant were of equal width (Fig. 7b, lanes 1, 2) whereas the mutant was higher than wild type 42 °C (Fig. 7b, lanes 3, 4). In NTD125-transfected cells, wild type p53 was at higher ratio (Fig. 7b, lanes 5, 7) than the mutant (Fig. 7b, lanes 6, 8). In ELISA, NTD93 showed partial stabilization of wild type (Fig. 7a, lanes 13, 14; Fig. 7b, lanes 11, 12) at 37 °C. However, NTD61 and NTD55 failed to show any protection. The above experiment thus established the chaperone-like stabilizing activity of p53-NTD that includes both the transactivation and proline-rich domain. Further, a time course analysis of NTD125 and p53 protein level in nuclear and cytoplasmic fractions was conducted for 36 hrs in NTD125 expressing KB cells. NTD125 was detected by anti-HA antibodies 6 hrs after transfection of NTD125-cDNA and was mostly nuclear until 33 hrs after which its level dropped (Fig. 7c). Interestingly, at 6th hr cytoplasmic p53 started migrating in to the nucleus (Fig. 7d). This result suggested that NTD125 stabilized cytoplasmic p53 in wild type conformation and initiated its nuclear translocation. Genotypically WT p53 in a mutant conformation promotes cell growth and behaves as a tumor suppressor only when present in the wild type conformation [27, 28]. NTD125 thus stabilized and induced nuclear translocation of cytoplasmic p53 supporting earlier observations that nuclear translocation of p53 could result in a change in the conformation from mutant to wild type [29-31]. In order to check whether this nuclear localized p53 is transcriptionally active, we performed luciferase reporter assay using p53 targeted gene promoter constructs such as Noxa, Bax, PUMA and p21. In NTD125- transfected cells, Noxa, Bax,

PUMA and p21 promoters were shown to be activated ~5.0, ~7.5, ~4.5, and ~5.0 fold respectively (Fig. 8a). In addition, RT-PCR analysis of p21, Noxa, Bax, PUMA and SUMO genes also yielded higher RNA expression of these genes in NTD125 expressing KB cells in comparison to control cells (Fig. 8b), thus confirming that nuclear p53 was transcriptionally active.

Discussion

Wild type p53 exists in two different conformational states, latent and active form in cells; the active form binds to DNA and is transcriptionally active whereas the latent form is devoid of these functions [32]. It exists in a conformational equilibrium between wild type and mutant conformation and equilibrium shifts in response to various stress conditions for binding to DNA and interaction with other proteins [25]. Interaction with N-ter specific antibodies PAb1801 has been shown to stabilize temperature-sensitive DNA-binding of wild-type and tumor derived mutant form of p53 through conformational stabilization [2] which suggests that NTD plays role in thermally sensitive, specific DNA binding of p53. It was proposed that p53-NTD can be involved in interdependent interaction with the C-terminus to regulate defined function of p53 [33]. CD studies of the full length p53 showed that NTD of p53 contains unstructured region in its native state [22]. Our experiments with highly purified recombinant NTD through CD analysis and IPP clearly showed that NTD125 binds to p53 and stabilized it at higher temperatures. Cryoelectron microscopy studies had earlier shown that in an intact p53 tetramer NTD of one molecule was positioned near CTD of another molecule thus forming an N/C node that was further confirmed by GST-pulldown assay and IPP [18].

We have demonstrated for the first time that the flexible p53-NTD that is devoid of tertiary structure possesses chaperone-like function in stabilizing p53 wild type conformation at higher temperature both *in vitro* and *in vivo*. Fluorescence based thermal aggregation assay, *in vitro* protection assay via IPP at various temperatures and ELISA confirmed that NTD125 displayed chaperone-like function in stabilizing the wild type conformation and restoring the mutant phenotype at elevated temperature. HSP90 and CHIP were earlier shown to stabilize WT p53 at higher temperature [24, 25].

We rationalized that the binding of NTD125 to p53-CTD might stabilize the core domain that, in turn, enhanced p53-DBS binding. Peptides were shown to stabilize p53 core domain [34] and stimulated p53-DBS binding [35]. EMSA analysis confirmed that NTD125 enhances p21-5'-DBS binding of p53 in dose dependent manner. Further, NTD restored p53

DBS binding of heat denatured p53 in an ATP-independent manner, unlike HSP90 [24]. Intrinsically disordered proteins were predicted to negatively correlate with the tendency of chaperone binding, although chaperone molecules binding would not assist in folding but might promote the assembly with partners in molecules [36]. p53-NTD interacts with multitude of protein factors that include molecular chaperones such as HSP90 [24], CHIP [25], HSP70 [37], and MDM2 [38] and it was shown to undergo disorder to order transition by interacting with MDM2 [39]. Short p53 TAD fragments in the intrinsically disordered p53 NTD domain were able to form 'induced helices' upon binding to target proteins [8, 40]. TAD2 in the NTD (aa 40-61) was also shown to fold into amphipathic alpha helices upon binding to replication protein A (RPA) [41] and Tfb1 subunit of yeast TFIIH [42].

Various synthetic compounds and small molecules have been identified that allowed mutant p53 to maintain active conformation and caused accumulation of active p53 in cells [43, 44] in order to improve antitumor therapy [45]. In KB cells that were transfected with NTD125, we have shown that p53 wild type conformation (PAb1620) was at a higher ratio than p53 mutant type conformation (PAb240) at elevated temperature. These results via IPP and *in vivo* ELISA confirmed that NTD protected and preserved WT p53 in native form. p53 NTD contains two separate transactivation domains TAD1 (aa residues 1-40), TAD2 (aa residues 40-61) and a proline-rich domain (aa residues 64-93) [1]. It is interesting that deletion of proline-rich domain (NTD55 and NTD61) resulted in loss of NTD chaperone function in cells. PRD was shown to contribute to p53 stability via Pin1 [46] and induction of p53-dependent apoptosis [47]. Earlier TAD2 along with PRD was identified for inducing pro-apoptotic genes or inhibition of anti-apoptotic genes [48]. Taken together, we concluded that transactivation domain along with PRD might be responsible for the observed chaperone-like function.

Nuclear translocation of p53 can result in a change in the conformation from mutant to wild type [29, 30] and genotypically WT p53 behaves as tumor suppressor in activating p53-downstream genes [28]. In NTD125 transfected cells, post 6 hrs, NTD125 was shown to co-translocate cytoplasmic p53 in to the nucleus. It is assumed that NTD125 might have triggered the activation of p53 for its nuclear translocation. The nuclear translocation of p53 can result in a change in the conformation from mutant to wild-type although these may be two separate events [29]. Under non-stress conditions, there exists equilibrium between the import and export of WT p53 in and out of nucleus. It was also proposed that

p53 might be escorted to the nucleus by chaperones such as HSP90 and the binding of HSP90 to the WT p53 inhibits the formation of multiple chaperone complexes with WT p53 [37]. Recently, we have shown that molecular chaperone CHIP co-translocated WT p53 into the nucleus and activated p53 gene transcription [25]. The NTD-mediated nuclear translocation of p53 further activated p53 downstream genes such as p21, Noxa, PUMA, SUMO, Bax. Based on above observations, we propose a model of p53 activation by NTD125 that might display chaperone-like function (Fig. 9).

The chaperone-like role of NTD125 both *in vitro* and in cells raises the possibility whether WT p53 might possess a self-chaperoning role as un-cleaved molecule; intra-molecular chaperone-like fragments occur frequently in proteins and such proteins would be prone to changing conditions and in particular, to mutations in the critical building block region [49]. α -synuclein and other chaperones require co-operativity between N- and C-ter [19] and an intra-molecular interaction between N- and middle region was essential for *in vivo* function of yeast HSP90 [50]. In best of our knowledge, this is the first report showing the presence of chaperone like activity within p53-N-ter region. As NTD125 could activate p53 signaling pathways in cells by activating its downstream genes; it would be of interest to explore the conversion of p53 mutant phenotype in to the wild type in cancer cells. Further study would aim at exploring the self chaperoning role of p53 in an intermolecular context and consequence of NTD125 expression in cellular system.

Materials and Methods

Plasmids, protein purification and Antibodies-

Vectors used and methods for purification of bacterially expressed His-p53, GST-p53 and GST-CHIP were described earlier [21]. pET32a-NTD125 and pET28a-NTD125 plasmids were used for expressing recombinant His-NTD125 in *E. coli* BL21 (DE3) cells. HA-tagged p53, NTD125 and deleted variants were expressed in mammalian system by cloning PCR amplified fragments in pNHA1 vector at *XbaI/EcoRI* site, generating, pNHA1-p53, pNHA1-NTD125, pNHA1-NTD93, pNHA1-NTD61, and pNHA1-NTD55 plasmids. Primers used for amplification are summarized in Supplementary Table. S1. For Luciferase reporter assay, pGL3-BAX, pGL3-Noxa, pGL3-p21, pGL3-PUMA and pSV- β -gal plasmids were used. Antibodies; anti-p53 (PAb1801), anti-p53 (PAb421), anti-p53 (PAb 1620), anti-p53 (PAb 240) were from Calbiochem; anti-p53 (C-19), anti-p53 (FL-393), anti-His, anti-GST and all secondary antibodies from Santa-Cruz and anti-HA from Babco were used.

Cells Culture, Transfection, Heat Shock Treatment and Immunoprecipitation-

KB cells were procured from NCCS, Pune, India, and maintained in Dulbecco's modified Eagle's medium (DMEM) (Sigma-aldrich) with 10 % FCS. Transfections were carried out using either Effectene Transfection Reagent (Qiagen) or EscortTM IV Transfection Kit (Sigma) according to manufacturer's instructions. Cells were processed for sample preparation after 24 hrs, 36 hrs post transfection or as described in the figures. For heat shock experiment, 24 hrs post-transfection, cells were grown at 42 °C for 75 min in CO₂ incubator and then processed for IPP/ *in vivo* ELISA assay. For IPP using conformation specific antibodies, cells were transfected, treated and processed as described earlier [21] except that the lysis was done in NP-40 lysis buffer (20 mM Tris-HCl pH 7.4, 100 mM NaCl, 10 % Glycerol, 1.0 % NP-40, 1mM EDTA and protease inhibitor cocktail). Eluted samples were resolved on 12% SDS-PAGE and probed using PAb C-19 antibodies.

Thermal denaturation curve and Fluorescence spectrophotometry (Aggregation assay)-

The heat denaturation studies were carried out by recording the change absorbance of 100 μ g of p53 or NTD125, diluted in 1 ml PBS at 280 nm wavelength in UV-visible spectrophotometer (CARY, 100 Bio, Varian) attached to temperature controller. The variation in temperature was done at the rate of 1 °C/min. The aggregation assay was performed as follows: p53 (1.0 μ M) was incubated at 37 °C and 45 °C with or without NTD125 (2.0 or 5.0 μ M). Thermal aggregation kinetics was monitored by measuring light scattering, in a fluorescence spectrophotometer (CARY Eclipse, Varian) attached to temperature controller, in the Peltier controlled thermostatted quartz cuvettes. All the measurements were done at the excitation and emission wavelengths of 340 nm with a spectral bandwidth of 5 nm.

Circular Dichroism (CD) Spectroscopy-

For CD spectroscopic analysis, all the measurements were done on J-815 Circular Dichroism System (Jasco), in the Far UV range from 200 to 260 nm using the cuvette of 0.1 cm pathlength. 200 μ g of p53 or NTD125 was diluted in 0.5 ml PBS and the spectra were collected at different temperatures. For each sample an average was taken of the three measurements at a scan rate of 20 nm/min. For interaction studies, 200 μ g each of p53 and NTD125 were mixed, diluted in 0.5 ml PBS and then incubated for 1 hr at the temperature at which spectra had to be recorded. The spectra were then taken at

different temperatures. For all the measurements, the spectrum of the buffer was deduced from the sample.

***In vitro* protection and co-immunoprecipitation assay-**

For *in vitro* protection assay, 2 µg of recombinant His-p53 was incubated with or without recombinant GST-CHIP (1:2) or His-NTD125 in (1:5) molar ratio. Protein mixture was then diluted to 100 µl in PBS (containing protease inhibitor cocktail) and incubated at different temperatures i.e. RT, 37 °C, 40 °C, 42 °C and 45 °C for 1 hr. Further volume of the sample was diluted to 500 µl and 1 µg of PAb C-19/ PAb1620/ PAb240 added to the mixture and incubated on a rotatory shaker for 1 hr at 4 °C. After that 50 µl of 10 % protein-A agarose (pre-saturated with BSA) was added to the sample and incubated for 2 hrs at 4 °C, with continuous stirring. After pelleting, beads were washed thrice with NP-40 washing buffer (0.5% NP-40 in PBS + protease inhibitor cocktail) and finally the immunocomplex was released in 50 µl of NP-40 washing buffer by adding SDS loading dye and boiling for 3 minutes. For assessment of restoration activity of NTD125, p53 was first denatured and then NTD125 was added to the mixture and incubated at 4 °C for another hr; finally immunoprecipitated using different antibodies. For co-immunoprecipitation assay, the entire procedure was repeated as above, only His-p53 and His-NTD125 were taken in (1:1) molar ratio. For immunoblotting 20 µl of eluted sample was resolved on 12 % SDS PAGE and semi-dry blotted on to nitrocellulose membrane, western blot was developed using PAb1801/ PAbDO1.

Electrophoretic Mobility Shift Assay-

The DNA binding activity of recombinant p53 was monitored by EMSA with or without NTD125. The EMSA reaction was set using 3 ng probe and 100 ng recombinant p53, as described previously [21]. Using radio-labeled p21-5' DBS site as probe [21], reaction mixtures were incubated for 30 minutes at RT and then loaded on to 4 % native-PAGE containing 0.5 X TBE buffer, subsequently, gel was dried and exposed for autoradiography. To visualize the effect of NTD125 on the DNA binding activity of p53, recombinant NTD125 in different amount (as shown in figures) was added to the p53 and incubated for 1 hr at 37 °C prior to set the reaction. Whereas to assess the restoration activity, p53 was first denatured and then incubated with NTD125 (in different molar ratios) at 4 °C for 1 hr before adding to reaction mixture. We used 5 µg of isolated nuclear extract for the EMSA, when KB-NE was used as the source of WT p53.

DNA-protein ELISA-

PAb421 (0.5 µg) diluted in 50 µl PBS was coated per well and incubated at 4 °C overnight, plate was then washed once with PBS and blocked using 200 µl of 1 % BSA in PBS for 1 hr. Plate was then washed thrice, 5 min each, with wash buffer (PBS + 0.05 % Tween20). After that WT p53 protein was bound to the antibody by adding 0.5 µg of p53 protein diluted in 50 µl PBS in the well and incubating it at 4 °C for 1 hr. To remove the unbound protein, plate was washed thrice, 5 min per wash, with wash buffer. Subsequently 0.5 µg of biotin labeled DBS diluted in 50 µl 1X GMS buffer was added in the well and incubated at 4 °C for 1 hr. Plate was washed again three times with wash buffer, and then 50 µl of 1:400,000 diluted Avidin Alkaline Phosphatase (AAP from Sigma) in PBS was added per well and incubated for 2 hrs. Washing was again done thrice with wash buffer, and the color was developed by adding 100 µl of 1mg/ml PNPP in AP buffer (50 mM Na₂CO₃, 1 mM MgCl₂, pH 9.8) and incubated at 37 °C. The reaction was then stopped by adding 100 mM EDTA, and absorbance was taken at 405 nm in the ELISA reader (Benchmark Plus Microplate reader, BioRad, USA). To study the DNA binding by heat denatured p53 protein, p53 was diluted in PBS, heat denatured at 37 °C for 1 hr in water bath with or without NTD125 and added on to the PAb421 coated wells, DBS was then added and bound DBS was detected using AAP.

ELISA-

An ELISA-based protein-protein interaction assay was utilized for p53- and NTD125 interaction studies. 96-well Maxisorp plates (Nunc) were coated with 50 µl of a 10 µg/ml (NTD125/CHIP/BSA) protein in PBS at 4 °C over night. The wells were rinsed with cold PBS at 4 °C three times. Blocking was done with 2 % BSA (Sigma) in PBS at 4 °C for 4 hrs. Following the blocking step, the wells were washed three times with PBS containing 0.01 % (v/v) Tween-20 (Sigma). p53 protein (0.5 µg) was diluted in 50 µl PBS, 0.05 % (v/v) Tween-20, 0.2 % (w/v) BSA and (in increasing concentration) added into NTD125 / CHIP/ BSA coated wells. After an incubation period of 90 min at 4 °C, the ELISA plates were washed with PBS containing 0.01 % Tween-20 three times. The p53 protein was detected using 0.2 µg of mouse monoclonal antibody PAb C-19 in 50 µl PBS, 0.05 % (v/v) Tween-20, 0.2 % (w/v) BSA and then AP-conjugated anti-mouse secondary antibody. Finally, 100 µl of alkaline phosphate substrate i.e. 1 mg/ml PNPP in AP-buffer (pH 9.6) was added and the enzymatic reaction was allowed to take place for 30 minutes at room temperature. The reaction was terminated by adding 50 µl of 0.1 M EDTA pH 8.0. The optical density was determined at 405 nm using

Microplate reader (BioRad). Total p53 concentration in cells was measured using PathScan^R Total p53 Sandwich Elisa Kit, from Cell Signaling TECHNOLOGY^R. The endogenous p53 level was observed in mock and NTD125 transfected KB cells in a time dependent manner. Cells were collected and washed twice with PBS. The cells were lysed and processed for detection of p53 according to manufacturer's protocol. For detection of HA-NTD125, wells were coated with polyclonal p53 antibody and protein was detected using monoclonal anti-HA antibody (12CA5) conjugated with reporter enzyme HRP (Direct HA detection western blot kit, Biochemia).

Sandwich ELISA-

Investigation of the p53 conformation *in vitro* was carried out using two-site ELISA. Firstly the wells were coated with p53 conformation specific monoclonal antibody PAb1620 or PAb240 at concentration of 50 ng/100 μ l per well in 0.1 M carbonate buffer (pH 9.2) at 4 °C for 16 h. The wells were rinsed with PBS three times. Blocking was done with 2 % BSA (Sigma) in PBS at 4 °C for 2 hrs. Following the blocking step, the wells were washed three times with PBS containing 0.05 % (v/v) Tween-20 (Sigma). p53 protein (100 ng) was diluted in 100 μ l of PBS, 0.05 % (v/v) Tween-20, 0.2 % (w/v) BSA with NTD125 (1:5) or without NTD125 were incubated at different temperatures for 1 hr, added in the wells and incubated for 90 min at 4 °C. The ELISA plates were then washed with PBS containing 0.05 % Tween-20 three times. p53 protein was detected using 50 ng of goat monoclonal antibody PAb C-19 in 50 μ l PBS, 0.05 % (v/v) Tween-20, 0.2 % (w/v) BSA and then AP-conjugated anti-goat secondary antibody. Finally detection was done as described earlier. Sandwich ELISA (*in vivo* ELISA) from cell lysate was done as follows; wells were coated with 100 μ l of 5 μ g/ml anti-p53 antibodies (PAb1620, PAb240 and PAb C-19) overnight at 4 °C. After washing thrice with TBS buffer (0.05 % Tween-20 in PBS), blocking was done using 5 % skimmed milk in TBS for 2 hrs at 4 °C. After washing the wells thrice with TBS, 200 μ g cell lysate in NP-40 buffer (normal/heat shocked) 1:1 v/v diluted in 5 % skimmed milk in TBS was added to each well and incubated at 4 °C for 2 hrs. Subsequently 100 μ l of anti-p53 polyclonal antibody FI-393 (1:1000 diluted) was added to each well and incubated at 4 °C for 2 hrs. Again after three quick washes, 100 μ l of AP-conjugated anti-rabbit secondary antibody (1:1000) was added to each well and kept at RT for another 2 hrs. ELISA was developed using 100 μ l of 1mg/ml PNPP solution in AP- buffer for 30 minutes and after terminating the

reaction O.D. was recorded at 405 nm on Microplate reader.

Preparation of Nuclear and Cytoplasmic extracts

KB cells were scraped with a rubber policeman, and pelleted. 200 μ l of cytoplasmic extraction reagent CER I (NE-PERTM Nuclear and Cytoplasmic Extraction Kit, Pierce Inc) was added per 20 μ l of packed cell volume, and the cell pellet was vortexed for 15 seconds. Cells were incubated in presence of CER I for 10 minutes, followed by incubation with 11 μ l of CER II for another minute. Lysed cells were centrifuged at 13,000 rpm for 5 minutes to pellet the intact nuclei. The supernatant containing the cytoplasmic fraction was carefully separated. The pelleted nuclei were resuspended in 100 μ l of NER I, vortexed for 15 seconds and incubated on ice for 45 minutes with periodic vortexing after every 10 minutes. After this, the suspension was centrifuged at 13,000 rpm and the supernatants containing the nuclear proteins were stored at -80 °C. Nuclear and cytoplasmic fractions were checked by western blotting using anti-actin and anti-RNA pol-II antibodies (data not shown).

Luciferase Reporter Assay

KB cells were plated in six-well plate the day before transfection such that they become 60–80% confluent before transfection. Reporter plasmid (1.0 μ g), full length promoter-constructs were transfected together with (1.0 μ g) expression vectors (pNHA1-NTD125) and (0.5 μ g) β -galactosidase-expression plasmid (pSV- β -gal; Promega) per well as per the manufacturer's instructions. For each transfection, DNA content was kept uniform by using empty vector for relative plasmid type. The cells were incubated at 37 °C, in CO₂ incubator, in serum free media for 6 hrs and then media was replaced with fresh complete DMEM media. After 24 hrs the cells were washed in cold PBS three times and lysed with 200 μ l of the 1 X lysis buffer (Promega) for 20 minutes at 4 °C, the lysate was then centrifuged at 14000 rpm for 5 min at 4 °C. Supernatant was collected and 20 μ l supernatant was used for the assay of luciferase activity using Luciferase reporter gene assay kit (Promega) as per the manufacturer's instruction. The β -galactosidase activity was determined using the β -galactosidase Enzyme Assay Kit (Promega). Luciferase activity was normalized by β -galactosidase activity and the data from triplicate determinations were expressed as mean \pm SD.

Isolation and RT-PCR

KB Cells were lysed in appropriate amount of Trizol (1 ml Trizol per well of a 6 well plate for cultured cells). Cells were repeatedly and vigorously

pipetted. Cells were then kept at room temperature for 5-10 mins, after which 200 µl of chloroform per 1 ml of Trizol was added and mixed thoroughly. The cells were again left at room temperature for 10 mins. Cells were then centrifuged at 12,000 rpm at 4 °C for 15 mins and the upper aqueous colorless layer was transferred to a fresh eppendorf tube. To this eppendorf tube, 75 µl Lithium Chloride (LiCl) followed by 1ml chilled Ethanol (EtOH) were added and kept at -20 °C for 2-3 hrs. The eppendorf tube was centrifuge at maximum speed for 15 minutes at 4 °C. The supernatant was discarded and 250 µl of 70 % EtOH was added and the tube was kept at room temperature for 2 minutes. The tube was again centrifuged at 7500 rpm for 5 minutes at 4 °C, the supernatant was then discarded and finally, the pellet was resuspended in RNA grade water till it was completely dissolved. Single Strand c-DNA was synthesized with sense and anti-sense primers using RevertAid™ H Minus First Strand cDNA Synthesis

Kit (Fermentas). The resulting cDNA was diluted (1:10) before proceeding with the PCR reaction. PCR was conducted in Mastercycler gradient (Brinkmann Instruments Inc., Westbury, USA). Each 50 µl PCR reaction employed cDNA, 2.5 U Taq polymerase (Eppendorf scientific Inc., Westbury, USA), 0.2 mM dNTPs and 0.5 µM primer. PCR products were resolved on 2 % agarose gel. The size of the PCR amplicon was determined by comparison with 100-bp DNA ladder (Promega, Madison, USA). Primers used for amplification of appropriate gene are summarized in Supplementary Table. S2.

Acknowledgements-We thank Dr. C. Lallemand for Noxa-pGL3 plasmid, Dr. R. Finch for p21-pGL3 and BAX-pGL3 plasmids and Dr. Tzippi Hershko for PUMA-pGL3 constructs. The research was partly supported by Department of Biotechnology, Govt. of India.

References-

1. Joerger AC, Fersht AR (2008) Structural biology of the tumor suppressor p53. *Annu Rev Biochem* 77, 557-582.
2. Hansen S, Lane DP, Midgley CA (1998) The N terminus of the murine p53 tumour suppressor is an independent regulatory domain affecting activation and thermostability. *J Mol Biol* 275, 575-588.
3. Dawson R, Muller L, Dehner A, Klein C, Kessler H, et al. (2003) The N-terminal domain of p53 is natively unfolded. *J Mol Biol* 332, 1131-1141.
4. Fields S, Jang SK (1990) Presence of a potent transcription activating sequence in the p53 protein. *Science* 249, 1046-1049.
5. Matas D, Sigal A, Stambolsky P, Milyavsky M, Weisz L, et al. (2001) Integrity of the N-terminal transcription domain of p53 is required for mutant p53 interference with drug-induced apoptosis. *EMBO J* 20, 4163-4172.
6. Baptiste N, Friedlander P, Chen X, Prives C (2002) The proline-rich domain of p53 is required for cooperation with anti-neoplastic agents to promote apoptosis of tumor cells. *Oncogene* 21, 9-21.
7. Roth J, Koch P, Contente A, Dobbstein M (2000) Tumor-derived mutations within the DNA-binding domain of p53 that phenotypically resemble the deletion of the proline-rich domain. *Oncogene* 19, 1834-1842.
8. Kussie PH, Gorina S, Marechal V, Elenbaas B, Moreau J, et al. (1996) Structure of the MDM2 oncoprotein bound to the p53 tumor suppressor transactivation domain. *Science* 274, 948-953.
9. Cain C, Miller S, Ahn J, Prives C (2000) The N terminus of p53 regulates its dissociation from DNA. *J Biol Chem* 275, 39944-39953.
10. Xirodimas DP, Lane DP (1999) Molecular evolution of the thermosensitive PAb1620 epitope of human p53 by DNA shuffling. *J Biol Chem* 274, 28042-28049.
11. Muller-Tiemann BF, Halazonetis TD, Elting JJ (1998) Identification of an additional negative regulatory region for p53 sequence-specific DNA binding. *Proc Natl Acad Sci U S A* 95, 6079-6084.
12. Protopopova M, Selivanova G (2003) Inhibition of p53 activity in vitro and in living cells by a synthetic peptide derived from its core domain. *Cell Cycle* 2, 592-595.
13. Hansen S, Hupp TR, Lane DP (1996) Allosteric regulation of the thermostability and DNA binding activity of human p53 by specific interacting proteins. *CRC Cell Transformation Group. J Biol Chem* 271, 3917-3924.
14. Matas D, Sigal A, Stambolsky P, Milyavsky M, Weisz L, et al. (2001) Integrity of the N-terminal transcription domain of p53 is required for mutant p53 interference with drug-induced apoptosis. *EMBO J* 20, 4163-4172.
15. Cregan SP, Arbour NA, Maclaurin JG, Callaghan SM, Fortin A, et al. (2004) p53 activation domain 1 is essential for PUMA upregulation and p53-mediated neuronal cell death. *J Neurosci* 24, 10003-10012.
16. Courtois S, Verhaegh G, North S, Luciani MG, Lassus P, et al. (2002) DeltaN-p53, a natural isoform of p53 lacking the first transactivation domain, counteracts growth suppression by wild-type p53. *Oncogene* 21, 6722-6728.
17. Bykov VJ, Issaeva N, Zache N, Shilov A, Hultcrantz M, et al. (2005) Reactivation of mutant p53 and induction of apoptosis in human tumor cells by maleimide analogs. *J Biol Chem* 280, 30384-30391.
18. Okorokov AL, Sherman MB, Plisson C, Grinkevich V, Sigmundsson K, et al. (2006) The structure of p53 tumour suppressor protein reveals the basis for its functional plasticity. *EMBO J* 25, 5191-5200.
19. Park SM, Jung HY, Kim TD, Park JH, Yang CH, et al. (2002) Distinct roles of the N-terminal-binding domain and the C-terminal-solubilizing domain of alpha-synuclein, a molecular chaperone. *J Biol Chem* 277, 28512-28520.
20. Bhattacharyya J, Das KP (1999) Molecular chaperone-like properties of an unfolded protein, alpha(s)-casein. *J Biol Chem*

- 274, 15505-15509.
21. Tompa P, Csermely P (2004) The role of structural disorder in the function of RNA and protein chaperones. *FASEB J* 18, 1169-1175.
 22. Bell S, Klein C, Muller L, Hansen S, Buchner J (2002) p53 contains large unstructured regions in its native state. *J Mol Biol* 322, 917-927.
 23. Kim AL, Raffo AJ, Brandt-Rauf PW, Pincus MR, Monaco R, et al. (1999) Conformational and molecular basis for induction of apoptosis by a p53 C-terminal peptide in human cancer cells. *J Biol Chem* 274, 34924-34931.
 24. Walerych D, Kudla G, Gutkowska M, Wawrzynow B, Muller L, et al. (2004) Hsp90 chaperones wild-type p53 tumor suppressor protein. *J Biol Chem* 279, 48836-48845.
 25. Tripathi V, Ali A, Bhat R, Pati U (2007) CHIP chaperones wild type p53 tumor suppressor protein. *J Biol Chem* 282, 28441-28454.
 26. Issaeva N, Friedler A, Bozko P, Wiman KG, Fersht AR, et al. (2003) Rescue of mutants of the tumor suppressor p53 in cancer cells by a designed peptide. *Proc Natl Acad Sci U S A* 100, 13303-13307.
 27. Milner J, Watson JV (1990) Addition of fresh medium induces cell cycle and conformation changes in p53, a tumour suppressor protein. *Oncogene* 5, 1683-1690.
 28. Sabapathy K, Klemm M, Jaenisch R, Wagner EF (1997) Regulation of ES cell differentiation by functional and conformational modulation of p53. *EMBO J* 16, 6217-6229.
 29. Gaitonde SV, Riley JR, Qiao D, Martinez JD (2000) Conformational phenotype of p53 is linked to nuclear translocation. *Oncogene* 19, 4042-4049.
 30. Zerrahn J, Deppert W, Weidemann D, Patschinsky T, Richards F, et al. (1992) Correlation between the conformational phenotype of p53 and its subcellular location. *Oncogene* 7, 1371-1381.
 31. Ryan JJ, Clarke MF (1994) Alteration of p53 conformation and induction of apoptosis in a murine erythroleukemia cell line by dimethylsulfoxide. *Leuk Res* 18, 617-621.
 32. Hupp TR, Meek DW, Midgley CA, Lane DP (1992) Regulation of the specific DNA binding function of p53. *Cell* 71, 875-886.
 33. Cain C, Miller S, Ahn J, Prives C (2000) The N terminus of p53 regulates its dissociation from DNA. *J Biol Chem* 275, 39944-39953.
 34. Friedler A, Hansson LO, Veprintsev DB, Freund SM, Rippln TM, et al. (2002) A peptide that binds and stabilizes p53 core domain: chaperone strategy for rescue of oncogenic mutants. *Proc Natl Acad Sci U S A* 99, 937-942.
 35. Selivanova G, Iotsova V, Okan I, Fritsche M, Strom M, et al. (1997) Restoration of the growth suppression function of mutant p53 by a synthetic peptide derived from the p53 C-terminal domain. *Nat Med* 3, 632-638.
 36. Hegyi H, Tompa P (2008) Intrinsically disordered proteins display no preference for chaperone binding in vivo. *PLoS Comput Biol* 4, e1000017.
 37. Zyllicz M, King FW, Wawrzynow A (2001) Hsp70 interactions with the p53 tumour suppressor protein. *EMBO J* 20, 4634-4638.
 38. Wawrzynow B, Zyllicz A, Wallace M, Hupp T, Zyllicz M (2007) MDM2 chaperones the p53 tumor suppressor. *J Biol Chem* 282, 32603-32612.
 39. Dunker AK (2007) Another window into disordered protein function. *Structure* 15, 1026-1028.
 40. Uesugi M, Verdine GL (1999) The alpha-helical FXXPhiPhi motif in p53: TAF interaction and discrimination by MDM2. *Proc Natl Acad Sci U S A* 96, 14801-14806.
 41. Bochkareva E, Kaustov L, Ayed A, Yi GS, Lu Y, et al. (2005) Single-stranded DNA mimicry in the p53 transactivation domain interaction with replication protein A. *Proc Natl Acad Sci U S A* 102, 15412-15417.
 42. Di Lello P, Jenkins LM, Jones TN, Nguyen BD, Hara T, et al. (2006) Structure of the Tfb1/p53 complex: Insights into the interaction between the p62/Tfb1 subunit of TFIIH and the activation domain of p53. *Mol Cell* 22, 731-740.
 43. Seo YR, Kelley MR, Smith ML (2002) Selenomethionine regulation of p53 by a refl-dependent redox mechanism. *Proc Natl Acad Sci U S A* 99, 14548-14553.
 44. Bykov VJ, Selivanova G, Wiman KG (2003) Small molecules that reactivate mutant p53. *Eur J Cancer* 39, 1828-1834.
 45. Beretta GL, Gatti L, Benedetti V, Perego P, Zunino F (2008) Small molecules targeting p53 to improve antitumor therapy. *Mini Rev Med Chem* 8, 856-868.
 46. Toledo F, Lee CJ, Krummel KA, Rodewald LW, Liu CW, et al. (2007) Mouse mutants reveal that putative protein interaction sites in the p53 proline-rich domain are dispensable for tumor suppression. *Mol Cell Biol* 27, 1425-1432.
 47. Sakamuro D, Sabbatini P, White E, Prendergast GC (1997) The polyproline region of p53 is required to activate apoptosis but not growth arrest. *Oncogene* 15, 887-898.
 48. Zhu J, Zhang S, Jiang J, Chen X (2000) Definition of the p53 functional domains necessary for inducing apoptosis. *J Biol Chem* 275, 39927-39934.
 49. Ma B, Tsai CJ, Nussinov R (2000) Binding and folding: in search of intramolecular chaperone-like building block fragments. *Protein Eng* 13, 617-627.
 50. Matsumoto S, Tanaka E, Nemoto TK, Ono T, Takagi T, et al. (2002) Interaction between the N-terminal and middle regions is essential for the in vivo function of HSP90 molecular chaperone. *J Biol Chem* 277, 34959-34966.

Figure Legends-

Fig. 1. NTD125 is highly thermostable **a.** UV spectra of NTD125 and p53. NTD125 is stable up to 50 °C whereas p53 starts melting at ~35 °C. **b.** Far-UV-spectra of NTD125 at 25 °C (■), 95 °C (▲) and after cooling down to 25 °C (□), shows that NTD125 was a less structured peptide and its secondary structure was completely reversible after cooling it down to 25 °C. **c.** CD spectra analysis of p53 (□), NTD125 (○), theoretical sum of both (Δ) and mixture of both (☆). The spectra of mixture were significantly different from the theoretical sum of individual spectra of NTD125 and p53 at different temperatures (i – 25 °C; ii – 37 °C; iii – 42 °C & iv – 45 °C); thus suggesting physical interaction between the peptides.

Fig. 2. NTD125 interacts with p53. **a.** ELISA showing interaction between NTD125 and p53. 50 µl of 10 µg/ml protein (BSA, lanes 1-8; CHIP, lanes 9-16; NTD125, lanes 17-24) was coated on to the wells and then p53 was added in increasing concentration, ELISA was developed using anti-p53 specific antibodies PAb C-19. CHIP and BSA were used as positive and negative controls respectively. **b.** Co-immunoprecipitation assay showing interaction of NTD125 with different conformations of p53. **c.** ELISA showing interaction of GST-NTD125 with His-p53 and His-CTD (lanes 1 & 3), whereas GST-NTD125 is unable to interact with His-NTD125. BSA is used as negative control.

Fig. 3. NTD125 stabilizes WT p53 in vitro. **a.** Loss of p53 wild type conformation (PAb1620) at higher temperature. Recombinant p53 was heated and conformational changes monitored with PAb1620 and PAb240 by IPP at (37-45 °C); gradual loss of wild type conformation was observed (Panel-1, lanes 2,5,8,11,14 & 16), mutant conformation was stable at (RT-42 °C) (Panel-1, lanes 3, 6, 9, 12) and decreased at 45 °C (Panel-1, lane 15). In presence of NTD125 wild conformation (37-45 °C) was protected (Panel-2, lanes 5, 8, 11, 14). Addition of recombinant CHIP (known chaperone of p53) also protected wild conformation of p53 (Panel-3, lanes 5, 8, 11, 14) at different temperatures (37-45 °C) **b.** Further, addition of NTD125 post incubating p53 at various temperature, restores wild conformation (lanes 5 and 8) and **c.** ELISA showing rise in mutant conformation (lanes 4, 6, 8, 10) at increasing temperature and **d.** protection of wild conformation in the presence of NTD125 (lanes 7, 11, 15, 19).

Fig. 4. Prevention of irreversible p53 thermal aggregation by NTD125. **a. & b.** Time dependent fluorescence studies at 340 nm show that at 37 °C and 45 °C, NTD125 (at 1:2 and 1:5 molar ratio) prevented irreversible p53 thermal aggregation.

Fig. 5. NTD125 stabilizes and restores DNA binding activity of heat denatured WT p53. **a.** EMSA showing role of NTD125 upon p53-DBS binding. 100 ng of p53 was incubated with 3 ng P³² labeled p21-5'-DBS with (lanes 4-7) or without (lane 3) PAb421. Addition of NTD125 (0.5- 2.0 µg) resulted in enhanced DBS binding (lanes 4-7). **b.** p53 DBS binding (lanes 2 & 3); loss of DBS binding after heating p53 at 37 °C for 1 hr (lane 4); Stabilization of DNA binding occurred after addition of NTD125 prior to heating (different molar ratios, lanes 5-8). **c.** in presence of Geldanamycin (5 µM), a HSP90 inhibitor, the loss of DNA binding after heating p53 at 37 °C (1 hr) (lane 4) and stabilization of DBS binding after adding NTD125 in increasing concentration (lanes 5-8). **d.** Restoration of DNA binding occurred after adding NTD125 (different molar ratios, lanes 1-4) post p53 denaturation step.

Fig.6. a. Lost activity of native p53 (lane 4) was also restored after adding NTD125 (lanes 5, 6 & 7) while using KB-NE as a source of WT p53. **b.** ELISA showing His-p53-DBS binding (lane 2), loss of DBS binding after heating p53 at 37 °C (lane 3) and stabilization of DBS binding (lane 4). **c.** ELISA showing GST-p53-DBS binding (lane 2), loss of DBS binding of p53 that was heated at 37 °C (lane 3) and stabilization (lane 4). PAb421 coated wells incubated with either p53 or heat-denatured p53 in presence or absence of NTD125 followed by addition of biotin-labeled p21-5'-DBS, color development was done with alkaline phosphatase conjugated Avidin.

Fig. 7. NTD125 activates and translocates cytoplasmic p53 in to the nucleus. **a.** *In vivo* ELISA showing NTD125 protecting p53 wild type conformation at physiological and elevated temperature. NTD constructs (NTD125, NTD93, NTD61 and NTD55) were transfected into KB cells and WCE (200 µg) was analyzed for estimating total cellular p53 (PAb C-19), p53 wild type (PAb1620) and mutant type (PAb240) conformation at various temperatures. Equal amount of wild and mutant form at 37 °C (lanes 1, 2) and rise in mutant form at 42 °C (lane 5) were observed whereas the presence of NTD125 and NTD93 decreased mutant form both at 37 °C and 42 °C (lanes 8, 11) and increased wild form (lanes 7, 10, 13); NTD61 and NTD55 failed to show chaperone-like function. **b.** Immunoprecipitation utilizing PAb1620 and PAb240 confirmed the above finding. NTD125 protected

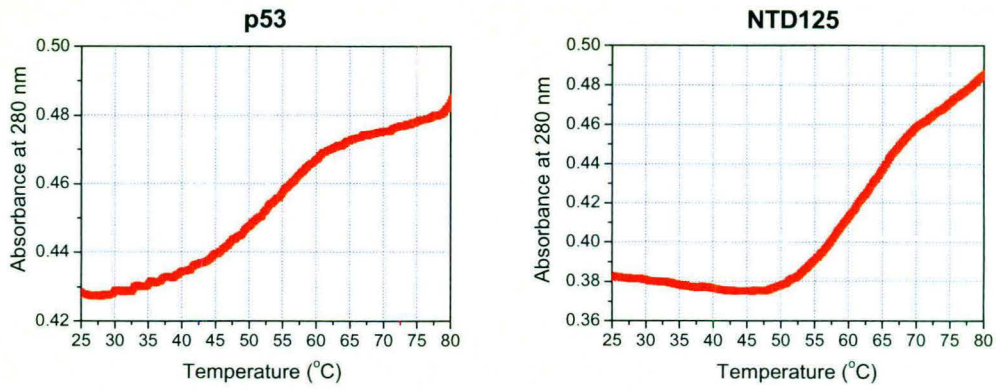
the wild form (PAb1620) when compared with KB control (compare lanes 3 & 7) at 42 °C, NTD93 partially protected the wild form (compare lanes 1 & 11; 3 & 13); NTD 61 and NTD55 failed to protect the wild form at 42 °C (compare lanes 3, 17 & 21). **c.** Time course ELISA showing p53 and NTD125 level post NTD125 transfection. PAb421 and HA-antibodies were used to estimate cellular (\square), cytoplasmic (Δ) and nuclear protein (\circ) level at every hr post NTD125 transfection; NTD125 enter nucleus at $\sim 5^{\text{th}}$ hr after transfection; the estimated amount of both nuclear and cellular NTD125 was approximately equal (left panel). **d.** In a synchronized manner most of the cytoplasmic p53 enters nucleus at $\sim 6^{\text{th}}$ hr post NTD125 transfection and the total cellular p53 was equal to the total cytoplasmic p53.

Fig. 8. NTD125 mediated activation of p53 downstream genes. **a.** Luciferase assay showing NTD125-mediated activation of Noxa, Bax, PUMA and p21 promoters. The promoter-luciferase constructs were transfected with or without NTD125 constructs and luciferase activity was monitored. Approximate activation of Noxa, Bax, PUMA and p21 promoter was 5.0, 7.5, 4.5, and 5.0 fold respectively. **b.** Reverse-transcriptase (RT) PCR showing higher expression of p21, NOXA, Bax, PUMA and SUMO genes in NTD125 expressing cells in comparison to only KB cells. Experiment was performed 24 hrs post NTD125 transfection.

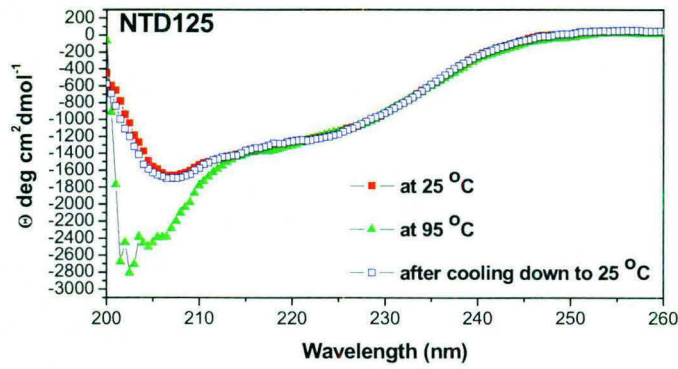
Fig. 9. A Model for activation of p53 through NTD125- NTD125 molecules interact with cytoplasmic p53 leading to stabilization of wild conformation that further initiate nuclear translocation of activated p53. Nuclear localized p53 activates transcription of downstream genes.

Fig. 1

a.



b.



c.

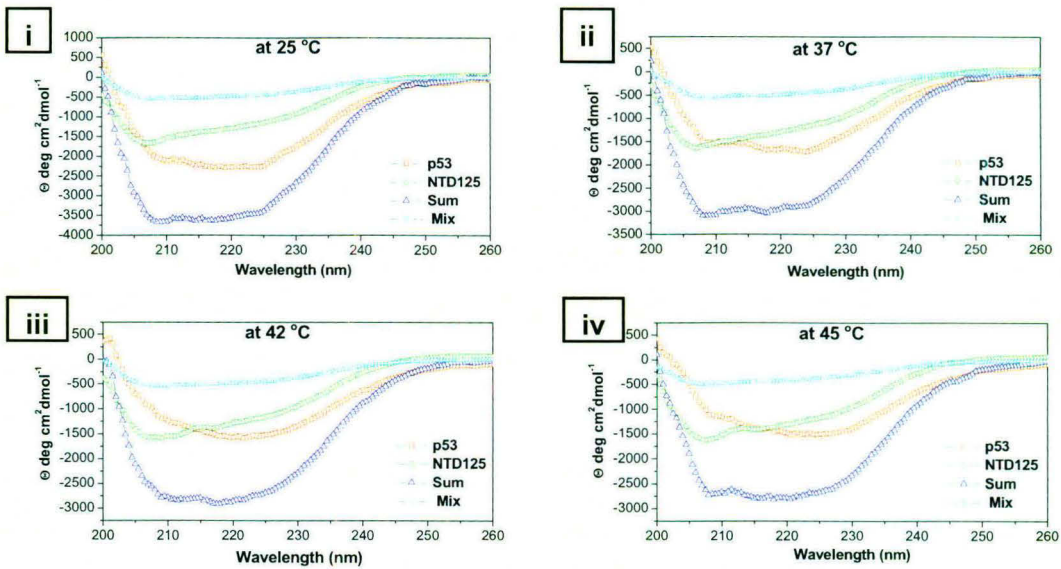
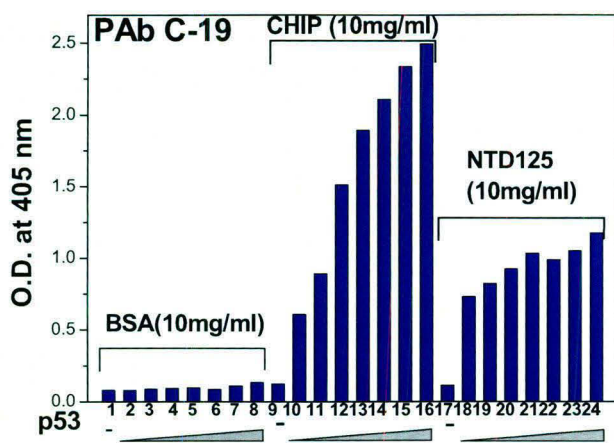
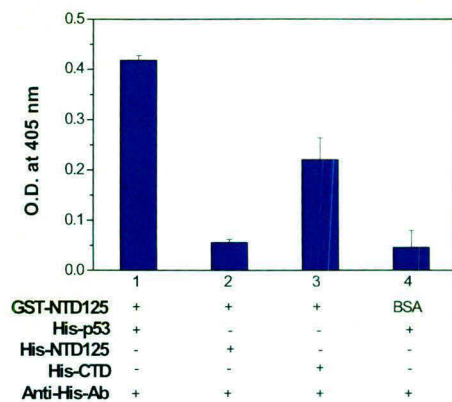


Fig. 2

a.



c.



Condition	1	2	3	4
GST-NTD125	+	+	+	BSA
His-p53	+	-	-	+
His-NTD125	-	-	-	-
His-CTD	-	-	+	-
Anti-His-Ab	+	+	+	+

b.

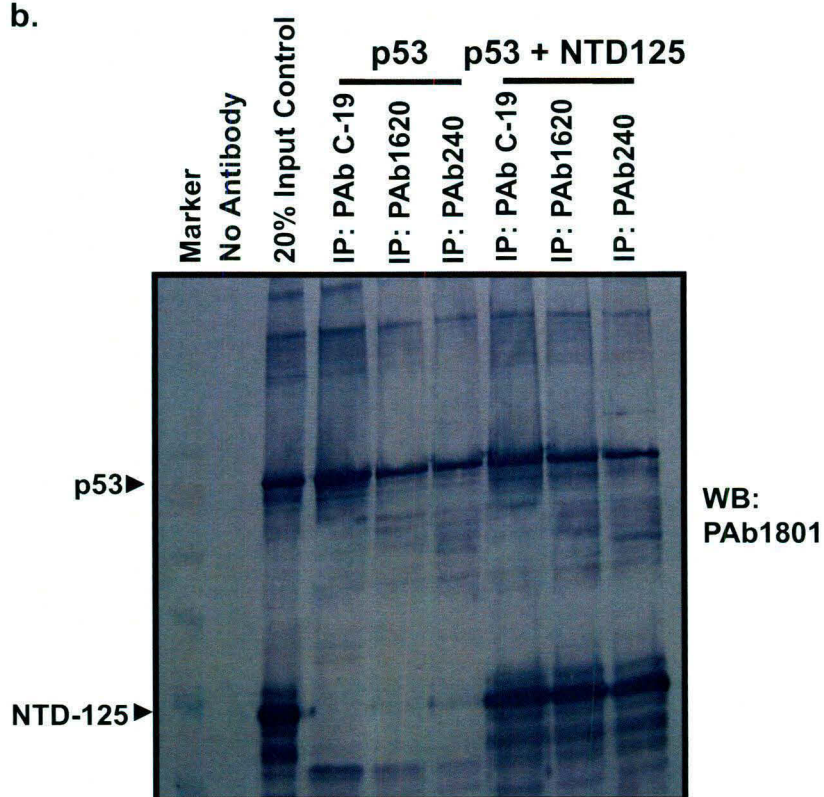
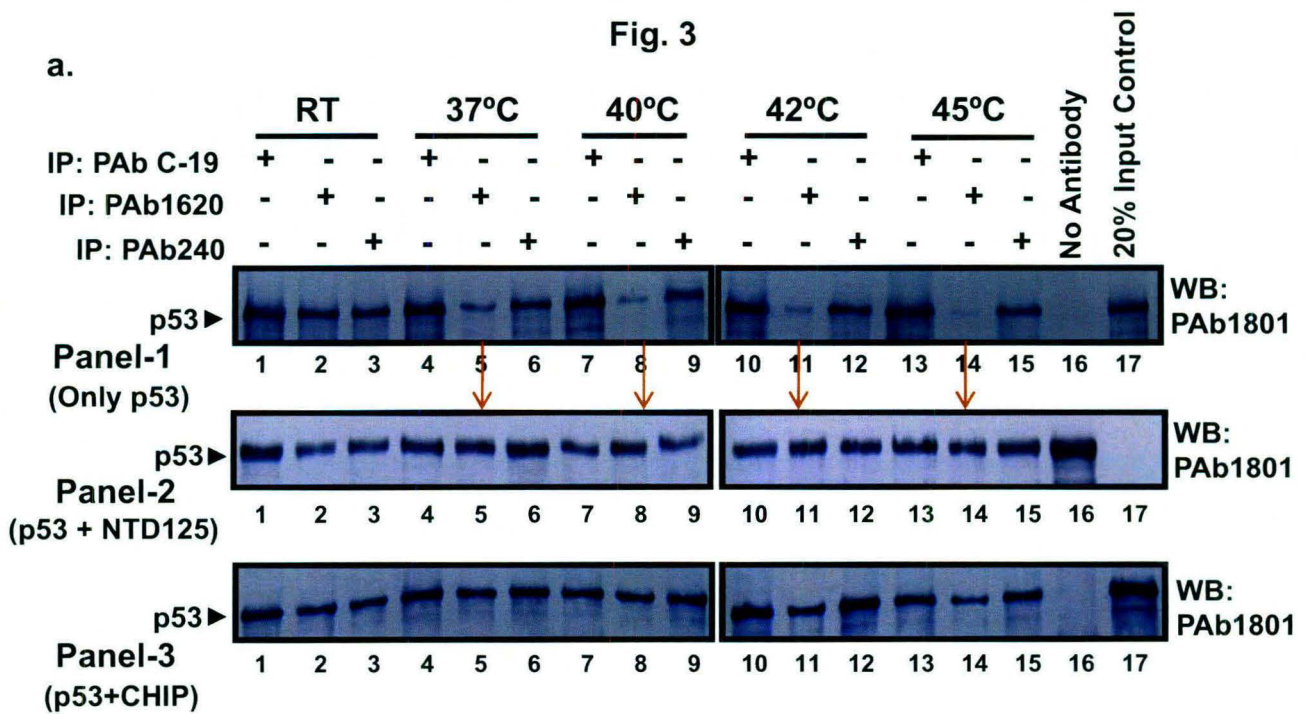
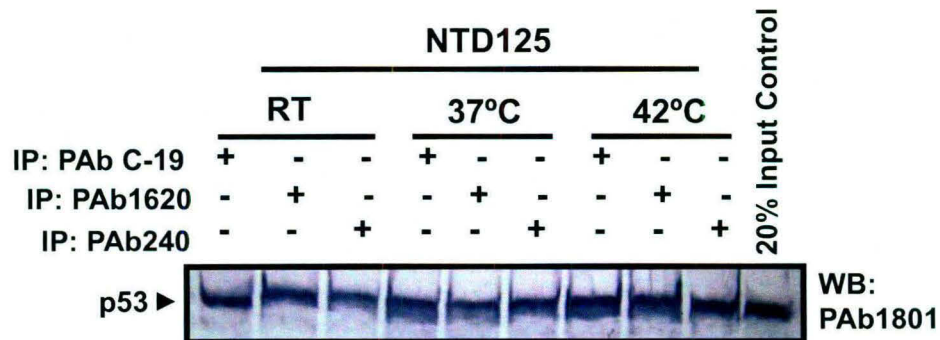


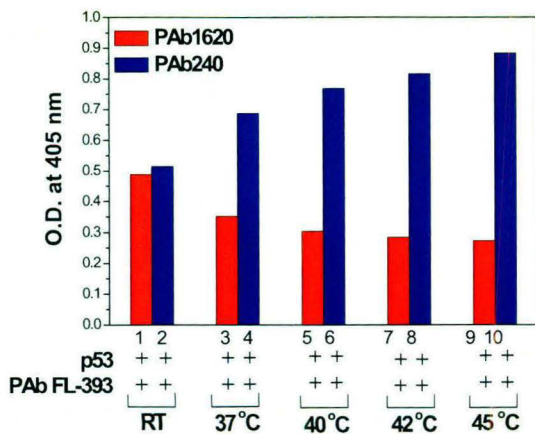
Fig. 3



b.



c.



d.

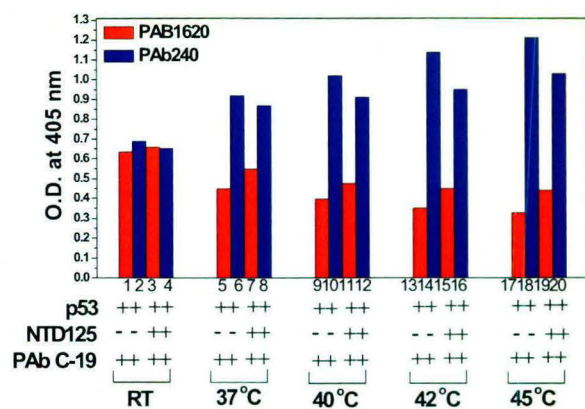
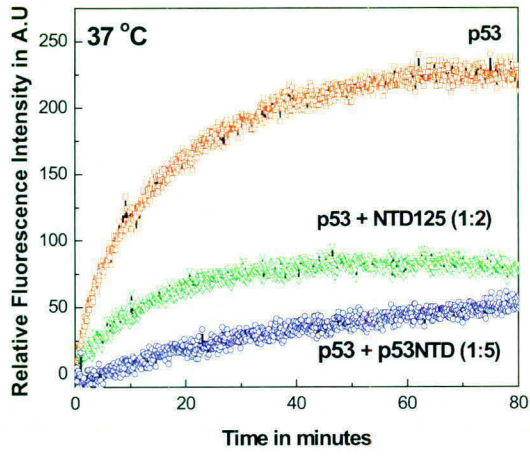


Fig. 4

a.



b.

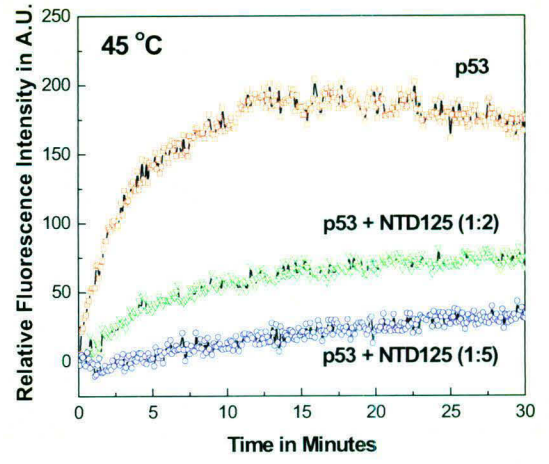
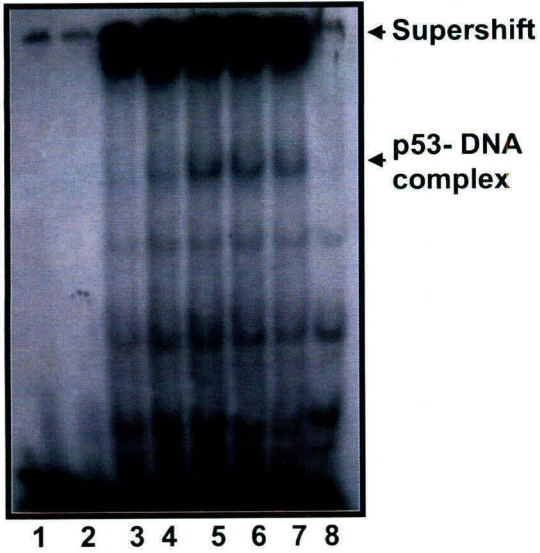


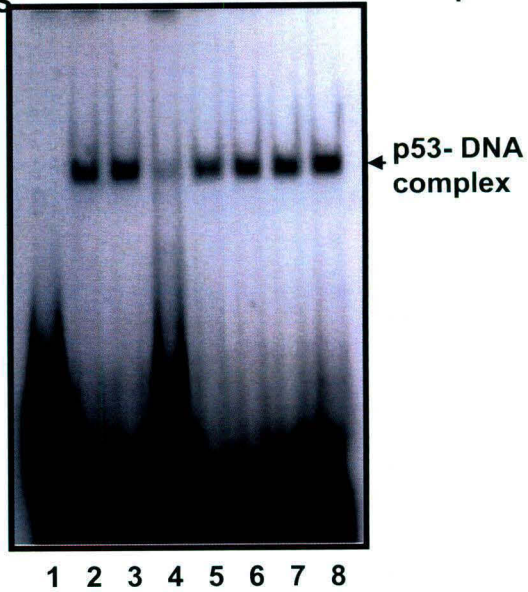
Fig. 5
b.

a.

-	-	+	+	+	+	+	-	PAb 421
-	+	-	0.5	1.0	1.5	2.0	-	NTD125 (μ g)
-	-	+	+	+	+	+	+	p53
+	+	+	+	+	+	+	+	Probe p21-5'-DBS

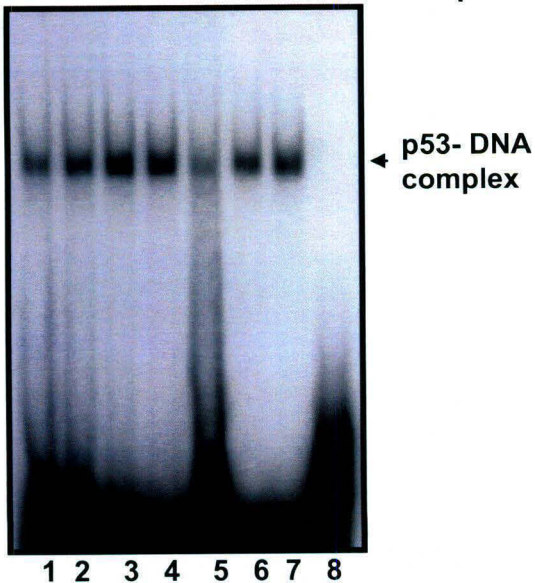


-	-	-	+	+	+	+	+	37 °C for 1 hr
-	-	+	-	1	2	5	10	NTD125 (molar ratio)
-	+	+	+	+	+	+	+	p53
+	+	+	+	+	+	+	+	Probe p21-5'-DBS



c.

+	+	+	+	+	+	+	+	Geldanamycin (5 μ M)
+	+	+	+	+	-	-	-	37 °C for 1 hr
1	2	5	10	-	-	+	-	NTD125 (molar ratio)
+	+	+	+	+	+	+	-	p53
+	+	+	+	+	+	+	+	Probe p21-5'-DBS



d.

1	2	5	10	-	-	+	-	NTD125 (molar ratio)
+	+	+	+	+	-	-	-	37 °C for 1 hr
+	+	+	+	+	+	+	-	p53
+	+	+	+	+	+	+	+	Probe p21-5'-DBS

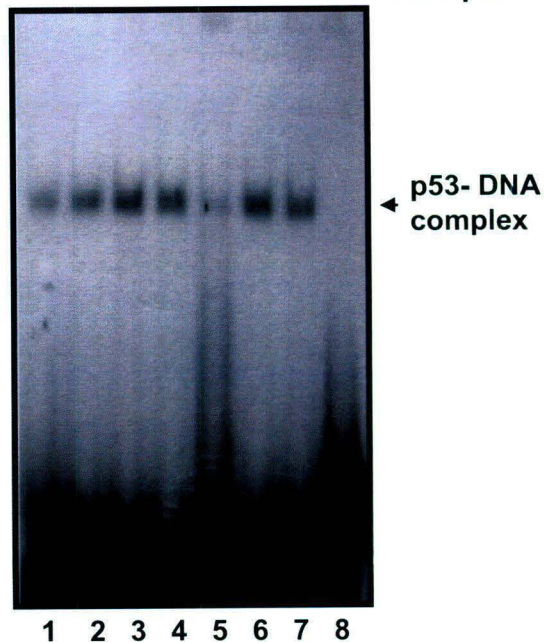


Fig. 6

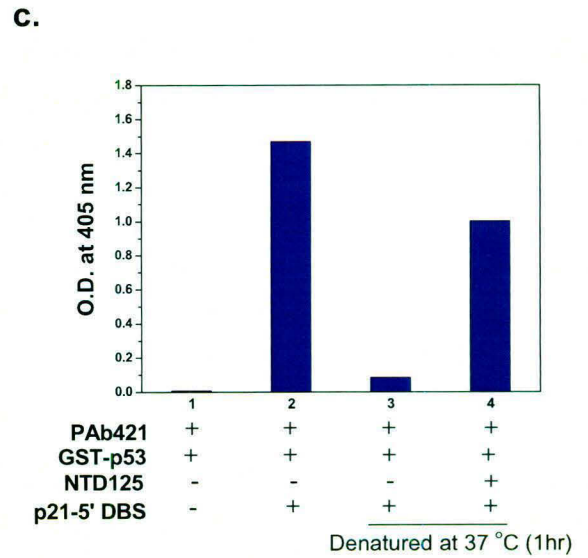
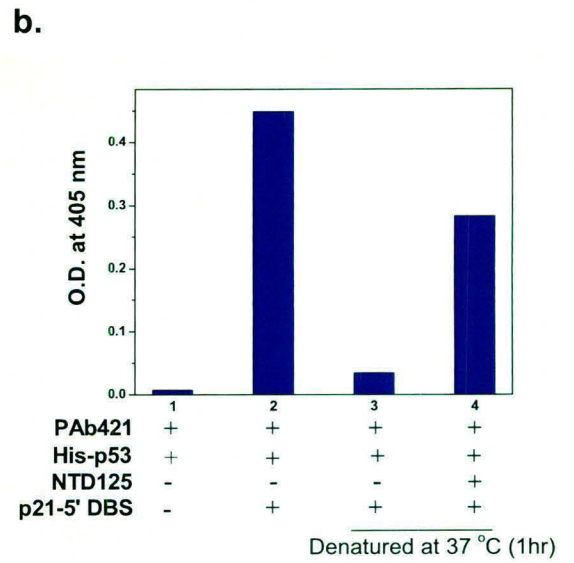
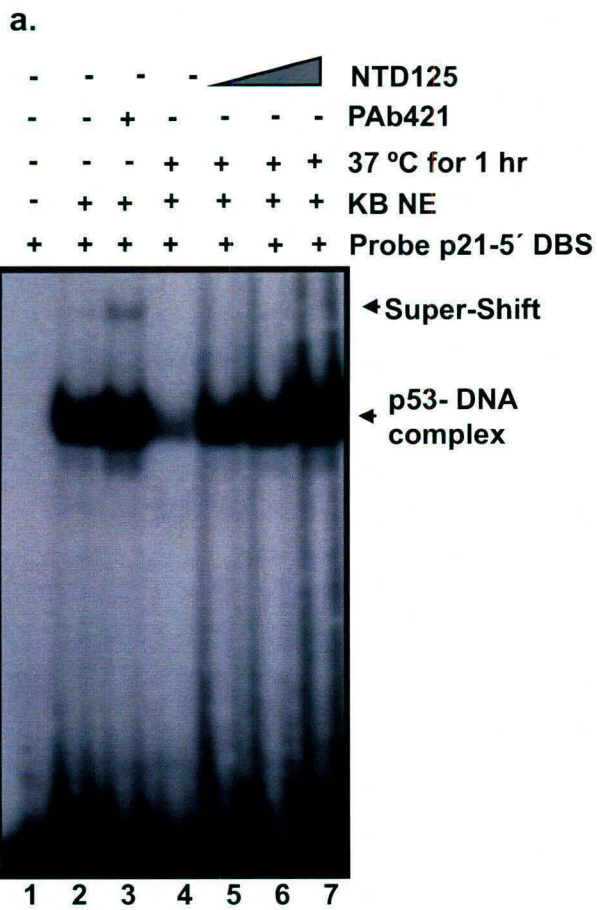
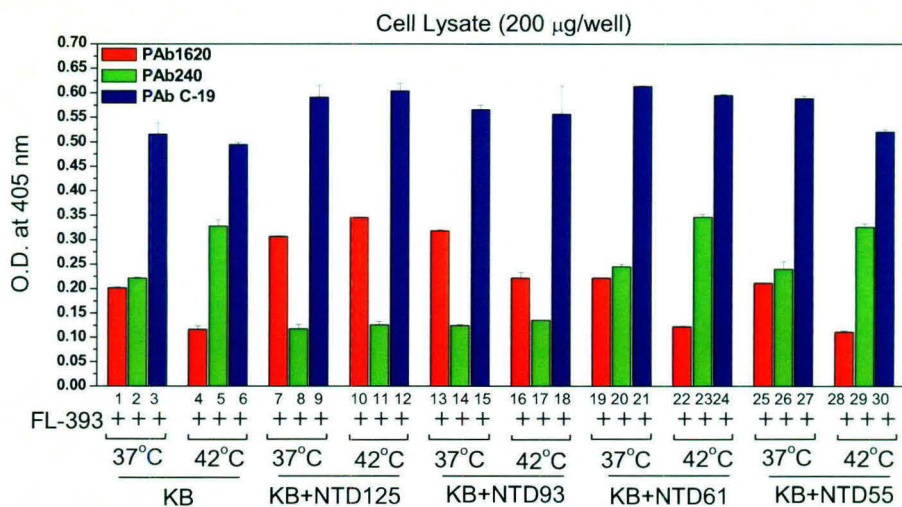
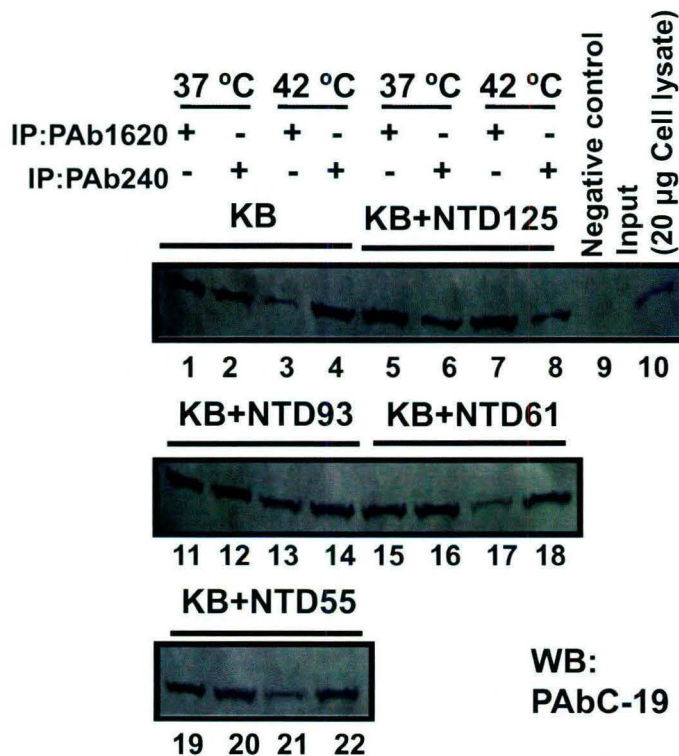


Fig. 7

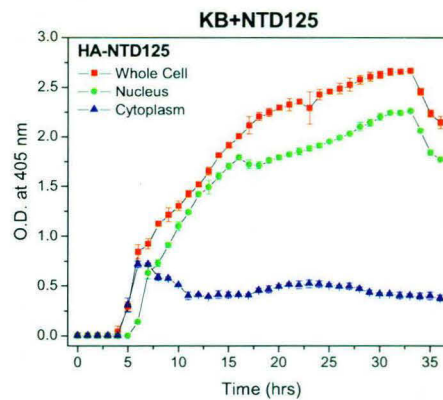
a.



b.



c.



d.

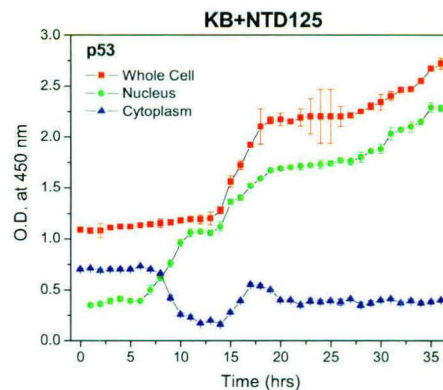
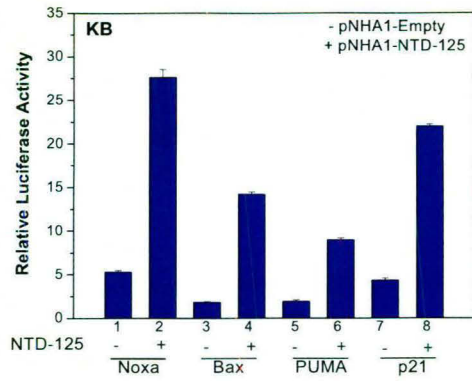


Fig. 8

a.



b.

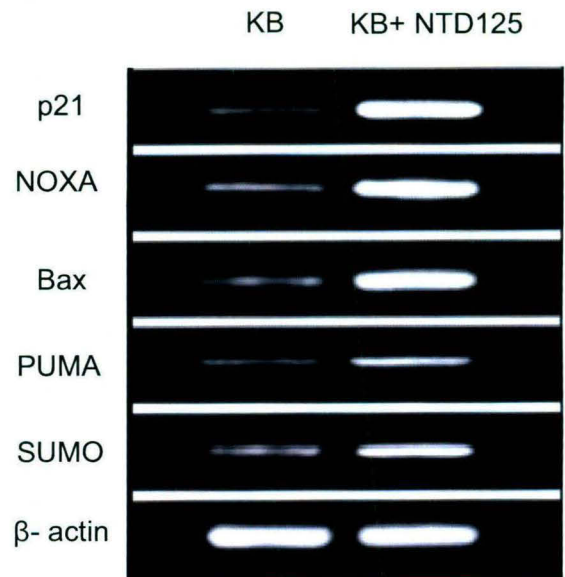
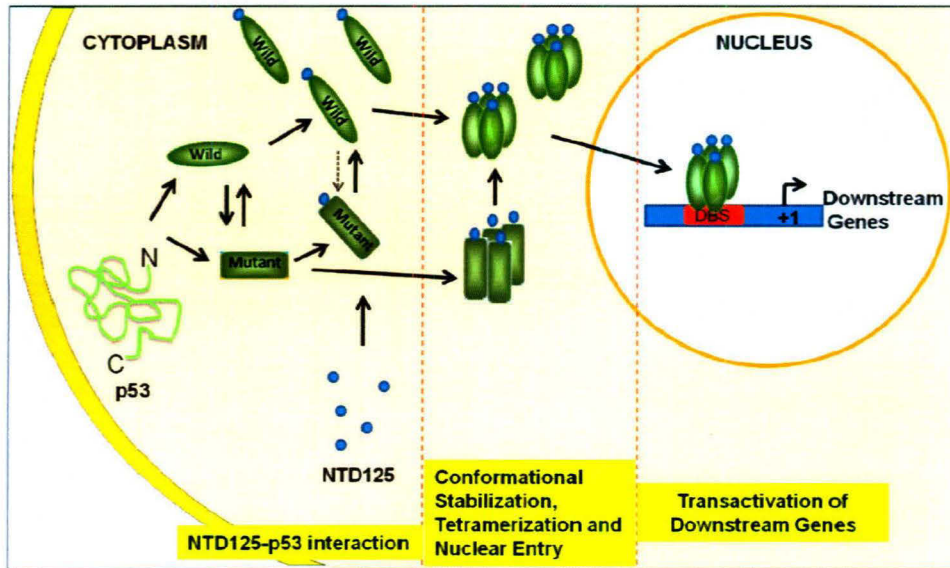


Fig. 9





Original article

Design, synthesis and characterization of some bioactive conjugates of curcumin with glycine, glutamic acid, valine and demethylenated piperic acid and study of their antimicrobial and antiproliferative properties

Shiv K. Dubey^a, Anuj K. Sharma^b, Upma Narain^c, Krishna Misra^{d,*}, Uttam Pati^b

^a Centre for Biotechnology, University of Allahabad, Allahabad 211002, India

^b Centre for Biotechnology, Jawaharlal Nehru University, New Delhi 110067, India

^c Kamla Nehru Hospital, Allahabad 211002, India

^d Indian Institute of Information Technology, Allahabad 211011, India

Received 10 May 2007; received in revised form 13 November 2007; accepted 22 November 2007

Available online 8 December 2007

Abstract

The monoesters of curcumin, a symmetric diphenol with valine and glycine have been prepared by a novel solid phase synthesis and its diesters with valine, glutamic acid and demethylenated piperic acid have been prepared by solution phase method. The assessment of their antimicrobial and anticancer (antiproliferative) activities suggested that diesters of curcumin are relatively more active than curcumin itself due to their increased solubility, slow metabolism and better cellular uptake. Furthermore, significant observation was that monoesters of curcumin have even better antimicrobial activity than their corresponding diesters, emphasizing the role of free phenolic group. The conjugate of curcumin with demethylenated piperic acid in which methylenedioxy ring was open also shows enhanced activity than the corresponding piperic acid conjugate, emphasizing the role of free phenolics in the transport or in the binding processes.

© 2007 Elsevier Masson SAS. All rights reserved.

Keywords: Curcumin; Piperic acid; Valine; Glutamic acid; Antimicrobial; Antiproliferative

1. Introduction

Curcumin [diferuloylmethane; 1,7-bis-(4-hydroxyl 3-methoxyphenyl)-1,6-heptadiene-3,5-dione; Scheme 1(I)] is the major pigmentary component of turmeric (*Curcuma longa*), a spice commonly used in India, better known as “Indian solid gold” due to its numerous therapeutic activities, its pharmacological safety and its colour. Curcumin occurs in turmeric along with its demethoxy and bis-demethoxy derivatives (curcuminoids). Curcumin has been shown to suppress carcinogenesis of the skin, liver, lung, colon, stomach and breast [1,2]. It has also been shown to inhibit the proliferation of a wide variety

of tumor cells in culture and promote apoptosis through cleavage of BID (a Bcl-2 family member protein) [3], cytochrome c release, down regulation of bcl-2 and activation of caspases [3]. It has been shown to lower blood cholesterol, promote wound healing, prevent skin wrinkling, inhibit inflammation, suppress rheumatoid arthritis and inhibit human immunodeficiency virus replication [4,5]. Curcumin mediates wide variety of therapeutic effects through the regulation of the transcription factors, nuclear factor kappa B [6–9] and activator protein, suppression of I κ B α kinase and c-jun N-terminal kinase and inhibition of expression of cyclooxygenase (COX) 2 [10,11], Cyclin D1, adhesion molecules, matrix metalloproteases [12] inducible nitric oxide synthase, HER2, epithelial growth factor (EGF) receptor, bcl-2, bcl-xl, and tumor necrosis factor (TNF) [13]. Pharmacologically, curcumin is quite safe and doses as high as 8 g/day have been administered orally to humans with no side effects.

* Corresponding author. Tel.: +91 0532 2465462/2467154 (Res); +91 0532 2922203 (Off); fax: +91 0532 2461376.

E-mail addresses: krishnamisra@hotmail.com, kkmisra@yahoo.com (K. Misra).



Telomerase targeted anticancer bioactive prodrug by antisense-based approach

Neha Kapoor^a, Anuj Kumar Sharma^b, Vishnu Dwivedi^c,
Anoop Kumar^b, Uttam Pati^b, Krishna Misra^{c,*}

^a Centre for Biotechnology, University of Allahabad, Allahabad 211002, India

^b Centre for Biotechnology, Jawaharlal Nehru University, New Delhi 110067, India

^c Chemistry department, University of Allahabad, Allahabad 211002, India

Received 30 March 2006; received in revised form 24 June 2006; accepted 1 August 2006

Abstract

A deoxy 11-mer oligonucleotide 5'-GTTAGGGTTAG-3', complementary to a repeat sequence of human telomerase RNA template has been linked through phosphate and a C-2 linker to a bioactive tetraglycine conjugate of curcumin, a well-known antitumor herbal spice component of turmeric. This molecule has been transfected into KB and HeLa cell lines and found to affect cell growth in the former. This DNA-curcumin-tetraglycine acts as a prodrug being targeted by antisense mechanism to telomerase.

© 2006 Elsevier Ireland Ltd. All rights reserved.

Keywords: Telomerase; KB cells; HeLa cells; Curcumin; Anticancer

1. Introduction

Recently, curcumin and related analogs and conjugates have been associated as remedy for various types of malignancies [1–10]. This trait is mainly derived from its antioxidant character [11,12]. Curcumin and its conjugates have been reported to inhibit several cell signaling pathways at multiple levels. Curcumin shows antiproliferative activity against tumor cells *in vitro* [13] and inhibits tumor promotion against skin, oral, intestinal and colon

carcinomas [14–16]. Previous studies have shown that curcumin affects a wide range of targets in cellular system, NF- κ B [17], p53 [18–20], c-jun [21] and telomerase [22] which are significant players in cell signaling, transcription regulation, apoptosis, cell cycle/division. Curcumin itself is well known to metabolise quickly in gut and liver. However, curcumin and a number of its conjugates have been reported to be having remarkably enhanced anti-pathogenic activity [23–26]. The masking of phenolic hydroxyls of curcumin with amino acids helps in better endocytosis and retention for a longer duration in the cell cytoplasm after enzymic hydrolysis. The curcumin-dieters are thus designed to act as prodrugs and get activated only under hypoxic conditions [27]. Our recent observation that tetra

* Corresponding author. Tel.: +91 0532 2465462/2467154 (Res); +91 0532 2922203 (Off); fax: +91 0532 2461389.

E-mail addresses: krishnamisra@hotmail.com, kkmisra@yahoo.com (K. Misra).